



UNIVERSIDAD  
DE MÁLAGA

**UNIVERSIDAD DE MÁLAGA**

Facultad de Ciencias

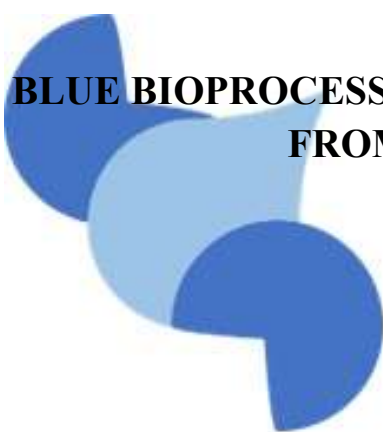
Doctorado en Biotecnología Avanzada



**UNIVERSIDAD DE LA FRONTERA**

Facultad de Ingeniería y Ciencias

Doctorado en Ciencias de la Ingeniería  
mención Bioprocesos



## **BLUE BIOPROCESS DEVELOPMENT OF NUTRACEUTICS FROM MARINE RED ALGAE**

**DOCTORAL THESIS IN FULFILLMENT OF  
THE REQUERIMENTS FOR THE DEGREE  
DOCTOR IN ADVANCED BIOTECHNOLOGY  
AND DOCTOR IN ENGINEERING SCIENCES  
WITH SPECIALIZATION IN BIOPROCESSSES**

**PABLO ANDRÉS CASTRO VARELA**

**DIRECTORES:**

**DR. FÉLIX DIEGO LÓPEZ FIGUEROA**

**DR. ROBERTO TEOFILO ABDALA DÍAZ**

**ESPAÑA-CHILE**


**2022**





UNIVERSIDAD  
DE MÁLAGA

AUTOR: Pablo Andrés Castro Varela

 <https://orcid.org/0000-0002-3886-1047>

EDITA: Publicaciones y Divulgación Científica. Universidad de Málaga



Esta obra está bajo una licencia de Creative Commons Reconocimiento-NoComercial-SinObraDerivada 4.0 Internacional:

<http://creativecommons.org/licenses/by-nc-nd/4.0/legalcode>

Cualquier parte de esta obra se puede reproducir sin autorización pero con el reconocimiento y atribución de los autores.

No se puede hacer uso comercial de la obra y no se puede alterar, transformar o hacer obras derivadas.

Esta Tesis Doctoral está depositada en el Repositorio Institucional de la Universidad de Málaga (RIUMA): [riuma.uma.es](http://riuma.uma.es)





## DECLARACIÓN DE AUTORÍA Y ORIGINALIDAD DE LA TESIS PRESENTADA PARA OBTENER EL TÍTULO DE DOCTOR

D./Dña PABLO ANDRES CASTRO VARELA

Estudiante del programa de doctorado EN BIOTECNOLOGÍA AVANZADA de la Universidad de Málaga, autor/a de la tesis, presentada para la obtención del título de doctor por la Universidad de Málaga, titulada: BLUE BIOPROCESS DEVELOPMENT OF NUTRACEUTICS FROM MARINE RED ALGAE.

Realizada bajo la tutorización de DR. FÉLIX LÓPEZ FIGUEROA y dirección de DR. ROBERTO ABDALA DÍAZ (si tuviera varios directores deberá hacer constar el nombre de todos)

DECLARO QUE:

La tesis presentada es una obra original que no infringe los derechos de propiedad intelectual ni los derechos de propiedad industrial u otros, conforme al ordenamiento jurídico vigente (Real Decreto Legislativo 1/1996, de 12 de abril, por el que se aprueba el texto refundido de la Ley de Propiedad Intelectual, regularizando, aclarando y armonizando las disposiciones legales vigentes sobre la materia), modificado por la Ley 2/2019, de 1 de marzo.

Igualmente asumo, ante a la Universidad de Málaga y ante cualquier otra instancia, la responsabilidad que pudiera derivarse en caso de plagio de contenidos en la tesis presentada, conforme al ordenamiento jurídico vigente.

En Málaga, a 9 de NOVIEMBRE de 2022

|   |                                       |
|---|---------------------------------------|
| Fdo.: PABLO CASTRO VARELA<br>Doctorando/a             | Fdo.: FÉLIX LÓPEZ FIGUEROA<br>Tutor/a |
| Fdo.: DR. ROBERTO ABDALA DÍAZ<br>Director/es de tesis |                                       |



## *Blue bioprocess development of nutraceuticals from marine red algae*

Esta tesis fue realizada en la modalidad de doble graduación mediante convenio entre la Universidad de La Frontera, Chile y la Universidad de Málaga, España bajo la supervisión conjunta por los siguientes directores:

Dra. Mónica Rubilar Díaz, Profesor Titular, perteneciente al Claustro del Doctorado en Ciencias de la Ingeniería mención Bioprocesos, adscrito al Departamento de Ingeniería Química de la Universidad de La Frontera, Chile.

Dr. Félix López Figueroa, Catedrático, perteneciente al Claustro del Doctorado en Biotecnología Avanzada, adscrito al Instituto Andaluz de Biotecnología y Desarrollo Azul, Departamento de Ecología y Geología, Facultad de Ciencias de la Universidad de Málaga, España.

Dr. Roberto Abdala Díaz, Profesor Contratado Doctor, perteneciente al Claustro del Doctorado en Biotecnología Avanzada, adscrito al Instituto Andaluz de Biotecnología y Desarrollo Azul, Departamento de Ecología y Geología, Facultad de Ciencias de la Universidad de la Málaga, España.

Es presentada para su revisión por los miembros de la Comisión Examinadora.

.....  
**Dr. Edgar Uquiche Carrasco**  
Director Programa de Doctorado en  
Ciencias de la Ingeniería mención  
Bioprocesos.

.....  
**Dra. Paz Robert Canales**  
Universidad de Chile

.....  
**Dr. Víctor Beltrán Vargas**  
Director Académico de Postgrado  
Universidad de La Frontera

.....  
**Dr. Paulo Díaz Calderón**  
Universidad de Los Andes

.....  
**Dr. Tomás Cordero Alcántara**  
Director Escuela de Doctorado  
Universidad de Málaga

.....  
**Dra. María Cristina Diez Jerez**  
Universidad de La Frontera

.....  
**Dra. Mónica Rubilar Díaz**  
Tutor de Tesis  
Universidad de La Frontera

.....  
**Dra. Mariela Bustamante López**  
Universidad de La Frontera

.....  
**Dr. Félix López Figueroa**  
Tutor de Tesis  
Universidad de Málaga

.....  
**Dra. Nathalie Korbee Peinado**  
Universidad de Málaga

.....  
**Dr. Roberto Abdala Díaz**  
Director de Tesis  
Universidad de Málaga



UNIVERSIDAD  
DE MÁLAGA

*“...La luz que oscila mensajes de secretos de juventud dialogó con seres mitológicos, dotados de quietud y dealidad de energéticos fotones...*

*...Qué hay detrás de esa sonrisa?*

*Energía y actitud...*

*...Qué hay en tus pupilas oscilantes?*

*Una imagen real e invertida....”*

*A los Jóvenes Investigadores del Mar, Poema de Calahonda.*



UNIVERSIDAD  
DE MÁLAGA

## Agradecimientos

*Agradezco a la Agencia Nacional de Investigación y Desarrollo de Chile (ANID) por la Beca Doctorado concedida (N°21180254) para la realización de esta tesis doctoral.*

*Agradezco a la Universidad de Málaga y la Agencia Iberoamericana de postgrado (AUIP) por la Beca Doctoral concedida para la realización de la tesis en Universidad de Málaga, España.*

*Se agradece al financiamiento otorgado por los proyectos FACCO (FEDER-JA-162) y NAZCA (PY20-00458) el cual la tesis doctoral fue asociada para la realización de los objetivos (Objetivos específicos 2, 3, 4 y 5) en Universidad de Málaga, España.*

*Agradezco a la Dirección de los Programas de Doctorado en Cs. de la Ing. mención Bioprocesos (UFRO), Dr. Edgar Uquiche Carrasco, y Doctorado en Biotecnología Avanzada (UMA), Dra. Carmen Beuzon López, por su buena disposición y gestión administrativa. Así como las diferentes ayudas económicas para las actividades científicas realizadas. A su vez, las respectivas unidades de relaciones internacionales Sra. María Paz Collio (UFRO) y Sr. José Ruiz (UMA), agradezco su importante labor internacional.*

*Deseo reconocer a mi Tutor de Chile, Dra. Mónica Rubilar Díaz por su compromiso, conocimientos, patrocinio, simpatía, ayuda, paciencia, colaboración, y gestión del proyecto doctoral que permitió vincularse con la industria de los bioprocesos.*

*Agradezco al Sr. Jaime Zamorano, Gerente de Desarrollo de la Empresa Gelymar S.A. por su asesoría industrial e interés en participar en este proyecto de tesis.*

*Deseo reconocer a mi Tutor de España, Dr. Félix López Figueroa por su pensamiento crítico transmitir y compartir enseñanzas, fraternidad, confianza y gran compromiso en aceptar la Tutoría de la plaza doctoral así como la instancia de colaborar en el Instituto IBYDA-UMA.*

*A su vez, reconocer a mi Director de España, Dr. Roberto Abdala Díaz por sus charlas y consejos, enseñanzas, humildad, confianza y su alto compromiso con el desarrollo de la tesis así como la vinculación con otros grupos de investigación.*

*A los Profesores Dra. Paula Célis Plá (UPLA), Dra. Julia Bejar (UMA), Dr. Manuel Mari-Beffa (UMA), Dr. Manuel López (UMA) y Dr. Antonio Martínez (UGR) por su alta disposición en colaborar y aportar sus conocimientos para la realización de este proyecto de tesis.*

*A mis compañeros del Doctorado UFRO (Erwin Werner, Claudio Alarcón, Eduardo Morales) y Doctorado UMA (Julia Vega y Víctor Robles) por la colaboración y la camaradería en el día a día.*



*Finalmente agradezco al personal técnico de ambos grupos de investigación Nicole Bobadilla, Unidad de tecnología y procesos-UTP UFRO, Cristina González y Marta Sánchez-Unidad de Biotecnología Azul-IBYDA UMA) en el soporte tecnológico para alcanzar con los objetivos propuestos.*

## Summary

*Sarcopeltis skottsbergii* is an endemic red alga species of the Southern Cone, with biliproteins as accessory pigments including R-phycoerythrin (R-PE). The production of *S. skottsbergii* is around 20,000 tons of dry alga per year. The evaluation of R-PE in a biorefinery model is still in the early stages in the field of algal biotechnology to be used in the food, pharmaceutical, cosmeceutical and nutraceutical industries. The objective of this Thesis is to present the current knowledge and the exploration of novel applications, encouraging the rational and integral utilization of this commercial specie. The Thesis is organized into six sections, covering information on the processing technologies for extraction (HPH and UAE) and protection (alginate/shellac by ionic gelation) of R-PE and fractions for functional foods and nutraceuticals, the *in vitro* and *in vivo* assessment of the biological activities, and alternative intensive production culture systems based on yellow light to saturate photosynthesis supplemented by blue light for R-PE accumulation. HPH method was the most efficient extraction method of R-PE. Furthermore, R-PE showed a positive correlation between the oxygen radical absorbance capacity (ORAC) in the best-selected extractions. An attractive non-aggressive extraction alternative with the biological activity of interest is suggested. From the residual supernatant generated by high-pressure homogenization, two soluble polysaccharides (neutral and acid fractions) were obtained with high biological activity. The acid polysaccharides, which had a relatively high sulfate content, exhibited significant antioxidant activity in superoxide radical assay (ABTS) and high anti-proliferative effects on melanoma (G-361), leukemia (U-937) and colon (HCT-116) carcinoma cells. The *in vivo* assay with zebrafish has shown a linear relationship between neutral and acid fractions concentration and growth retardation at 72 hpf  $\text{mg}^{-1} \text{ml}^{-1}$  with a  $\text{LC}_{50}$  of about  $1.45 \text{ mg ml}^{-1}$  and  $1.25 \text{ mg ml}^{-1}$ , respectively. These results indicated that the *in vitro* antitumoral assays, *in vivo* model and

antioxidant activities of the two polysaccharides may be related to the combined effects of sulfate or galactose contents.

The encapsulation of alginate/shellac reached an EE value of 97.5% and led to higher R-PE contents at the end of digestion compared with R-PE non-encapsulated, suggesting a protective role. From permeate streams, equivalent to the absorption of R-PE encapsulated, the bioavailability was 2.5 times significantly higher than R-PE non-encapsulated. A high selectivity index ( $> 10$ ) was observed for the R-PE extract on the HCT-116 human colon cancer cell line. The alginate/shellac as a wall material and ionic gelation technology used may determine the release of the R-PE pigment at an intestinal site and their effect antiproliferative on health. Yellow light with the incidence of blue light as an interesting factor in the culture of red microalgae improves high-quality R-PE compound and maintained stable biomass productivity, to improve the quality of bioprocess production for nutraceutical industry. This Thesis complemented understanding the potential of algae for traditional and novel functional products.

## Resumen

Esta tesis doctoral se centra en desarrollar un bioproceso azul sostenible y alternativo, basado en procesos de extracción verde (ultrasonido y homogenización de alta presión), protección por biomateriales orgánicos (alginato de sodio y shellac) y efectos de biodisponibilidad gastro/oral de R-ficoeritrina (R-PE) de *Sarcopeltis skottsbergii* en líneas celulares de tejidos bucales y enzimas gastrointestinales mediante reactores químicos. Además, la fotosaturación para la acumulación de R-ficoeritrina así como la recuperación de biocompuestos del proceso residual aplicando un modelo de biorrefinería de algas.

En el **capítulo 1** se desarrolla una contextualización de los antecedentes sobre el uso de las algas a nivel alimentario con un especial enfoque en los pigmentos ficobilínicos que acumulan el alga roja *Sarcopeltis skottsbergii*. La producción de *S. skottsbergii* ronda las 20.000 toneladas de alga seca al año. La evaluación de R-PE en un modelo de biorrefinería aún se encuentra en etapas tempranas en el campo de la biotecnología de algas para su uso en las industrias alimenticia, farmacéutica, cosmeceútica y nutracéutica. El objetivo de esta Tesis es presentar el conocimiento actual y la exploración de aplicaciones novedosas, fomentando el aprovechamiento racional e integral de esta especie comercial. La Tesis está organizada en seis secciones, cubriendo información sobre las tecnologías de procesamiento para la extracción (Homogeneización a alta presión-HPH y Extracción asistida por ultrasonido-UAE) y protección (alginato/goma laca por gelificación iónica) de R-PE y la simulación dinámica de el tracto gastrointestinal humano para el estudio de la biodisponibilidad y bioaccesibilidad de R-PE en encapsulados. Asimismo, la recuperación de fracciones de polisacáridos para alimentos funcionales y nutracéuticos, la evaluación in vitro de las actividades biológicas y sistemas alternativos de cultivo intensivo de producción basados en luz amarilla para saturar la fotosíntesis complementada con luz azul para acumulación de R-PE.

La primera etapa del trabajo doctoral (**Capítulo 2**) se enfoca en dilucidar y potenciar las algas marinas como fuentes importantes de sustancias naturales bioactivas. En este aspecto, se ha demostrado que muchos metabolitos aislados (por ejemplo, proteínas, lípidos, polisacáridos, etc.) de algas marinas poseen actividades biológicas y beneficios potenciales para la salud. Por lo tanto, ha surgido una nueva tendencia para aislar e identificar componentes y compuestos bioactivos de las algas marinas. Una característica particularmente interesante de las algas marinas es su riqueza en pigmentos naturales (NP). Por lo tanto, muchos pigmentos naturales, como las ficobiliproteínas como la ficoeritrina aislada de algas marinas, han llamado mucho la atención en los campos de la alimentación, la cosmética y la farmacología. Nuevas técnicas de extracción y separación con enfoque en compuestos hidrofílicos es necesario evaluar y mejorar los rendimientos de extracción,

Las tecnologías de extracción, especialmente aquellas consideradas como procesos limpios, como los métodos que involucran la extracción de agua, han llamado la atención para explorar los recursos marinos para obtener ingredientes funcionales. Como se mencionó anteriormente, las ficobiliproteínas son las clases importantes de proteínas presentes en micro y macroalgas. Las proteínas marinas pueden proporcionar numerosas ventajas sobre las enzimas tradicionales utilizadas en el procesamiento de alimentos debido a su actividad y estabilidad en condiciones de reacción inusuales y extremas. Como las ficobiliproteínas son intracelulares, se requiere la disrupción celular para su liberación eficiente durante la extracción. Hay varios métodos disponibles para la extracción de ficobilinas, como el choque osmótico, maceración en presencia de nitrógeno líquido en tampón fosfato, congelar la molienda, congelación y descongelación, ultrasonidos (US) y homogeneización. Sin embargo, estos métodos se informan para la caracterización y el análisis fisicoquímico de las ficobiliproteínas y no tienen como objetivo el procesamiento posterior. Según Jacotet-Navarro et al., (2016) el objetivo de los procesos de extracción verde es lograr una tasa de

extracción más rápida, un uso más efectivo de la energía, una mayor transferencia de masa y calor, un tamaño reducido del equipo, una reducción en el número de procesos pasos y sin daño bioactivo. La aplicación de estas tecnologías también tiene como objetivo preservar el entorno natural y sus recursos. Al ser una tecnología verde, US ha llamado la atención de los investigadores por su aplicación en industrias alimenticias y afines. US actúa creando compresión y descompresión a través de ondas de sonido a una frecuencia  $>20$  kHz. Se han identificado varios mecanismos de acción de los ultrasonidos, que incluyen fragmentación, erosión, efecto sonocapilar, sonoporación, cizallamiento local y destrucción-detexturización de la matriz de la pared celular vegetal. Un efecto general de estos mecanismos da como resultado la ruptura de la pared celular. Sin embargo, el grado relativo de contribución de un mecanismo dado puede variar con el tipo de biomasa y los parámetros del proceso. Al emplear US, se pueden lograr mayores rendimientos de extracción en un tiempo de proceso bajo ( el grado relativo de contribución de un mecanismo dado puede variar con el tipo de biomasa y los parámetros del proceso. Al emplear US, se pueden lograr mayores rendimientos de extracción en un tiempo de proceso bajo el grado relativo de contribución de un mecanismo dado puede variar con el tipo de biomasa y los parámetros del proceso. Al emplear US, se pueden lograr mayores rendimientos de extracción en un tiempo de proceso bajo y a menudo, a bajas temperaturas y, por lo tanto, más adecuado para compuestos termolábiles. En procesos de extracción asistidos por ultrasonido, se observaron mayores rendimientos ( $>70\%$ ) para biomoléculas como carotenoides de residuos de granada, lípidos de microalgas y antocianinas de arándano. Además, US tiene la ventaja de la escalabilidad directa debido a su capacidad de generar zonas de cavitación de intensidad progresivamente alta y, por lo tanto, adecuado para la ampliación del proceso industrial.

La extracción mediante ultrasonido se puede combinar con otras técnicas, como extracción por reflujo térmico, tratamiento a alta presión,  $\text{CO}_2$  supercrítico y microondas para extraer y

no dañar los compuestos bioactivos. En una revisión reciente de Yi et al., (2019) el tratamiento de alta presión, que se considera una de las tecnologías más ecológicas, mostró un tiempo de extracción considerablemente más corto y un mayor rendimiento en comparación con otras técnicas convencionales. Además, el uso de temperaturas suaves hace que este proceso sea especialmente atractivo en la extracción de compuestos bioactivos termosensibles. En otro reporte, Yang y Wei (2015) desarrollaron un método eficiente para extraer compuestos bioactivos de la planta *Rabdosia rubescens* combinando extracción por reflujo de calor (convencional, solvente: etanol) y extracción asistida por ultrasonido (frecuencia de 40 kHz y potencia de 185 W, con agitación). Los autores concluyeron que la combinación de técnicas de extracción redujo el tiempo de procesamiento y aumentó el rendimiento de extracción de compuestos bioactivos. Sin embargo, después de la extracción de R-ficoeritrina, el extracto de proteína debe concentrarse y purificarse previamente, lo que generalmente es costoso y requiere muchas etapas. Entre los métodos de separación de concentrados, la tecnología de membrana se centra en el uso de una membrana semipermeable para separar un líquido en dos fracciones diferentes al permitir selectivamente el paso de algunos compuestos mientras se impide el paso de otros compuestos, generalmente en función del peso molecular. Las tecnologías de membrana son métodos alternativos prometedores para concentrarse en proteínas de algas, así como para probar nuevos ingredientes tecnofuncionales y bioactivos. Tienen la ventaja de ser un método de separación no térmico y respetuoso con el medio ambiente. Las tecnologías de membrana más utilizadas incluyen microfiltración, ultrafiltración, nanofiltración y ósmosis inversa.

La ruptura de la pared celular resistente es un paso crítico necesario para aumentar la disponibilidad de proteínas de algas para la extracción. Las tecnologías de membrana son muy adecuadas para usar con algas marinas como parte de un proceso de biorrefinería para maximizar la valorización de todos los componentes dentro de las algas y evitar la presencia

de metales pesados en el producto final. Se podría usar una combinación de tecnologías de membrana para aislar proteínas de algas usando los mismos principios de corte de peso molecular que se usan en la industria láctea. En la industria láctea, la microfiltración (MF) se utiliza para prolongar la vida útil de la leche sin ningún tratamiento térmico mediante la eliminación de microorganismos, al tiempo que conserva el sabor general y los atributos sensoriales. MF podría usarse para eliminar componentes de la pared celular de algas y bacterias con un peso molecular superior a 200 kDa. Luego, la ultrafiltración (UF) podría usarse para aislar proteínas y otras macromoléculas entre 1 y 200 kDa, de manera similar a como se usa en la industria láctea para generar fracciones enriquecidas de menos de 10, 5, 3 y 1 kDa. La nanofiltración (NF) podría luego usarse para eliminar sales monovalentes para minimizar la presión osmótica, seguida de ósmosis inversa (RO) para reducir el volumen de líquido. De hecho, las tecnologías de membrana ya se han utilizado para aislar células de microalgas enteras y varios componentes de algas marinas. Se informó que la microfiltración de flujo tangencial es un método eficiente para recuperar entre el 70% y el 89% de la biomasa de algas de los tratamientos de aguas residuales. La UF se utilizó anteriormente junto con la extracción con CO<sub>2</sub> supercrítico y el ultrasonido para aislar polisacáridos de la macroalga *Sargassum pallidum*. Se aislaron polisacáridos con actividades antioxidantes de la macroalga verde *Ulva fasciata* utilizando extracción con agua caliente seguida de varias etapas de UF con tamaños de poro cada vez más pequeños. Además, se usó UF para aislar la proteína ficoeritrina de la macroalga *Grateloupia turuturu* luego de la homogeneización celular, que se informó que retiene el 100% de la proteína sin desnaturalización. Alternativamente, se podría aplicar una UF de dos etapas para el enriquecimiento de proteínas de algas.

Por lo tanto, la extracción y separación de R-PE de la biomasa de macroalgas, así como la metodología seguida, son extremadamente importantes para mantener las bioactividades. La falta de metodologías estandarizadas de extracción y separación ha impedido la aprobación



oficial de las ficobiliproteínas o sus fracciones derivadas para aplicaciones alimentarias, farmacéuticas, dermatológicas, nutracéuticas u otras aplicaciones comerciales hasta la fecha.

Finalmente, nuestro estudio demuestra que la extracción de R-PE de *S. skottsbergii* fue optimizada por RSM, utilizando UAE y HPH. RSM demostró ser útil para la extracción de PE en el rango de optimización probado, proporcionando un modelo con un buen acuerdo entre los resultados experimentales y predichos. HPH obtuvo la extracción más eficiente, rindiendo 5.7 mg R-PE g<sup>-1</sup> DW de biomasa en las condiciones óptimas (300 MPa, 2 pases con agua destilada), 50-60 % superior a los rendimientos de PE obtenidos con UAE. La variable más crucial en el proceso de extracción fue el nivel de presión, con concentraciones más altas de R-PE usando agua destilada. *S. skottsbergii* reveló una excelente fuente de R-ficoeritrina y actividad antioxidante, y su aplicación como ingrediente bioactivo podría sugerirse para la industria alimentaria.

En el **capítulo 3** se desarrollan los principales desafíos en cuanto a la protección de ficoeritrina, previamente optimizada su extracción (**capítulo 2**). La ficoeritrina, al ser un compuesto basado en proteínas, requiere algunas formas de protección antes de que pueda incorporarse como ingrediente especializado en matrices alimentarias. Al respecto, varios investigadores han demostrado que la encapsulación es un método efectivo y económico para mantener la estabilidad de las ficobiliproteínas y especialmente de la ficocianina (otro pigmento de la ficobiliproteína, con coloración azul). Sin embargo, la estabilización con ficoeritrina orientada a preservar las propiedades biotecnológicas aún es reducida y requiere mayor investigación.

Una alternativa para proteger este tipo de compuestos bioactivos es encapsularlos en un soporte sólido como microcápsulas, aumentando así su estabilidad química, además de proteger y mejorar la biodisponibilidad a nivel gastrointestinal. Cabe señalar que el éxito del sistema de encapsulación depende principalmente de la técnica utilizada, las condiciones del proceso y el

tipo de material de encapsulación. En los últimos años, el uso de la técnica de encapsulación por electrocoextrusión, a través del mecanismo de gelificación iónica, se ha considerado como una tecnología de encapsulación prometedora para la producción de cápsulas core-shell, que van desde micrómetros hasta milímetros. La electro-coextrusión es un proceso simple, económico y fácil de operar, para producir cápsulas uniformes en tamaño y forma. El principio se basa en rotura el flujo laminar aplicando una frecuencia vibratoria con una amplitud definida a un tamaño determinado. Diferentes tipos de polímeros hidrofílicos e hidrofóbicos, como alginato, poli-L-lactida, poli(DL-lactida-co-glicolida), polidimetilsiloxano, fotopolímero y manteca de cacao, se han utilizado en electro-coextrusión. Para fabricar cápsulas con diferentes fluidos centrales es necesario proteger soluciones proteicas, soluciones acuosas, emulsiones, suspensiones celulares y aceites encapsularon una suspensión celular. Por ejemplo, dentro de una capa de alginato de calcio de 0,36 mm de diámetro y 90 m de espesor por electro-coextrusión, fue superado el problema de fuga celular que se presenta con el uso de perlas de alginato de calcio. Choi et al., (2010) fabricaron microcápsulas de alginato de calcio con núcleo y cubierta, en el rango de tamaño de 200–1000 m, por electro-coextrusión para la entrega controlada de factores de inducción osteogénica de células madre. A pesar de los estudios citados anteriormente sobre cápsulas de alginato húmedas de tamaño micro, actualmente hay poca información disponible sobre la electrocoextrusión de cápsulas de alginato de núcleo y cubierta visibles de tamaño macro en forma seca.

Las características de las cápsulas de núcleo-envoltura producidas por electrocoextrusión, como la apariencia externa, el tamaño, el grosor de la cubierta, la textura, el comportamiento de liberación del núcleo y la estabilidad, podrían estar influenciadas principalmente no solo por factores relacionados con el fluido de la cubierta, como la concentración de polímero, viscosidad, densidad, tensión superficial y conductividad eléctrica, sino también por factores relacionados con el proceso, como las tasas de flujo del núcleo y la carcasa, la relación de la

tasa de flujo de la carcasa y el núcleo, el voltaje aplicado, la temperatura, el tamaño de la boquilla, la distancia entre la punta de la boquilla y la superficie del baño gelificante, la concentración del agente gelificante, el tiempo de gelificación y el método de secado. Sin embargo, los efectos de tales factores sobre las características de las cápsulas de alginato con núcleo y cubierta, especialmente de las cápsulas de alginato secas y de tamaño macro, no se han estudiado sistemáticamente.

Actualmente, existe un interés creciente en el uso de cápsulas a base de polímeros de fuentes naturales, debido a su capacidad de renovación, biodegradabilidad, biocompatibilidad y no toxicidad. Por ejemplo, el alginato es un polisacárido aniónico natural ampliamente utilizado para preparar sistemas de encapsulación de cápsulas o perlas debido a sus interesantes propiedades fisicoquímicas, biocompatibilidad, amplia disponibilidad y bajo costo. La funcionalidad de las perlas de alginato depende en gran medida de su permeabilidad y estabilidad fisicoquímica. Esta cápsula de alginato tiene una retención y liberación selectiva, que la convierte en un buen vehículo para aplicaciones biotecnológicas; sin embargo, la porosidad relativamente alta no es adecuada para algunas aplicaciones industriales. La difusión de moléculas pequeñas como la glucosa y el etanol no se ve afectada por la matriz de alginato, mientras que se ha demostrado que la difusión de proteínas más grandes de los geles depende de su peso molecular. Se ha informado sobre la difusión de varias proteínas de perlas de alginato, incluida la inmunoglobulina G (IgG), el fibrinógeno y la insulina. El aumento de la concentración de alginato en las perlas disminuye la velocidad de difusión de las proteínas desde el gel. Por lo tanto, para controlar sus propiedades fisicoquímicas, se han desarrollado varias estrategias para mejorar la eficiencia de la encapsulación. De esta forma, la incorporación de polímeros naturales adicionales, en combinación con alginato, podría controlar las propiedades fisicoquímicas de la matriz final y mejorar la eficiencia de encapsulación. Entre ellos, destaca la goma laca como una resina natural secretada por insectos

principalmente del sudeste asiático del género *Kerria*, siendo un polímero natural renovable, no tóxico, biodegradable y comercialmente disponible (Empresa NOVATEC). Consiste en una mezcla compleja de ácidos alifáticos y alicíclicos. Los componentes principales son el ácido aleurítico, así como los ácidos jalárico y shellólico. En los últimos años, el biopolímero de goma laca ha atraído un gran interés, desarrollar diferentes tipos de sistemas de encapsulación. Las experiencias han validado su incorporación como una capa externa adicional para recubrir las cápsulas. La combinación de alginato/goma laca se ha utilizado para fabricar perlas de aceite por extrusión por gelificación iónica. Sin embargo, aún no se ha utilizado para desarrollar microcápsulas mediante la técnica de encapsulación por extrusión por gelificación iónica para la protección de bioactivos hidrofílicos como el R-PE. Al respecto, en nuestro estudio proporcionó información sobre las condiciones del proceso para preparar perlas con un alto EE% de R-PE y la evolución bajo microcápsulas de digestión gastrointestinal *in vitro*. Las variables de proceso para el encapsulado de R-PE se obtuvieron utilizando un caudal de alimentación de 20 mL h<sup>-1</sup>, 5 cm de distancia y 5 gr L<sup>-1</sup> de CaCl<sub>2</sub>. La encapsulación en condiciones óptimas mostró un 97,5% mostrando una buena coincidencia con los valores predictivos de OTE (97%). Las perlas presentaban una forma semiesférica y estaban libres de poros con un tamaño de 1,2 mm. Sugerimos que el sistema de encapsulación de R-PE se pueda incorporar a una matriz alimentaria para aplicaciones nutraceuticas.

En relación al **capítulo 4** se desarrolla cómo es posible que los compuestos que acumulan las algas pueden ser realmente absorbidos al sistema gastrointestinal y finalmente otorgar el efecto terapéutico. En este sentido, las algas se comercializan cada vez más como "alimentos funcionales" o "nutraceuticos"; estos términos no tienen estatus legal en muchas naciones, pero describen alimentos que contienen compuestos bioactivos o fitoquímicos, que pueden beneficiar la salud, más allá del papel de la nutrición básica (por ejemplo, antiinflamatorios, prevención de enfermedades). Muchos estudios reportan el potencial nutricional o contenido

bioactivo de diferentes algas, pero pocos de ellos cuantifican la biodisponibilidad de nutrientes y fitoquímicos de los alimentos de algas. El concepto “biodisponibilidad”, fue definido por Carbonell-Capella et al., (2014) “como una combinación de bioactividad y bioaccesibilidad”, donde bioaccesibilidad se refiere a la liberación de la matriz alimentaria, transformaciones durante la digestión y transporte a través del epitelio digestivo, mientras que la bioactividad abarca la absorción en los tejidos, el metabolismo y los efectos fisiológicos. Debido a las dificultades, tanto prácticas como éticas, en términos de medir la bioactividad, la fracción de un determinado compuesto o su metabolito que llega a la circulación sistémica puede considerarse bioaccesible, pero no necesariamente bioactiva. La mayoría de las evaluaciones publicadas de la bioactividad de los alimentos de algas se basan en pruebas *in vitro* a corto plazo, utilizando extractos de algas que con frecuencia tienen una composición mal definida y baja pureza, por lo que una comprensión clara de su valor alimenticio es muy limitada. En particular, se revela una falta de información sobre el comportamiento de los componentes alimentarios de las algas en el intestino. De ese modo, la digestión se refiere a la degradación física y bioquímica de los alimentos y el contenido de nutrientes en preparación para la absorción en el cuerpo. La digestión comienza en la boca con la masticación, que reduce el tamaño de las partículas y mezcla los alimentos con la saliva. La enzima salival predominante es la alfa ( $\alpha$ )-amilasa, que es específica para los enlaces de glucosa  $\alpha(1\rightarrow4)$ , y la amilasa salival humana es más activa que la de otros primates. La pepsina y los pepsinógenos comienzan la digestión de proteínas en el estómago, con la ayuda del ácido clorhídrico que desnaturaliza las proteínas y libera nutrientes de la matriz alimentaria. Las lipasas producidas en la boca y el estómago inician el proceso de digestión de los triacilglicerolos. El páncreas descarga una mezcla de tripsina, quimotripsina, carboxipeptidasas,  $\alpha$ -amilasa, lipasa y otras enzimas que, respectivamente, digieren proteínas y péptidos, almidones, triacilglicerolos y otros compuestos en el intestino delgado. La mezcla de proteasas, amilasa y lipasa se conoce colectivamente

como pancreatina; La pancreatina porcina se utiliza a menudo como modelo de sistemas de digestión *in vitro* humanos modelo. Finalmente, la alta digestibilidad de la ficoeritrina permitiría una mayor absorción de la proteína, o de hecho, de sus aminoácidos o péptidos cortos. Debido a que las proteasas digestivas humanas tienen su especificidad por los enlaces cerca de ciertos aminoácidos, es importante verificar que las secuencias de proteínas de algas puedan ser digeridas por las proteasas humanas. La digestibilidad de las proteínas se puede evaluar simulando las condiciones gastrointestinales mediante protocolos estándar. Hay varios tipos de métodos de digestión *in vitro* que se usan comúnmente para alimentos; estos se pueden dividir en métodos estáticos y dinámicos. Estos modelos pretenden simular las condiciones fisiológicas del tracto gastrointestinal superior, es decir, las fases oral, gástrica y del intestino delgado. La mayoría de los modelos dinámicos han demostrado ser adecuados para simular la digestión de alimentos y productos farmacéuticos en diferentes grupos de población y para diferentes propósitos. Por ejemplo, para un método estático, Gajaria et al., (2017) y Kazir et al., (2019) encontraron una correlación entre el valor estándar de digestión de la proteína de caseína extraída y las actividades antioxidantes de la macroalga roja *Gracilaria* sp. Estos resultados indican que las proteínas de algas extraídas pueden ser hidrolizadas por enzimas digestivas, lo que puede aumentar la posibilidad de su absorción en el intestino con actividad biológica. para un método estático. Gajaria et al., (2017) y Kazir et al., (2019) encontraron una correlación entre el valor estándar de digestión de la proteína de caseína extraída y las actividades antioxidantes de la macroalga roja *Gracilaria* sp. Estos resultados indican que las proteínas de algas extraídas pueden ser hidrolizadas por enzimas digestivas, lo que puede aumentar la posibilidad de su absorción en el intestino con actividad biológica para un método estático.

En nuestro estudio, la digestión *in vitro* mostró que las perlas de alginato/goma laca tenían una biodisponibilidad 2,5 veces mayor que el extracto de R-PE no encapsulado en la digestión en

la etapa intestinal con una concentración de 0,31 mg de R-PE. Finalmente, el R-PE cargado en el encapsulado puede ser utilizado como un potencial sistema de liberación de extracto acuoso y dar una respuesta terapéutica de acuerdo a los valores de IC<sub>50</sub> (144 µg mL<sup>-1</sup>) encontrados para el R-PE para cáncer de colon.

El **capítulo 3** se enfoca en la reutilización de residuos mediante el concepto de biorefinería asociados a los procesos de extracción de la ficoeritrina. En general, la mayoría de los productos y subproductos de alimentos marinos se están convirtiendo y utilizando como alimentos funcionales valiosos a través del desarrollo reciente en la industria de bioprocesos marinos. Esto se debe a la presencia de compuestos bioactivos que son un poderoso antioxidante por naturaleza y se utilizan como alimentos funcionales y nutracéuticos donde dependen de los efectos fisiológicos.

El término 'nutracéutico', acuñado por la Fundación para la Innovación en Medicina, se refiere a cualquier sustancia que sea un alimento o parte de un alimento y proporcione beneficios médicos o de salud, incluida la prevención y el tratamiento de enfermedades. Un nutracéutico puede ser un nutriente natural, ya sea un producto aislado o purificado, generalmente presentado en forma medicinal o en una matriz no alimenticia, en forma de polvo o tableta, como suplementos dietéticos o productos a base de hierbas.

Muchos estudios se han dedicado al reconocimiento del potencial antioxidante de las proteínas naturales provenientes de algas debido a su actividad antioxidante de amplio espectro (atribuida a diversas cadenas laterales de aminoácidos), gran abundancia y fácil disponibilidad en la naturaleza. De hecho, se han aislado varios productos terapéuticos de algas de poblaciones tropicales y subtropicales y pocos de ellos han sido evaluados por su potencial anticancerígeno. Los efectos preventivos del cáncer de la clorofila *a* y sus derivados se han estudiado ampliamente, con especial énfasis en su efecto antimutagénico *in vitro* contra numerosos

mutágenos dietéticos y ambientales. Varios estudios han utilizado ensayos de mutagenicidad bacteriana. Respectivamente, Los pigmentos marinos derivados de algas también se han investigado con respecto a su actividad antimutagénica/antigenotóxica. luteína,β-caroteno y clorofila aislados del alga roja *Porphyra tenera* han demostrado actividad antimutagénica en bacterias *Salmonella typhimurium*. Se han publicado interesantes estudios de investigación sobre los carotenoides y sus cualidades anticancerígenas. Ishikawa et al., (2008) demostraron los efectos de la fucoxantina y su metabolito desacetilado, el fucoxantínol, contra la leucemia de células T adultas. Las actividades inhibitorias de fucoxantina y fucoxantínol fueron más fuertes que las deβ-caroteno y astaxantina. La leucemia de células T del adulto es una neoplasia maligna mortal de los linfocitos T causada por la infección por el virus de la leucemia de células T humana tipo 1 y sigue siendo curable. Por lo tanto, los carotenoides podrían ser agentes terapéuticos potencialmente útiles para pacientes adultos con leucemia de células T. En el caso de la fucoxantina, se redujo notablemente la viabilidad de las líneas celulares de cáncer de colon humano y el tratamiento con fucoxantina indujo la fragmentación del ADN. La exposición a la fucoxantina disminuyó el nivel de la proteína supresora de la apoptosis (Bcl-2), lo que sugiere que el mecanismo anticancerígeno de la fucoxantina produce un mecanismo de apoptosis. También se ha observado el efecto inductor de apoptosis de la fucoxantina en líneas celulares de cáncer de próstata humano (PC-3, DU-145 y LNCaP) (Kotake et al., 2001). Mientras tanto, el efecto antiproliferativo y la inducción de apoptosis por fucoxantina en células de cáncer de colon humano (Caco-2, HT-29 y DLD-1) fueron observados por Hosokawa et al., (2004). Además, también demostraron el efecto antiinflamatorio de la fucoxantina aislada de las líneas celulares RAW 264.7 estimuladas con LPS de *Myagropsis myagroidesin*.

Por otro lado, se encontraron fracciones efectivas de polisacáridos principalmente en cianobacterias, aunque recientemente se ha demostrado el potencial de compuestos de macroalgas rojas y verdes como potentes agentes inmunomoduladores. Además, los



fotoprotectores UV, los aminoácidos tipo micospolina (MAAs), extraídos principalmente de algas rojas, también presentan actividad inmunológica.

Las ficobiliproteínas de algas adquieren una gran importancia debido a sus propiedades inmunopotenciadoras, antiinflamatorias, anticancerígenas, antioxidantes y nutricionales, y estas propiedades podrían proporcionar un avance vital en la investigación del cáncer. La ficoeritrina contiene grupos prostéticos llamados bilinas, útiles para la prevención y tratamiento de enfermedades causadas por daño oxidativo como el cáncer. Además, la estabilidad de su estructura y la linealidad de sus grupos cromóforos son las que le confieren sus propiedades saludables, de forma que cuanto más estable se comporta la molécula, mayor es el abanico de aplicaciones biotecnológicas que se le pueden atribuir. Recientemente, Senthilkumar et al., (2018) han demostrado el efecto anticancerígeno de la R-PE obtenida de la macroalga *Portieria hornemannii* contra la línea celular HepG2. Otro estudio informó una formulación nanoteranóstica que utiliza R-PE como molécula terapéutica y de diagnóstico dirigida a las células de cáncer de mama triple negativas. Sin embargo, los informes sobre los efectos hepatoprotectores de la R-PE son escasos, especialmente en modelos animales. Estudios previos indicaron que tanto la ficocianina como la ficoeritrina son posibles eliminadores de radicales libres. La ficobiliproteína posee actividad eliminadora de radicales hidroxilo y peroxilo tanto en modelos *in vitro* como *in vivo*. Del mismo modo, que R-PE tenía la capacidad de eliminar los radicales libres, incluidos, superóxido y óxido nítrico y radicales hidroxilo además de mostrar actividad antiperoxidativa de lípidos *in vivo*. Sin embargo, aún no se han evaluado los informes de los efectos anticancerígenos del R-PE encapsulado, lo que podría mejorar el efecto terapéutico con la liberación controlada. Al respecto, los compuestos encontrados en el residuo, permiten concluir que los dos polisacáridos sulfatados extraídos de las algas rojas *S. skottsbergii* después de la extracción previa de ficoeritrina por homogeneización a alta presión (extracción asistida por HPH) después de un enfoque de

biorrefinería exhibieron actividades antioxidantes, antitumorales y se observaron relaciones dosis-efecto. Específicamente, el polisacárido ácido con alto contenido de sulfato y galactosa mostró la mayor actividad en los ensayos de barrido de radicales en el ensayo de radicales ABTS, es decir, una tasa de barrido de radicales del 20% a la concentración entre 300-500  $\mu\text{g mL}^{-1}$ . La actividad antitumoral de la fracción ácida fue significativamente mayor en todas las líneas celulares de cáncer analizadas que la de la fracción neutra. Sin embargo, la fracción neutra con el contenido más bajo de sulfato y galactosa exhibió una actividad de nivel medio en el ensayo de barrido de radicales, pero tuvo actividades antitumorales más altas contra las células cancerosas de melanoma G-361 con un alto índice selectivo de 14.22 y baja toxicidad en células sanas de fibroblastos. Las fracciones de polisacáridos recuperadas de un bioproceso sobrenadante como biocompuestos antitumorales y antioxidantes podrían aplicarse en las industrias cosmecéutica y alimentaria.

El **capítulo 5** se enfoca en la producción, disponibilidad y accesibilidad sean eficientes a partir de una materia prima producida de manera sostenible, siendo este el pilar básico de la biorrefinería de algas marinas. Sin embargo, la biodisponibilidad del recurso en el medio ambiente es finita. La explotación actual del recurso algal es un cuello de botella para el proceso que está afectando a la biodiversidad marina (incluidas otras especies de algas, peces e invertebrados). Por lo tanto, los sistemas de cultivo eficientes combinan la producción de materia prima de biorrefinería de algas de alta calidad con una contribución a la mitigación del cambio climático. Esto se puede lograr mediante el fortalecimiento de la capacidad marina para la captura de  $\text{CO}_2$ , mientras que el cultivo de algas marinas en sistemas de cultivo contribuye a la economía circular.

Se hace referencia a la economía circular para resaltar la sostenibilidad del cultivo de algas marinas al ofrecer una mayor eficiencia en la valorización de los recursos (economía) y la mitigación del cambio climático (medio ambiente). Por lo tanto, para mejorar el rendimiento

de biomasa y metabolitos, es necesario aumentar la eficiencia fotosintética y la optimización de la absorción de luz mediante el ajuste del aparato captador de luz para lograr un equilibrio óptimo de fotosíntesis/fotoprotección, en lugar de simplemente maximizar la absorción de luz del espectro de luz fotosintético activo. (PAR) entre 400-700 nm.

Según sus diferencias de pigmentación en general, las algas se clasifican en tres filos principales: Rhodophyta (macroalgas rojas), Chlorophyta (macroalgas verdes) y Phaeophyta (macroalgas marrones). La existencia de los diversos fitopigmentos en las macroalgas se ve afectada por su hábitat marino. En consecuencia, debido a que las macroalgas verdes tienen la capacidad de absorber grandes cantidades de energía luminosa, son abundantes en las aguas costeras, mientras que las macroalgas marrones y rojas se pueden encontrar a mayores profundidades donde la penetración de la luz solar está restringida. En los organismos fotosintéticos, la luz se puede utilizar como fuente de información ambiental para controlar procesos metabólicos como el crecimiento, la reproducción y la morfogénesis.

Las microalgas duplican su biomasa celular en menos de 1 día y pueden crecer 100 veces más rápido que las plantas terrestres. Las microalgas pueden alcanzar productividades de 40 a 50 g de peso seco (PD)  $m^{-2} d^{-1}$ . Desempeñan un papel importante en la fijación de  $CO_2$  debido a su capacidad para utilizar  $CO_2$  de 10 a 50 veces más eficientemente que las plantas, convirtiendo la energía solar en energía química. Ciertas especies de macroalgas presentan una alta tasa de crecimiento en tanques bajo acuicultura multitrófica integrada, es decir, 10-14%  $d^{-1}$  (*Ulva* spp), 10-16%  $d^{-1}$  (*Porphyra* spp.), 3,5%  $d^{-1}$  (*Undaria pinnatifida*) o 6,7%  $d^{-1}$  (*Gracilariopsis longissima*) (Pérez Lloréns et al., 2016). La productividad en macroalgaje cultivado en tanques puede alcanzar valores de 21-20 g PS  $m^{-2} d^{-1}$  en *Gracilaria* spp.

Además de la irradiación, la calidad de la luz tiene un efecto sobre la composición bioquímica y el crecimiento, ya que los fotorreceptores de las algas son responsables de todas las reacciones

dependientes de la luz, y los cambios en las condiciones de luz conducen a la aclimatación cromática. Las algas necesitan fotorreceptores para su desarrollo general, como es el caso de las plantas, para el cambio entre las diferentes etapas del ciclo de vida, para controlar el aparato fotosintético y para orientarse durante sus etapas de vida móviles. Solo cinco tipos principales de fotorreceptores sensoriales (proteínas BLUF, criptocromos, fototropina, fitocromos y rodopsinas) se utilizan en la naturaleza para regular los procesos metabólicos. López-Figueroa et al., (1990) detectaron dominios conservados en proteínas similares a fitocromos entre algas verdes y rojas contra plantas superiores etioladas, a saber, la región del N-terminal (anticuerpos Z2B3 y Z4BS). Sin embargo, las algas pardas no coinciden con las que se encuentran en la región N-terminal del fitocromo. Lamparter (2004) mencionó que durante la evolución de los fitocromos de plantas y cianobacterias, el sitio de unión del cromóforo ha cambiado de una cisteína cercana al extremo N-terminal de la proteína, el sitio de unión de la biliverdina, a una cisteína que se encuentra dentro del llamado dominio GAF. y sirve como sitio de unión de fitocromobilina o ficocianobilina. Mientras que Rockweel et al., (2014) demuestran que los fitocromos de algas no se limitan a las respuestas de rojo y rojo lejano. En cambio, diferentes fitocromos de algas pueden detectar la luz naranja, verde e incluso azul. algas pardas no coinciden encontradas en la región N-terminal del fitocromo.

Entonces, los organismos pueden cambiar su composición de pigmentos y obtener una ventaja en diferentes ambientes, y el pigmento responsable de la recolección de la luz incidente se volverá predominante. La fotosíntesis requiere el pigmento de reacción central clorofila-a; pigmentos accesorios (ficoeritrina, ficocianina y aloficocianina), clorofila b, c y d; y carotenoides, que ayudan a ampliar el rango de absorción de la luz. Las longitudes de onda azul y roja son las principales bandas de absorción de todas las clorofilas. Los nuevos desarrollos en los sistemas de producción buscan aumentar la disponibilidad de luz y la eficacia para la producción de biomasa de microalgas y pigmentos fotosintéticos y macroalgas, y dichos

cambios se pueden realizar en términos de distribución de luz, intensidad y/o fuente. Se pueden usar espectros de pico estrecho para actuar directamente sobre la fotorrespuesta del organismo. La ventaja de complementar la luz es la posibilidad de mantener el metabolismo fotosintético en su nivel óptimo mientras se activan otras vías a través de varias respuestas fotomorfogénicas. Por ejemplo, el uso de luz blanca con luz roja suplementada aumentó la producción de lípidos en la microalga *Ettlia oleoabundans*. La ventaja de complementar la luz es la posibilidad de mantener el metabolismo fotosintético en su punto óptimo mientras se activan otras vías a través de diversas respuestas fotomorfogénicas. Se han observado resultados similares en macroalgas.

Al usar LED azules y rojos mixtos, la producción de biomasa celular fue a menudo más alta que la obtenida usando solo LED rojos. Sin embargo, aún no se ha determinado una relación de mezcla óptima para la máxima producción de biomasa celular porque la captura de fotones por la clorofila de las algas depende de múltiples factores, incluida la arquitectura celular, la composición de los pigmentos y la disposición de los cloroplastos. Las bombillas de luz incandescente producen principalmente luz amarilla, naranja o roja. Las bombillas fluorescentes estándar de "blanco frío" emiten principalmente una luz de color amarillo verdoso. Las lámparas de vapor de sodio de baja presión (lámparas SOX), que emiten principalmente a 589 nm, son fuentes eficientes de PAR, que emiten niveles relativamente bajos de radiación infrarroja (IR) y calor. La tasa de crecimiento y la actividad fotosintética fueron óptimas bajo SOX en las macroalgas rojas. Las microalgas producen un importante metabolito intracelular en respuesta a condiciones de estrés lumínico. Según las respuestas de las microalgas, las longitudes de onda específicas mejorarán la productividad de productos intracelulares específicos con luz artificial. Luz amarilla (SOX) es posible obtener la saturación de la fotosíntesis en una banda de longitud de onda sin ningún fotorreceptor fotomorfogénico conocido y sin interferencia con otros fotorreceptores no fotosintéticos conocidos en las

longitudes de onda de luz azul, verde o roja y la radiación UV, lo que lleva a la acumulación de compuestos a través de vías no fotosintéticas.

Por tanto, los retos de este trabajo son (i) optimizar la extracción respetuosa con el medio ambiente por UAE y HPH, el fraccionamiento por matriz de disolventes acuosos y los procesos de purificación para concentrar el R-PE de forma rápida y no agresiva; (ii) desarrollar una formulación novedosa basada en alginato-goma laca para proteger el R-PE y (iii) mantener los efectos biológicos con liberación controlada a nivel gastrointestinal para el desarrollo de ingredientes no tóxicos a base de algas para alimentos funcionales y aplicaciones nutracéuticas.

Además, el abastecimiento de materia prima será un punto crítico donde será necesario realizar estudios para un desarrollo sustentable del proceso, evitando la extracción de bancos naturales y sus efectos negativos. Para ello se han realizado evaluaciones en base a la intensidad y calidad de la luz, con el fin de estimular el crecimiento y compuestos bioactivos como el R-PE en el alga roja *Porphyridium cruentum*. Al respecto, hemos reportamos en nuestro, por primera vez para el período experimental, la factibilidad de usar luz SOX (luz amarilla) como luz fotosintética a irradiancia saturada de la actividad de fotosíntesis sin reducir la concentración de biomasa de *P. cruentum*. Este estudio demuestra que la luz amarilla con la incidencia de la luz azul es un factor interesante en el cultivo de microalgas rojas, para mejorar los compuestos de alta calidad y mantener estable la productividad de la biomasa. A pesar de que comparamos solo una pequeña cantidad de factores en un rango muy estrecho, los datos muestran que *P. cruentum* tiene un gran potencial para la producción de pigmento de ficoeritrina para colorantes naturales comerciales o proteínas para diferentes mercados, como piensos/alimentos. Se propone el uso de luz SOX o filtros de color amarillo con suplemento de luz azul en la nueva generación de tecnología de fotobiorreactores para cultivar especies de algas rojas con el objetivo de mejorar la calidad de la producción de ficoeritrina.

## TABLE OF CONTENTS

|  |    |
|--|----|
| Agradecimientos / Acknowledgements   | 4  |
| Summary  | 6  |
| Resumen  | 8  |
| List of Tables   | 29 |
| List of Figures  | 30 |
| <b>CHAPTER I. General Introduction</b>   | 32 |
| 1.1 Introduction   | 33 |
| 1.2 Hypothesis   | 52 |
| 1.3 General objective  | 52 |
| 1.4 Specific objectives  | 53 |
| <b>CHAPTER II. Title <i>Highly efficient water-based extraction of biliprotein R-Phycoerythrin from marine the red macroalga <i>Sarcopeltis skottsbergii</i> by ultrasound and high-pressure homogenization methods.</i></b> | 54 |
| Introduction   | 57 |
| Materials and methods  | 60 |
| Optimization by High pressure homogenization method  | 71 |
| Optimization by Ultrasound method  | 72 |
| Antioxidant activities and pigments quantification   | 76 |
| Discussion   | 80 |
| <b>CHAPTER III. <i>A sequential recovery extraction and biological activity of water-soluble sulfated polysaccharides from the polar red macroalgae <i>Sarcopeltis skottsbergii</i></i></b>                                  | 90 |
| Introduction   | 93 |
| Materials and methods  | 96 |

|   |     |
|---|-----|
| Extraction of Polysaccharides (neutral and acid fractions)  | 97  |
| Chemical characterization of polysaccharides  | 98  |
| Antioxidant and biological activities of polysaccharides on cell lines  | 99  |
| Discussion  | 107 |
| <b>CHAPTER IV. <i>High R-phycoerythrin bioavailability through alginate/shellac beads with enhanced antiproliferative activity.</i></b>               | 118 |
| Introduction  | 121 |
| Material and methods  | 125 |
| Optimization of the encapsulation of R-PE by ionic gelation   | 126 |
| Characterization of the beads   | 127 |
| Bioaccessibility and bioavailability of R-PE during in vitro digestion assay by dynamic gastrointestinal model SIMUGIT.                               | 128 |
| Discussion  | 142 |
| <b>CHAPTER V. <i>Photobiological effects on biochemical composition in Porphyridium cruentum (Rhodophyta) with a biotechnological application</i></b> | 131 |
| Introduction  | 148 |
| Materials and methods   | 155 |
| Photosynthetic variables respect to the fluorescence in Chlorophyll a   | 157 |
| Effect of quality of light on growth and accumulation of bio-compounds  | 167 |
| Discussion  | 169 |
| <b>CHAPTER VI. <i>General discussion, conclusions and future perspectives</i></b>   | 178 |
| 4.1 General discussion  | 179 |
| 4.2 General conclusions/Conclusiones generales  | 189 |
| 4.3 Future perspectives   | 193 |
| <b>CHAPTER VII. List of Appendices</b>  | 196 |



## LIST OF TABLES

|   |     |
|---|-----|
| Table I.2 Central composite design for ultrasound-assisted method and yield (YPE) results from response surface method analysis.....  | 45  |
| Table II.2 Central composite design for high-pressure homogenization-assisted method and yield (YPE) from response surface method analysis.....   | 46  |
| Table III.2 Characteristics of extracts obtained under selected conditions for ultrasonication (US) and high-pressure homogenization (HPH) methods.....   | 61  |
| Table IV.2 . Pigment composition (phycoerythrin content, chlorophyll <i>a</i> and total carotenoids of the aqueous extract of <i>S. skottsbergii</i> under selected conditions for ultrasound (US) and high-pressure homogenization (HPH).....  | 62  |
| Table I.3 Total carbon (C), nitrogen (N), ratio C/N, hydrogen (H) and sulfur (S) (%) obtained in the biomass and polysaccharides (neutral and acid) from <i>Sarcopeltis skottsbergii</i> . ....   | 87  |
| Table II.3 Content of monosaccharides in neutral and acid polysaccharide analyzed by gas-liquid chromatography-mass spectrometry (GC-MS).....   | 87  |
| Table III.3 Cytotoxicity index (IC <sub>50</sub> ) and selective index (SI) for different fractions of polysaccharides in the different cell lines : 1064 sK (human gingival fibroblasts cell line), HCT-116 (human colon cancer), G-361 (human melanoma cancer), U-937 (human leukemia cancer).....                            | 90  |
| Table I.4 Encapsulation efficiency of R-PE, sphericity factor, and particle size using the orthogonal matrix L <sub>4</sub> (2 <sup>3</sup> ) .....   | 120 |
| Table II.4 Cytotoxicity index (IC <sub>50</sub> ) and selective index (SI) for R-PE encapsulate and non-encapsulate on the different cell lines : 1064 sK (human gingival fibroblasts cell line), HCT-116 (human colon cancer), G-361 (human melanoma), U-937 (human leukemia).....   | 125 |
| Table I.5 Parameters of growth (maximum cell density (N <sub>max</sub> ), maximum growth rate (k <sub>max</sub> ), dry weight (per culture volume) and biomass productivity (mg ml <sup>-1</sup> day <sup>-1</sup> ) obtained in one-liter batch regime under five different combined treatments of light in a harvest day..... | 150 |
| Table II.5 Biochemical composition (soluble proteins, biliproteins content, total carbohydrates, and antioxidant activity) of the biomass of <i>Porphyridium cruentum</i> grown in one-liter batch regime under five different combined treatments of light sources and quality.....  | 151 |
| Table III.5 Total lipids and fatty acids composition of <i>Porphyridium cruentum</i> in one-liter batch regime under five treatments of light. Values are expressed as % total lipids and fatty acids by dry biomass.....   | 152 |

## LIST OF FIGURES

|   |     |
|---|-----|
| Figure I.1 Utilization of seaweed and seaweed-derived components in food and non food applications.....   | 17  |
| Figure II.1 Frontiers in functional foods (adapted from Doyon and Labrecque, 2008) .....  | 27  |
| Figure III.1 Flow diagram of the application of the photobiology for biotechnology applications.....  | 33  |
| Figure I.2 Summarizing scheme of the procedure for the extraction of R-Phycoerythrin from <i>S. skottsbergii</i> . *RSM Optimization.....   | 48  |
| Figure II.2 Response surface (3D) plots to illustrate the effect between the amplitude wave ( $X_1$ ) and ultrasonic time ( $X_2$ ) by solvent extraction on the extraction yield: a) effect between $X_1$ and $X_2$ under phosphate buffer, b) effect between $X_1$ and $X_2$ under distilled water. ....  | 57  |
| Figure III.2 Response surface (3D) plots to display the effect between the pressure ( $X_1$ ) and passes ( $X_2$ ) by solvent extraction on the extraction yield: A) effect between $X_1$ and $X_2$ under phosphate buffer, B) effect between $X_1$ and $X_2$ under distilled water.....  | 58  |
| Figure IV.2 Total antioxidant activities (ORAC and DPPH) of the aqueous extract of <i>S. skottsbergii</i> under selected conditions for ultrasound-assisted extraction (UAE) and high-pressure homogenization (HPH).....  | 67  |
| Figure V.2 Principal component analysis to pigments quantification and antioxidant activity in <i>S. skottsbergii</i> with respect to the extraction methods.....   | 69  |
| Figure I.3 Schematic representation of the biorefinery concept for the recovery of the neutral and acid polysaccharides.....  | 81  |
| Figure II.3 FTIR spectra of the neutral and acid polysaccharides.....   | 92  |
| Figure III.3 Scavenging effects % of the sample of biomass, neutral and acid fractions in ABTS radical from <i>S. skottsbergii</i> .....  | 93  |
| Figure IV.3 Survival (%) of cell lines exposed to different concentrations of neutral polysaccharides. (A) Survival (%) of HTC-116 cell line; (B) Survival (%) of U-937 cell line; (C) Survival (%) of G-361 cell line.....   | 97  |
| Figure V.3 Survival (%) of cell lines exposed to different concentrations of acid polysaccharides. (A) Survival (%) of HTC-116 cell line; (B) Survival (%) of U-937 cell line; (C) Survival (%) of G-361 cell line.....   | 98  |
| Figure I.4 Process and work conditions to form alginate/shellac beads and <i>in vitro</i> digestion simulating analysis. * Taguchi experimental design: Independent variables and two levels of work.....   | 107 |
| Figure II.4 Flow diagram of the dynamic <i>in-vitro</i> Gastrointestinal-Tract-Simulating Membrane Bioreactor (SimuGIT). ....   | 116 |
| Figure III.4 Confocal microscopic for 1) design point N°1 (97.5%EE) and 2) presence of R-phycoerythrin by fluorescence.....   | 118 |
| Figure IV.4 Morphology of the beads by scanning microscopy (SEM) for a) design point N°1, b) design point N°4 and c) magnification of 500X for the surface of the beads of the design point N°4.....  | 119 |
| Figure V.4 Bioaccessibility (%) of R-PE extract and encapsulates during <i>in vitro</i> gastrointestinal digestion.....   | 121 |
| Figure VI.4 Bioavailability (%) of R-PE extract and encapsulates during <i>in vitro</i> gastrointestinal digestion.....   | 122 |
| Figure VII.4 Sodium dodecyl sulphate polyacrylamide gel electrophoresis (SDS-PAGE) profile of R-PE encapsulated from different stage <i>in vitro</i> simulated digestion (simuGIT). 50µg of protein were loaded into the corresponding lane. MW: Molecular weight marker; D:Duodenn; RS30': Retentate streams at 30min; RS180': Retentate streams at 180min; PS30': Permeate streams at 30min; PS180': Permeate streams at 180min; M:mouth; S: Stomach..... | 123 |
| Figure VIII.4 R-PE release from alginate/shellac capsules during 250min at different pH-values.....   | 124 |
| Figure I.5 Principal Components diagram in relation to physiological responses in <i>Porphyridium cruentum</i> culture at the end of the experimental period respect to the light treatments.....   | 146 |

|   |     |
|---|-----|
| Figure II.5 Maximal quantum yield ( $F_v/F_m$ ) in <i>Porphyridium cruentum</i> in function of time and qualities of lights interactions, for the next treatments.....                              | 147 |
| Figure III.5 Photosynthetic efficiency ( $\alpha_{ETR}$ ) in <i>Porphyridium cruentum</i> in function of the time and qualities of lights interactions ( $p < 0.05$ ), for the next treatments..... | 148 |
| Figure IV.5 Maximal electron transport rate ( $ETR_{max}$ ) or productivity in the culture for <i>Porphyridium cruentum</i> culture for the time and qualities of lights interactions.....          | 148 |
| Figure V.5 Maximal non-photochemical quenching ( $NPQ_{max}$ ) or photoprotective indicator in the culture of <i>Porphyridium cruentum</i> , under time and qualities of lights interactions.....   | 149 |
| Figure I.6 Schematic of general blue bioprocess from <i>Sarcopeltis skottsbergii</i> .....  | 165 |
| Figure II.6 Schematic of general upstream and downstream blue bioprocess proposal for future applications from red algae (Macro and microalgae).....  | 178 |

---

# CHAPTER I:

## General introduction

---

## CHAPTER I: General introduction

Substantial research efforts are being focused on the identification and characterization of functional food ingredients that might prevent chronic disease or optimize health, a trend supported by growing consumer demand. The marine ecosystem has the potential to supply high added-value ingredients that exhibit multiple activities, and algae are promising organisms for providing both essential compounds for human nutrition and novel bioactive substances with medicinal and pharmaceutical value (Smit, 2004), suited for developing functional foods (Holdt and Kraan, 2011).

The complex algal composition and the presence of valuable chemical fractions support the rational and integral utilization of algae as a primary biomass feedstock, in the same way as terrestrial biomass from forest or agricultural origin. The possibility of obtaining a range of products from algal biomass involving environmentally friendly technologies conforms to a sustainable approach fitting into the concept of biorefinery. Knowledge of composition, functionality and bioactivity is essential for the future development of multi-step, multi-purpose processes to enable rational exploitation of algae (Figure I.1).

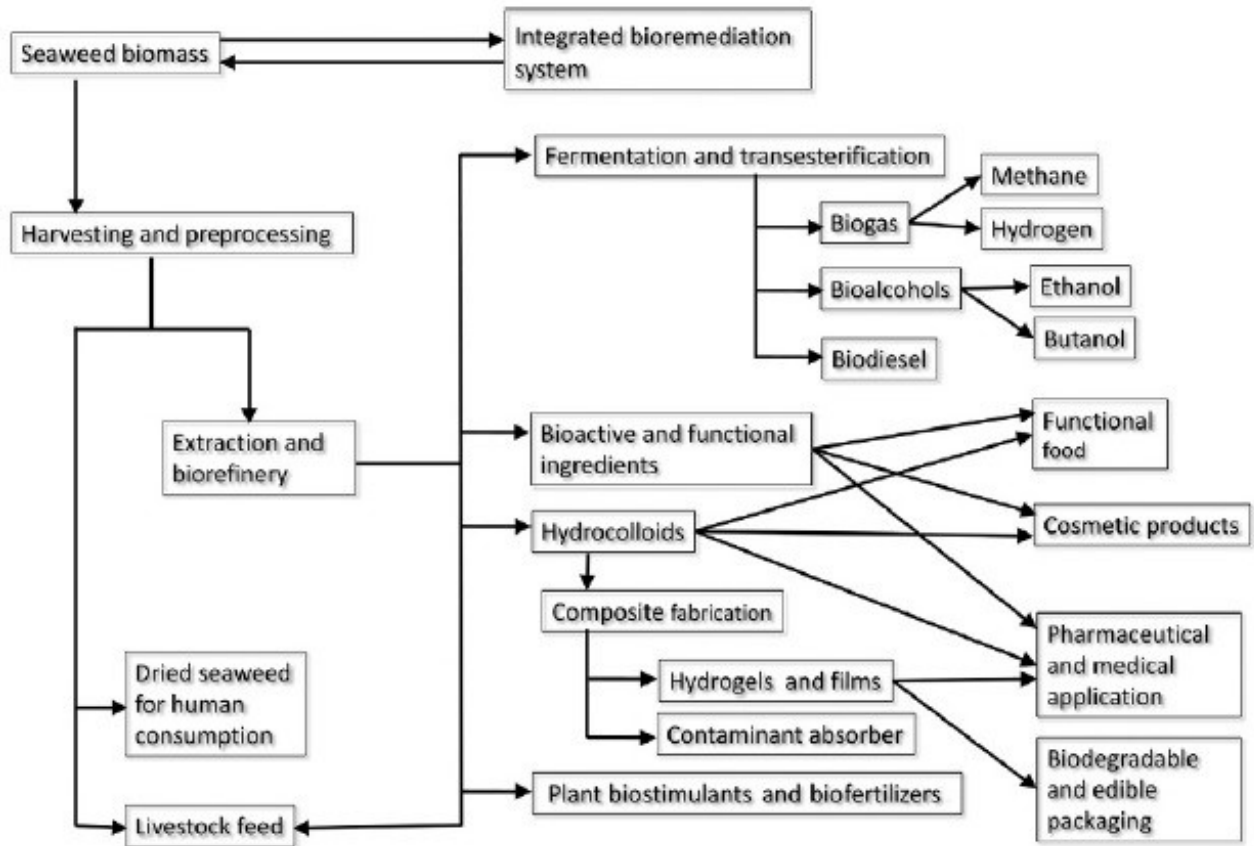


Figure I.1. Utilization of seaweed and seaweed-derived components in food and non food applications. (Lange et al., 2020).

Therefore, this proposal seeks to develop specialized ingredients from vegetal origin based on phycoerythrin-enriched extracts with red coloration from macroalgae. This is a phycobilinic pigment, hydrophilic and protein based compound, which has proven healthy activities such as antioxidant, stimulator of the immune system, anti-inflammatory, antiviral, hepatoprotective and anticarcinogenic) (Soni et al., 2009, Dominguez, 2013; Thangam et al., 2015; Senthilkumar et al., 2013, 2018). Phycobiliproteins are water-soluble pigments found in the cytoplasm or in the stroma of the chloroplast. Red micro and macroalgae, Cyanobacteria and Cryptophyta are the only source for reddish-red pigment, phycoerythrin, which acts as the major light-harvesting pigment, and their main function is to trap light energy between 495 and 650 nm wavelengths and transfer it to Phycocyanin, allophycocyanin and finally to chlorophyll a (P680) of the photosynthetic reaction center of Photosystem II. *Sarcopeltis skottsbergii* is a phycoerythrin-producing species, endemic to the South America (Buschmann et al., 2008). The

Antarctic Peninsula (63° 23'S) (Westernmeyer and Ramírez, 1978) from the Magallanes Region is the main producer of *S. skottsbergii* biomass of the country, with the production of near twenty thousand tons of dry alga. The valuation of phycoerythrin in a model of biorefinery is still incipient in algal biotechnology area and thus have great prospects in the food, pharmaceutical, cosmeceutical, and nutraceutical industries (Huang et al., 2021). However, the application of R-Phycoerythrin as a bioactive compound in dietary matrices could lead to problems of production and stability, caused by aggressive technology extraction conditions and environmental factors such as light, temperature and humidity, causing its degradation, generating products of poor quality, with reduced health-promoting properties (Torres et al., 2019), that is why as stabilization strategy to maintain its healthy properties it is protection through encapsulation will be used.

### **Extraction and separation of algae compounds**

In recent years, marine algae have served as important sources of bioactive natural substances. Moreover, many metabolites isolated (e.g. proteins, lipids, polysaccharides, etc) from marine algae have been shown to possess biological activities and potential health benefits. Therefore, a new trend to isolate and identify bioactive compounds and constituents from marine algae has emerged. One particular interesting feature in marine algae is their richness in natural pigments (NPs). Therefore, many natural pigments, such as phycobiliproteins as phycoerythrin isolated from marine algae have attracted much attention in the fields of food, cosmetic and pharmacology. Novel extraction and separation techniques with focus on hydrophilic compounds its necessary evaluate and improve the extraction yields, reduce processing time and reduce environmental damage caused by toxic solvents (Mittal et al., 2017)

Extraction technologies, especially those considered as clean processes such as methods involving water extraction have gained attention to explore marine resources for obtaining functional ingredients. As previously mentioned, phycobiliproteins are the important classes of proteins present in micro- as well as macroalgae. Marine proteins can provide numerous advantages over traditional enzymes used in food processing due to their activity and stability under unusual and extreme reaction conditions (Ciko et al., 2018). As the phycobiliproteins are intracellular, cell disruption is required for their efficient release during extraction. There are several methods available for extraction of phycobilins such as osmotic shock (Kawsar et al., 2011), maceration in the presence of liquid nitrogen in phosphate buffer (Munier et al., 2014), freeze grinding (Galland-Irmouli et al., 2000), freezing and thawing (Senthilkumar et al., 2013), ultrasonication (US) (Le Guillard et al., 2015), and homogenization (Pereira et al., 2020). However, these methods are reported for characterization and physicochemical analysis of phycobiliproteins and they are not with the purpose of downstream processing. According to Jacotet-Navarro et al., (2016) the objective of the green extraction processes is to achieve a faster extraction rate, more effective use of energy, increased mass and heat transfer, reduced equipment size, a reduction in the number of processing steps and no bioactive damage. The application of these technologies is also intended to preserve the natural environment and its resources (Silva et al., 2016). Being green technology, US has attracted the attention of researchers for its application in food and allied industries (Chemat et al., 2017). US acts by creating compression and decompression through sound waves at frequency  $>20$  kHz. Several mechanisms for the action of ultrasound have been identified, which include fragmentation, erosion, sonocapillary effect, sonoporation, local shear stress and destruction-detexturation of plant cell wall matrix (Chemat et al., 2017). An overall effect of these mechanisms, results in disruption of cell-wall. However, the relative extent of contribution of a given mechanism may vary with the type of biomass and process parameters.



By employing US, higher extraction yields can be achieved at low process time (Youssouf et al., 2017) and often at low temperatures and hence more suitable for thermolabile compounds (Pereira et al., 2020). In ultrasound assisted extraction processes, higher yields (>70%) were observed for biomolecules such as carotenoids from pomegranate waste (Goula et al., 2017), lipids from microalgae (Guldhe et al., 2014) and anthocyanins from blueberry (Yang et al., 2022). Further, US has advantage of direct scalability due to its ability of generate progressively high intensity cavitation zones and therefore suitable for scale-up of the industrial process (Torres et al., 2021).

Extraction using ultrasound can be coupled with other techniques such as extraction heat-reflux, high pressure treatment, supercritical CO<sub>2</sub>, and microwave in order to extract and no damage to bioactive compounds. In a recent review by (Yi et al., 2019) high pressure treatment, that is considered one of the greenest technologies, showed a considerably shorter extraction time and higher yield compared to other conventional techniques. Moreover, the use of mild temperatures makes this process especially attractive in the extraction of thermosensitive bioactive compounds. In other report, Yang and Wei (2015) developed an efficient method to extract bioactive compounds from the plant *Rabdosia rubescens* by combining heat reflux extraction (conventional, solvent: ethanol) and ultrasound-assisted extraction (40 kHz frequency and power of 185 W, with agitation). The authors concluded that the combination of extraction techniques reduced the processing time and increased the extraction yield of bioactive compounds. Therefore, it is important to integrate emerging and green technologies such as UAE or HPH to make better use of a highly abundant marine biomass like macroalgae.

Nevertheless, after R-phycoerythrin extraction, protein extract has to be concentrated and pre purified, which is generally expensive and requires many stages. Among the separation methods of concentrate, the membrane technology has a focus on the use of a semi-permeable

membrane to separate a liquid into two different fractions by selectively allowing some compounds to pass through while impeding other compounds, typically based on molecular weight. Membrane technologies are promising alternative methods to concentrate on algal proteins, as well as testing novel techno-functional and bioactive ingredients. They have the advantage of being non-thermal and environmentally-friendly separation method (Kumar et al., 2013). The most commonly used membrane technologies include microfiltration, ultrafiltration, nanofiltration, and reverse osmosis.

Disruption of the tough cell wall is a critical step required in order to increase the availability of algal proteins for extraction (Barba et al., 2015). Membrane technologies are well suited to use with seaweed as part of a biorefinery process to maximize valorization of all components within algae while avoiding the presence of heavy metals in the final product (Yaich et al., 2011). A combination of membrane technologies could be used to isolate algal proteins using the same principles of molecular weight cut-offs used in the dairy industry. In the dairy industry, microfiltration (MF) is used to extend the shelf-life of milk without any thermal treatment by removing microorganisms, while preserving overall taste and sensory attributes. MF could be used to remove algae cell wall components and bacteria with a molecular weight greater than 200 kDa. Ultrafiltration (UF) could then be used to isolate proteins and other macromolecules between 1 and 200 kDa, similar to the way it is used in the dairy industry to generate enriched fractions less than 10, 5, 3 and 1 kDa. Nanofiltration (NF) could then be used to remove monovalent salts to minimize osmotic pressure, followed by reverse osmosis (RO) to reduce fluid volume (Kumar et al., 2013). Indeed, membrane technologies have already been used to isolate whole microalgae cells and several seaweed components. Tangential flow microfiltration was reported as an efficient method for recovering 70%–89% of algal biomass from wastewater treatments (Petruševski et al., 1995). UF was previously used in conjunction with supercritical CO<sub>2</sub> extraction and ultrasound to

isolate polysaccharides from the macroalgae *Sargassum pallidum* (Ye et al., 2008; 2009). Polysaccharides with antioxidant activities were isolated from green macroalgae *Ulva fasciata* utilizing hot water extraction followed by several stages of UF with increasingly smaller pore sizes (Shao et al., 2013). Furthermore, UF was used to isolate phycoerythrin protein from macroalgae *Grateloupia turuturu* following cell homogenization, which was reported to retain 100% of the protein without denaturation (Denis et al., 2009). Alternatively, a two-stage UF could be applied for algal protein enrichment, as demonstrated by the separation of polysaccharide components in the microalgae *Tetraselmis suecica* using HPH followed by UF separate in membranes with different pore size (Safi et al., 2013).

Therefore, the extraction and separation of R-PE from macroalgal biomass as well as the methodology followed are extremely important in order to keep the bio-activities. The lack of standardized extraction and separation methodologies has prevented the official approval of phycobiliproteins or their derived fractions for food, pharmaceutical, dermatological, nutraceutical or other commercial applications to date.

### **Encapsulation of bioactive compounds as a stabilization strategy**

Phycoerythrin, being a protein-based compound, requires some forms of protection before it can be incorporated as a specialized ingredient in food matrices. In this regard, several researchers have shown that encapsulation is an effective and economical method to maintain the stability of phycobiliproteins and especially phycocyanin (another phycobiliprotein pigment, with blue coloration) (Yan et al., 2014; Pan-utai and Iamtham, 2018). However phycoerythrin stabilization oriented to preserve the biotechnological properties are still reduced and requires further investigation.

An alternative to protect this type of bioactive compounds is to encapsulate them in a solid support such as in microcapsules, thus increasing their chemical stability, as well as protecting

and improving the bioavailability at the gastrointestinal level (Sotomayor-Gerding et al., 2016; Morales et al., 2017; Piornos et al., 2017; Acevedo et al., 2018). It should be noted, that the success of the encapsulation system depends mainly on the technique used, process conditions and type of encapsulating material (Tan et al., 2009). In recent years, the use of the electro-coextrusion encapsulation technique, through the mechanism of ionic gelation, has been considered as a promising encapsulation technology for the production of core-shell capsules, ranging from micrometers to millimeters (Phawaphuthanon et al., 2014). Electro-coextrusion is a simple, economical and easy to operate system, to produce uniform capsules in size and shape. The principle is based on breaking the laminar flow by applying a vibrational frequency with a defined amplitude to a certain size. Different types of hydrophilic and hydrophobic polymers, such as alginate, poly-L-lactide, poly (DL-lactide-co-glycolide), polydimethylsiloxane, photopolymer and cocoa butter, have been used in electro-coextrusion to make capsules with different fluids central to protect, such as protein solutions, aqueous solutions, emulsions, cell suspensions and oils (Phawaphuthanon et al., 2014). Lewinska et al., (2008) encapsulated a cell suspension within a calcium-alginate shell of 0.36 mm diameter and 90  $\mu$ m thickness by electro-coextrusion, in order to overcome the cell leakage problem encountered by the use of calcium-alginate beads. Choi et al., (2010) fabricated core-shell calcium-alginate microcapsules, in the size range of 200–1000  $\mu$ m, by electro-coextrusion for the controlled delivery of osteogenic inductions factors of stem cells. In spite of the studies cited above on micro-sized wet alginate capsules, there is little information, currently available, on the electro-coextrusion of macro-sized, visible core-shell alginate capsules in dried form.

The characteristics of core-shell capsules produced by electro-coextrusion, such as outward appearance, size, shell thickness, texture, core release behaviour, and stability, could be mainly influenced not only by shell fluid-related factors, such as polymer concentration, viscosity, density, surface tension, and electrical conductivity, but also by process-related factors, such

as core and shell flow rates, shell-to-core flow rate ratio, applied voltage, temperature, nozzle size, distance between the nozzle tip and the surface of gelling bath, gelling agent concentration, gelling time, and drying method (Lewinska et al., 2008; Choi et al., 2010;). However, the effects of such factors on the characteristics of core-shell alginate capsules, especially of dried and macro-sized alginate capsules, have not been systematically studied.

Currently, there is a growing interest in the use of capsules based on polymers from natural sources, due to their capacity for renewal, biodegradability, biocompatibility and non-toxicity (Ben Messaoud et al., 2016). For example, alginate is a natural anionic polysaccharide widely used to prepare capsule or pearl encapsulation systems due to its interesting physicochemical properties, biocompatibility, wide availability and low cost (Pawar and Edgar, 2012; Lupo et al., 2015). The functionality of alginate beads depends to a large extent on their permeability and physicochemical stability. This alginate capsule has a retention and selective release, that makes it a good carrier for biotechnology applications; however, relatively high porosity is not adequate for some industrial applications (Mancini et al., 1999). Diffusion of small molecules such as glucose and ethanol is unaffected by the alginate matrix while diffusion of larger proteins from the gels has been shown to be dependent on their molecular weight (Martinsen et al., 1991). The diffusion of several proteins from alginate beads has been reported including immunoglobulin G (IgG) (Chevalier et al., 1987) fibrinogen and insulin (Gombotz and Wee, 2012). Increasing the concentration of alginate in the beads decreases the rate of diffusion of the proteins from the gel. Therefore, to control its physicochemical properties, several strategies have been developed to improve the efficiency of encapsulation. In this way, the incorporation of additional natural polymers, in combination with alginate, could control the physicochemical properties of the final matrix and improve the encapsulation efficiency (Tan et al., 2009; Ben Messaoud et al., 2016). Among them, shellac stands out as a natural resin secreted by insects mainly in Southeast Asia of the genus *Kerria*, being a renewable natural

polymer, non-toxic, biodegradable and commercial available (NOVATEC Company). It consists of a complex mixture of aliphatic and alicyclic acids. The main components are aleuritic acid, as well as jalaric and shellolic acids (Stummer et al., 2010). In recent years, the shellac biopolymer has attracted significant interest, to develop different types of encapsulation systems. Experiences have validated its incorporation as an additional external layer to coat capsules (Limmatvapirat et al., 2008; Ben Messaoud et al., 2016). The combination of alginate / shellac has been used to make oil beads by extrusion by ionic gelation (Morales et al., 2017). However, it has not yet been used to develop microcapsules by means of the extrusion by ionic gelation encapsulation technique for the protection of hydrophilic bioactives such as R-PE.

### **Digestion and bioavailability**

Algae are increasingly being marketed as “functional foods” or “nutraceuticals”; these terms have no legal status in many nations, but describe foods that contain bioactive compounds or phytochemicals, that may benefit health, beyond the role of basic nutrition (e.g., anti-inflammatory, disease prevention) (Bagchi, 2006; Hafting et al., 2012; Cofrades et al., 2013). Many studies report the nutritional potential or bioactive content of different algae, but few of them quantify the bioavailability of nutrients and phytochemicals from algal foods. The concept “bioavailability”, was defined by Carbonell-Capella et al., (2014) “as a combination of bioactivity and bioaccessibility”, where bioaccessibility refers to the release from the food matrix, transformations during digestion and transport across the digestive epithelium, while bioactivity encompasses uptake into tissues, metabolism, and physiological effects. Because of the difficulties, both practical and ethical, in terms of measuring bioactivity, the fraction of a given compound or its metabolite that reaches the systemic circulation (Holst and Williamson, 2008) can be considered bioaccessible, but not necessarily bioactive. Most published evaluations of bioactivity of algal foods are based on short-term *in vitro* tests, using algal extracts that frequently are of ill-defined composition and low purity, so a clear understanding

of their food value is highly constrained. Particularly, a lack of information concerning the behaviour of algal food components in the gut is revealed. In that way, one of the questions we hope to answer is if the R-PE has bioactivity properties and if the protection can be maintained as the conditions for therapeutic effect at the intestinal level.

Digestion refers to the physical and biochemical degradation of foods and the nutrients contents in preparation for absorption into the body. Digestion begins in the mouth with chewing, which reduces particle size and mixes food with saliva (Brodkorb et al., 2019). The predominant salivary enzyme is alpha ( $\alpha$ )-amylase, which is specific for  $\alpha(1\rightarrow4)$  glucose linkages, and human salivary amylase is more active than that from other primates (Boehlke et al., 2015). Pepsin and the pepsinogens begin protein digestion in the stomach, aided by hydrochloric acid that denatures proteins and releases nutrients from the food matrix. Lipases produced in the mouth and stomach begin the process of digesting triacylglycerols. The pancreas discharges a mixture of trypsin, chymotrypsin, carboxypeptidases,  $\alpha$ -amylase, lipase, and other enzymes that respectively digest proteins and peptides, starches, triacylglycerols, and other compounds in the small intestine (Gropper and Smith, 2013). The mixture of proteases, amylase, and lipase are collectively known as pancreatin; porcine pancreatin is often used as model of model human *in vitro* digestion systems. Finally, high digestibility of phycoerythrin would enable greater absorption of the protein, or in fact, its amino acids or short peptides. Because human digestive proteases have their specificity to bonds near certain amino acids, it is important to verify that the algal protein sequences can be digested by the human proteases. Protein digestibility may be assessed by simulating gastro-intestinal conditions by standard protocols (Minekus et al., 2014). There are several types of *in vitro* digestion methods that are commonly used for food; these can be divided into static and dynamic methods. These models aim to simulate the physiological conditions of the upper gastrointestinal tract, namely the oral, gastric and small intestinal phases. Most dynamic models (Kong and Singh, 2010) have been shown

to be suitable for simulating the digestion of foods and pharmaceutical products in different population groups and for different purposes (Dupont, 2018). For example, for a static method, Gajaria et al., (2017) and Kazir et al., (2019) both found a correlation between the digestion standard value of the casein protein extracted and antioxidant activities of the red macroalgae *Gracilaria* sp. These results indicate that the algal proteins extracted can be hydrolyzed by digestive enzymes, which may increase the possibility of its absorption in the intestine with biological activity.

### Bioactivity of the algal compounds in cell lines

Most of the marine food products and by-products are being converted and utilized as valuable functional foods through recent development in marine bioprocess industry. This is due to the presence of bioactive compounds which are a powerful antioxidant in nature and are used as functional foods and nutraceuticals where depended of the physiological effects (Ngo et al., 2011) (Figure II.1).

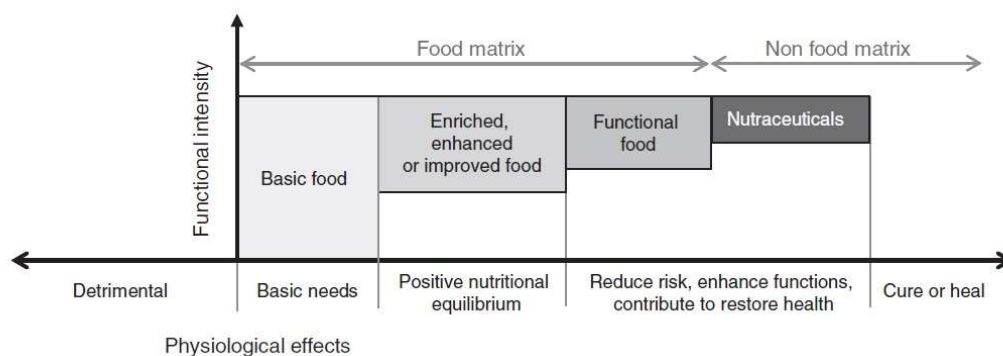


Figure II.1. Frontiers in functional foods (adapted from Doyon and Labrecque, 2008) and frontiers in nutraceuticals (adapted from Palthur et al.,2010).

The term ‘nutraceutical’, coined by the Foundation of Innovation in Medicine (de Felice, 1992), refers to any substance that is a food or a part of a food and provides medical or health



benefits, including the prevention and treatment of disease. A nutraceutical may be a natural nutrient, either an isolated or purified product, generally presented in medicinal form or in a non-food matrix, in powder or tablet form, such as dietary supplements, or herbal products (Klimas et al., 2008) (Figure II.1).

Many studies have been devoted toward the recognition of antioxidant potential of natural proteins originated from algae because of their broad spectrum antioxidant activity (attributed by diverse aminoacid side chains), great abundance and easy availability in nature. In fact, several therapeutic products have been isolated from algae of subtropical and tropical populations and few of them have been screened for their anticancer potential (Manilal et al., 2009; Xu et al., 2017). Cancer preventive effects of chlorophyll *a* and its derivatives have been extensively studied, with particular emphasis on their in vitro antimutagenic cell lines effect against numerous dietary and environmental mutagens (Ferruzzi et al., 2007). A number of studies have used bacterial mutagenicity assays. Accordingly, marine pigments algae-derived have also been investigated with regard to their antimutagenic/antigenotoxic activity. Lutein,  $\beta$ -carotene and chlorophyll isolated from the red algae *Porphyra tenera* have demonstrated antimutagenic activity in bacterial, *Salmonella typhimurium* (Okai et al., 1996). Exciting research studies have been published regarding carotenoids and its anticancer qualities. Ishikawa et al., (2008) showed anti-adult T-cell leukemia effects of fucoxanthin and its deacetylated metabolite fucoxanthinol. The inhibitory activities of fucoxanthin and fucoxanthinol were stronger than those of  $\beta$ -carotene and astaxanthin. Adult T-cell leukemia is a fatal malignancy of T lymphocytes caused by human T-cell leukemia virus type 1 infection and remains in curable. Therefore, carotenoids could be potentially useful therapeutic agents for adult T-cell leukemia patients. In the case of fucoxanthin remarkably reduced the viability of human colon cancer cell lines and treatment with fucoxanthin induced DNA fragmentation. Exposure to fucoxanthin decreased the level of apoptosis suppressing protein (Bcl-

2), suggesting that anticancer mechanism of fucoxanthin bring through apoptosis mechanism. Apoptosis inducing effect of fucoxanthin in human prostate cancer cells lines (PC-3, DU-145 and LNCaP) has also been observed (Kotake et al., 2001). Meanwhile, anti-proliferative effect and apoptosis induction by fucoxanthin in human colon cancer cells (Caco-2, HT-29 and DLD-1) were observed by Hosokawa et al., (2004). In addition, they also demonstrated anti-inflammatory effect of fucoxanthin isolated from *Myagropsis myagroidesin* LPS-stim-ulated RAW 264.7 cell lines.

On the other hand, effective fractions of polysaccharides were found mainly in cyanobacteria, although recently, the potential of red and green macroalgae compounds as potent immunomodulatory agents has been shown (Tabarsa et al., 2018). In addition, the UV photoprotectors, mycosporine-like amino acids (MAAs), extracted mainly from red algae (Álvarez-Gomez et al., 2016), also present with immunological activity (Suh et al., 2014).

Algal phycobiliproteins gain huge importance due to their immuno-enhancing, anti-inflammatory, anticarcinogenic, antioxidant, and nutritional properties and these properties could provide vital breakthrough in cancer research (Belay, 2002; Dammeyer and Frankenberg-Dinkel, 2006; Senthilkumar et al., 2013). Phycoerythrin containing prosthetic groups called bilines, useful for the prevention and treatment of diseases caused by oxidative damage such as cancer (Senthilkumar et al., 2013). In addition, the stability of its structure and the linearity of its chromophore groups are what give its healthy properties, so that the more stable the molecule behaves, the greater the range of biotechnological applications that can be attributed to it. Recently, Senthilkumar et al., (2018) have demonstrated the anticancer effect of R-PE obtained from macroalgae *Portieria hornemannii* against HepG2 cell line. Another study, reported a nanotheranostic formulation using R-PE as therapeutic and diagnostic molecule targeting triple negative breast cancer cells (Thangam, et al., 2015). However, reports on the hepato-protective effects of R-PE are scarce especially using animal models. Previous

studies indicated that both, phycocyanin and phycoerythrin, are potential free radical scavengers. Phycobiliprotein possesses hydroxyl and peroxy radical scavenging activity in both *in vitro* and *in vivo* models (Vadiraja, et al., 1998; Bhat and Madyastha, 2000;). Likewise, that R-PE had the ability to scavenge free radicals including, superoxide and nitric oxide and hydroxyl radicals besides showing anti-lipid peroxidative activity *in vivo* (Soni et al., 2006). However, reports of anti-cancer effects of encapsulated R-PE have not yet been evaluated, which could improve the therapeutic effect with controlled release.

### **Light spectrum influences the production of algae biomass**

Efficient production, availability, and accessibility of a sustainably produced biomass feedstock is the basic pillar of seaweed biorefinery. However, the bioavailability of the resource in the environment is finite (Lange et al., 2020). The current exploitation of the algal resource is a bottleneck for the process that is affecting marine biodiversity (including other species of seaweed, fish, and invertebrates). Thus, efficient culture systems combine production of high-quality, algae biorefinery feedstock with a contribution to climate change mitigating his can be achieved by strengthening marine capacity for CO<sub>2</sub> sequestration while seaweed cultivation in culture systems where contributes to the circular economy (Lange et al., 2021).

The circular economy is referred to highlighted the sustainability of seaweed cultivation by delivering both improved resource valorization efficiency (economy) and climate change mitigation (environment). Thus, to enhance biomass and metabolite yield, it is necessary to increase photosynthetic efficiency and optimization of light absorption through adjustment of the light-harvesting apparatus to achieve optimal balance of photosynthesis/photoprotection, rather than just maximizing light absorption from the light spectrum photosynthetic active region (PAR) between 400-700 nm (Larkum et al., 2003; Jerez et al., 2016; Peralta et al., 2019).

Based on their pigmentation differences in general, algae are classified into three major phylum: Rhodophyta (red macroalgae), Chlorophyta (green macroalgae), and Phaeophyta (brown macroalgae). The existence of the diverse phytopigments in macroalgae is affected by their marine habitat. Accordingly, because green macroalgae have the ability to absorb large amounts of light energy, they are abundant in coastal water, whereas brown and red macroalgae can be found at greater depths where sunlight penetration is restricted. In photosynthetic organisms, light can be used as a source of environmental information to control metabolic processes such as growth, reproduction, and morphogenesis (Rüdiger and Figueroa, 1992; Pagels et al., 2020).

Microalgae double their cell biomass in less than 1 day and can grow 100 times faster than terrestrial plants (Tredici, 2010). Microalgae can reach productivities of 40-50 g Dried Weight (DW) m<sup>-2</sup> d<sup>-1</sup> (Acien et al., 2016; Masojidek et al., 2021). They play an important role in CO<sub>2</sub> fixation due to their ability to utilize CO<sub>2</sub> 10–50 times more efficiently than plants, converting the solar energy to chemical energy (Khan et al., 2009; Li et al., 2008; Lam et al., 2012). Certain macroalgal species presents high growth rate in tanks under integrated multitrophic aquaculture i.e. 10-14% d<sup>-1</sup> (*Ulva* spp), 10-16% d<sup>-1</sup> (*Porphyra* spp.), 3,5% d<sup>-1</sup> (*Undaria pinnatifida*) or 6.7% d<sup>-1</sup> (*Gracilariopsis longissima*) (Pérez Lloréns et al., 2016). The productivity in macroalage cultured in tanks can reach values of 21-20 g DW m<sup>-2</sup> d<sup>-1</sup> in *Gracilaria* spp, 44.0 in *Ulva* species and 20-30 in *Hypnea* spp (Gómez Pinchetti et al , 2011)

In addition to the irradiance, light quality has effect on the biochemical composition and growth as photoreceptors in algae are responsible for all light-dependent reactions, and changes in light conditions lead to chromatic acclimation (Montgomery, 2017). Algae need photoreceptors for their general development, as is the case in plants, for the switch between different stages of the life cycle, for controlling the photosynthetic apparatus and for orientation during their motile life stages (Hagemann, 2008). Only five major types of sensory photoreceptors (BLUF-

proteins, cryptochromes, phototropin, phytochromes and rhodopsins) are used in nature to regulate the metabolic processes (Lopez-Figueroa et al., 1990; Hagemann, 2008; Lamparter 2004; Rockwell et al., 2014). López-Figueroa et al., (1990) detected conserved domains in phytochrome-like proteins between green and red algae against etiolated higher plants, viz., the region of the N-terminal (antibodies Z2B3 and Z4BS). However, brown algae not match found at N-terminal region of phytochrome. Lamparter (2004) mentioned during the evolution of plant and cyanobacterial phytochromes, the chromophore binding site has changed from a cysteine close to the N-terminus of the protein, the biliverdin attachment site, to a cysteine which lies within the so-called GAF domain and serves as phytochromobilin or phycocyanobilin attachment site. While Rockweel et al., (2014) demonstrate that algal phytochromes are not limited to red and far-red responses. Instead, different algal phytochromes can sense orange, green, and even blue light.

Then, the organisms are able to change their pigment composition and obtain an advantage in different environments, and the pigment responsible for the harvesting of the incident light will become predominant (Bennett and Bogorad 1973; Walter et al., 2011). Photosynthesis requires core reaction pigment chlorophyll-*a*; accessory pigments (Phycoerythrin, phycocyanin and allophycocyanin), chlorophyll *b*, *c*, and *d*; and carotenoids, which help to extend the range of light absorption. Blue and red wavelengths are the main absorption bands of all chlorophylls (Richmond, 2003). New developments in production systems want to increase light availability and efficacy for the production microalgal biomass and photosynthetic pigments (Assunção et al., 2022) and macroalgae (López Figueroa, 1991; Figueroa et al., 1995), and such changes can be done in terms of light distribution, intensity, and/or source. Narrow peak spectra can be used to act directly on the photo-response of the organism (Schulze et al., 2014). The advantage of supplementing light is the possibility to keep the photosynthetic metabolism in its optimum

while other pathways are activated through various photomorphogenic responses (Yang and Weathers, 2014; Suyono et al., 2015) (Figure III.1).

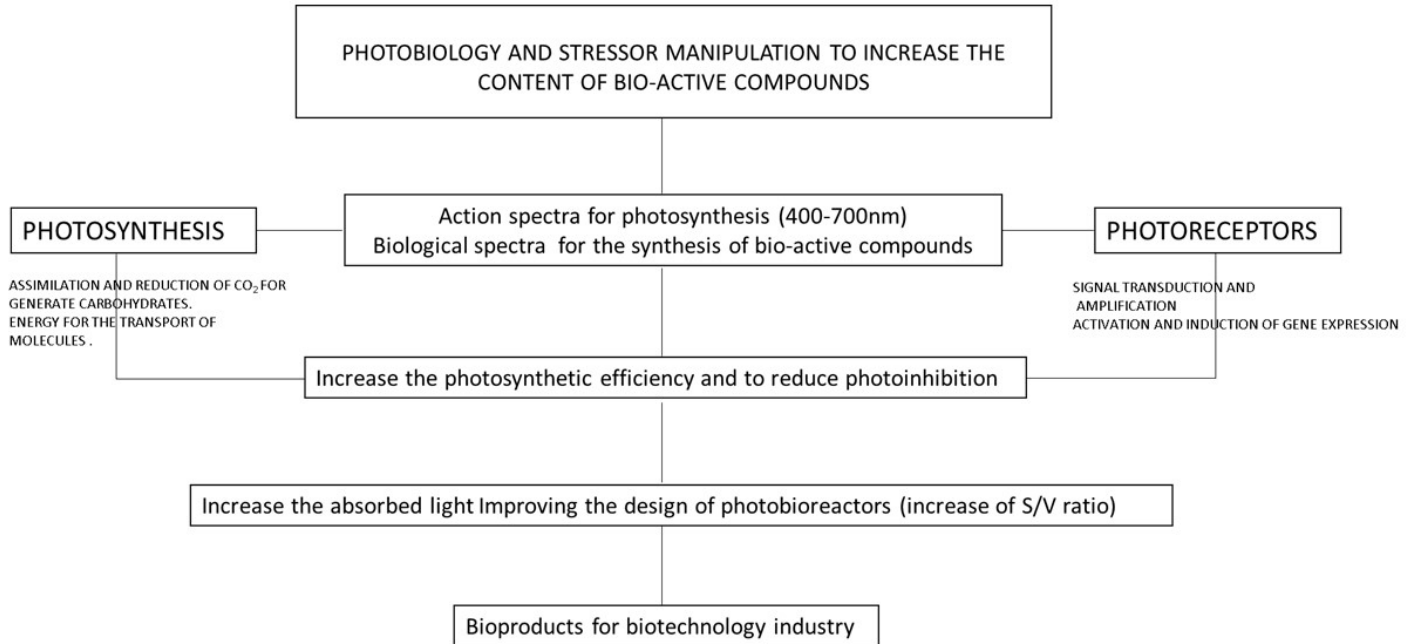


Figure III.1. Flow diagram of the application of the photobiology for biotechnology applications. (From Figueroa F.L. Module class dissertation 2022).

For example, the use of white light with supplemented red light increased the lipid production in the microalga *Ettlia oleoabundans* (Yang and Weathers, 2014). The advantage of supplementing light is the possibility to keep the photosynthetic metabolism in its optimum while other pathways are activated through various photomorphogenic responses (Yang and Weathers, 2014; Suyono et al., 2015). Similar results have been observed in macroalgae (Figueroa et al., 1995; Häder and Figueroa, 1997; Aguilera et al., 1997)

Using mixed blue and red LEDs, cell biomass production was often higher than that obtained using red LED alone (Pagels et al., 2020; Assunção et al., 2022). However, an optimal mixing ratio for maximum cell biomass production has not yet been determined because the capture of photons by algal chlorophyll depends on multiple factors including cellular architecture,

pigment composition, and chloroplast arrangement (Schulze et al., 2014). The incandescent light bulbs mostly produce yellow, orange or red light. Standard “cool white” fluorescent bulbs emit mostly yellow-green light (Wobbe et al., 2016; Baer et al., 2016). The low-pressure sodium vapor lamps (SOX lamps), emitting mainly at 589 nm, are efficient sources of PAR, which emit relatively low levels of infrared radiation (IR) and heat (Sager et al., 1982). Growth rate and photosynthetic activity were optimal under SOX in the red macroalgae (Aguilera et al., 1997; 2000). The microalgae produce an important intracellular metabolite in response to light stress conditions. Based on the microalgal responses, the specific wavelengths will enhance the productivity of specific intracellular products with artificial light. Yellow light (SOX) it is possible to obtain saturation of photosynthesis in a wavelength band without any known photomorphogenic photoreceptor (Segovia et al., 2003) and without interference with other known non photosynthetic photoreceptors in the wavelengths of blue, green, or red light and UV radiation, leading to accumulation of compounds through non-photosynthetic pathways (Rüdiger and López-Figueroa, 1992; Hegemann et al., 2001; Rockwell et al., 2014; Pagels et al., 2020).

Therefore, the challenges of this work is (i) to optimize the environmentally friendly extraction by UAE and HPH, fractionation by aqueous solvents matrix and purification processes to concentrated the R-PE in a fast and non-aggressive way; (ii) to develop a novel formulation based on alginate-shellac to protect R-PE and (iii) maintain biological effects with controlled release at gastrointestinal level for development of non-toxic algae-based ingredients for functional foods and nutraceutical applications.

In addition, the supply of raw material will be a critical point where it is necessary to carry out studies for a sustainable development of the process, avoiding extracting from natural banks and its negative effects. For this, evaluations have been carried out based on the intensity and

quality of light, in order to stimulate growth and bioactive compounds such as R-PE in the red algae *Porphyridium cruentum*.

## **Hypothesis**

The application of the biorefinery process based on the extraction methods (ultrasound assisted extraction and high-pressure homogenization) on the *Sarcopeltis skottsbergii* biomass can obtain valuable products: (i) the high yield, and purity of Phycobiliprotein (R-PE) and the combination with ionic gelation encapsulation by alginate/shellac mixture biomaterial to allow the bioaccessibility of R-PE at an intestine level with biological activity, (ii) the recovery of supernatant residues with sulfated polysaccharides maintaining the antioxidant and antiproliferative activities to be used as nutraceutical ingredients.

The sustainably produced of biomass enrichment with Phycobiliprotein (R-PE) can be efficient production culture system by the manipulation of light PAR spectra on the red algae *Porphyridium cruentum*.

## **General objective**

To develop a nutraceutical ingredient of R-phycoerythrin concentrate and polysaccharides from the macroalgae *Sarcopeltis skottsbergii* (Rhodophyta) using a green technology for the extraction, ionic gelation to encapsulate it and to characterize its digestibility and bioactivity by *in vitro* systems.

## **Specific objectives**

1. To optimize the extraction and separation processes of R-phycoerythrin from *S. skottsbergii* by using two green technologies (ultrasound and high pressure homogenization) and evaluation of the antioxidant capacity.



2.To optimize encapsulation conditions by external ionic gelation for the alginate/shellac mixture as biomaterials to microencapsulate phycoerythrin from *S. skottsbergii*.

3.To characterize the digestibility and bioactivity of the nutraceutical ingredient of phycoerythrin by means of an *in vitro* system (enzymatic reaction and cellular culture).

4.To evaluate antioxidant capacity of neutral and acid polysaccharides and their antiproliferative effects on cell lines: human fibroblasts (1064sk, CIC-UGA, ES), immortalized human keratinocytes (HACAT, ATCC, USA), human leukemia cell line (U-937, ATCC, USA), human malignant melanoma (G-361, ATCC, USA) and colon cancer cell line (HCT-116, ATCC, USA).

5.To evaluate the bioproduction of R-PE under yellow light saturation (587nm) and the combination of blue (440nm), green (560)nm and red (660nm) light PAR spectra on the red algae *Porphyridium cruentum*.

---

# CHAPTER II.

## **Highly efficient water-based extraction of biliprotein R-Phycoerythrin from marine the red macroalga *Sarcopeltis skottsbergii* by ultrasound and high-pressure homogenization methods.**

This chapter has been published in *Frontiers in Marine Science*, Section Marine Biotechnology and Bioproducts. Castro-Varela P, Celis-Pla PSM, Figueroa F and Rubilar M (2022) Highly Efficient Water-Based Extraction of Biliprotein R-Phycoerythrin From Marine the Red-Macroalga *Sarcopeltis skottsbergii* by Ultrasound and High- Pressure Homogenization Methods. *Front. Mar. Sci.* 9:877177. Doi: 10.3389/fmars.2022.877177

---

**CHAPTER II. Highly efficient water-based extraction of biliprotein R-Phycoerythrin from marine the red macroalga *Sarcopeltis skottsbergii* by ultrasound and high-pressure homogenization methods**

Pablo Castro-Varela<sup>1,2</sup>, Paula S.M. Célis-Plá<sup>3</sup>, Félix L. Figueroa<sup>2</sup>, Mónica Rubilar<sup>4</sup>

<sup>1</sup>Institute of Blue Biotechnology and Development (IBYDA), Experimental Centre Grice Hutchinson, Universidad de Málaga, Lomas de San Julian, 2, 29004 Málaga, Spain. ([pablo.castro@uma.es](mailto:pablo.castro@uma.es); [p.castro07@ufromail.cl](mailto:p.castro07@ufromail.cl)).

<sup>2</sup>Doctorate in Engineering Sciences with specialization in Bioprocesses, Faculty of Engineering and Sciences, Universidad de La Frontera, Temuco, Chile.

<sup>3</sup>Laboratory of Coastal Environmental Research, Center of Advanced Studies-HUB Ambiental, Universidad de Playa Ancha, Traslaviña, Viña del Mar, Chile. ([paulacelispla@upla.cl](mailto:paulacelispla@upla.cl) )

<sup>4</sup>Department of Chemical Engineering, Faculty of Engineering and Sciences, Universidad de La Frontera, Temuco, Chile. ([monica.rubilar@ufrontera.cl](mailto:monica.rubilar@ufrontera.cl) )

**Keywords:** R-phycoerythrin, *Sarcopeltis skottsbergii*, ultrasound, high-pressure homogenization, red algae

## ABSTRACT

*Sarcopeltis skottsbergii* is an endemic species of the Southern Cone, with R-phycoerythrin (R-PE) as an accessory photosynthetic pigment. The production of *S. skottsbergii* is around 20,000 tons of dry alga per year. The evaluation of R-PE in a biorefinery model is still in the early stages in the field of algal biotechnology and will be used in the food, pharmaceutical, cosmeceutical, and nutraceutical industries. This work evaluated the cell disruption and separation processes by using two green technologies, ultrasound-assisted extraction (UAE) and high-pressure homogenization (HPH), to obtain an R-PE-enriched extract from *S. skottsbergii*. A two-level, three-factor central composite design (CCD) and response surface methodology (RSM) were carried out to optimize the extraction conditions, including the factors for UAE (time, amplitude, and solvent) and HPH (pressure, number of passes, and solvent).

Additionally, a second-order polynomial fit was performed to fit the experimental data by the green method. HPH method was the most efficient extraction method under the conditions obtained from 100-400 MPa pressure power, 2-3 passes, and distilled water as solvent. Furthermore, the experimental extraction yields ranged from 4.4-5.7 mg of PE g<sup>-1</sup> of dry biomass under the optimal extraction conditions (400 MPa; 2 passes), which agreed with the predictive yield of 4.6-5.5 mg g<sup>-1</sup> DW. The ultrafiltration membrane used for the separation process for both methods exhibited a rejection of R-PE concentrated at 30 KDa. Furthermore, R-PE showed a positive correlation between the oxygen radical absorbance capacity (ORAC) in the best-selected extractions. After the extraction, the same pattern was observed in Chlorophyll *a* and total carotenoids with DPPH. Thus, an attractive non-aggressive extraction alternative with biological activity of interest is suggested for formulating biotechnological products for the food industry.

## INTRODUCTION

Phycobiliproteins are water-soluble proteins and pigments found in the cytoplasm or the stroma of the chloroplast (Glazer et al., 1976; Pagels et al., 2019). Red micro and macroalgae, Cyanobacteria and Cryptophytes, are the only sources of reddish-red pigment, R-phycoerythrin (R-PE), and their primary function is to trap light energy between 495 and 650 nm wavelengths and transfer it to chlorophyll *a* of the photosynthetic reaction center of Photosystem II through other biliproteins such as phycocyanin and allophycocyanin (Sekar and Chandramohan, 2008; Castro-Varela et al., 2021; Roy and Pabbi, 2022). R-PE is an oligomeric protein of 240 kDa with three subunits  $\alpha$  (about 16 kDa),  $\beta$  (about 21 kDa), and  $\gamma$  (about 39 kDa), and they are bound to specific cysteines by thioether bonds (Li et al., 2019b). The study of phycobiliproteins focuses mainly on therapeutic (bioactive) applications, i.e., anti-inflammatory, antiviral, hepatoprotective, and anticarcinogenic capacities of R-PE have been reported (Thangam et al., 2015; Senthilkumar et al., 2018; Ulagesan et al., 2021).

Red algae often contain high levels of proteins (Hasan R. and Fao, 2009; Manivannan et al., 2009; Gómez-Ordóñez et al., 2010) in contrast to brown algae, which has a lower content (Angell et al., 2016). In this sense, the nutritional and biological properties based on the protein in R-PE from red algae could be used as functional ingredients in several phases of food fortification, such as *Kappaphycus alvarezii* (fish cutlet), *Gelidium amansii* (hamburger patties), or *Porphyra umbilicalis* (restructured meats) (Mamatha et al., 2007; Moreira et al., 2010; Jeon and Choi, 2012; Le Guillard et al., 2015; Angell et al., 2016; Ngamnikom et al., 2017). The red macroalga *Sarcopeltis skottsbergii* (formerly *Gigartina skottsbergii*), endemic to the Southern Cone (Buschmann et al., 2008), presents a high content of the R-PE, sulfated polysaccharide and mycosporine-like amino acids (MAAs) (Roleda et al., 2008).

R-PE is among the phycobilisomes connected to Photosystem II in chloroplasts; thus, cell disruption is required for the efficient release during the extraction process. There are several

available methods for extraction of phycobiliproteins such as osmotic shock (Kawsar et al., 2011), maceration in the presence of liquid nitrogen in phosphate buffer (Munier et al., 2014), freeze grinding (Galland-Irmouli et al., 2000), freezing and thawing (Senthilkumar et al., 2013), ultrasonication (US) (Le Guillard et al., 2015), and homogenization (Pereira et al., 2020). Due to the complexity of structures and properties of bioactive compounds and the structure of the extracted materials, there is no available universal extraction protocol (Ciko et al., 2018). For this reason, it is essential to carry out extraction studies that allow us to obtain a high yield and bioactivity from the biological material (Michalak and Chojnacka, 2014) by applying advanced extraction techniques (Ciko et al., 2018).

Therefore, exploring cost-effective extraction and separation methods for R-PE is necessary. Disruption of the rigid cell wall is a critical step required to increase the availability of algal proteins for extraction (Barba et al., 2015). Recently, extraction technologies, especially those considered green processes such as methods involving extraction with water, have gained attention for exploring marine resources to obtain functional ingredients.

Ultrasound-assisted extraction (UAE) has garnered the attention of researchers for its application in the food and allied industries (Michalak and Chojnacka, 2014; Chemat et al., 2017) and acts by creating compression and decompression through sound waves at the frequency of 20 kHz. Thus, several mechanisms for UAE action have been identified, including fragmentation, erosion, sonocapillary effect, sonoporation, local shear stress, and destruction-detexturation of plant cell wall matrix (Le Guillard et al., 2015; Chemat et al., 2017). An overall effect of these mechanisms results in disruption of cell wall. However, the relative extent of the contribution of a given mechanism varies with the type of vegetal biomass and process parameters such as amplitude wave or time (Alexandre et al., 2017; Chemat et al., 2017). Another modern non-conventional alternative method to recover intracellular components is high-pressure homogenization (HPH), considered one of the greenest technologies, which has

exhibited a considerably shorter extraction time and higher yield than conventional techniques (Ciko et al., 2018). This method is typically performed by forcing a liquid through a narrow nozzle at high pressure and establishing high shear stress. The use of mild temperatures makes this process especially appealing in extracting thermosensitive bioactive compounds (Alexandre et al., 2017). Membrane technologies are well suited for use with seaweed as part of a biorefinery process to maximize the valorization of all components within algae and avoid the presence of heavy metals in the final product (Yaich et al., 2011). Some researchers have suggested that the combination of extraction technologies and the incorporation of membrane technologies could be used to isolate algal proteins employing the same principles of molecular weight cut-offs used in the dairy industry. Ultrafiltration (UF) membranes constitute a physical barrier that retain all compounds larger than the membrane molecular weight cut-off. UF could then be used to isolate proteins and other macromolecules between 1 and 200 kDa, as has been validated on an industrial scale (food and feed industry) to generate enriched fractions less than 10, 5, 3 and 1 kDa. UF was used to isolate R-PE protein from macroalgae *Grateloupia turuturu* following cell homogenization, retaining about 100% of the protein without denaturation (Denis et al., 2009).

In this regard, determining a behavior pattern between R-PE and the extraction method, we could consider a new attribute that reinforces the use of green methods for sustainability and development of a bioprocess. In fact, there is no universal extraction protocol that ensures the quality of the structures and properties of the pigments (Liu et al., 2019); therefore, it is believed that a specific extraction process must be established for each biological material extracted to obtain extracts with desirable bioactivity and high yield.

Response surface methodology (RSM) is a statistical tool used to determine and enhance the optimal experimental conditions to achieve maximum yields with minimum time and resource consumption (Wani et al., 2017). In this way, this study aimed to optimize the extraction

process to obtain crude extracts with a higher yield of phycoerythrin from *S. skottsbergii* using RSM. Two green methods, UAE and HPH, including the variables for UAE (time, amplitude, and solvent) and HPH (pressure, number of passes, and solvent), were investigated for their influence on the yield of the extracts. UF technology, antioxidant activity, soluble protein content, and photosynthetic pigments were tested to evaluate the concentration and purity of R-PE in the aqueous extracts.

## MATERIAL AND METHODS

### Algal biomass

Biomass of the marine macroalgae *S. skottsbergii* (Rhodophyta) is distributed along the coast of Chile, from Corral (39° 88' S) (Westermeyer and Ramírez, 1978) to the Antarctic Peninsula (63° 23'S) (Bischoff-Bäsmann and Wiencke, 1996a). In this study, the macroalgae were provided from the Magallanes Region by Gelymar S.A., Puerto Montt, Chile. The biomass was washed with filtered and distilled water to remove sand particles, epiphytes, and other undesirable materials before transporting under cold conditions to the Universidad de La Frontera, Temuco, Chile. Biomass was lyophilized (Biobase BK-FD18PT) for 48h, and substrate samples were carefully milled with a grinder machine (Sindelen Mol165IN, China) until particle size was less than sieve screen number 18 (1 mm openings). The samples were sieved using a Ro-Tap testing sieve shaker (model RX-29-10, W.S. Tyler, Mentor, OH) through a set of sieves (ASTM E11:95). The average particle diameter ( $d_p = 0.70$  mm) was determined using Equation 1 of the standard method S319.3 (ASAE S319.3 Method of Determining and Expressing Fineness of Feed Materials by Sieving).

$$d_p = \log^{-1} \left[ \frac{\sum_{i=1}^{n-1} w_i \log \bar{d}_i}{\sum_{i=1}^n w_i} \right] \quad (\text{Eq. 1})$$



$\bar{d}_i$  (mm) is the geometric mean diameter of particles on  $i$ th sieve, or  $(d_i \times d_{i+1})^{1/2}$  where  $d_i$  is the nominal sieve aperture size of the  $i$ th sieve and  $d_{i+1}$  is the nominal sieve aperture size, in  $i$ th sieve  $w_i$  is the mass of particles with an average diameter of  $\bar{d}_i$ . The biomass was stored at  $-18 \pm 2$  °C, and the desired quantity of biomass was taken out as and when required for the experimentation.

### **Experimental design**

The RSM, with a central composite design (CCD), was employed for the evaluation of the effect of the variable on the phycoerythrin yield extracted with UAE and HPH. For the case of the UAE method, amplitude percentage (30 to 90 %) and time (10 to 30 min) in the solvent (water or phosphate buffer) were tested. For the HPH methods, factors include the pressure (100 to 500 MPa) and the passes (1 to 3) through the solvent (water or phosphate buffer). The experiments were designed according to a 22 factorial design with three central points for both methods. The range of independent variables, the response levels, and the results of the complete design composed of 22 experimental runs performed in random order is listed in Tables 1 and 2. All the trials were performed in triplicate. Three-dimensional response surface plots were generated by varying the variables within the experimental region. The goodness of fit of the model was evaluated by analysis of variance. The results were analyzed in Design-Expert v. 12.0 (Stat-Ease Inc., Minneapolis, USA). The design was fitted to a reduced quadratic model expressed by a polynomial regression equation.

Different statistical criteria to evaluate the model were considered. Values close to 1 for  $R^2$ , lower than 10 for covariance, and higher than 4 for adequate precision were considered desirable for model acceptance. Adequate precision measures signal-to-noise ratio related to the contrast in predicted response concerning its associated error. The statistical significance was based on the total error criteria with a 95% confidence level.

Table I.2. Central composite design for ultrasound-assisted method and yield (YPE) results from response surface method analysis.

| <b>Run</b> | <b>Amplitude<br/>wave<br/>(%)</b> | <b>Time<br/>(min)</b> | <b>Solvent for extraction</b> | <b>Y<sub>PE</sub><br/>(mg g<sup>-1</sup>)</b> |
|------------|-----------------------------------|-----------------------|-------------------------------|---|
| 1          | 30                                | 10                    | Phosphate buffer              | 0.602 ± 0.02                                  |
| 2          | 90                                | 10                    | Phosphate buffer              | 0.689 ± 0.05                                  |
| 3          | 30                                | 30                    | Phosphate buffer              | 0.739 ± 0.08                                  |
| 4          | 90                                | 30                    | Phosphate buffer              | 0.658 ± 0.09                                  |
| 5          | 30                                | 20                    | Phosphate buffer              | 0.722 ± 0.10                                  |
| 6          | 90                                | 20                    | Phosphate buffer              | 0.646 ± 0.09                                  |
| 7          | 60                                | 10                    | Phosphate buffer              | 0.886 ± 0.08                                  |
| 8          | 60                                | 30                    | Phosphate buffer              | 0.759 ± 0.07                                  |
| 9          | 60                                | 20                    | Phosphate buffer              | 0.882 ± 0.12                                  |
| 10         | 60                                | 20                    | Phosphate buffer              | 0.835 ± 0.13                                  |
| 11         | 60                                | 20                    | Phosphate buffer              | 0.827 ± 0.51                                  |
| 12         | 30                                | 10                    | Distilled water               | 1.700 ± 0.01                                  |
| 13         | 90                                | 10                    | Distilled water               | 2.256 ± 0.02                                  |
| 14         | 30                                | 30                    | Distilled water               | 1.969 ± 0.03                                  |
| 15         | 90                                | 30                    | Distilled water               | 2.141 ± 0.09                                  |
| 16         | 30                                | 20                    | Distilled water               | 2.076 ± 0.08                                  |
| 17         | 90                                | 20                    | Distilled water               | 2.285 ± 0.03                                  |
| 18         | 60                                | 10                    | Distilled water               | 2.029 ± 0.01                                  |
| 19         | 60                                | 30                    | Distilled water               | 2.291 ± 0.13                                  |
| 20         | 60                                | 20                    | Distilled water               | 2.552 ± 0.12                                  |
| 21         | 60                                | 20                    | Distilled water               | 2.451 ± 0.14                                  |
| 22         | 60                                | 20                    | Distilled water               | 2.685 ± 0.11                                  |

Table II.2. Central composite design for high-pressure homogenization-assisted method and yield (YPE) from response surface method analysis.

| Run | Pressure<br>(MPa) | Passes | Solvent extraction | Y <sub>PE</sub><br>(mg g <sup>-1</sup> ) |
|-----|-------------------|--------|--------------------|--|
| 1   | 100               | 1.00   | Phosphate buffer   | 4.284 ± 0.01                             |
| 2   | 500               | 1.00   | Phosphate buffer   | 3.771 ± 0.13                             |
| 3   | 100               | 3.00   | Phosphate buffer   | 4.348 ± 0.1                              |
| 4   | 500               | 3.00   | Phosphate buffer   | 3.196 ± 0.02                             |
| 5   | 100               | 2.00   | Phosphate buffer   | 5.170 ± 0.01                             |
| 6   | 500               | 2.00   | Phosphate buffer   | 4.425 ± 0.03                             |
| 7   | 300               | 1.00   | Phosphate buffer   | 4.514 ± 0.02                             |
| 8   | 300               | 3.00   | Phosphate buffer   | 3.209± 0.05                              |
| 9   | 300               | 2.00   | Phosphate buffer   | 4.736 ± 0.04                             |
| 10  | 300               | 2.00   | Phosphate buffer   | 4.361± 0.05                              |
| 11  | 300               | 2.00   | Phosphate buffer   | 4.631 ± 0.12                             |
| 12  | 100               | 1.00   | Distilled water    | 4.957 ± 0.11                             |
| 13  | 500               | 1.00   | Distilled water    | 5.249 ± 0.10                             |
| 14  | 100               | 3.00   | Distilled water    | 5.193 ± 0.08                             |
| 15  | 500               | 3.00   | Distilled water    | 4.972 ± 0.09                             |
| 16  | 100               | 2.00   | Distilled water    | 4.873 ± 0.09                             |
| 17  | 500               | 2.00   | Distilled water    | 4.889 ± 0.08                             |
| 18  | 300               | 1.00   | Distilled water    | 5.557 ± 0.04                             |
| 19  | 300               | 3.00   | Distilled water    | 5.727 ± 0.02                             |
| 20  | 300               | 2.00   | Distilled water    | 5.533 ± 0.11                             |
| 21  | 300               | 2.00   | Distilled water    | 5.46 ± 0.11                              |
| 22  | 300               | 2.00   | Distilled water    | 4.631 ± 0.12                             |

### **Extraction procedure.**

The procedure followed for R-PE extraction from *S. skottsbergii* is schematized in Figure I.2. For all the runs or experiments, freeze-dried biomass of *S. skottsbergii* (5 g) was suspended in 500 mL of solvent (phosphate buffer at pH=6.5 or distilled water) and homogenized by magnetic stirrer at room temperature for 5 min. Then, the extraction was carried out by UAE or HPP, according to the experimental design. After extraction, the samples were centrifuged (Eppendorf Centrifuge 5810R, Billerica, EUA) at 4,000 rpm for 10 min at 4 °C and the pellet was discarded. The supernatant was further filtered through a PTFE 0.45 µm membrane (VWR, North America) and analyzed to determine its R-PE purity, protein content, antioxidant activity, chlorophyll, and carotenoid pigments.

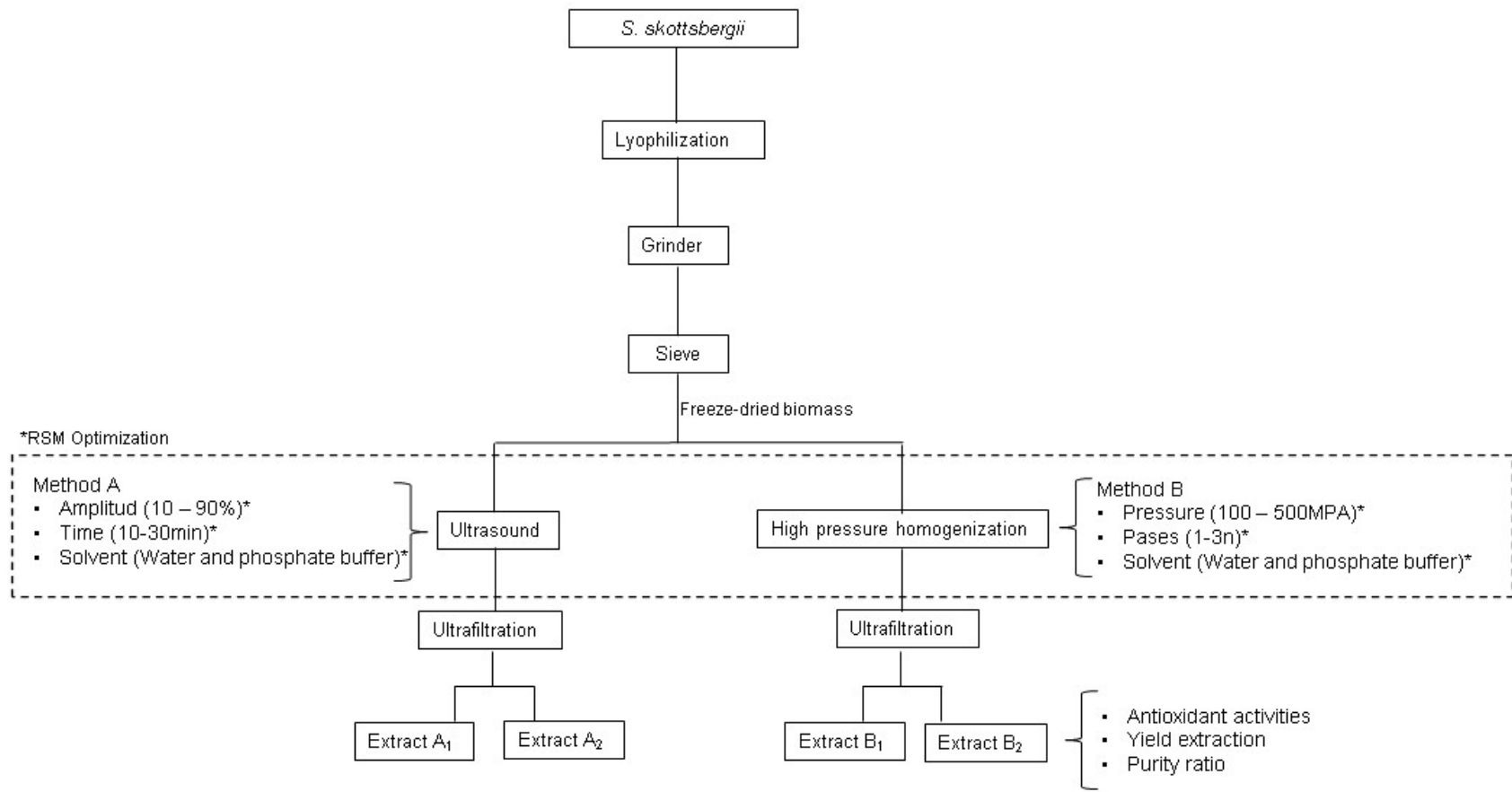


Figure I.2. Summarizing scheme of the procedure for the extraction of R-Phycocerythrin from *S. skottsbergii*. \*RSM Optimization

### **Ultrasound-assisted extraction (UAE)**

The biomass/solvent suspension was placed either in an ultrasonic probe (Sonics VC-505 Vibra Cell Digital Ultrasonic with 3/4" (19 mm) probe, 500 W, 20 KHz, Newtown, CT, USA) for different periods (10-30 min) and amplitude (10-90 %). The probe was inserted into the sample container at about 0.5 cm from the bottom. After UAE, the sample was immediately cooled in an ice bath to avoid overheating to ensure good homogeneity of the sample. After disruption, samples were centrifuged, collected, and analyzed by spectrophotometry at 565 nm (see Eq. 4, 5 and 6).

### **High-pressure homogenization assisted (HPH) extraction**

The biomass/solvent suspension was carried out in high-pressure equipment (Gea Niro Soavi, Homogenizer Panda Plus 2000, Germany) for a different number of passes (1-3) at different pressures (100-500 MPa). The cell suspension was well mixed in the supply tank before disruption to ensure good homogeneity. After disruption, samples were centrifuged, collected, and analyzed by spectrophotometry at 565 nm (see Eq. 4, 5 and 6).

### **Ultrafiltration procedure.**

The extracts with the best phycoerythrin yields from methods A and B were selected to concentrate phycoerythrin using the ultrafiltration stage. Concentrated preparation was carried out following the method proposed by Dennis et al., (2009) with modifications. 500  $\mu$ L of algal extract solution were taken and transferred into Amicon tubes of 30 kDa porosity. They were centrifuged for 20 min at 4 °C. The volumes of the samples (precipitate and permeate) and the phycoerythrin content in both fractions were determined by spectrophotometry at 565 nm (see Eq. 4, 5 and 6).

### **Biochemical analyses total carbon, hydrogen, nitrogen, and sulfur in biomass.**

Total carbon (C), hydrogen (H), nitrogen (N), and sulfur (S) were determined from dry biomass (20 mg) using the total combustion technique in the LECO TruSpec Micro CHNSO-Elemental Analyzer according to the manual. This technique is based on the complete and instantaneous oxidation of the sample by pure combustion with controlled oxygen at a temperature of up to 1050 °C (C, H, N, S) and pyrolysis at 1300°C (O) for decomposition of O as CO and oxidation to CO<sub>2</sub>. The resulting combustion products, CO<sub>2</sub>, H<sub>2</sub>O, SO<sub>2</sub>, and N<sub>2</sub>, are quantified by a selective IR absorption detector (C, H, S) and TCD (N) differential thermo-conductivity sensor. The result of each element (C, H, N, S) was expressed in percentage to the weight of the sample.

### **Total and soluble protein content**

Total protein content was calculated by multiplying the total internal nitrogen content by a factor of 4.59 reported by (Lourenço et al., 2002) for the red alga *S. skottsbergii*. After extraction treatments, the soluble protein content (PC) of the aqueous extract is spectroscopically determined (Bradford, 1976). Briefly, 200 µL of Bradford reagent was diluted with 790 µL distilled water and mixed with 10 µL soluble extracts or bovine serum albumin (BSA, Sigma, MO, USA). The absorbance was read at 730 nm (Biotek Synergy HT) after 5 min of incubation at room temperature. Measurements were performed at least in triplicate.

### **Photosynthetic pigments**

Chl<sub>a</sub> and total carotenoid concentrations were determined through 15 mL aliquots per extraction treatment, using 0.45 µm Millipore filters. In darkness, the pigment concentration was extracted at 2 % (W/V) methanol for 24 h at 4 °C. After centrifugation at 5,000 g for 10

min, the absorption was measured using a Thermo Fisher UV-Vis spectrophotometer (Waltham, MA, USA), using the mathematical equation according to (Ritchie, 2008) for Chl *a* (see Eq. 1) and for the total carotenoids, the equations reported by (Parsons and Strickland, 1963) (see Eq. 2). The results were expressed by  $\mu\text{g mL}^{-1}$  of volume of extract.

$$\text{Chlorophyll } a \text{ (Chl } a) = 11.4711 * (A_{664} - A_{750}) - 1.6841 * (A_{691} - A_{750}) \quad (\text{Eq. 2})$$

$$\text{Total Carotenoid} = 10 * (A_{480} - A_{750}) \quad (\text{Eq. 3})$$

The content of the phycobiliprotein pigments in the phosphate buffer and water extract processed was spectrophotometrically determined at 565 nm, 620 nm, and 650 nm using the dichromatic equations (Eq. 4, 5, and 6) reported by (Bennett and Bogobad, 1973). All the data were normalized against 750 nm. The results were expressed by dry weight of biomass. Triplicate samples were taken from each treatment.

$$\text{Phycocyanin (R - PC)} = \text{Abs620} - \left[ 0.7 * \left( \frac{\text{Abs650}}{7.38} \right) \right] \quad (\text{Eq. 4})$$

$$\text{Allophycocyanin (A - PC)} = \text{Abs650} - \left[ 0.19 * \left( \frac{\text{Abs620}}{5.65} \right) \right] \quad (\text{Eq. 5})$$

$$\text{Phycoerythrin (R - PE)} = \text{Abs565} - [2.8 * (\text{R - PC}) - (1.34) * (\text{A - PC}/12.7)] \quad (\text{Eq. 6})$$

The purity of phycoerythrin (extract purity, EP) in the aqueous extract was defined as the ratio between the absorbance measurements at 565 and 280 nm, using the following equation (Sudhakar et al., 2015):

$$\text{EP} = \frac{\text{Abs565}}{\text{Abs280}} \quad (\text{Eq. 7})$$



The extraction yield of phycoerythrin ( $\text{mg g}^{-1}$  Dried Weight) was calculated using the concentration of phycoerythrin (PE,  $\text{mg ml}^{-1}$ ), the volume of the extraction solvent (V, ml), and the mass of the dry biomass defined in the following equation (Sudhakar et al., 2015):

$$\text{Yield (mg g}^{-1}\text{)} = \frac{R - PE * V}{\text{Biomass}} \quad (\text{Eq.8})$$

### **Antioxidant capacity (DPPH and ORAC analyses)**

The antioxidant activity DPPH (2,2-diphenyl-1-picrylhydrazyl) assay (i.e.,  $\text{EC}_{50}$ ) according to (Blois, 1958) was estimated by reducing the stable free radical DPPH. The aqueous supernatant measurements were used for DPPH analysis; 150 mL of DPPH were added to each extract. This solution of DPPH was prepared in 90% methanol (90MeOH:10H<sub>2</sub>O) in 20 mL at a concentration of 1.27 mM. The reaction was complete after 30 min in a dark room at  $\sim 20$  °C and the absorbance was read at 517 nm in a Thermo Fisher spectrophotometer (Waltham, MA, USA). A calibration curve made with DPPH was used to calculate the remaining concentration of DPPH in the reaction mixture after incubation. Values of DPPH were expressed as  $\text{mg DW mL}^{-1}$ . Ascorbic acid was used as a positive control (Celis-Plá et al., 2014b).

The antioxidant capacity was analyzed in aqueous macroalgae extracts determined by the ORAC method described by (Fukumoto and Mazza, 2000). The reaction was carried out in 75 mM phosphate buffer (pH 7.4). The sample (100  $\mu\text{L}$ ) and the fluorescein (100  $\mu\text{L}$ ; 0.082 mM final concentration) solution were placed in the well of the microplate (black 96-well plates; Biotek, Synergy HT, USA). A 2,2'-Azobis (-amidino propane) dihydrochloride (AAPH) solution (100  $\mu\text{L}$ ; 0.15 M final concentration) was rapidly added using a multichannel pipette. The plate was immediately placed in the plate reader (Biotek, Synergy HT), and the fluorescence was recorded every minute for 150 min at 37 °C. Excitation and emission filters were 485-P and 520-P, respectively. The plate was automatically agitated prior to each reading. All reaction mixtures were prepared in triplicate and at least three independent runs were

performed for each sample. Blank using phosphate buffer instead of the antioxidant solution and calibration solutions using Trolox (0–8 mM final concentration) as the antioxidant was also performed in the same run. The area under the fluorescence decay curve (AUC) was calculated using the KC4 v.3.4 software, and finally, the ORAC value was expressed as mg Trolox equivalent mL<sup>-1</sup> substrate (mg TE mL<sup>-1</sup>).

### **Statistical analysis**

The interactive effect on the aqueous extracts selected, purity index, protein content, antioxidant activities, and pigment composition among extraction methods were evaluated through ANOVA (Underwood, 1996). For the ANOVA, two fixed factors were measurements for the solvent extraction: 1) ultrasound-assisted extraction, and 2) high pressure-assisted extraction. After significant effects, the interaction was determined with a *posteriori* the Student Newman Keuls (SNK) test (Underwood, 1996). Homogeneity of variance was evaluated using the Cochran test and visual inspection of the residuals (Underwood, 1996). In addition, the Pearson coefficient was calculated to determine the correlation pattern between antioxidant activity and photosynthetic pigments extracted by using the different mentioned methods. All analyses were performed using SPSS v.21 (IBM, USA).

The general variation patterns among biochemical variables, antioxidant activity and pigments composition measured in *S. skottsbergii* were explored using a multivariate approach. A principal component analysis (PCA) was performed for this purpose based on Euclidean distance using PERMANOVA+ for the PRIMER 6 package (Anderson et al., 2008). This multivariate ordination was used to investigate the variation of the content of biochemical responses concurrently by observing the ordination plot.

## RESULTS

### Chemical Assessment.

Total carbon ( $28.38 \pm 0.5$ ) and sulfur contents ( $5.63 \pm 0.05$ ) were higher than the nitrogen content ( $5.46 \pm 0.18$ ) (Table S1; see supplementary material). The C:N index in *S. skottsbergii* was  $23.85 \pm 0.49$ .

### Ultrasound-assisted extraction method

The extraction yields of R-PE as a function of the amplitude wave, time, and solvent for extraction (phosphate buffer and distilled water) are shown in Table I.2. The  $Y_{PE}$  ranged from 0.6-0.8 mg PE  $g^{-1}$  DW for phosphate buffer.

In comparison,  $Y_{PE}$  ranged from 1.7-2.6 mg PE  $g^{-1}$  DW in distilled water (Table S2; see supplementary material).

The mathematical model represents the extraction yield as a function of the independent variables (amplitude wave and time) in each solvent at the chosen ranges; these models are expressed according to the following equations:

$$Y_{ultrasound/buffer\ phosphate} = 0.8452 - 0.1569X_1^2 \quad (Eq. 10)$$

$$Y_{ultrasound/water} = 2.51 + 0.1562X_1 - 0.2566X_1^2 - 0.2771X_2^2 \quad (Eq. 11)$$

where  $X_1$  and  $X_2$  are the UAE amplitude wave (%) and time (min), respectively. The statistical significance of the regression model was demonstrated through the  $F$ -test and  $p$ -value ( $p < 0.05$ ).

For phosphate buffer, the ANOVA showed that there are statistically significant differences ( $p < 0.05$ ) in amplitude wave, with  $R^2$  0.84 and lack of fit of 4.91 ( $p$ -value = 0.170) ( $p > 0.05$ ) (Table S3; see supplementary material).

The most significant effect on R-PE extraction is the quadratic effect of amplitude wave (+0.15). For distilled water, the amplitude wave and time have significant differences in the yield extraction of R-PE, with  $R^2$  0.89 and a lack of fit of 1.34 (p-value =0.170) ( $p>0.05$ ) (Table S2; see supplementary material). The most significant effect on R-PE extraction is the linear and quadratic effect of amplitude wave (+0.15 and -0.25, respectively) and the quadratic effect of time (-0.27).

The linear positive and negative interaction effects suggest that the extraction yield increases by using distilled water as a solvent with an increase in the amplitude and, in addition, the extraction time is reduced. This effect can be observed in Figure II.2B, where the surface response plot illustrates the combined effect of the variables in the extraction yield trend.

### **High-pressure homogenization method**

The experimental result of the extraction yields of R-PE as a function of the pressure, number of passes and solvent for extraction (phosphate buffer and distilled water) are shown in Table II.2. In phosphate buffer, the  $Y_{PE}$  ranged from 3.1-5.1 mg g<sup>-1</sup> of R-PE by dry biomass. The  $Y_{PE}$  ranged from 4.6-5.7 mg g<sup>-1</sup> of R-PE for distilled water by dry biomass. The ANOVA applied to the data and the second-order model (Eq. 12 and 13) selected are summarized in Table S4 (see supplementary material). The mathematical model represents the extraction yield as a function of the independent variables (pressure and number of passes) for each extraction solvent in the chosen ranges; the models are written according to the following equations:

$$Y_{HPH/buffer\ phosphate} = 4.57 - 0.40X_1 - 0.786X_2^2 \quad (Eq. 12)$$

$$Y_{HPH/water} = 5.48 + 0.2537X_1 - 0.4217X_2^2 \quad (Eq. 13)$$

where  $X_1$  and  $X_2$  pressure (MPa) and the number of passes, respectively. The statistical significance of the regression model was demonstrated through the  $F$ -test and  $p$ -value ( $p < 0.05$ ). The response surfaces of Eq. 12 and 13 are displayed in Table S4 and S5, respectively (see supplementary material).

In the analysis of HPH by using phosphate buffer, the ANOVA showed that there are statistically significant differences in pressure and number of passes without interactions, with  $R^2$  0.86 and lack of fit 3.65 ( $p > 0.05$ ) (see supplementary material).

From the HPH model using phosphate buffer, the most significant effects on R-PE extraction are the linear effect of pressure (-0.40) and time (-0.78), whereas for the water solvent, the model shows similar effects of pressure (+0.25) and time (-0.42) on R-PE. The variables tested to increase the extraction yield indicating that the extraction is efficient use a range of pressure between 100-500 MPa and between 1-3 of a number of passes. Figures 3A and 3B represent the surface response plots illustrating the effects that the combinations of variables have on the extraction yield of phycoerythrin. The range of interest that optimizes the response at a pressure between 100-300 MPa, 2-3 passes with distilled water as solvent, is shown in Figure III.2B. The maximum predicted optimization point is 390.2 MPa, with two passes with distilled water. This condition was experimentally validated through performance responses of the purity index and was consistent with the predictive yield.

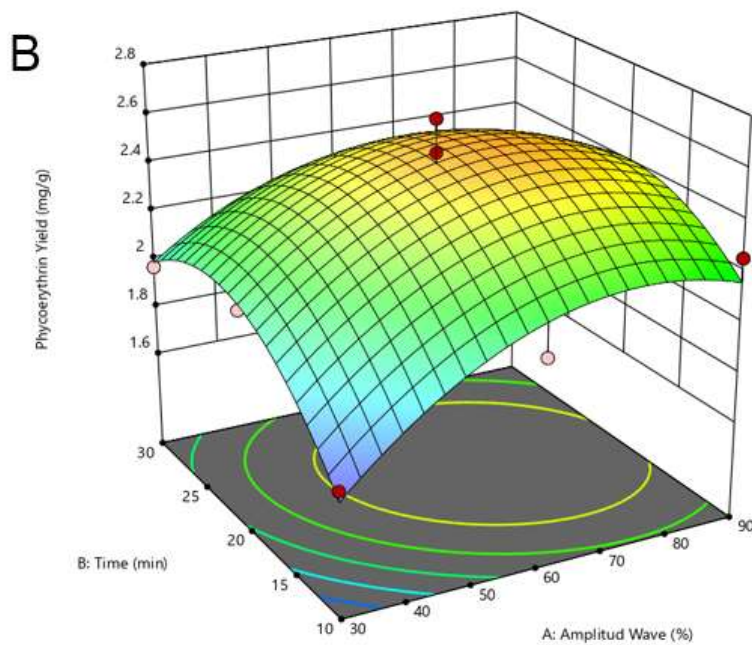
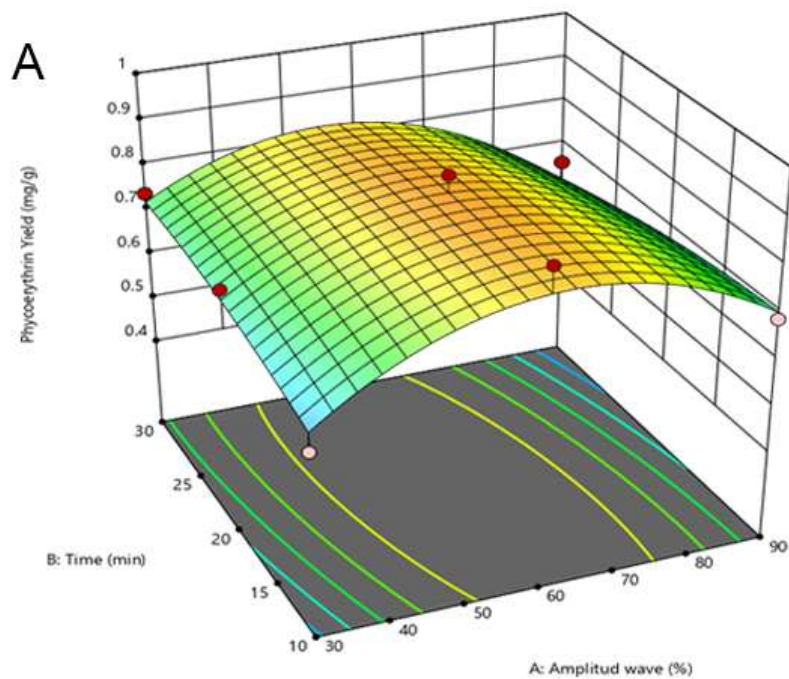


Figure II.2. Response surface (3D) plots to illustrate the effect between the amplitude wave ( $X_1$ ) and ultrasonic time ( $X_2$ ) by solvent extraction on the extraction yield: a) effect between  $X_1$  and  $X_2$  under phosphate buffer, b) effect between  $X_1$  and  $X_2$  under distilled water.

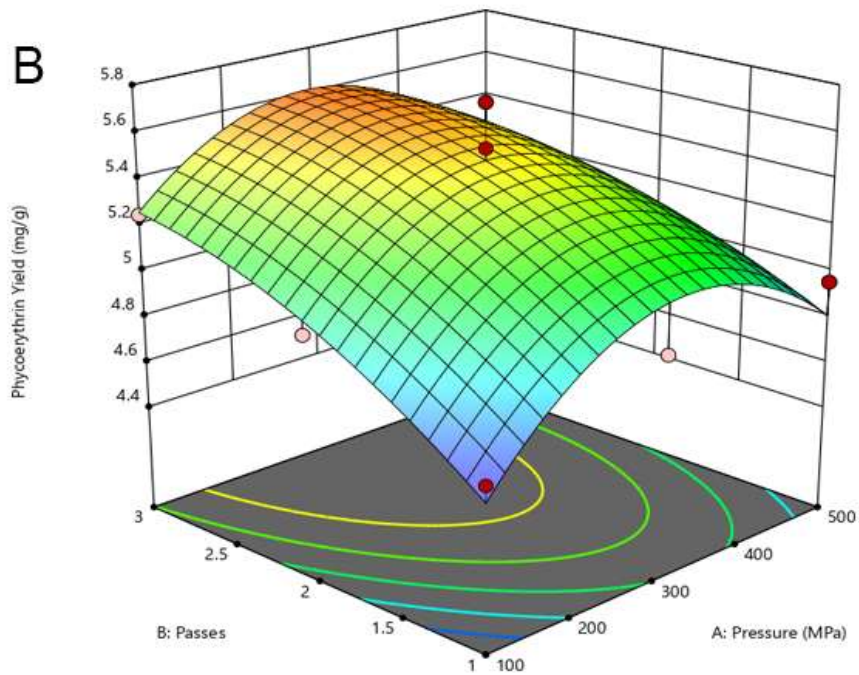
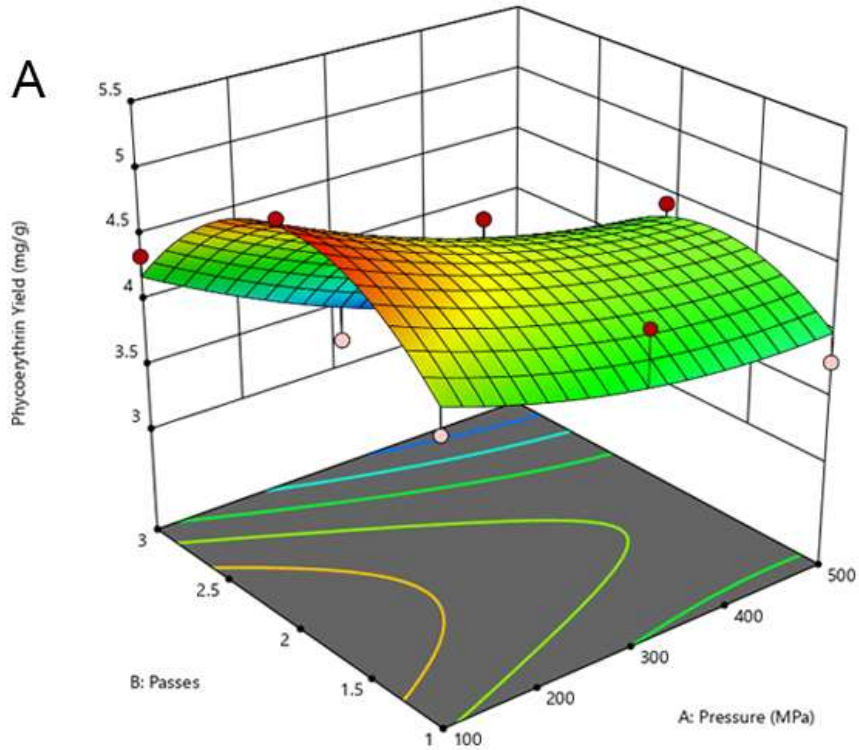


Figure III.2. Response surface (3D) plots to display the effect between the pressure ( $X_1$ ) and passes ( $X_2$ ) by solvent extraction on the extraction yield: A) effect between  $X_1$  and  $X_2$  under phosphate buffer, B) effect between  $X_1$  and  $X_2$  under distilled water.

## CHARACTERIZATION OF SELECTED EXTRACTS (R-PE YIELD, PURITY INDEX, ANTIOXIDANT ACTIVITIES AND SOLUBLE PROTEIN)

### R-PE Yield and Purity Index

According to our results, distilled water was the best extraction agent for UAE and HPH ( $p < 0.05$ ; Tables 3 and 4). The operational conditions selected for UAE were 60% of amplitude wave and 20 min. For HPH, the conditions selected were 300 MPa and two passes. The extraction yields of R-PE for UAE were  $2.3 \text{ mg g}^{-1} \text{ DW}$  and for HPH was  $5.7 \text{ mg g}^{-1} \text{ DW}$ , which were close to the values predicted by the second-order model of  $2.3 \text{ mg R-PE g}^{-1} \text{ DW}$  and  $5.6 \text{ mg R-PE g}^{-1} \text{ DW}$ , respectively. Thus, the second-order model was validated by these results. The quality of the phycoerythrin-enriched extract of these selected conditions is provided in Table III.2.

From the criterion (R-PE yield) of selected extract conditions by methods A (UAE) and B (HPH), the ultrafiltration process was applied for both methods. For the UAE, extracts A<sub>1</sub> are in distilled water and A<sub>2</sub> in phosphate buffer. B<sub>1</sub> extracts are in distilled water for the B extraction, and B<sub>2</sub> in phosphate buffer. The results showed that the 30 KDa polyethersulfone (PES) membrane allowed 100% PE recovery in all extracts obtained by UAE (Extracts A<sub>1</sub> and A<sub>2</sub>) and HPH (extracts B<sub>1</sub> and B<sub>2</sub>). The purity index of R-PE (A565/A280) was significantly higher in A<sub>2</sub> and B<sub>1</sub>. Among the treatments, B<sub>1</sub> extracts of HPH had the highest extraction yield, which reached 1.57, 0.42 times greater than extract A<sub>1</sub> obtained by UAE (Table III.2).



### **Antioxidant Activities**

The antioxidant activity by DPPH method ranged from 3.3 to 11.0 (% w/w dry biomass), showing significant differences among the extractions (Figure IV.2; Table S6)(see supplementary material). HPH had the highest level of antioxidant activity with distilled water ( $11.0 \pm 2.5$  %). On the other hand, the ORAC activity differed significantly among the different extraction treatments. The activity increased under both extraction treatments (UAE and HPH) in distilled water concerning the maceration method. However, the distilled water showed the highest activity detected between UAE and HPH. The antioxidant activity ranged between  $3.70 \pm 0.62$  and  $10.40 \pm 0.77$  % for the UAE conditions evaluated, while under HPH the ORAC was between  $3.30 \pm 0.32$  and  $11.0 \pm 2.5$  % (Table IV.2). The positive correlations were obtained between the antioxidant activity and the analyzed molecules. Chlorophyll *a* showed a positive correlation ( $r=0.80$  and carotenoids ( $r=0.73$ ) with antioxidant activity using the DPPH method (Table S7; see supplementary material). At the same time, phycoerythrin showed a positive correlation ( $r=0.75$ ) with the ORAC method (Tables S6 and S7; see supplementary material).

### **Multivariate analyses**

According to the extraction treatments, the principal component analyses (PC diagram, according to Figure V.2) showed a positive correlation of the first axis (81 percentage of total variation) with the samples for M1, M2, A2 and B2. Conversely, the variables phycoerythrin, carotenoids, ORAC, Chla and DPPH were highest in the samples of B1 and A1 extract and were positively correlated with the second axis (13.3 percentage of total variation) with intermediate values for *S. skottsbergii* (Figure V.2).

Table III.2. Characteristics of extracts obtained under selected conditions for ultrasonication (US) and high-pressure homogenization (HPH) methods. The average values  $\pm$  standard deviations of 3 replicates per treatment are shown. Different letters in a row indicate significant differences ( $p < 0.05$ ) (ANOVA, Student Newman Keuls,  $p < 0.05$ ). A1: Ultrasound (60 % amplitude; 10 min; water); A2: Ultrasound (60 % amplitude; 20 min; phosphate buffer); B1: High pressure (300 MPa; 2 passes; water); B2: High pressure (300 MPa; 2 passes; phosphate buffer).

| Experimental condition                                  | Extract A (US)                |                              | Extract B (HPH)              |                              |
|---|-------------------------------|------------------------------|------------------------------|------------------------------|
|   | A1                            | A2                           | B1                           | B2                           |
| Yield average ( $\text{mg g}^{-1}$ )                    | 2.17 $\pm$ 0.10 <sup>b</sup>  | 1.67 $\pm$ 0.3 <sup>a</sup>  | 5.67 $\pm$ 0.42 <sup>d</sup> | 4.55 $\pm$ 0.34 <sup>c</sup> |
| Purity (not concentrated)<br>( $A_{565}/A_{280}$ )      | 0.30 $\pm$ 0.005 <sup>b</sup> | 0.18 $\pm$ 0.01 <sup>a</sup> | 0.34 $\pm$ 0.05 <sup>d</sup> | 0.26 $\pm$ 0.01 <sup>c</sup> |
| Purity (concentrated at 30KDa)<br>( $A_{565}/A_{280}$ ) | 1.15 $\pm$ 0.02 <sup>b</sup>  | 0.86 $\pm$ 0.01 <sup>a</sup> | 1.57 $\pm$ 0.01 <sup>c</sup> | 0.95 $\pm$ 0.01 <sup>b</sup> |
| Soluble protein (%)                                     | 1.6 $\pm$ 1.0 <sup>a</sup>    | 1.5 $\pm$ 1.11 <sup>a</sup>  | 1.73 $\pm$ 1.10 <sup>a</sup> | 2.6 $\pm$ 0.32 <sup>b</sup>  |

Table IV.2. Pigment composition (phycoerythrin content, chlorophyll *a* and total carotenoids of the aqueous extract of *S. skottsbergii* under selected conditions for ultrasound (US) and high-pressure homogenization (HPH). The average values  $\pm$  standard deviations of 3 replicates per treatment are shown. Different letters indicate significant differences ( $p < 0.05$ ) (ANOVA, Student Newman Keuls,  $p < 0.05$ ). M1: Maceration by water; M2: Maceration by phosphate buffer; A1: Ultrasound by water; A2: Ultrasound by phosphate buffer; B1: High pressure by water; B2: High pressure by phosphate buffer.

| Extraction method | Extraction solvent | Phycoerythrin<br>(mg g <sup>-1</sup> DW) | Chlorophyll <i>a</i><br>( $\mu$ g DW mL <sup>-1</sup> ) | Total Carotenoids<br>( $\mu$ g DW mL <sup>-1</sup> ) |
|-------------------|--------------------|--|---|--|
| M1                | Distilled water    | 0.65 $\pm$ 0.38 <sup>c</sup>             | 0.08 $\pm$ 0.04 <sup>a</sup>                            | 0.31 $\pm$ 0.12 <sup>a</sup>                         |
| M2                | Phosphate buffer   | 1.32 $\pm$ 0.73 <sup>a</sup>             | 0.10 $\pm$ 0.04 <sup>a</sup>                            | 0.40 $\pm$ 0.11 <sup>a</sup>                         |
| A1                | Distilled Water    | 2.17 $\pm$ 0.10 <sup>e</sup>             | 0.62 $\pm$ 0.03 <sup>e</sup>                            | 2.13 $\pm$ 0.13 <sup>e</sup>                         |
| A2                | Phosphate buffer   | 1.67 $\pm$ 0.03 <sup>b</sup>             | 0.17 $\pm$ 0.05 <sup>b</sup>                            | 0.96 $\pm$ 0.02 <sup>b</sup>                         |
| B1                | Distilled water    | 5.67 $\pm$ 0.42 <sup>d</sup>             | 0.42 $\pm$ 0.01 <sup>d</sup>                            | 1.91 $\pm$ 0.05 <sup>d</sup>                         |
| B2                | Phosphate buffer   | 4.55 $\pm$ 0.34 <sup>c</sup>             | 0.24 $\pm$ 0.01 <sup>c</sup>                            | 1.37 $\pm$ 0.02 <sup>c</sup>                         |

## DISCUSSION

Red seaweed, such as *Porphyra* sp. (Nori), has a relatively high protein content (Mouritsen et al., 2018; Abdala-Díaz et al., 2019). However, in our study, the measured content of protein for *S. skottsbergii* (5.46 % DW) was lower than that of *Porphyra* sp. (Rhodophyta) (15.6 % DW), but higher than the brown alga *Laminaria ochroleuca* (Phaeophyceae) (alginate source) (4.8% DW) reported by Abdala-Díaz et al., (2019). Protein levels may vary in different species, geographical areas, seasons, and extraction methodologies (Pereira et al., 2020). Seaweed, especially red seaweed, appears to be an essential source of proteins and biliproteins (Mouritsen et al., 2018; Pereira et al., 2020). On the other hand, it has been seen that the degree of sulfation is related to bioactivity consistent with protein or polysaccharides. It is unknown if more significant bioactivity is present in this species related to sulfating of organic compounds. Carrageenan-based delivery systems present excellent performance in the delivery of bioactive ingredients, which can improve the stability and bioavailability of bioactive ingredients (Huang et al., 2021).

Generally, the R-PE yield depends on the extraction solvent. However, the yield decreased over 20 min of exposure to UAE. This situation can be attributed to the pigment denaturation due to the amplitude wave, which increases the extracted temperature (48 °C; data not shown). In this sense, more than 20 min is not recommended for *S. skottsbergii*, assuming that the chloroplast is slightly damaged, explaining the low release of R-PE (Pereira et al., 2020). Similar conclusions were reported by Simovic et al., (2022), who found a reduction of R-PE over 45 °C from the macroalga *Porphyra purpurea* (Rhodophyta) using the high-pressure method. Knowing the individual and combined effects of each variable on R-PE extraction, a model was constructed to predict the optimal conditions at which higher R-PE yields can be extracted. The range optimizes the response at an amplitude between 60-90%, 10-20 min extraction time, and distilled water as solvent. At the same time, the optimal predicted point is 68% amplitude

ultrasound, and 18 min with distilled water. These observations agree with Pereira et al., (2020), who found that between 15-20 min under an ultrasound probe would result in a high yield of phycoerythrin from the red alga *Gracilaria gracilis*. Although the researchers did not include the evaluation of amplitude wave, the extraction was done using phosphate buffer. This suggests that the effects of extraction yield depend on the extraction solvent and the species of the macroalga used. Mittal et al., (2017) analyzed different green technologies and observed that a sustainable yield of the phycoerythrin extraction was obtained by a combination of the ultrasound probe with homogenization under phosphate buffer solvent.

However, the extractions yields are reduced ( $0.16 \text{ mg of R-PE g DW}^{-1}$ ) compared to this study. As a extraction solvent, distilled water is the primary factor that enhances the extraction of phycoerythrin and is less influenced by the combined effects of ultrasound wave (%) and time in *S. skottsbergii* (Figure II.2A and 2B; Table II.2). These observations are in agreement with Jubeau et al., (2013), Sudhakar et al., (2015), and Tan et al., (2020), who reported higher levels when using distilled water for phycoerythrin extraction. The literature suggests that the UAE has the advantage of direct scalability due to its ability to generate high-intensity cavitation zones progressively and, therefore, suitable for scale-up of the industrial process (Le Guillard et al., 2015; Rodrigues et al., 2018). Previous studies have reported the successful extraction of phycobiliproteins using ultrasonic waves from other types of algae, such as the microalga *Porphyridium purpureum* (formerly *Porphyridium cruentum*) (Rhodophyta) and the macroalga *Dasyisiphonia japonica* (formerly *Heterosiphonia japonica*) (Rhodophyta) (Román et al., 2002; Benavides and Rito-Palomares, 2006; Sun et al., 2009). In this sense, Sharma et al., (2020) found that duty cycle variables and electrical acoustic intensity have significantly enhanced the C-phycoerythrin from *Oscillatoria* sp. (Cyanobacteria), whereas Ardiles et al., (2020) found the maximum R-PE yield was obtained under optimal US conditions (amplitude wave 100% and 15 min for *Porphyridium cruentum* (Rhodophyta)). However, when longer

treatment periods were used (>20 min), a degradation of phycobiliproteins was observed (Figure II.2A and 2B) (decrease in maximum absorbance), consistent with other studies (Rodrigues et al., 2018; Pereira et al., 2020).

Using high-pressure homogenization (HPH), we observed that the distilled water as an extraction solvent increases the R-PE yields with pressure and number of passes as a combined effect. Similar results were found by Sudhakar et al., (2015) and Jubeau et al., (2013), showing that water as extraction solvent can increase the yield of phycoerythrin extracts from red algae, as was observed in this study with *S. skottsbergii*. Our results suggest that the release of phycoerythrin can be promoted with distilled water due to accelerated molecule diffusion and solubility of other proteins. However, heat can also induce the degradation of the extracted bioactive compounds. The high amplitude of UAE (between 75-90% wave amplitude) and HPH (>450 MPa) produces a higher temperature (average of 40 °C; data not shown).

The macroalgae studied usually grow in the cold water (<10 °C) along the Magallanes coast of Chile; thus, the bioactive components could be susceptible to increased heat. These might explain why high pressure and high ultrasound caused a decrease in the phycoerythrin content of the extract. Similar results were observed by Pereira et al., (2020), where the pressure at 600 MPa induced an increase in the extracted temperature, promoting pigment denaturation. Simovic et al., (2022) reported that contrary to high temperature, the high-pressure (HP) treatment showed that a significant concentration at 450 MPa had a less destructive effect on R-PE color intensity from the macroalga *Porphyra purpurea* (Rhodophyta). However, the yields are less even if a range similar to our range optimization of 100-300 MPa is worked with. This difference may be due to the different species of red algae and geographical latitude because the morphology of the cell wall and accumulation of metabolites can vary despite R-phycoerythrin being the pigment with the highest proportion in red algae.

On the other hand, ice crystals are formed during the freezing step (Soni et al., 2006), which, when thawed, break down the cell walls and release the intracellular content directly (Hardouin et al., 2014). Therefore, the treatment with freeze biomass can be used to achieve higher yields. Similar results were observed by Pereira et al., (2020), where the samples frozen at  $-80\text{ }^{\circ}\text{C}$  obtained higher R-PE yields than those at room temperature. Ghosh and Mishra (2020) found that the interaction between buffer molarity (0.1 to 1 M) and the number of freeze-thaw cycles ( $-70$  to  $27\text{ }^{\circ}\text{C}$ ) was most significant for modeling the response optimization of phycoerythrin from *Lyngbya* sp. (Cyanobacteria). Tan et al., (2020) showed similar results with the combination of freezing at  $-80\text{ }^{\circ}\text{C}$  (2 h) and thawing at  $25\text{ }^{\circ}\text{C}$  (24 h) as optimal temperature and extraction time to obtain the highest number of phycobiliproteins for *Arthrospira* sp. (Cyanobacteria). However, several studies have shown that this increase was not significant due to the high content of cellulose deposited in the cell wall (Kannaujiya et al., 2017; Thoisen et al., 2017).

Regarding other species of red macroalgae, previous studies have shown that the extractions by mortar maceration of *Gracilaria corticata* and *Gracilaria canaliculata* (formerly *Gracilaria crassa*) yielded  $0.78\text{ mg R-PE g}^{-1}\text{ DW}$  and  $0.5\text{ mg R-PE g}^{-1}\text{ DW}$ , respectively. These values are still lower than by the HPH method but similar to our maceration extraction ( $0.65\text{ mg R-PE g}^{-1}\text{ DW}$ ). Previous results by Astorga-España et al., (2017), in the same species of *S. skottsbergii* by using phosphate buffer under the maceration method showed yields ranging from  $0.057\text{-}0.078\text{ mg g}^{-1}\text{ DW}$ . These differences can be attributed to the extraction method, solvent (phosphate or water), seasonal harvest, and red macroalgae species. However, our work demonstrates high yield levels found in distilled water either by HPH or UAE. In this sense, we believe that the sulfated polysaccharides are released into the matrix because of the increase in temperature, which increases the viscosity of polysaccharides.

Consequently, the cell shear stress is high in this water, allowing the release of a greater quantity to the phosphate buffer. The next step of this work is to study the degree of shear stress at the level of the extraction matrix and comparison between extraction solvents. Therefore, this is a new report of a commercial species where different green extraction methods and solvents are compared. Considering that *S. skottsbergii* is a commercial species, the cost of extraction using distilled water is lower than phosphate buffer, prior to the carrageenan extraction processes, visualizing a possible cost-effective biorefinery of this macroalga in local industry in Chile.

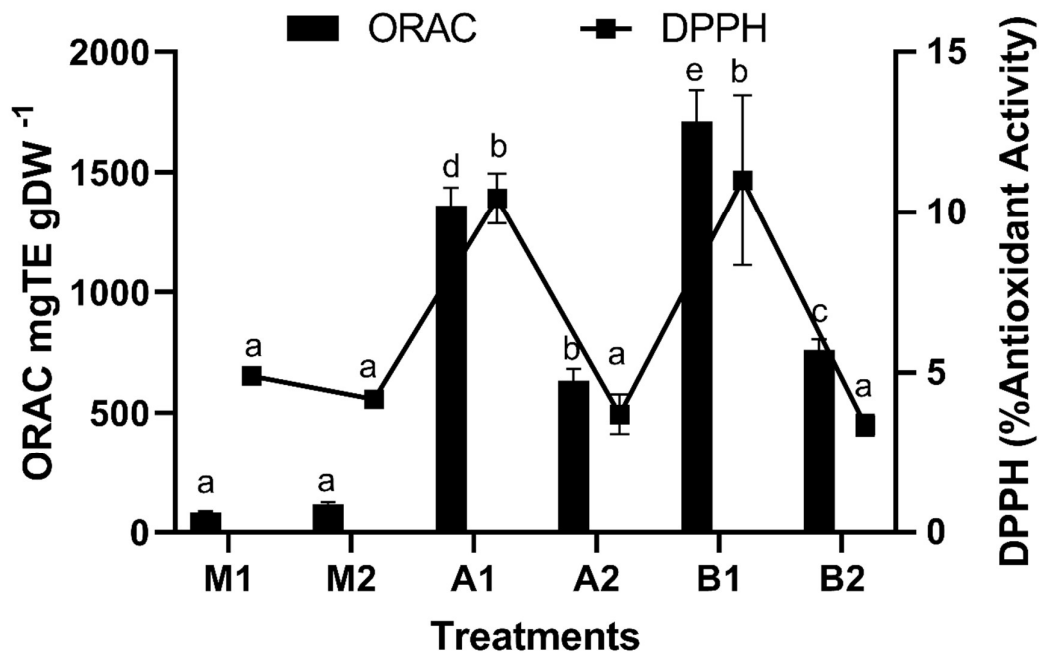


Figure IV.2. Total antioxidant activities (ORAC and DPPH) of the aqueous extract of *S. skottsbergii* under selected conditions for ultrasound (US) and high-pressure homogenization (HPH). The average values  $\pm$  standard deviations of 3 replicates per treatment are shown. Different letters indicate significant differences ( $p < 0.05$ ) (ANOVA, Student Newman Keuls,  $p < 0.05$ ). According to the extraction methods; M1: Maceration by water; M2: Maceration by



phosphate buffer; A1: Ultrasound by water; A2: Ultrasound by phosphate buffer; B1: High pressure by water; B2: High pressure by phosphate buffer.

From the observations in Figures 2 and 3, our results could be helping to improve the pigment, which remains at a desirable level, considering its commercial importance and potential applications in the functional food sector or supplement market.

Most of the *S. skottsbergii* proteins are more soluble in the extracts A<sub>1</sub> and B<sub>1</sub> than A<sub>2</sub> and B<sub>2</sub>, but not phycoerythrin, which is found more in water solutions (Jubeau et al., 2013; Sudhakar et al., 2015). This explains why the purity ratios are higher in distilled water than in phosphate buffer. The soluble proteins detected reached 2.6±0.32% and 1.73±1.1% using phosphate buffer and distilled water, respectively (p<0.05; Table 5). This result is in agreement with the report by Jubeau et al., (2013), where a higher purity ratio (0.79) in distilled water than in a culture medium was detected by applying a two-step high-pressure process in the microalga *Porphyridium purpureum*. Purification yields obtained here and for Denis et al., (2009) were different because of the biomass treatment, but the concentration of the R-PE was the same in the 30 KDa PES membrane. The permeate flux obtained during the filtration in the 30 kDa PES membrane was similar in all treatments, allowing for retention of all R-PE with no significant accumulation of unwanted molecules. Moreover, from an industrial point of view, PES membranes are more widely used than cellulose regenerated ones due to their lower fragility and higher resistance to chemicals, pH, and temperature variations (Denis et al., 2009; Mittal et al., 2017).

When using HPH in distilled water (pH 7.0), the levels are higher than in phosphate buffer (pH 6.5). It is precisely in distilled water where the high levels of phycoerythrin (treatment B1) and chlorophyll and total carotenoids (treatment A1) are found. This could be related to an increase in temperature and the release of polysaccharides that tend to increase the viscosity of the

matrix. This situation could change the pattern of the cells towards the pressure and the amplitude of the wave, as well as the solubility of PE, being higher in water as the solvent by both methods (UAE and HPH) compared to other solvents.

The R-PE in *S. skottsbergii* influenced by HPH with water solvent reached  $5.67 \text{ mg g}^{-1}$  by dry biomass. The content pigment in red algae is highly dependent on the perceived light intensity and quality of light (Castro-Varela et al., 2021). However, we suggest the application of HPH to release more R-PE content without reducing the stability, as shown in the purity index (Table III.2; Figure III.2). Thus, these results reinforce using phycobiliproteins (aqueous extracts) from a new source of *S. skottsbergii* for nutraceutical or pharmacological applications (Jung et al., 2016; Mittal et al., 2019).

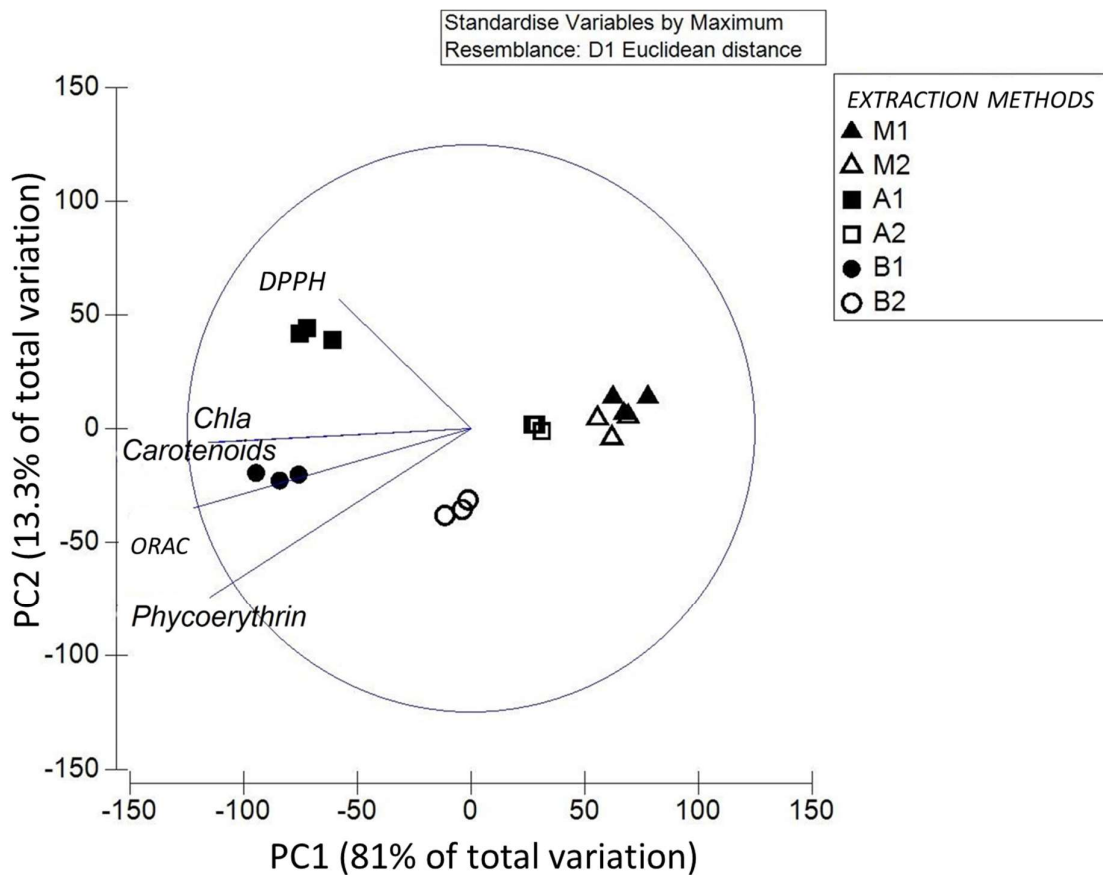


Figure V.2. Principal component analysis for pigment quantification and antioxidant activity in *S. skottsbergii* with respect to the extraction methods. M1: Maceration by water; M2:

Maceration by phosphate buffer; A1: Ultrasound by water; A2: Ultrasound by phosphate buffer; B1: High pressure by water and B2: High pressure by phosphate buffer.

There are still few studies that evaluate the impact of the extractive technique on the bioactive compound, which makes it difficult to compare our results with other works on pigment process optimization. In this respect, we consider that our work is the first approach to the state of the pigmentary material of this red macroalga after method extractions, and is of high interest as several authors have valued it for food applications (Le Guillard et al., 2015; Khanra et al., 2018; Liu et al., 2019; Mittal et al., 2019).

Biliproteins showed a positive correlation with the antioxidant activity of different red algae and cyanobacteria (Sekar and Chandramohan, 2008; Pagels et al., 2019). The pigments and antioxidant capacity of the water extract from the *S. skottsbergii* show a good relation. Biliprotein concentrations can vary depending on environmental factors like irradiance, light quality, pH or nutrients (Korbee et al., 2005b; Celis-Plá et al., 2014b; Astorga-España et al., 2017; Pagels et al., 2019). The extraction can also influence the content, e.g., a great number of authors used the freezing and thawing method (Niu et al., 2006). However, our observations showed significant antioxidant properties, which were increased with the enhancement of R-PE concentration in water solvent using the UAE and HPH methods. Although our study does not use a chromatographic technique for purification and determines the polyphenols and polysaccharides, the centered extract of R-PE could be part of a synergy of these compounds in the redox activity attributable to this macroalga.

## CONCLUSIONS

The extraction of R-PE from *S. skottsbergii* was optimized by RSM, using UAE and HPH. RSM proved useful for PE extraction in the tested optimization range, providing a model with

good agreement between the experimental and predicted results. HPH obtained the most efficient extraction, yielding 5.7 mg R-PE g<sup>-1</sup> DW biomass at the optimal conditions (300 MPa, 2 passes with distilled water), 50-60 % higher than the PE yields obtained with UAE. The most crucial variable in the extraction process was the pressure level, with higher concentrations of R-PE using distilled water. *S. skottsbergii* revealed an excellent source of R-phycoerythrin and antioxidant activity, and its application as a bioactive ingredient could be suggested for the food industry.

#### **AUTHOR CONTRIBUTIONS**

PCV, PCP, FLF, MR conceived and designed the experiments; PCV performed the experiments; all authors analyzed the data and co-wrote the paper.

#### **SUPPLEMENTARY MATERIAL**

<https://www.frontiersin.org/articles/10.3389/fmars.2022.877177/full#supplementarymaterial>

#### **FUNDING**

The research leading to these results has received funding from National Agency of Development and Research of Chile (PhD Scholarship N°21180257) and Andalusian government, Spain (Project FACCO, UMA18-FEDER JA-162).

#### **CONFLICT OF INTEREST STATEMENT**

The authors declare that the research was conducted in the absence of any commercial or financial relationships that could be construed as a potential conflict of interest.

## **ACKNOWLEDGMENTS**

We want to express our gratitude to Mr. Jaime Zamorano, Director of Development, from the GELYMAR S.A. for collaborate with this research project. We also want to thank to the Photobiology and Biotechnology of Aquatic Organisms research group (FYBOA, RNM-295) and the Institute of Blue Biotechnology and Developmen (IBYDA), University of Malaga due to the use of laboratory equipments and acknowledgments of the Laboratory of Coastal Environmental Research (LACER, University of Playa Ancha) for the technical support. P.S.M.CP thanks to CEA 22-20 project of the University of Playa Ancha regular competition research 2019.

---

# CHAPTER III:

## **A sequential recovery extraction and biological activity of water-soluble sulfated polysaccharides from the polar red macroalgae *Sarcopeltis skottsbergii***

This chapter has been submitted for evaluation in Marine Biotechnology Journal. Castro-Varela P., Rubilar M., Rodriguez B., Figueroa L.F., Abdala R. (2022). A sequential recovery extraction and biological activity of water-soluble sulfated polysaccharides from the polar red macroalgae *Sarcopeltis skottsbergii*. (*In revision*).

---

## CHAPTER III: A sequential recovery extraction and biological activity of water-soluble sulfated polysaccharides from the polar red macroalgae

### *Sarcopeltis skottsbergii*

Pablo Castro-Varela<sup>1,2</sup>, Mónica Rubilar<sup>3</sup>, Bruna Rodrigues<sup>4</sup>, Félix L. Figueroa<sup>1</sup>, Roberto Abdala-Díaz<sup>1</sup>

<sup>1</sup>Malaga University, Andalusian Institute of Blue Biotechnology and Development (IBYDA), Experimental Centre Grice Hutchinson, Lomas de San Julián, 2, 29004-Malaga, Spain. ([pablo.castro@uma.es](mailto:pablo.castro@uma.es) ; [felixfigueroa@uma.es](mailto:felixfigueroa@uma.es); [abdala@uma.es](mailto:abdala@uma.es))

<sup>2</sup>Doctorate in Engineering Sciences with specialization in Bioprocesses, Faculty of Engineering and Sciences, Universidad de La Frontera, Temuco, Chile.

<sup>3</sup>Department of Chemical Engineering, Faculty of Engineering and Sciences, Universidad de La Frontera, Temuco, Chile. ([monica.rubilar@ufrontera.cl](mailto:monica.rubilar@ufrontera.cl))

<sup>4</sup>Laboratory of Phycology, Department of Botany, Federal University of Santa Catarina, Florianopolis 88049-900, SC, Brazil. [bruna.rm01@gmail.com](mailto:bruna.rm01@gmail.com)

**Keywords:** Recovery extraction, Sulfated polysaccharides, Antioxidants Activity, Antitumor Active, Red seaweed.

## Abstract

Algal biomass is comprised of a variety of biochemical components that make it a viable raw material for use in a variety of applications using a biorefining process. From the residual supernatant generated by high-pressure homogenization for the extraction of the R-phycoerythrin pigment, two soluble polysaccharides (neutral and acid fractions) were obtained. The composition of total carbon (C), hydrogen (H), nitrogen (N), and sulfur (S), gas chromatography-mass spectrometry (GC-MS), Fourier transform infrared (FTIR-ATR) spectroscopy, antioxidant capacity (ABTS) and antiproliferative *in vitro* activities were evaluated. The two polysaccharides, which had a relatively high sulfate content, exhibited significant antioxidant activity in superoxide radical assay (ABTS) and high anti-proliferative effects on G-361, U-937, HCT-116 cancer cells. A high selectivity index ( $> 10$ ) was observed for the extract on G-361 and U-937 cell lines. However, inhibitory effects on the growth of 1064sK healthy fibroblast cells too. Neutral fraction polysaccharides with the lowest sulfate content gained relatively lower radical scavenging rates but showed significantly higher antitumor activities on G-361 melanoma cancer cells and non-toxicity on healthy cells. These results indicated that the *in vitro* antitumor and antioxidant activities of the two polysaccharides may be related to the combined effects of sulfate content and galactose content from the residual supernatant bioprocess. Potential interest for the cosmeceutical or nutraceutical industry is suggested.



## **Introduction**

An important part of the objectives of the blue bioeconomy is sustainable valorization of the aquatic biomass, marine, wild catch as well as aquaculture, to complement the terrestrial production of food, feed, non-food (biomaterials and chemicals) and bioenergy (Sanjeeva and Jeon, 2018). Seaweed is not only known as a rich source of nutrients but also as an important source of bioactive components. For centuries, seaweed has been used as both therapeutic and traditional medicines in many countries such as China and Korea (Kang et al., 2016; Sanjeeva and Jeon, 2018). In recent years, studies have shown that seaweed possesses polysaccharides with high antioxidant (Souza et al., 2012), anti-inflammatory, anticoagulant, antiangiogenic, and antitumor activities (Yan et al., 2019). In general, the bioactive properties and their compounds vary from species to species. Most of the bioactive compounds in seaweed are typically from the aqueous extracts. This is probably due to the known traditional practice in several parts of the world where seaweed is boiled, infused with hot water, or prepared as a soup to extract their medicinal properties before being consumed by the patient (Tjahjana et al., 2009; Liu et al., 2012). Furthermore, a very important difference, essential for biorefinery processing, is that seaweed does not have the recalcitrant lignin such as lignocellulosic materials characteristic for terrestrial plants (Martone et al., 2009).

The new and upcoming use seaweed bioprocessing is facilitating the development of new types of higher-value products, which are not just tasty but also gut-health-promoting ingredients. The main challenge, which determines the industrial utilization of seaweed potential, in addition to biomass availability, is the development of efficient extraction methods while preserving most of the intrinsic qualities of the raw material, with its functionalities and bioactivities intact. Several procedures exist for extracting and separating biologically active compounds from the algal biomass. Traditional extraction techniques for seaweed generally consist of maceration of the material in solvents for several hours at temperatures ranging from

ambient to 50–60 °C (Heffernan et al., 2016). Commonly used solvents include methanol, dichloromethane, or ethanol. Such conditions are quite severe and cause decomposition of most of the biologically active compounds and these solvents also have toxic effects. Thus, the primary challenge when extracting algal bioactive compounds will be to find a compromise between the cost of production of sufficient quantities and quality of compounds in the shortest timeframe, finding the optimum processing condition, and meeting the principles of green chemistry and green technology (Ponthier et al., 2020)

Recent trends to limit the use of chemicals have promoted the development of greener solvents, such as subcritical water extraction alone (González-Ballesteros and Rodríguez-Argüelles, 2020) or with ionic liquids as catalysts (Gereniu et al., 2018). Moreover, methods assisted by microwaves (Ponthier et al., 2020), ultrasound (Youssouf et al., 2017) or high pressure (Pereira et al., 2020), which reduces operation time and energy consumption compared with conventional extraction methods, are being used more frequently. However, depolymerization exhibits lower gel strength and viscosity (Gereniu et al., 2018).

High molecular weight polymers (up to 5000 kDa, average 200-800 kDa) are approved for food applications, whereas degraded polysaccharides (10-20 KDa) are not authorized (Cotas et al., 2020a). However, interesting activities of these degraded polysaccharides such as antitumor, antiviral, antibacterial, or immunostimulant have been reported (Luo et al., 2010; Tecson et al., 2021; Torres et al., 2021).

A water-soluble polysaccharide has several biological activities, as is common for a sulfated polysaccharide extracted from algae, with activities ranging from anticoagulant and antithrombotic, to immunomodulatory, antiviral, and antitumor effects (Guan et al., 2017). A role of sulfated polysaccharides from algae as antineoplastic agents has also been suggested. Several investigations have reported that sulfated polysaccharides have antiproliferative activity in cancer cell lines in vitro, as well as inhibitive activity in tumors growing in mice

(Rocha De Souza et al., 2006). Interest is increasing in several areas, such as pharmaceutical, environmental, and biosensor applications (Ooi et al., 2015; Esmaeili et al., 2017), as well as for drug administration approaches (Li et al., 2014) and tissue engineering (Popa et al., 2015). South America is the main producer of *Sarcopeltis skottsbergii* biomass. Chile produces about twenty thousand tons of dry alga to be commercialized mainly in Europe and Asia. The valuation of compounds in a biorefinery model is still in the early stages in algal biotechnology and thus have great prospects in the food, pharmaceutical, cosmeceutical, and nutraceutical industries (Juin et al., 2015; Jacotet-Navarro et al., 2016; Pereira et al., 2020).

Therefore, the modification of the process variables of technologies for the extraction and separation of sulfated polysaccharide from macroalgal biomass as well as the methodology followed are extremely important to keep extracts with high yield and the biotechnology properties. In previous studies in our group, we optimized water extraction by high-pressure homogenization (HPH-Assisted extraction) to recover R-phycoerythrin pigment from the red algae *S. skottsbergii*. The residue generated from the phycoerythrin aqueous extract was sequentially characterized found high proportion of polysaccharides (neutral and acid) compounds. The aim of this study was to determine the chemical composition and biological activities of the residual water fraction by high-pressure homogenization. Both types of sulfated polysaccharides (neutral and acid) were characterized by chemical analyses (CHNS; FTIR; GC-MS) and the antioxidant activity (ABTS) and cytotoxic effects on different human tumor lines such as human colon cancer (HCT-116), human melanoma (G-361), human leukemia (U-937) and in the human gingival fibroblasts cell line (1065SK) were assessed.

## Materials and Methods

### Algal biomass

Biomass from the marine macroalgae *Sarcopeltis skottsbergii* (Rhodophyta) is distributed along the coast of Chile, from Puerto Montt to the Antarctic Peninsula (63° 23'S) (Bischoff-Bäsmann and Wiencke, 1996b). In this study, the macroalgae was provided from the Magallanes Region by Gelymar Company S.A., Puerto Montt, Chile. The biomass was washed with filtered and distilled water to remove sand particles, epiphytes, and other undesirable materials before transporting under cold conditions to the Universidad de La Frontera, Temuco, Chile. Biomass was lyophilized (Biobase BK-FD18PT) for 48 h and the substrate samples were carefully milled with a grinder machine (Sindelen Mol165IN, China) until the particle size was less than US sieve screen number 18 (1 mm openings). The samples were sieved using a Ro-Tap testing sieve shaker (model RX-29-10, W.S. Tyler, Mentor, OH) through a set of sieves (ASTM E11:95). The average particle diameter ( $d_p = 0.70$  mm) was determined using Equation 1 of standard method S319.3 (American Society of Agricultural Engineers Standards, 2000).

$$d_p = \log^{-1} \frac{[\sum_{i=1}^{n-1} w_i \log \bar{d}_i]}{\sum_{i=1}^n w_i} \quad (1)$$

$\bar{d}_i$  (mm) is the geometric mean diameter of particles on  $i$ th sieve, or  $(d_i \times d_{i+1})^{1/2}$  where  $d_i$  is the nominal sieve aperture size of the  $i$ th sieve, and  $d_{i+1}$  is the nominal sieve aperture size in the next one larger than  $i$ th sieve.  $w_i$  is the mass of particles with an average diameter of  $\bar{d}_i$ . The biomass was stored at  $-18 \pm 2$  °C and the desired quantity of biomass was taken out as and when required for the experimentation.

### Biochemical analyses Total Carbon, Hydrogen, Nitrogen and Sulfur in biomass.

Total carbon (C), hydrogen (H), nitrogen (N), and sulfur (S) were determined from dry biomass (20 mg) using the total combustion technique used in the LECO TruSpec Micro CHNSO-Elemental Analyzer according to the manual. This technique is based on the complete and instantaneous oxidation of the sample by pure combustion with controlled oxygen at a temperature of up to 1050°C (C, H, N, S) and pyrolysis at 1300°C (O) for decomposition of O as CO and oxidation to CO<sub>2</sub>. The resulting combustion products, CO<sub>2</sub>, H<sub>2</sub>O, SO<sub>2</sub>, and N<sub>2</sub>, are subsequently quantified by a selective IR absorption detector (C, H, S) and TCD (N) differential thermo-conductivity sensor. The result of each element (C, H, N, S) is expressed in % with respect to the weight of the sample.

### **Polysaccharide extraction from the supernatant**

The neutral and acid polysaccharides were extracted from the water residues from R-phycoerythrin extraction under high-pressure optimization according to the method reported by Castro-Varela et al., (2022) (Fig. I.3). For this, neutral polysaccharides were stirred at 90°C and precipitated with the addition of ethanol (v/v) (Sun et al., 2014) and acid polysaccharide with N-cetylpyridinium bromide (Cetavlon) (Sigma-Aldrich, St. Louis, MO, USA) 2% (W/V) for 24 h (Abdala-Díaz et al., 2019). Then, polysaccharides were centrifuged at 4500 rpm for 5 min, 4 °C. The supernatant was discarded, and 10 mL of 4-M NaCl (Sigma-Aldrich, St. Louis, MO, USA) were added. This mix was stirred until completely dissolved. Once cooled, the ethanol was placed in a ratio 1:1 (% v/v) and kept at 4°C for 24 h. After centrifugation at 4500 rpm, 5 min, 4°C, the pellet containing the polysaccharides and salts was placed on a dialysis membrane (Sigma-Aldrich, St. Louis, MO, USA) in a 0.5M NaCl solution overnight at 4°C. Then, the dialyzed EPS was centrifuged at 4500 rpm for 5 min, 4°C, and washed with absolute ethanol. Finally, acid and neutral polysaccharides from supernatant extraction conditions (in

triplicate, n = 3) were stored at -80°C and subsequently lyophilized (Lyophilizer Cryodos, Telstar, Spain).

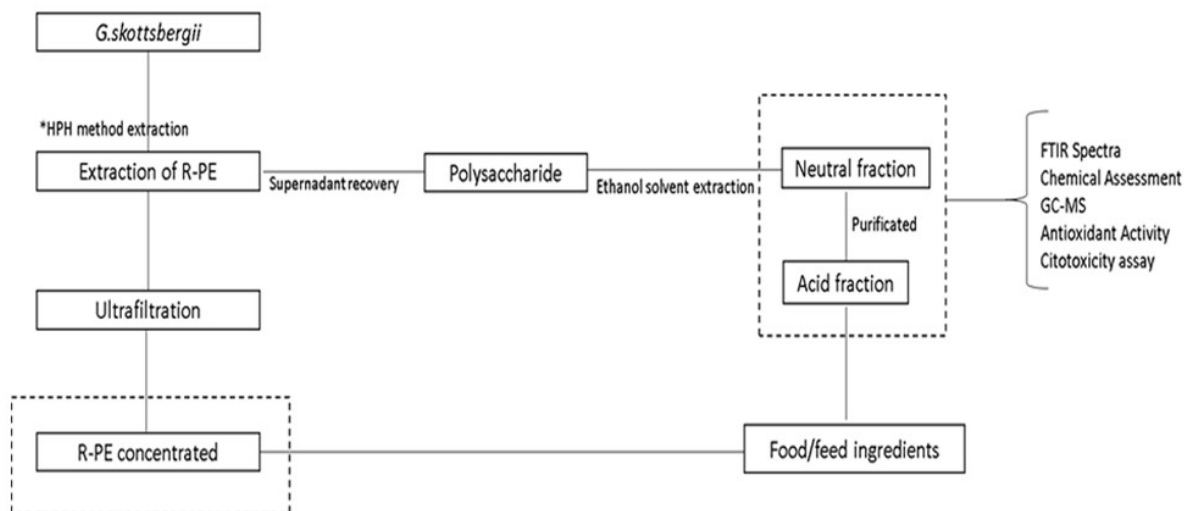


Figure I.3. Schematic representation of the biorefinery concept for the recovery of the neutral and acid polysaccharides. \*Optimized extraction by Castro-Varela et al., (2022).

### Total Carbon, Hydrogen, Nitrogen, and Sulfur in Polysaccharides

Total carbon (C), nitrogen (N), and sulfur (S) were determined from the extracted polysaccharides using the total combustion technique used in the LECO TruSpec Micro CHNSO-Elemental Analyzer. This technique is based on the complete and instantaneous oxidation of the sample by pure combustion with controlled oxygen at a temperature of up to 1050 °C (C, H, N, S) and pyrolysis at 1300 °C (O) for decomposition of O as CO and oxidation to CO<sub>2</sub>. The resulting combustion products, CO<sub>2</sub>, H<sub>2</sub>O, SO<sub>2</sub>, and N<sub>2</sub>, were subsequently quantified by a selective IR absorption detector (C, H, S) and TCD (N) differential thermoconductivity sensor. The result of each element (C, H, N, S) is expressed in % with respect to the weight of the sample.

### **Infrared Analysis of Polysaccharides**

Fourier transform infrared (FTIR) spectra of the polysaccharides were obtained by using self-supporting pressed disks 16 mm in diameter from a mixture of polysaccharides and KBr (1% w/w) with a hydrostatic press at a force of  $15.0 \text{ tcm}^{-2}$  for 3 min. The FTIR spectra were obtained with a Thermo Nicolet Avatar 360 IR spectrophotometer (Thermo Electron Inc., USA), having a resolution of  $4 \text{ cm}^{-1}$  with a DTGS detector and using an OMNIC 7.2 software (bandwidth  $50 \text{ cm}^{-1}$ , enhancement factor 2.6) in the  $400\text{--}4000 \text{ cm}^{-1}$  region. Baseline adjustment was performed using the Thermo Nicolet OMNIC software to flatten the baseline of each spectrum. The OMNIC correlation algorithm was used to compare sample spectra with those of the spectral library (Thermo Fisher Scientific, USA).

### **Antioxidant Activity (ABTS) Free-Radical Method**

The ability of the polysaccharides to scavenge free radicals was evaluated using an ABTS assay according to Re et al., (1999) with few modifications. Antioxidant capacity as 2,2'-azino-bis(3-ethylbenzothiazoline-6-sulfonic acid (ABTS) Assay Scavenging of Free Radical in Sulfated Polysaccharides and Biomass. The ABTS radical cation was produced through the reaction with ABTS. An aqueous solution containing was mixed 7 mM ABTS solution with 2.45 mM potassium persulfate for 16 h in the dark at room temperature. After incubation, the well-mixed solution was diluted to an absorbance of 0.7 at 413 nm with deionized water. The final concentrations of polysaccharide solution were: 25, 50, 75, 100, 150, 200, 300, 400, and  $500 \mu\text{g mL}^{-1}$ . For biomass, 100 mg DW in 1.5 mL of phosphate buffer was made. A total of 50  $\mu\text{L}$  of these samples were mixed with 940  $\mu\text{L}$  of phosphate buffer and 10  $\mu\text{L}$  of ABTS solution. The resulting mixture was measured with a spectrophotometer at 413 nm. ABTS radical scavenging capacity was calculated according to the following equation:

$$AA\% = [(A0 - A1)/A0] * 100 \quad (2)$$

where, A0 is the absorbance of the ABTS radical in phosphate buffer at time 0 and A1 is the absorbance of the ABTS radical solution mixed with the sample after 8 min. All determinations were performed in triplicate (n = 3) (Vijayabaskar and Vaseela, 2012).

### **Cell Cultures**

To perform the cytotoxicity analysis, the five following cell lines were chosen: human fibroblasts (1064sk, CIC-UGA, ES), human leukemia cell line (U-937, ATCC, USA), human malignant melanoma (G-361, ATCC, USA), and colon cancer cell line (HCT-116, ATCC, USA) stored in liquid nitrogen in the cell culture unit of the Central services for research support (SCAI) of Malaga University (UMA). To maintain the cells, 1064sk, G-361 and HCT-116s were previously cultured using Dulbecco's modified Eagle's medium (DMEM) (Capricorn Scientific, ref. DMEM-HPSTA) supplemented with 10% fetal bovine serum (Biowest, ref. S1810-500), 1% penicillin–streptomycin solution 100× (Capricorn Scientific, ref. PS-B), and 0.5% of amphotericin B (Biowest ref. L0009-100). U-937 were grown in RPMI-1640 medium (BioWhittaker, ref. BE12-167F) supplemented with 10% fetal bovine serum (Biowest ref. S1810-500), 1% penicillin–streptomycin solution 100×, and 0.5% of amphotericin B. In the case of the cells in suspension (U-937), was harvested upon reaching 70–75% confluence and centrifuged at 1500 rpm for 5 min at room temperature. Once centrifuged, the corresponding test or the subculture of the cells was carried out. The cells were kept under subconfluence in an atmosphere-controlled incubator with 5% CO<sub>2</sub> at 37 °C.

### **Analytic Method (MTT assay)**

For cancer and healthy cell viability assay, U-937, HTC-116, G-361 and 1064sk cells were incubated at polysaccharide concentrations of 5 to  $4.76 \times 10^{-6}$  mg mL<sup>-1</sup> in serial dilutions (1:1)



from the alga *S. skottsbergii*. The experiment was conducted individually with each cell line in a 96-well microplate for 72 h (37 °C, 5% CO<sub>2</sub> in a humid atmosphere). The proliferation of these cell lines was estimated by the MTT (3-(4,5-dimethylthiazol-2-yl)-2,5-diphenyltetrazolium bromide) assay (Abdala-Díaz et al., 2011). Briefly, a volume of 10 µL of the MTT solution (5 mg mL<sup>-1</sup> in phosphate buffered saline) was added to each well. The plates were incubated at 37 °C for 4 h. The yellow tetrazolium salt of MTT was reduced by mitochondrial dehydrogenases of metabolically active viable cells to form insoluble purple formazan crystals. Formazan was dissolved by the addition of acid-isopropanol (150 µL of 0.04 N HCl<sup>2</sup> propanol) and measured spectrophotometrically at 550 nm (Micro Plate Reader 2001, Whittaker Bioproducts, USA). The relative cell viability was expressed as the mean percentage of viable cells compared with the untreated cells. Four samples for each tested concentration were included in each experiment. Measurements were carried out in independent experiments in triplicate.

### **Calculation of the selectivity index (SI)**

The selectivity index determines the cytotoxic selectivity of the compounds tested and is calculated by the ratio between the IC<sub>50</sub> as indicated in the following equation:

$$SI = \frac{IC_{50} \text{ OF health cell}}{IC_{50} \text{ of cancer cell}}$$

According to Quispe et al., (2006) and Valdés-García et al., (2003), a selective compound presents a SI over 10.

### **Gas Chromatography–Mass Spectrometry (GC-MS)**

#### **Hydrolysis and Derivatization of Polysaccharides**

Polysaccharide samples (2 mg) and monosaccharide standards were treated with the same procedure. First, 100 µL of the standard stock solution of 1 mg mL<sup>-1</sup> of each monosaccharide

was dried under nitrogen gas flow. Second, the samples of polysaccharides, and a mixture containing the standard monosaccharides included in the IS (Internal Standard), were methanolized in 2 mL methanol/3 M HCl at 80 °C for 24 h. The monosaccharides glucose, galactose, rhamnose, fructose, mannose, xylose, apiose and myo-inositol (Internal Standard, IS), as well as pyridine, hexane and methanol/3 M HCl solution, were purchased from Sigma-Aldrich. Then, the saccharides were washed with methanol and dried under nitrogen gas flow. Third, the trimethylsilyl reaction was accomplished with 200 µL of Tri-Sil HTP (Thermo Fisher Scientific, Franklin, MA, USA). Each vial with the sample was heated to 80 °C for 1 h. The derivatized sample was cooled at room temperature and dried under a stream of nitrogen. Fourth, the dry residue was extracted with hexane (2 mL) and centrifuged. Finally, the hexane solution containing silylated monosaccharides was concentrated and reconstituted in hexane (200 µL), filtered and transferred to a GC-MS autosampler vial. Sample preparation and analyses were performed in triplicate.

### **Gas Chromatography-Mass Spectrometry (GC-MS) Analysis**

GC/MS analyses were performed using a Trace GC gas chromatograph (Thermo Scientific), Tri Plus autosampler and DSQ mass spectrometer quadrupole (Thermo Scientific). The column was ZB-5 Zebron, Phenomenex (5% phenyl, 95% dimethylpolysiloxane) with dimensions of 30 m × 0.25 mm i.d. × 0.25 µm. The column temperature program started at 80 °C (held 2 min) and underwent a gradient of 5 °C/min to reach a final temperature of 230 °C. The carrier gas was helium (flow 1.2 mL/min). The injection volume was 1 µL in splitless mode at 250 °C. The source and MS transfer line temperature were 230 °C. The mass spectrometer was set for a Select Ion Monitoring (SIM) program in electron ionization mode (EI) at 70 eV. The TMS-derivatives were identified by characteristic retention times and mass spectrum compared to those of the standards that were used for the identification of

monosaccharides. The compounds were identified by comparing the mass spectra with those in the National Institute of Standards and Technology (NIST 2014) library.

### **Statistical analysis**

The values obtained were expressed as means  $\pm$  standard deviations (SD) or standard error of the mean (SEM) depending on the case. To determine the statistical differences between each treatment, a one-way analysis of variance (ANOVA) was performed followed by a Student Newman Keuls (SNK) test (Underwood, 1996). Homogeneity of variance was evaluated using the Cochran test and visual inspection of the residuals (Underwood, 1996). All analyses were performed using SPSS v.21 (IBM, USA).

## **Results**

### **Chemical Assessment in biomass and Polysaccharide.**

Total carbon and sulfur contents were higher than the nitrogen content in biomass (Table I.3). The polysaccharides from *S.skottsbergii* presented the highest percentage in carbon, hydrogen, and sulfur, the latter being the content of a higher order in acid polysaccharide compared to the neutral polysaccharides. In the case of nitrogen, the neutral polysaccharides had a higher percentage than those acid polysaccharides. The molar C/N ratio was 1.72 times higher in the case of acid polysaccharides ( $121.02 \pm 0.4$ ) versus neutral polysaccharides ( $70.0 \pm 0.3$ ) (Table I.3).

### **Gas Chromatography–Mass Spectrometry (GC-MS)**

According to the monosaccharide TMS (trimethylsilyl) derivatives composition, the neutral fraction of polysaccharide, Glc (32.37%) was the major component, followed by Gal (28.37%) (Table II.3). The other acid fraction of polysaccharides, five types of monosaccharide TMS derivatives, such as Rhamnose (Ram), Xylose (Xyl), Mannose (Mann), Galactose (Gal),

Glucose (Glc) were detected through GC-MS analysis. The main monosaccharides were Gal, accounting for 67.21% of the polysaccharide. From the different peaks identified, the high values of Ram, Xyl, Mann and Glc accounted for 0.1%, 0.29%, 0.12%, 2.27%, respectively (Table II.3).

**Table I.3.** Total carbon (C), nitrogen (N), ratio C/N, hydrogen (H) and sulfur (S) (%) obtained in the biomass and polysaccharides (neutral and acid) from *Sarcopeltis skottsbergii*. The data represent the average  $\pm$  standard deviation (n = 3)

|                         | C                | N               | C/N              | H                | S                |
|-------------------------|------------------|-----------------|------------------|------------------|------------------|
| Total biomass           | 28.38 $\pm$ 0.5  | 1.19 $\pm$ 0.04 | 23.85 $\pm$ 0.49 | 4.83 $\pm$ 0.07  | 5.63 $\pm$ 0.05  |
| Neutral polysaccharides | 39.924 $\pm$ 0.2 | 0.57 $\pm$ 0.01 | 70.0 $\pm$ 0.3   | 7.219 $\pm$ 0.04 | 1.889 $\pm$ 0.02 |
| Acid polysaccharides    | 25.968 $\pm$ 0.1 | 0.214 $\pm$ 0.3 | 121.02 $\pm$ 0.4 | 4.086 $\pm$ 0.08 | 3.478 $\pm$ 0.03 |

**Table II.3.** Content of monosaccharides in neutral and acid polysaccharide analyzed by gas-liquid chromatography-mass spectrometry (GC-MS).

| Fraction of polysaccharides | Monosaccharide  | Retention time (min) | %     |
|-----------------------------|-----------------|----------------------|-------|
| Neutral polysaccharides     | Galactose (Gal) | 28.21                | 1.30  |
|                             | Galactose (Gal) | 29.06                | 5.28  |
|                             | Galactose (Gal) | 29.29                | 28.37 |
|                             | Glucose (Glc)   | 30.41                | 32.37 |
|                             | Glucose (Glc)   | 29.71                | 21.60 |
|                             | Glucose (Glc)   | 30.22                | 7.34  |
|                             | Glucose (Glc)   | 32.38                | 3.74  |
| Acid polysaccharides        | Rhamnose (Ram)  | 19.39                | 0.10  |
|                             | Rhamnose (Ram)  | 21.08                | 0.01  |
|                             | Xylose (Xyl)    | 21.98                | 0.23  |
|                             | Xylose (Xyl)    | 24.21                | 0.04  |
|                             | Xylose (Xyl)    | 26.94                | 0.29  |
|                             | Mannose (Mann)  | 27.81                | 0.12  |

|                 |       |       |
|-----------------|-------|-------|
| Galactose (Gal) | 28.24 | 67.21 |
| Galactose (Gal) | 29.08 | 25.31 |
| Galactose (Gal) | 29.3  | 1.66  |
| Glucose (Glc)   | 29.73 | 2.27  |
| Glucose (Glc)   | 30.24 | 0.78  |
| Galactose (Gal) | 30.44 | 1.92  |
| Glucose (Glc)   | 32.39 | 0.05  |

Xyl = Xylose; Mann = Mannose; Gal = Galactose; Glc = Glucose; Ram= Rhamnose.

### Fourier Transform Infrared Spectroscopy

The FTIR spectroscopy of the polysaccharides obtained from *S.skottsbergii* revealed the presence of several bands (Fig. II.3). In general, both polysaccharides show the characteristic peaks were very close. The strong and wide signal localized between bands 3500 and 2800  $\text{cm}^{-1}$  was also observed at approximately 1500–1300 and 1000–800  $\text{cm}^{-1}$ . However, peaks at 3000-2800  $\text{cm}^{-1}$  and 1500-1400  $\text{cm}^{-1}$  were only detected for acid polysaccharides. In fact, the peaks at 900-800  $\text{cm}^{-1}$  and 1600-1400  $\text{cm}^{-1}$  were caused by the bending vibrations of C-O-S of sulfate in an axial position and C-O of uronic acids respectively. The peaks between 1200  $\text{cm}^{-1}$  and 1000  $\text{cm}^{-1}$  were attributed to the sugar ring and glycosidic bond C-O stretching vibrations. Bands centered at 3500-3400  $\text{cm}^{-1}$  and 2900-2800  $\text{cm}^{-1}$  were assigned to hydrogen bonded O-H stretching vibrations and C-H stretching vibrations respectively.

### Antioxidant Capacity (ABTS Assay) in Biomass and Sulfated Polysaccharides

Antioxidant activity was evaluated in neutral biomass and fractions of polysaccharide. In the total antioxidant capacity (expressed as percentage of the radical scavenging capacity), all samples showed activity (Fig. III.3). The total biomass and neutral polysaccharide showed the lowest activity with 13 and 15% of scavenging effects, respectively. Moreover, the acid polysaccharide had the greatest activities with approximately 20% of scavenging effects.

Significant differences ( $p \leq 0.05$ ) were observed between the antioxidant activity of biomass, neutral and acid fractions of polysaccharide (Fig III.3).

### **Cell Viability of Lines HTC-116, G-361, U-937 and 1064SK**

The cytotoxicity of neutral and acid polysaccharides was determined in the human cancer cells (HCT-116; G-361; U-937) and healthy cells (1064sk). After the treatment of the cells with increasing concentrations of the two samples, cell proliferation was evaluated using the MTT assay. As shown in Fig. III.4 and III.5, all the samples exhibited relatively high inhibition ratios at all concentration levels and demonstrated a dose-dependent inhibition on the growth of cancer cells. It was observed that the lowest  $IC_{50}$  value in G-361 with neutral polysaccharides was  $243.2 \pm 2.56 \text{ mg mL}^{-1}$ , in U-937  $IC_{50}$  cells was  $561.6 \pm 10.23 \text{ mg mL}^{-1}$ , in HCT-116  $IC_{50}$  cells was  $963.9 \pm 11.63 \text{ mg mL}^{-1}$  (Figure V.3; Table III.2). For acid polysaccharides the lowest  $IC_{50}$  value in G-361 cells  $IC_{50}$  was  $0.6 \pm 1.86 \text{ mg mL}^{-1}$ , while in U-937  $IC_{50}$  was  $1.2 \pm 2.4 \text{ mg mL}^{-1}$  and in HCT-116 was  $283.6 \pm 12.3 \text{ mg mL}^{-1}$  (Figure IV.3; Table III.3). On the other hand, in the healthy cells line in 1064sK the neutral and acid polysaccharides were  $3459 \pm 18.3 \text{ mg mL}^{-1}$  and  $53.6 \pm 3.3 \text{ mg mL}^{-1}$ , respectively. The highest SI values calculated for the acid fraction extract also belonged to the three above-mentioned cell lines including G-361 ( $> 83.4$ ), U-937 ( $> 45.4$ ) and HCT-116 ( $> 0.19$ ) compared to the other cell lines (Table III.3). The SI values calculated for the neutral fractions for all the cell lines were low, ranging between 3.59 and 14.22, depending on the cell line, indicating higher effectiveness of the acid fraction extract on the cancer cell lines compared to neutral fractions polysaccharides. These results show an acute cytotoxic effect on the cancer and healthy cells where the acid polysaccharide presented relatively high antitumor activities against G-361 cells.

Table III.3. Cytotoxicity index (IC<sub>50</sub>) and selective index (SI) for different fractions of polysaccharides in the different cell lines : 1064 sK (human gingival fibroblasts cell line), HCT-116 (human colon cancer), G-361 (human melanoma cancer), U-937 (human leukemia cancer).

| Fraction of polysaccharides | Healthy and carcinoma active cell lines | Cytotoxicity Index IC <sub>50</sub> (μg mL <sup>-1</sup> ). | Selectivity Index (SI) |
|-----------------------------|---|---|------------------------|
| Neutral polysaccharides     | 1064sK                                  | 3459±18.3   | -                      |
|                             | HCT-116                                 | 963.9±11.63   | 3.59                   |
|                             | U-937                                   | 561.6±10.23   | 6.16                   |
|                             | G-361                                   | 243.2±2.56  | 14.22                  |
| Acid polysaccharides        | 1064sK                                  | 53.6±3.3  | -                      |
|                             | HCT-116                                 | 283.6±12.3  | 0.19                   |
|                             | U-937                                   | 1.2 ±2.4  | 45.40                  |
|                             | G-361                                   | 0.642 ±1.86   | 83.4                   |

## DISCUSSION

Our work is the first to use polysaccharides recovered from aqueous fractions derived from phycoerythrin extraction and their potential bioactivity from *S. skottsbergii* (Fig. I.3). Low temperature has been proposed to extract low-molecular-weight carrageenan and to maintain reducing, antiradical and anticoagulant activities, probably due to the higher sulfate content, which would be lost after hot water, acid and alkali treatments (Gómez-Ordóñez et al., 2014). From our observations, high-pressure homogenization offers a process efficiency of depolymerization where desulfation was not observed. It has been seen that the degree of sulfation is much higher in acid than total aqueous fraction (Table I.3), which could be evidence of its greater bioactivity. In the same vein, Fenoradosa et al., (2012) reported that high-pressure homogenization on the polysaccharide of *Halymenia durvillei* (red algae) showed its

feasibility and effectiveness and that an advantage of high-pressure depolymerization was the ease and speed of the preparation. In this sense, del Del Río et al., (2021) reported the use of microwave hydrothermal treatment for the multiproduct valorization of the invasive macroalgae *Sargassum muticum*, allowing the recovery of a liquid phase rich in fucoidan-derived compounds (up to 4.81 gL<sup>-1</sup>), oligomers and phenols with the antioxidant capacity of interest in the feed/food sector. On the other hand, ultrasound-assisted processes, both alkaline and aqueous, shortened extraction times compared to the conventional method, avoiding degradation of labile compounds, showing a slight variation in sulfate, AG and Gal contents and viscosity in the red algae *Hypnea musciformis* (Rafiquzzaman et al., 2017). Youssouf et al., (2017) reported that they doubled the yields attained in four-eight longer times with conventional extraction without affecting the chemical structure and molar mass distribution of carrageenans.

The FTIR spectra suggest that aqueous supernatant from *S.skottsbergii* have different polysaccharides in their cell wall mainly due to the different absorption in the range of 4,000 to 500 cm<sup>-1</sup> (Fig. 2). The broad stretching peak around 3,500 cm<sup>-1</sup> is characteristic of the hydroxyl group, while the weak stretching band at 3,000 cm<sup>-1</sup> suggests C–H bonds in neutral and acid polysaccharide. By contrast, the peak at 1,600 cm<sup>-1</sup> has been shown to indicate the presence of cyclic alkene C–C bonds(Pereira et al., 2009), whereas the peaks between 1,400 and 1000 cm<sup>-1</sup> are attributed to C-O stretching vibration (Parages et al., 2012) and to a combination of N–H bending and C–H stretching vibration in amide complexes. On the other hand, the peak of strong intensity at 1,250 cm<sup>-1</sup> could be attributed to the S=O (ester sulfate; Mollet et al., 1998) stretching vibration, which is associated with the spatial distribution of sulfated groups where the acid polysaccharide has greater intensity.



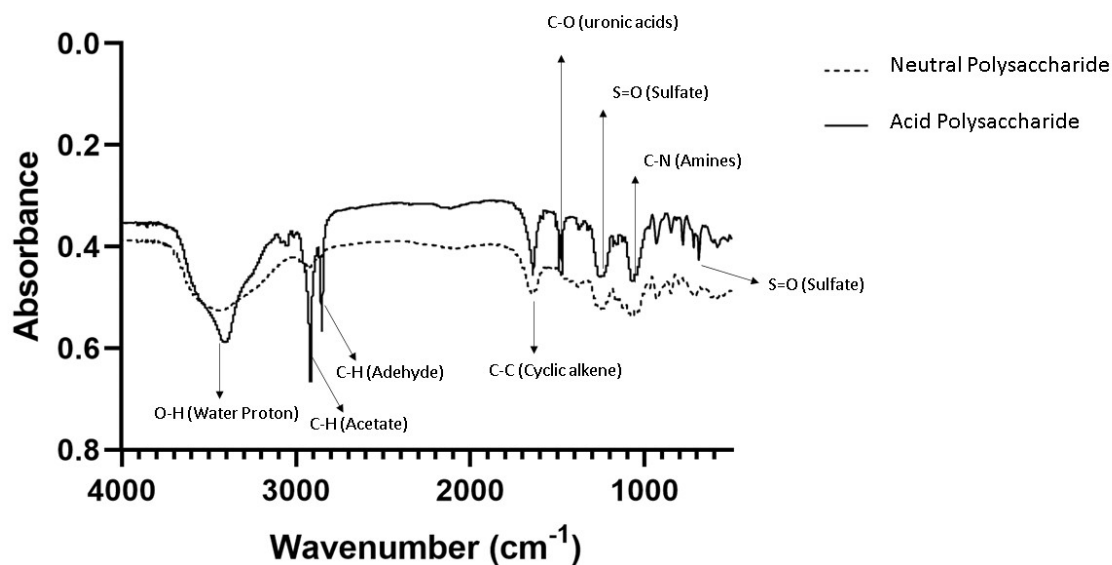


Figure II.3. FTIR spectra of the neutral and acid polysaccharides.

The antioxidant capacity of sulfated polysaccharides was measured using an assay based on electron transfer. In this study, we employed the  $ABTS^+$  cation radical as an oxidant. As illustrated in Fig. 3,  $ABTS$  radical scavenging activities of neutral and acid polysaccharide and concentration-dependent radical scavenging activity was also observed. But in general, the two polysaccharide samples exhibited lower scavenging activities (<50%) at all tested concentrations. Unlike excellent performances in concentrations between 300 and 500  $\mu\text{g L}^{-1}$ , the scavenging rates of acid polysaccharide was higher than 20% with the high sulfate content of 3.47%, while neutral polysaccharide achieved a radical scavenging average of 15%. Different radical scavenging activities of acid polysaccharide might suggest that the chemical composition had a certain effect on antioxidant activity. Studies over the last several years have revealed that sulfated polysaccharides from a number of types of seaweed have an appreciable antioxidant capacity. For example, sulfate polysaccharides from *Mastocarpus stellatis* (Red algae) had a significant positive correlation between sulfate and  $ABTS$  ( $r=0.83$ ) (Gómez-Ordoñez et al., 2014). Similar results in acid polysaccharide from *Gelidium corneum* (Red

algae) and *Porphyra umbilicalis* (Red algae) also showed significant antioxidant capabilities in hydroxyl radical scavenging assays (Abdala-Díaz et al., 2019). Multifunctional antioxidant capacity of different polysaccharide fractions in seaweed can be directly correlated to increasing sulfate content (Jiménez-Escrig et al., 2011) or to decreasing molecular weight of polysaccharides (Zhou et al., 2008). Our results suggested that sulfate content could be shown a relevant effect on radical scavenging of acid fractions compared to the neutral fractions. However, the high sulfate content in the total biomass showed lower ABTS activity. In this regard, the synergy between the compounds and the antioxidant activity does not always have to be directly proportional to the expected response, although it should be tested by other analyses such as DPPH, ORAC, among others.

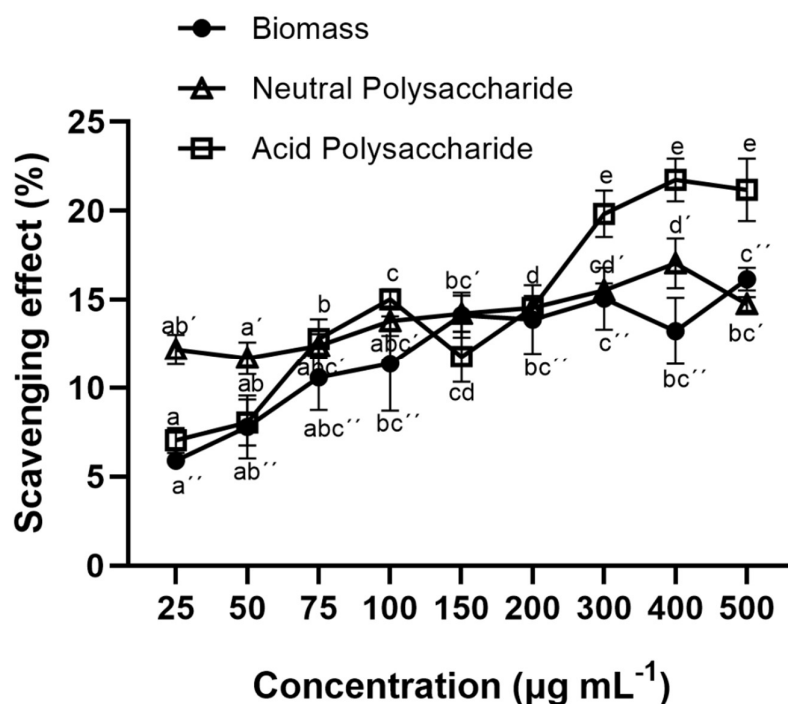


Figure III.3. Scavenging effects (%) of the sample of biomass, neutral and acid fractions in ABTS radical from *S. skottsbergii*. Different points with the same letter correspond to different concentrations with no significant differences between them (post-hoc Student-Newman-Keuls test).

The monosaccharide composition of the acid fractions show high amounts of galactose and small amounts of rhamnose, xylose, mannose and glucose (Table II.3). They are the most sulfated extracts. The neutral fractions only contained glucose and galactose. The polymerization was higher in acid than the neutral fraction with high-pressure homogenization. Then, high-pressure homogenization as a pretreatment before hot water was enough to allow further breakdown of the complex polysaccharide, very different to those of the neutral fractions. Mateos-Aparicio et al., (2018) found in *Gigartina pistillata* (Red algae) lower depolymerization (only two monosaccharides) with sequential extraction when using a lower temperature (60°C) with a water solvent. While Cotas et al., (2020b) in the same species *Gigartina pistillata* found high depolymerization with the modification of the concentration of alkaline solvent before the treatment with hot water (85-90 °C). On the other hand, Torres et al., (2021) did not analyze the profile of the monosaccharides of the biopolymer detected in the red algae *Mastocarpus stellatus*, but it is clear that the use of ultrasound-assisted extraction is a practical method for the degradation for the polysaccharides leading to low molecular weight oligosaccharides with new functionalities and bioactivities. The differences between the weight and content of monosaccharides are due to the physiological and nutritional stress of the macroalgae caused by environmental conditions, the different methods of extraction, derivatization, and analysis strategies (Álvarez-Viñas et al., 2019; Torres et al., 2019; Cotas et al., 2020a). Our results showed that the treatment to enhance the extraction process performance could be a pre-treatment before the hot water extraction of polysaccharides in shorter times than with conventional extraction. This considering a previous process temperature of 46 °C under high-pressure homogenization.

It has been reported that the sulfated groups played a major role in the suppression of cancer cell growth by binding with cationic proteins on the cell surface, and the polysaccharides with higher sulfate contents exhibited stronger antitumor activities *in vitro* (Rocha De Souza et al.,

2006; Parages et al., 2012; Xu et al., 2017; Abdala-Díaz et al., 2019b; Zhang et al., 2022). Interestingly, in this work, neutral and acid fractions of polysaccharides which had higher sulfate contents showed markedly higher antitumor activities against the G-361 cells, U-937 and HCT-116 cells. However, the neutral polysaccharide with the lowest sulfate content also exhibited inhibition (Table I.3). A previous study also showed that uronic acid could affect their antitumor and immunomodulatory activities (Shao et al., 2013). In this sense, our work did not detect uronic acid in either polysaccharide; however, there were significantly higher inhibition ratios. Similar results were found by Sheng et al., (2007), where different fractions of polysaccharides extracted from *Chlorella pyrenoidosa* exhibited high antitumor activity, exhibiting galactose and rhamnose as the main monosaccharides.

Therefore, uronic acid may not be the only factor that determines the antitumor activities of the two polysaccharides. Combined with the results from the antioxidant *in vitro* test, we infer that the higher antitumor and antioxidant activities of the two polysaccharides may be related to comprehensive effects of their sulfate contents; however, the relation between the chemical characteristics and bioactivities of polysaccharides needs further investigation. On the other hand, the anticancer activity of carrageenan has been reported to be closely related to its molecular weight. When native carrageenan was hydrolyzed in boiling water with HCl acid for 4 h, a significant increase in anticancer activity occurs (Yuan et al., 2005; Zainal-Arifin et al., 2014). However, carrageenan hydrolyzed in a microwave oven showed little improvement in anticancer activity (Ponthier et al., 2020). This suggests that the anticancer activity of carrageenan could be significantly enhanced by lowering its molecular weight only when it is depolymerized under mild conditions (Sun et al., 2015; Torres et al., 2019). In our case, when high-pressure homogenization was used, apparently depolymerization is suggested, where high levels of cytotoxicity index (IC<sub>50</sub>) on G-361, U-937 and HCT-116 was observed. Zainal-Arifin et al., (2014) reported similar results, when effects of carrageenan from *Eucheuma*

*denticulatum* (red algae) on human colon cancer Caco-2 with  $I_{50}=1000$  ( $\mu\text{g mL}^{-1}$ ) was analyzed, while in our analyses on HCT-116, the acid polysaccharides from *S. skottsbergii* presented 3.6 times higher cytotoxicity. In addition, the incorporation of ultrasound-assisted extraction can enhance the activity as reported by Torres et al., (2021) comparing the conventional extraction of carrageenan with ultrasound extraction. The cytotoxicity was 3.39 times more effective against in the same cancer cell line HT-29 than that reported by Suganya et al., (2016).

The low  $IC_{50}$  values for G-361 ( $0.642 \pm 13$ ) and U-937 ( $1.2 \pm 7$ ) as well as the high SI values for the extract in these cells ( $> 83.4$  for G-361 and  $> 45.4$  for U-937) suggest acid polysaccharide as a promising therapeutic candidate particularly on skin and blood cancers. Knowing that the greater the SI value is, the more selective it is and that SI values over 10 indicate general toxicity (Quispe et al., 2006; Valdés-García et al., 2003), we concluded that compared to neutral fractions, ( $< 14.22$ ), acid fraction extracts are better candidates for growth suppression of all the examined cell lines with SI values  $> 10$  (Table III.3). The fractionation of polysaccharides by extractive green systems such as high pressure could be an important effect due to the high affinity with biology systems. Future studies in an *in vivo* system are necessary to relate antiproliferative and antioxidant activities as potential nutraceuticals.

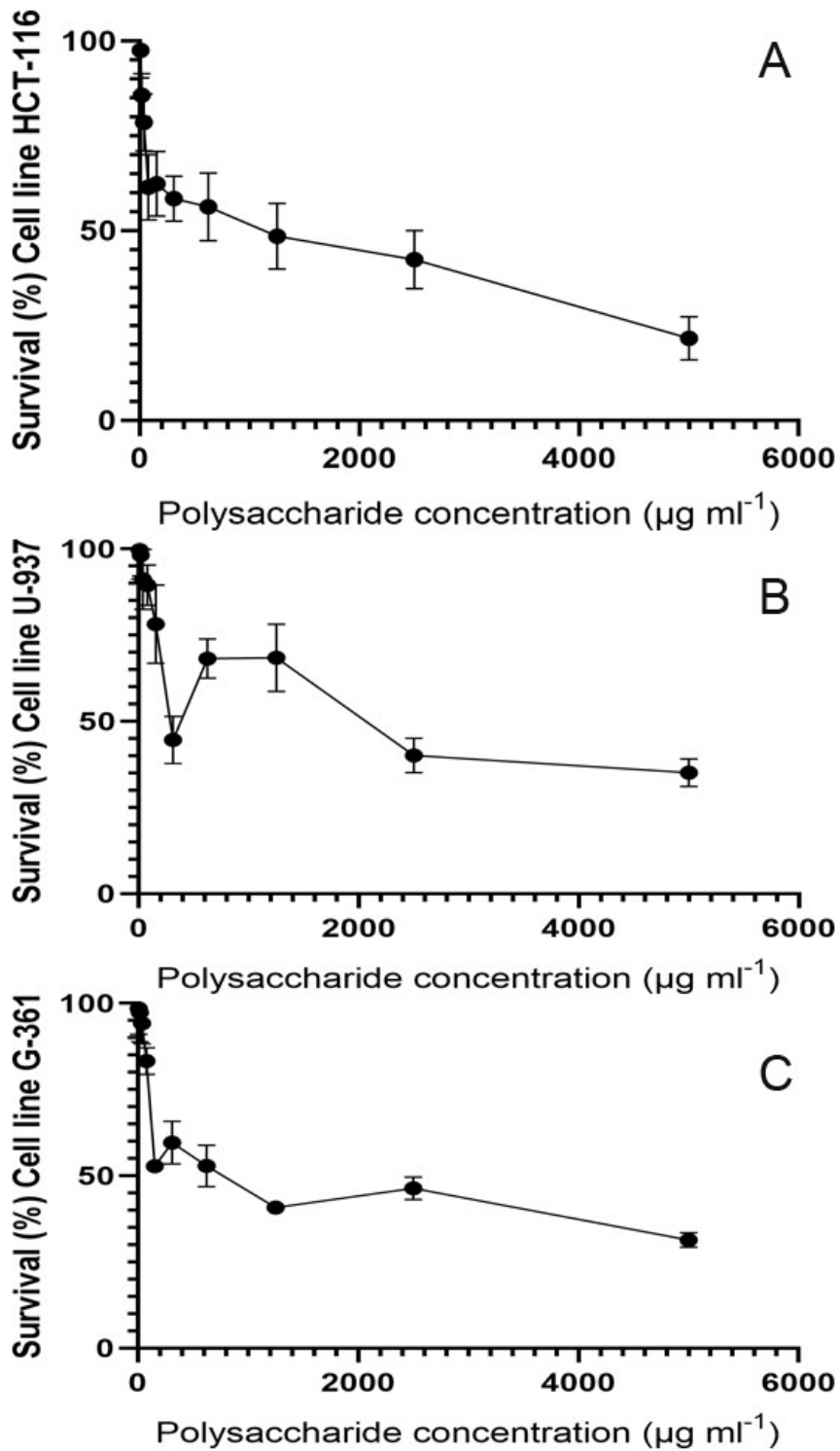


Figure IV.3. Survival (%) of cell lines exposed to different concentrations of neutral polysaccharides. (A) Survival (%) of HTC-116 cell line; (B) Survival (%) of U-937 cell line; (C) Survival (%) of G-361 cell line.

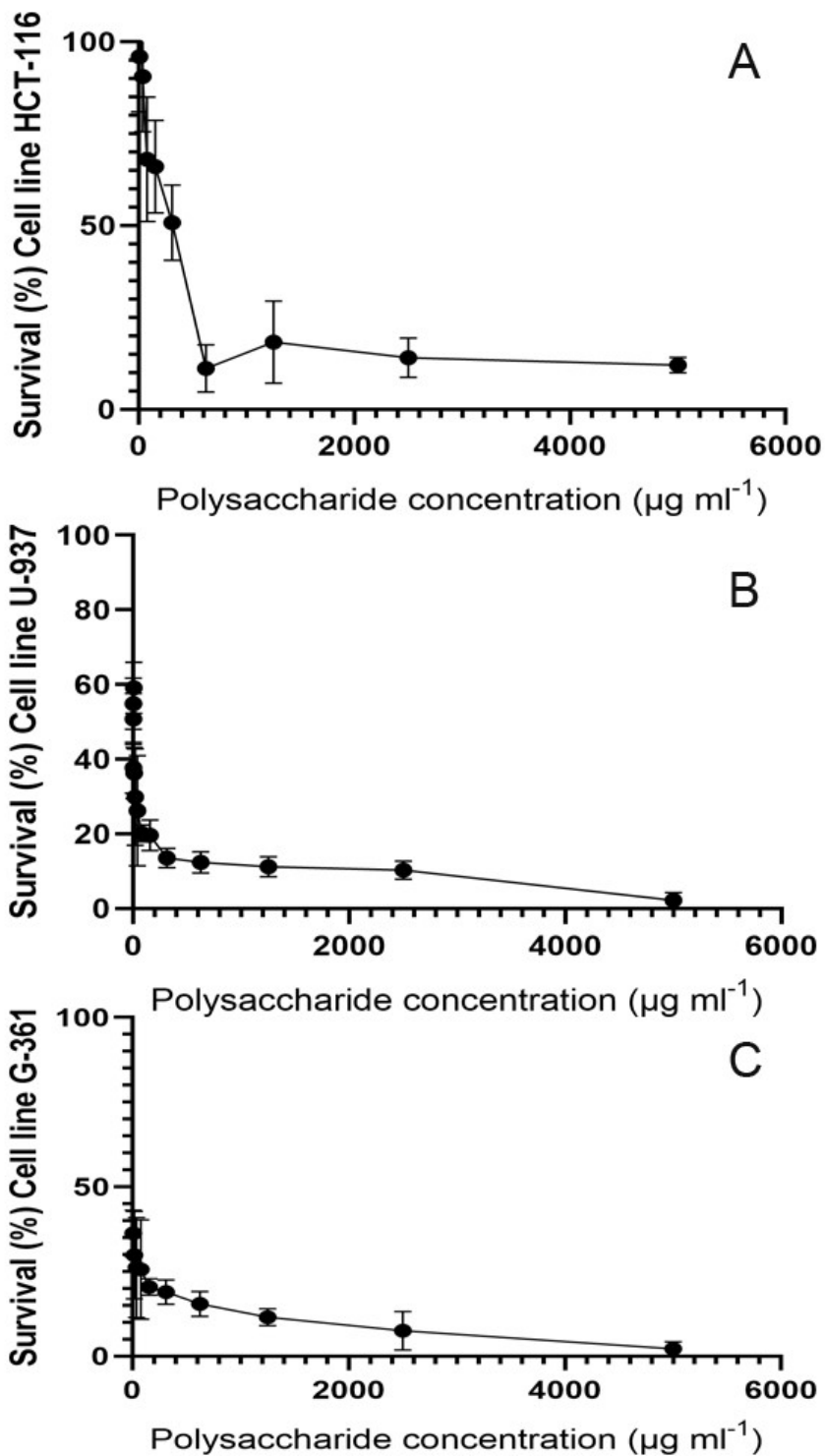


Figure V.3. Survival (%) of cell lines exposed to different concentrations of acid polysaccharides. (A) Survival (%) of HCT-116 cell line; (B) Survival (%) of U-937 cell line; (C) Survival (%) of G-361 cell line.

Finally, the two sulfated polysaccharides extracted from the red algae *S. skottsbergii* after previous extraction of phycoerythrin by high-pressure homogenization (HPH-assisted extraction) water extraction following a biorefinery approach exhibited antioxidant, antitumor activities, and dose-effect relations were observed. Specifically, acid polysaccharide with high sulfate and the galactose contents showed the highest activity in scavenging radical assays in the ABTS radical assay, i.e., a radical scavenging rate of 20% at the concentration between 300-500 $\mu\text{g mL}^{-1}$ . The antitumor activity of the acid fraction was significantly higher in all cancer cell lines tested than that of the neutral fraction. However, the neutral fraction with the lowest sulfate content and galactose content exhibited a middle level activity in the scavenging radical assay, but had higher antitumor activities against G-361 melanoma cancer cells with a high selective index of 14.22 and low toxicity on fibroblast healthy cells. Polysaccharide fractions recovered from a supernatant bioprocess as antitumor and antioxidant biocompounds could be applied in the cosmeceutical and food industries.

## ACKNOWLEDGMENTS

We want to express our gratitude to Mr. Jaime Zamorano, Director of Development, from GELYMAR Company for collaborating on this research project. We also want to thank the Photobiology and Biotechnology of Aquatic Organisms research group (FYBOA, RNM-295) and the Institute of Blue Biotechnology and Development (IBYDA), Malaga University. P.C.V. is grateful to the Universidad de La Frontera, Universidad de Málaga, Asociación Iberoamericana de Postgrado (AUIP) and National Agency of Research and Development of Chile (ANID; N°21180254) for a PhD scholarship.



## **FUNDING INFORMATION**

This study was supported by the Project “Blue nutricosmeceuticals with cyanobacteria and macroalgae (NAZCA)-Nutricosmeceútica azul con cianobacterias y algas (NAZCA-) PY20-00458 by the Adalusian Government, Spain.

## **CONFLICT OF INTEREST**

The authors declare that there are no conflicts of interest.

## **AUTHOR CONTRIBUTIONS:**

Conceptualization, P.C-V., M.R., F.L.F. and R.A-D.; methodology, B.R. and P.C-V.; experiments, P.C-V and B.R.; data curation, P.C-V, B.R. and M.R.; validation, P.C-V and B.R.; writing original draft preparation, P.C-V.; writing-review and editing, P.C-V., M.R., F.L.F. and R.A-D.; visualization, P.C-V; supervision, M.R., F.L.F. and R.A-D. All authors have read and agreed to the published version of the manuscript.

---

# CHAPTER IV:

## **High R-phycoerythrin bioavailability through alginate/shellac beads with enhanced antiproliferative activity.**

This chapter has been submitted for a patentability study by the Department of innovation unit of the Universidad de La Frontera, Chile.

Authors: Pablo Castro-Varela, Mónica Rubilar, Roberto Abdala Díaz y Félix López Figueroa.

---

## **CHAPTER IV: High R-phycoerythrin bioavailability through alginate/shellac beads with enhanced antiproliferative activity.**

**Pablo Castro-Varela<sup>1,2</sup>, Mónica Rubilar<sup>3</sup>, Manuel López<sup>4</sup>, Antonio Martines-Ferez<sup>5</sup>,  
Roberto Abdala-Díaz<sup>2</sup>, Félix L. Figueroa<sup>2</sup>**

<sup>1</sup>Doctorate in Engineering Sciences with specialization in Bioprocesses, Faculty of Engineering and Sciences, Universidad de La Frontera, Temuco, Chile.

<sup>2</sup>Institute of Blue Biotechnology and Development (IBYDA), Experimental Centre Grice Hutchinson, Lomas de San Julián, 2, 29004-Málaga, Universidad de Málaga, Spain.

<sup>3</sup>Department of Chemical Engineering, Faculty of Engineering and Sciences, Universidad de La Frontera, Temuco, Chile.

<sup>4</sup>Department of Chemical Engineering, Faculty of Sciences, Universidad de Málaga, Spain.

<sup>5</sup>Department of Chemical Engineering, Faculty of Sciences, Universidad de Granada, Spain.

**Keywords:** alginate/shellac, ionic gelation, simulated gastrointestinal digestion, antiproliferative activity

## Abstract

This work aimed to evaluate alginate/shellac mixture as wall material to develop aqueous phycoerythrin (R-PE) encapsulation system by external gelation and to determine the effect of encapsulation on the release properties of R-PE during simulated gastrointestinal digestion. Taguchi method to formulate beads with a high R-PE encapsulation efficiency (EE) was implemented. The effect of the variables: Feeding flow (90 and 20 mL h<sup>-1</sup>), distance (5 and 10 cm) and CaCl<sub>2</sub> (5 and 15 g L<sup>-1</sup>) were optimized and characterized the bead size, sphericity factor (SF) and total R-PE content of beads. Finally, the optimal alginate/shellac beads were submitted to *in vitro* dynamic gastrointestinal digestion. The results show that the beads formed under optimal conditions reached an EE value of 97.5%. The CaCl<sub>2</sub> concentration and feeding flow were the variables that most affect the R-PE EE. The beads obtained were semi-spherical, and non-aggregated with a particle size of 1.2 mm and SF 0.09. The release of R-PE from alginate/shellac was affected at acid pH 1; however, the concentration was under 10% of R-PE total content. The R-PE extract and R-PE encapsulated were partially degraded in gastric and intestinal conditions; the mouth did not detect signals from the protein profile. The encapsulation of alginate/shellac led to higher R-PE contents at the end of digestion compared with R-PE non-encapsulated, suggesting a protective role. From permeate streams, equivalent to the absorption of R-PE encapsulated, the bioavailability was 2.5 times significantly higher than R-PE non-encapsulated. A high selectivity index (> 10) was observed for the R-PE extract on the HCT-116 human colon cancer cell line. The alginate/shellac as a wall material and ionic gelation technology used may determine the release of the R-PE pigment at an intestinal site and their effect antiproliferative on health.

## Introduction

Evidently, the success of diverse nano/micro-encapsulation strategies hinges upon the potential of constructing a biocompatible wall material, which enables high loading of bioactive agents with zero premature release of the payload prior to attaining the destination (Assadpour et al., 2020; Rostamabadi et al., 2020). Biocompatibility of the wall matrix, high loading of desired bioactive components and providing a release mechanism through a controlled manner are some factors that should be considered in the selection of such matrices to serve as an efficacious delivery vehicle (Falsafi et al., 2020).

As one of the important classes of food-based encapsulation systems, biopolymeric nano/microparticles can be constructed via a single biopolymer matrix (through the precipitation process of carbohydrates or desolvation mechanism of proteins) (Joye and McClements, 2014); nanogels of particular biopolymers (e.g., alginate, whey/soy protein, chitosan, etc.) (Araiza-Calahorra & Sarkar, 2019; Hosseini & Rajaei, 2020); nano- tubes/fibrils of whey proteins (Khanh Nguyen et al., 2019); as well as complexation mechanism of two oppositely charged biopolymers (commonly a protein and a polysaccharide) (Devi et al., 2017).

Polysaccharide-based capsules are of a general importance in the encapsulation field (Madene et al., 2006). Their main functions are the successful encapsulation, transportation and controlled release of the capsule content to the external environment (Hu et al., 2008). For example, alginate is a natural anionic polysaccharide widely used to prepare capsule or pearl encapsulation systems due to its interesting physicochemical properties, biocompatibility, wide availability and low cost (Pawar and Edgar, 2012). The functionality of alginate beads depends to a large extent on their permeability and physicochemical stability. This alginate capsule has a retention and selective release, that makes it a good carrier for biotechnology applications; however, relatively high porosity is not adequate for some industrial applications (Mancini et

al., 1999). To overcome this problem, blends of alginate and other polymers such as shellac may be used to reduce wall porosity (Burgain et al., 2011; Chew et al., 2015). Shellac is a natural polymer from the insect *Kerria lacca* and it is considered a food additive by FDA (The United States Food and Drug Administration). In addition, it has a protective effect in the gastric fluid, which is an advantage when used in microcapsules to improve probiotic resistance (Schell and Beermann, 2014; Strummer et al., 2010). Thanks to its excellent film forming and protective properties, nontoxicity and biodegradability, this natural polymer is widely used as adhesives, thermoplastics, sealants, insulating materials, and coating materials in food and pharmaceutical industries (Aulton et al., 1995) and was also used as an oleogelator (Patel et al., 2013).

In recent years, the shellac biopolymer has attracted significant interest, to develop different types of encapsulation systems. Experiences have validated its incorporation as an additional external layer to coat capsules (Ben Messaoud et al., 2016). The combination of alginate and shellac has been used to protect aqueous extract of riboflavin by internal and external gelation (Ben Messaoud et al., 2016), microorganisms like probiotics (Silva et al., 2016) and lipophilic (sunflower oil) compounds to develop an oil encapsulation system by external gelation (Morales et al., 2017).

Since the extracted algal proteins are intended for human consumption, it is crucial to determine their digestibility under human gastric and intestinal conditions. High digestibility would enable greater absorption of the protein, or in fact, its amino acids or short peptides. Because human digestive proteases have their specificity to bonds near certain amino acids, it is important to verify that the algal protein can be digested by the human proteases. Protein digestibility may be assessed by simulating gastro-intestinal conditions by standard protocols (Minekus et al., 2014). Moreover, it is important to highlight that the biological activity of

algae proteins may decrease or be modified by the digestive enzymes during their passage through the gastrointestinal tract prior crossing the intestinal barrier into the blood circulation system (Xu et al., 2019). Additionally, it is crucial to carry out *in vitro* and *in vivo* bioavailability and bioaccessibility studies, as more scientific evidence is needed to support the benefits of algae compounds described so far, in order to validate their efficacy, especially *in vivo* (Pimentel et al., 2020).

The phycoerythrin (R-PE) is an oligomeric protein of 240 kDa with three subunits  $\alpha$  (about 16 kDa),  $\beta$  (about 21 kDa) and  $\gamma$  (about 39 kDa), and they are bound to specific cysteines by thioether bonds (Li et al., 2019). The study of phycobiliproteins focuses mainly on therapeutic (bioactive) applications, i.e., anti-inflammatory, antiviral, hepatoprotective, and anticarcinogenic capacities of R-PE have been reported (Thangam et al., 2015; Senthilkumar et al., 2018; Ulagesan et al., 2021). In previous studies in our group, we optimized by high-pressure homogenization (HPH-Assisted extraction) extraction R-phycoerythrin pigment from red algae *Sarcopeltis skottsberggi*. The concentrated extract is characterized by high yield, satisfactory purity and antioxidant activities.

Considering the potential of alginate/shellac model system to protect hydrophilic and lipophilic compounds and the advantages of the extrusion and co-extrusion process, this study aimed to develop alginate/shellac beads by external gelation as a model system to encapsulate efficiently R-phycoerythrin. Also, evaluate the effect of *in vitro* simulated gastrointestinal digestion and cytotoxic effects on different human tumor lines on the R-phycoerythrin beads. The optimal process conditions to prepare beads with efficiency encapsulation (EE) were determined by the Taguchi method with orthogonal array  $L_4(2^3)$ . The effect of the variables of flow rate, distance and concentration of calcium chloride ( $\text{CaCl}_2$ ) solution on the EE were evaluated. The particle size, release properties, confocal laser microscopy (CLSM) and scanning electron microscopy

(SEM) were investigated. The best obtained with optimal conditions were selected and evaluated their parameters of bioaccessibility and bioavailability processes on the simulation gastrointestinal system (SIMUGIT) and cytotoxic effects on different human tumor lines such as human colon cancer (HCT-116), human melanoma (G-361), human leukemia (U-937) and in the human gingival fibroblasts cell line (1065SK).

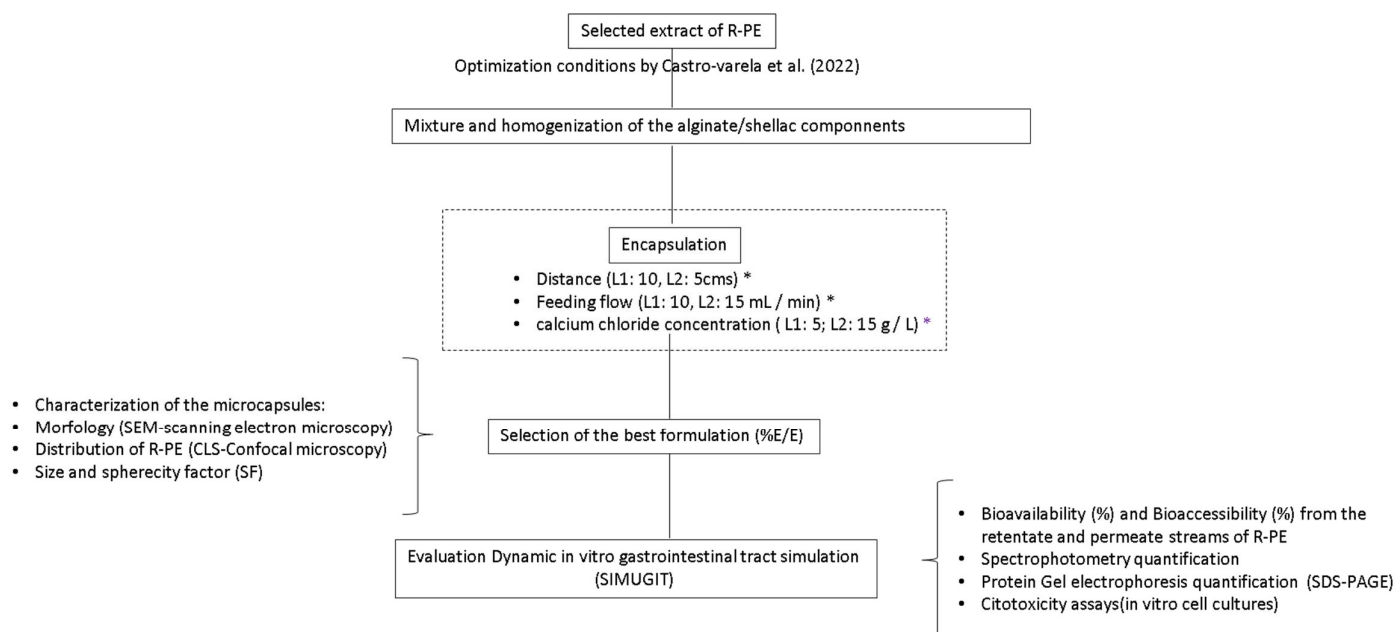


Figure I.4. Process and work conditions to form alginate/shellac beads and *in vitro* digestion simulating analysis. \* Taguchi experimental design: Independent variables and two levels of work.



## Materials and Methods

### Materials

Alginate and calcium chloride were purchased from Sigma Aldrich (St. Louis, MO). The Aqueous Shellac Solution NORELAC B20 was obtained from Norevo (Germany). NORELAC B20 is a 25% solids ammoniated aqueous shellac solution based on a selected shellac of high and uniform quality refined by solvent extraction. The bioactive, R-Phycocerythrin (biliprotein pigment), was obtained from the red algae *Sarcopeltis skottsbergii* previous optimization of extraction processes (Castro-Varela et al., 2022).

### Formulation of wall material (WM)

Sodium alginate solution (20 g/L) was prepared by mixing the alginate powder with distilled water under agitation at 700 rpm using a magnetic stirrer. Suspension was maintained under gentle agitation (1 h) until complete hydration and let stand for 60 min for deaeration. The wall material was prepared by mixing an alginate solution (20 g/L) and shellac solution (250 g/L) at a ratio of 75/25 (%v/v), with continuous agitation (30 min) at 500 rpm using a magnetic stirrer. Then, the pH of the resulting solution was adjusted to pH 7.5 with 1 M NaOH solution.

### Formulation of beads by external gelation.

Fig. 1 illustrates the process to prepare the alginate/shellac beads system with the bioactive (B). The B/WM ratios (80/20 to 20/80 % v/v) were prepared by mixing the bioactive (R-PE) with the previously prepared WM using continuous agitation (200 rpm for 15 min). The B/WM ratios were extruded by controlled flow system pump (SyringePump, Inc.) through of a 0.3 mm nozzle and dripped into 100 mL of a gelling bath containing CaCl<sub>2</sub> (5-15 g/L) to produce the beads.

The gelling bath was prepared by dissolving the CaCl<sub>2</sub> in an ethanol/ water mixture (1:1 v/v). The flow rate (30-90 mL/h) and the distance (5-15 cm) from the tips of the syringe to the surface of the gelling bath were evaluated. The beads formed were allowed to stand in the gelling bath for 30 min to ensure crosslinking.

### Experimental design for aqueous encapsulation

To optimize the encapsulation of R-PE with high EE (%), an experimental Taguchi design was applied. A matrix L4(2<sup>3</sup>) with three independent variables and two levels of work (L1 and L2) were used, applying the criterion 'bigger is better': fed flow solutions of Bioactive (R-PE)/WM (variable Flow; L1:20 mL/h; L2:90 mL/h), distance to the surface of the gelling bath (variable Distance; L1:5cms; L2:15cms) and concentration of calcium chloride solution (variable CaCl<sub>2</sub>; L1:5 and L2:15 g/L). The optimized theoretical equation (OTE) was determined by considering the average of the response with the greatest impact, identifying the most important variables and levels of work.

$$OTE = T + [(V_1, L_1) - T] + [(V_2, L_2) - T] + [(V_3, L_2) - T] \quad (Eq. 1)$$

where V is the variable, T is the average of the responded of experimental runs, L corresponds to the working levels.

### Determination of encapsulation efficiency (EE) of R-PE load

The phycoerythrin concentration (R-PE) was determined spectrophotometrically, using the equation of Bennett and Bogorad, (1973) as follows:

$$Phycocyanin (R - PC) = Abs620 - \left[ 0.7 * \left( \frac{Abs650}{7.38} \right) \right] \quad (Eq. 2)$$

$$Allophycocyanin (A - PC) = Abs650 - \left[ 0.19 * \left( \frac{Abs620}{5.65} \right) \right] \quad (Eq. 3)$$

$$\text{Phycoerythrin (R - PE)} = \text{Abs}_{565} - [2.8 * R - PC] - (1.34) * (A - PC/12.7)] \quad (\text{Eq. 4})$$

The encapsulation efficiency of microcapsule was calculated, following the method of Ge et al., (2009) with some modifications, by measuring the concentration of not-coated phycoerythrin and the concentration of phycocyanin added at the beginning of the microencapsulation process as follows:

$$EE(\%) = \frac{\text{initial concentration of R - PE} - \text{concentration of uncoated R - PE}}{\text{initial concentration of R - PE}} \times 100$$

### **Physicochemical properties of phycoerythrin microcapsules**

#### **Sphericity factor (SF)**

The size and shape of the beads were determined using the ImageJ software (National Institutes of Health, USA). A digital camera coupled to a binocular microscope was used to capture the images of the beads. SF was used to indicate the roundness of the beads, as described by Chan (2011), where a value equal to zero indicates a perfect sphere and higher values indicate a greater degree of shape distortion. SF was calculated according to Eq.:

$$SF = \frac{D_{max} - D_{per}}{D_{max} + D_{per}} \quad (\text{Eq 5})$$

where  $D_{max}$  is the maximum diameter passing through the bead centroid (mm) and  $D_{per}$  is the perpendicular diameter to  $D_{max}$  passing through the bead centroid (mm). All samples were assayed in triplicate to determine the mean and standard error. The bead size and shape were determined based on the measurement of 50 beads per sample.

## **Gastrointestinal-Tract-Simulating Membrane Bioreactor (GITSMB)—SimuGIT**

The dynamic gastrointestinal simulator system used (SimuGIT) was developed by the Research Group TEP025 of the Department of Chemical Engineering of the University of Granada and Malaga (Rivas-Montoya et al., 2016) (Figure I.I.4.1). The dynamic in-vitro Gastrointestinal-Tract-Simulating Membrane Bioreactor GITSMB (SimuGIT), schematically shown in Figure I.I.4, consists of a continuous stirred-tank reactor (CSTR) connected in series to a continuous plug-flow tubular reactor (PFTR) equipped with a monochannel tubular ceramic microfiltration membrane. The CSTR used to simulate the gastric digestion in the stomach is a benchtop fermenter supplied by Braun Biotech International (model Biostat B). It comprises a conventional autoclavable stirred tank glass vessel equipped with an impeller stirrer (180 W, model Rushton) and a proportional-integral-derivative (PID) unit control system for the temperature, level, foam, dissolved oxygen, and pH. The control system unit includes an RS-422 interface that enables the control of the CSTR with a computer. The CSTR has an external jacket to maintain constant temperature, such that the temperature in the vessel is measured by means of a Pt-100 digital sensor and is accurately controlled ( $T_{\text{setpoint}} \pm 0.1 \text{ }^{\circ}\text{C}$ ) by the PID loop connected to a thermostatic laboratory bath. The CSTR system also has sampling and reagent addition inlets by means of several peristaltic pumps (Eyela, modelMP-3). The pH inside the CSTR is measured by a pH electrode (Hamilton, model Easyferm Plus K8) immersed in the vessel and adjusted by an own-made pH control system based on data acquisition modules, which acts on two different peristaltic pumps that dose the acid and basic solutions (HCl or NaHCO<sub>3</sub>). The digested solution exiting the CSTR is continuously driven to the PFR. To this end, the PID control system acts on impulsion and return peristaltic pumps (two of the four peristaltic pumps integrated in the benchtop fermented, as previously described), such that by varying the flow rates of these pumps, it is possible to regulate the pressure inside the hydraulic circuits, as well as the product filtration rate. In addition to this own-developed

control pressure mechanism, the operating pressure can be adjusted accurately (P setpoint  $\pm$  10 mmHg) with a spring-loaded pressure-regulating valve (SS-R4512MM-SP model, Swagelok) and monitored by a digital pressure gauge (Endress + Hauser, model Ceraphant PTC31). The continuous PFR connected in series to the CSTR serves for the simulation of the conditions in the intestine. It consists of a cylindrical tube made of stainless steel (provided by Prozesstechnik GmbH, Basel, Switzerland) equipped with a monochannel ceramic microfiltration (MF) membrane in tubular configuration provided by Atech Innovations GmbH. The MF membrane used for the experiments is an inorganic one of  $\alpha$ -Al<sub>2</sub>O<sub>3</sub> active surface with a mean pore diameter equal to 0.2  $\mu$ m and molecular weight cut-off in the range 1.2 kDa (model 20N). The dimensions of the selected membrane are 1000 mm in length, 6 mm in duct diameter, and  $2 \pm 0.5$  mm in thickness. This type of MF membrane also ensures a series of advantageous characteristics, such as high resistance to temperature (suitable for steam sterilization at 121 °C) and pressure (up to 10 bar) during the cleaning protocols, pH stability (0 to 14), possibility of back pulsing, very high abrasion resistance (against aggressive chemical reagents), optimal permeability recovery, as well as high selectivity and performance, and long lifetime service. The PFR is integrated with the CSTR by means of a drive and return system made of chemically resistant polyethylene tubes. Finally, a precision electronic mass balance with USB connectivity (Sartorius, model Quintix 5102, accuracy equal to 1 mg) is coupled to an automatic sampling and data registration system in order to register values of permeate (bioaccessible fraction that crossed the membrane) with time.

### **GITSMB Conditions**

- Gastric Phase

When the trial began, the bath temperature that keeps the reactor jacket warm was set at 37.5  $\pm$  1 °C throughout the process, and the reactor stirring speed was set at 50 rpm to simulate the

peristaltic movements of the stomach. Next, 800 mL of GSF and 14 mL of SSF were prepared using the reagents in accordance with Brodkorb et al., (2019). The concentrations used of each reagent for each fluid were pre-established in accordance with Brodkorb et al., (2019). Once prepared, the GSF was introduced into the reactor and heated to a temperature of 37.5 °C. At this point, the pH dropped to 3, as the empty stomach was simulated before adding the food with the microcapsules. In parallel, 20 g of water mineral were weighed and 1g of phycoerythrin were added. Since two different samples (encapsulated of phycoerythrin and nonencapsulated) were chosen, two separate tests were carried out. The SSF was then mixed with the food preparation + microcapsules; 1 mL alpha-amylase solution (75 U/mL), 0.1 mL  $\text{CaCl}_2 \cdot 2\text{H}_2\text{O}$  of concentration 0.3 M, and 4.9 mL distilled water were added (final salivary fluid to food preparation ratio of 1:1). The mixture was shaken for 2 min and the pH was adjusted to 7 (if necessary). Once the GSF was hot, the mixture of the food with the SSF was added to the reactor tank, stirred for a few seconds, and an initial sample was taken. Then, a 10 mL solution of pepsin (2000 U) and 50 mg of phospholipid (Lipoid p45) were added, and the pH was adjusted to 3 by controlled dosing of 6 M HCl. From this moment on, a sample was taken every 5 min for the next half-hour.

- Duodenum Phase

When the gastric phase ended with the last sample taken, the pH of the GSF was raised to 6.5 by dosing 1 M  $\text{NaHCO}_3$  at a rate of 2.05 mL/min and a sample was taken after adjustment. This pH simulates the action of pancreatic juices on the food being digested. Intestinal enzymes were added: 10 mL solution of pancreatic lipase (2000 U/mL), biliary salts (for a final concentration of 5 mM), 10 mL solution of pancreatin (10%), and 1 mL solution of trypsin (50 mg/assay). Digestion in the duodenum takes about 10 min after the addition of enzymes, and a

sample was taken after that digestion period. The approximate total duration of this phase (including pH rise, addition of enzymes, and digestion) was 30 min.

- **Intestinal Absorption Phase**

To simulate intestinal absorption, fluids from the bioreactor were pumped to flow through the modular filtration system CSTR into the PFTR, where filtration through the 0.05 $\mu$ m membrane size was chosen for these trials, based on tests carried out previously (Abad et al., 2019; González et al., 2019). The system overpressure limit was set at 50 mmHg, so that the diffusion of phycoerythrin through the membrane was only due to passive transport. It is important to remind that the ionization characteristics of a compound can have a profound effect on the rate of its transfer by passive diffusion because only the unionized species are capable of passive diffusion across the membrane. Once the circuit was primed and fluids began to fall into the bioreactor, the intestinal absorption phase was considered to have begun and lasted 180 min. Samples were taken at 30, 60, 90, 120, 150, and 180 min. Two samples were taken each time, one from the fluid filtrated through the membrane (permeate) and another from the retained fluid, which forms part of the colonic residue (retained).

In summary, each simulation test lasted approximately 4 h: Gastric phase (30 min), duodenal phase (30 min), and intestinal absorption phase (180 min). Each trial was conducted in duplicate. Throughout the trial, the system program generated a data file in which all the events and processes that occurred during the simulation were recorded. This file was then processed in the computer to obtain information on all the variables.

### **Analysis of the Samples**

All samples collected during the assay were refrigerated and, subsequently, the concentration of phycoerythrin present in the fluids in each sample was measured using spectrophotometry

analysis according to the Bennet & bogoard, (1976). The concepts of release or bioaccessibility and bioavailability were used in order to measure the amount of phycoerythrin released along the digestive tube that is present in the chymus and the amount absorbed by the membrane, respectively. The release corresponds to the pigment fraction delivered by microcapsules in the gastrointestinal tract during the gastric and duodenal phases, and was calculated using Equation (6), adapted from Rivas-Montoya et al., (2016). When release and precipitation processes took place simultaneously, the same equation was used to calculate the bioaccessible percentage as the released and non-precipitated fraction in the chymus. On the other hand, bioavailability corresponds to the pigment fraction absorbed by difusion through the membrane during the intestinal absorption phase, and was calculated using Equation (7), adapted from Ariza et al., (2018).

$$\text{Bioaccessibility (\%)} = \frac{\text{pigment phycoerythrin in chymuss}}{\text{initial pigment phycoerythrin in microcapsules}} \times 100 \quad \text{Eq. 6}$$

$$\text{Bioavailability (\%)} = \frac{\text{phycoerythrin amount in IAS}}{\text{initial pigment phycoerythrin in microcapsules}} \times 100 \quad \text{Eq. 7}$$

where IAS means intestinal absorption samples. In both equations, the amounts of phycoerythrin present in the chymus and in the microcapsules are expressed in milligrams of R-PE by total biomass ( $\text{mg g}^{-1}$ ).

### **Cell Cultures and MTT assay in microcapsules.**

To perform the cytotoxicity analysis was carried out according the methodology described in Chapter III (section cell cytotoxicity) following cell lines were chosen: human fibroblasts (1064sk, CIC-UGA, ES), human leukemia cell line (U-937, ATCC, USA), human malignant melanoma (G-361, ATCC, USA), and colon cancer cell line (HCT-116, ATCC, USA).



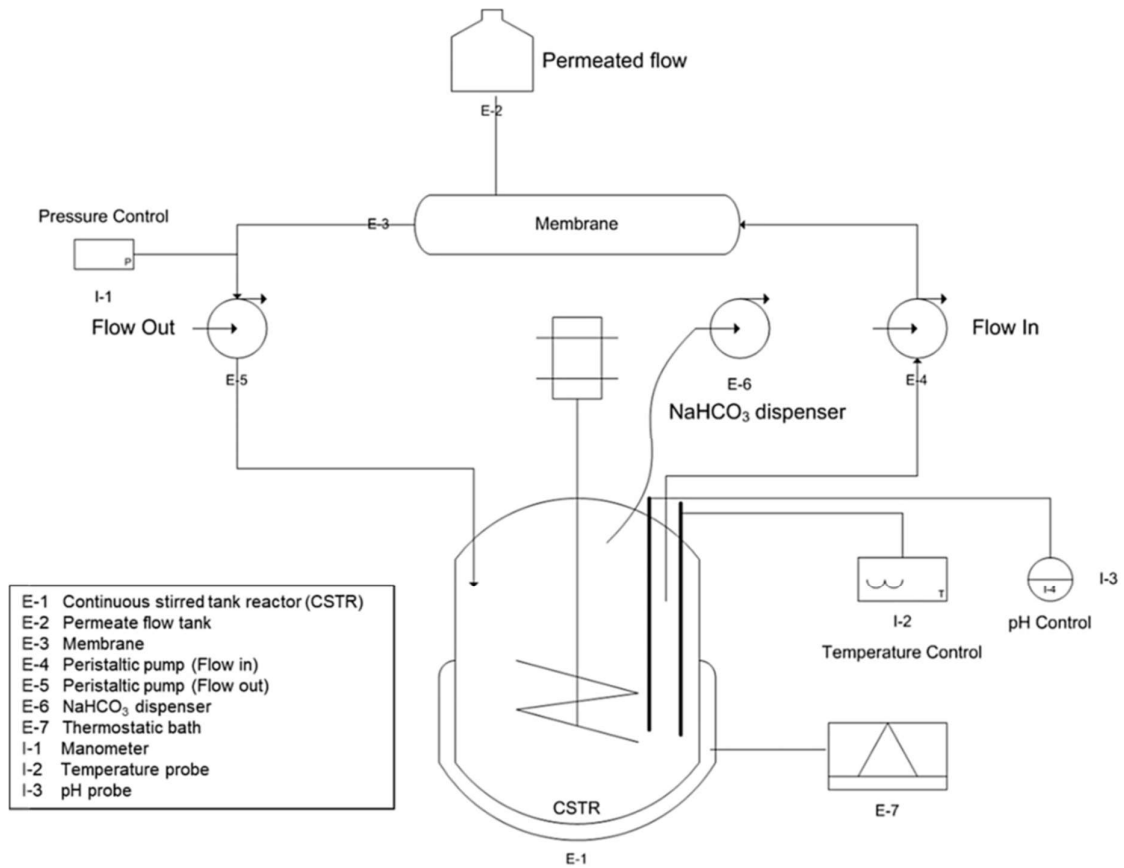


Figure I.I.4. Flow diagram of the dynamic *in-vitro* Gastrointestinal-Tract-Simulating Membrane Bioreactor (SimuGIT). (Rivas-Montoya et al., 2016).

## Results

The different combinations of alginate and shellac were tested for liquid-core matrix. Only the formulation alginate/shellac (75/25 % V/V) was satisfactory to determine the basic process conditions of bead preparation. Thus, the effect of the process variables (Flow rate, distance and concentration of  $\text{CaCl}_2$ ) on the EE of R-PE was investigated (Figure II.4). For this 80% of alginate/shellac mixture (wall material) was mixed with 20% of R-PE extract, and then extruded and dripped into  $\text{CaCl}_2$  solution for 30 min of gelation to form beads. The R-PE encapsulation process was optimized where included the effect of three independent variables flow rate (90 and 20  $\text{mL min}^{-1}$ ), distance (10 and 5 cm) and  $\text{CaCl}_2$  (5 and 15  $\text{g L}^{-1}$ ) on %EE were evaluated. Table I.4 shows the results of EE (%), particle size and SF obtained with the different conditions. The range of EE values obtained was between 89 and 97%. From Taguchi design, a higher  $\text{CaCl}_2$  concentration, lower flow rate and high distance resulted in a high EE.

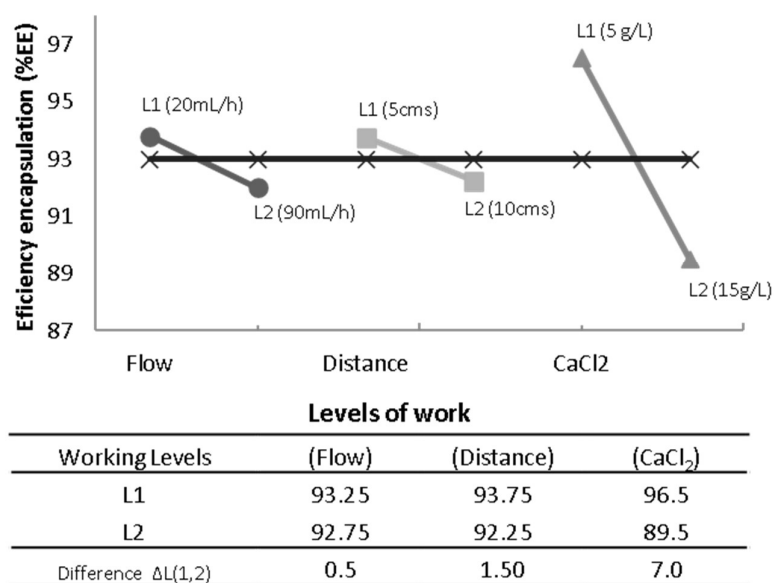


Figure II.4. Effect of the working levels of each variable on the encapsulation efficiency.

Figure II.4. shows the effect of the working levels of each variable on the encapsulation efficiency (degree of incline of the slope as a response to EE). The difference between level 1 and level 2 for a variable, the higher the change magnitude of the response. The variable  $\text{CaCl}_2$  showed a higher influence on the EE with an average difference of 7.0 units between the responses of working-level 1 ( $\text{L1}:5 \text{ g L}^{-1}$ ) and working-level 2 ( $\text{L2}:15 \text{ g L}^{-1}$ ), followed by the variable distance showed an influence on the EE with a difference of 1.50 units between the levels. The variable flow rate with a difference of 0.5 units between the two working levels. Therefore, the variable  $\text{CaCl}_2$  presented the highest difference compared with flow rate and distance. Thus, the R-PE pigment can be more efficiently encapsulated in beads coated with a low  $\text{CaCl}_2$  ( $<15 \text{ g L}^{-1}$ ) due to the formation of encapsulating matrix where that coating the capsules by  $\text{Ca}^{2+}$  reticulation of shellac leads to the formation of a uniform and smooth layer at the surface of alginate capsules compared to capsules prepared at  $15 \text{ g L}^{-1}$  of  $\text{CaCl}_2$  generating the formation of a non-uniform external layer.

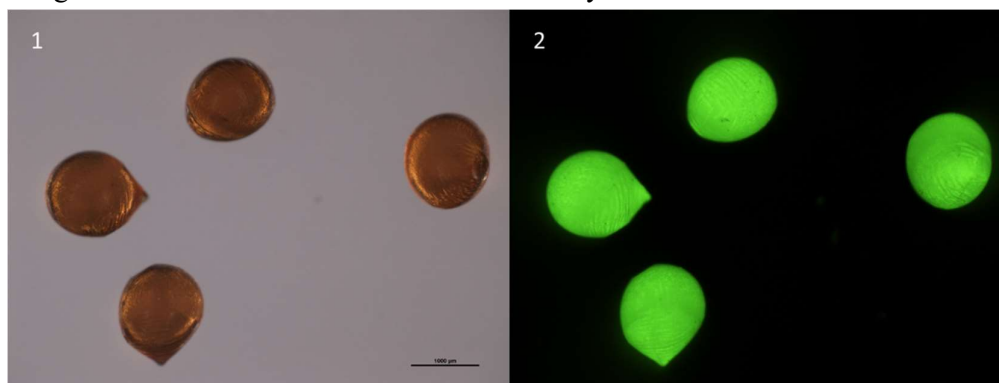


Figure III.4. Confocal microscopic for 1) design point N°1 (97.5%EE) and 2) presence of R-phycoerythrin by fluorescence.

The fluorescence observation of the aqueous-core alginate/shellac capsules are shown in Figures III. 4. In Figure IV.4 shows SEM images of optimal alginate/shellac beads from design point 1, which reached the highest EE. The image shows that the bead surfaces are smooth and free of pores, which is important for the stability of the beads because the pores facilitate the

exit or loss of the R-PE. However, the beads from design point 2 and 3 shows non-uniform particles and rough surfaces. Figure III.4 shows the R-PE distribution in the beads that was observed by confocal microscopy (CLSM). The pigment R-PE was identified by the fluorescent of the chromophores group after the external gelation process. A fluorescence of high intensity was emitted which was homogeneously distributed throughout the polymeric matrix in all design points. The bead size was between 10-50 mm according to the design points. Additionally, the lowest SF value was found in design point 1, reaching 0.04, whereas design point 3 showed the highest SF value 0.358. According to Chang et al., (2011), beads with an SF value lower than 0.05 are considered spherical beads. Thus, semi-spherical beads were obtained in our study. Additionally, the irregular head shape was observed with high distance (10 cm) and high  $\text{CaCl}_2$  ( $15 \text{ g L}^{-1}$ ) which correspond on the EE decrease (Table1).

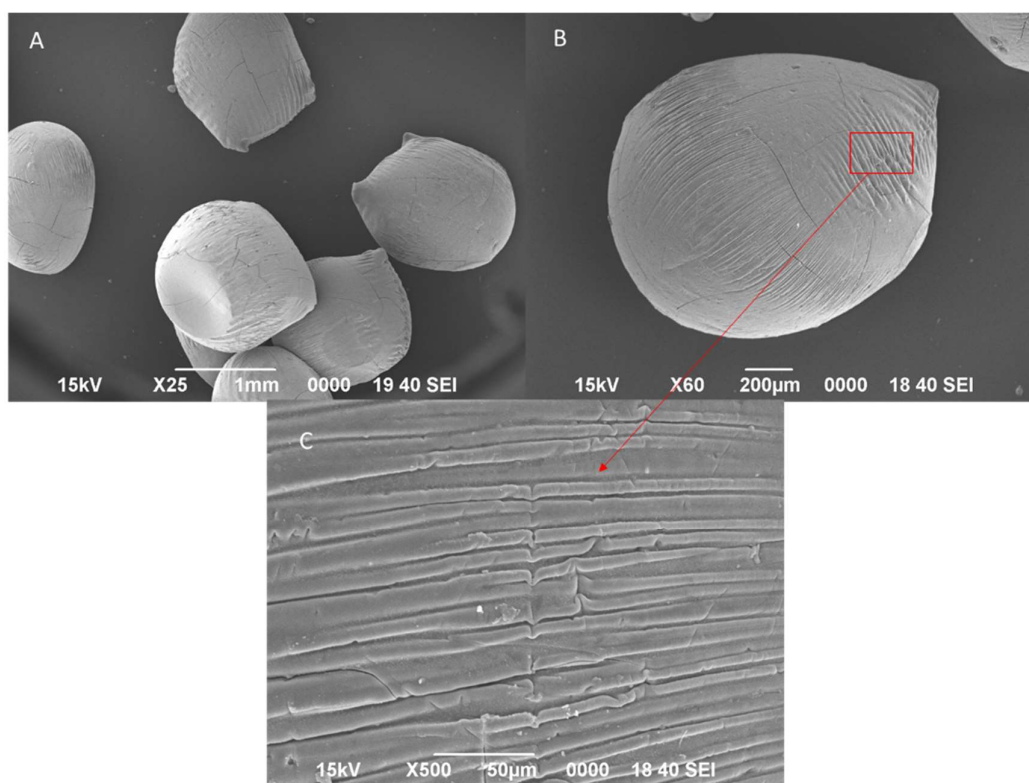


Figure IV.4. Morphology of the beads by scanning microscopy (SEM) for a) design point N°1, b) design point N°4 and c) magnification of 500X for the surface of the beads of the design point N°4.

The coefficients of determination ( $R^2$ ) for the independent variables Flow, Distance, and  $\text{CaCl}_2$  were 2.5, 4.2 and 90.7%, respectively. The coefficient of determination for these three variables was significant ( $p < 0.05$ ) with  $R^2 = 97.4\%$  indicating a good affinity or association of the independent variables with the EE. The optimized theoretical equation (OTE) for EE was determined employing Eq. 1, where T is equal to 97% which is the total average of the response of experimental runs and L corresponds to the working levels of the equation. The OTE contributed to 97% of the response, showing a close coincidence with the optimal experimental value (Point N°1: 97.5%). These results confirmed that the combination between the control variables and working levels were enough to determine an optimum.

Table I.4. Encapsulation efficiency of R-PE, sphericity factor, and particle size using the orthogonal matrix  $L_4 (2^3)$ .

| Design point | Orthogonal Matrix $L_4 (2^3)$ |                |                                       | Characterization of beads |               | Efficiency of encapsulation |
|--------------|-------------------------------|----------------|---------------------------------------|---------------------------|---------------|-----------------------------|
|              | Flow (mL/h)                   | Distance (cms) | $\text{CaCl}_2$ (gr $\text{L}^{-1}$ ) | Sphericity factor (SF)    | Size (mm)     | %EE                         |
| 1            | 20 ( $L_1$ )                  | 5 ( $L_1$ )    | 5 ( $L_1$ )                           | $0.06 \pm 0.02$           | $1.2 \pm 0.2$ | $97.5 \pm 0.7$              |
| 2            | 20 ( $L_1$ )                  | 10 ( $L_2$ )   | 15 ( $L_2$ )                          | $0.10 \pm 0.03$           | $1.6 \pm 0.1$ | $89 \pm 1.41$               |
| 3            | 90 ( $L_2$ )                  | 5 ( $L_1$ )    | 15 ( $L_2$ )                          | $0.09 \pm 0.05$           | $1.1 \pm 0.2$ | $90 \pm 1.41$               |
| 4            | 90 ( $L_2$ )                  | 10 ( $L_2$ )   | 5 ( $L_1$ )                           | $0.07 \pm 0.01$           | $1.1 \pm 0.1$ | $95.5 \pm 0.71$             |

Figure V.4 shows the bioaccessibility of R-PE from encapsulated and non-encapsulated during intestinal digestion. The encapsulation of R-PE significantly influenced the bioaccessibility and bioavailability of pigment R-PE. The bioaccessibility of R-PE extract was significantly higher than alginate/shellac microparticles, reaching values around 30.4% at 180 min. While the bioaccessibility from R-PE encapsulated just was detected in gastric and intestinal phases reached values of 20.25% at the end of the intestinal digestion (180 min).

The bioavailability of R-PE with and without encapsulates at the end of intestinal digestion is presented in Figure VI.4. Comparing R-PE samples, we observed that encapsulates of R-PE presented the highest percentages (6.0%) of bioavailability when compared to R-PE non-encapsulated (2.41%) at 180 min of intestinal digestion. At the beginning of the intestinal absorption phase (permeate samples), it was noted that small percentages of R-PE non-encapsulated and encapsulated from the initial total content were available and passed through the membrane. We observed during each digestion time for all samples was increased the R-PE content showed similar contents, but at the end of the intestinal digestion, a significance difference was detected at 180 min reached for R-PE non-encapsulated and encapsulated 0.123 and 0.31 mg of R-PE /g of biomass, respectively.

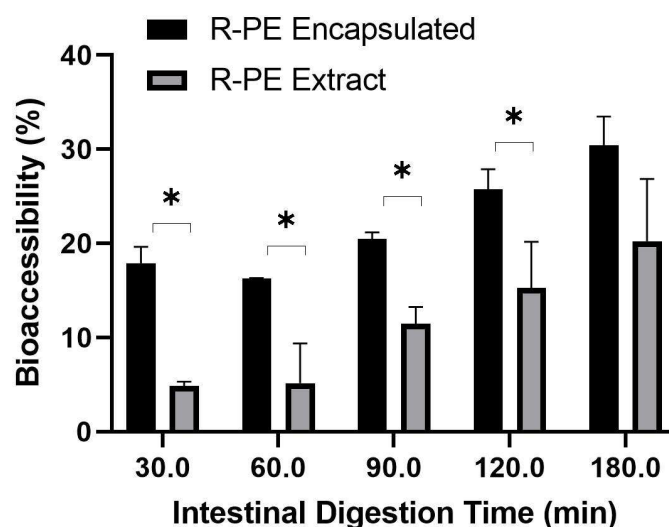


Figure V.4. Bioaccessibility (%) of R-PE extract and encapsulates during *in vitro* gastrointestinal digestion. Bars with asterisk indicate significance difference ( $p < 0.05$ ) between R-PE encapsulated and R-PE extract.

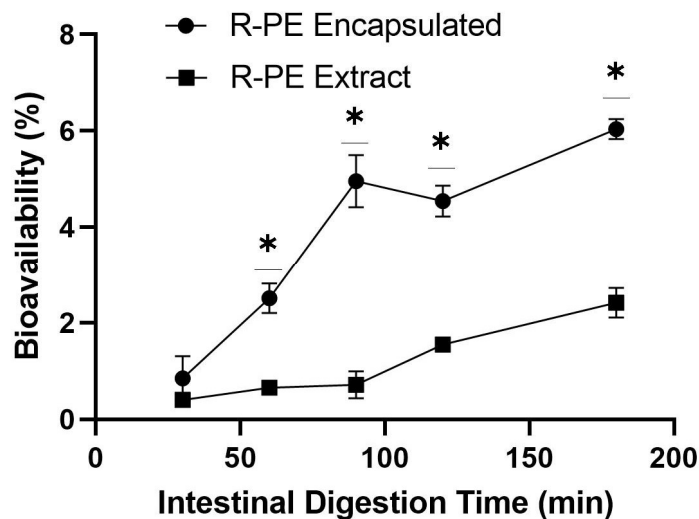


Figure VI.4. Bioavailability (%) of R-PE extract and encapsulates during in vitro gastrointestinal digestion. Line with asterisk indicate significance difference ( $p < 0.05$ ) between R-PE encapsulated and R-PE extract.

Figure VII.4 outline SDS-PAGE profile of the different stage of the digestion samples, where multiple protein bands ranging from 20 to 100 kDa can be observed, except for the mouth and stomach. More intense bands eluted in duodenum and intestine at round 50, 20-37 kDa, suggesting that some bands correspond to Phycoerythrin. Thus, it is possible to understand that the matrix core of the encapsulation of the phycoerythrin has a good resistance to mouth and stomach levels because no signal was reported. However, in the intestine signals between concentrated and permeated phases, are similar in the intense bands in the different times of reaction (30 and 180 min). Finally, it is possible to suggest that the phycoerythrin has a good control release in the function of matrix encapsulation formulated at the intestine level. These results have a good coincidence with the release test evaluated in different pH (1-5), where the R-PE encapsulated at pH 1 does not exceed 10 % of release content, while at pH 3 and 5 it remains, which is possible to suggest a release controlled after 180 min of exposure from the encapsulating matrix (Figure VIII.4).

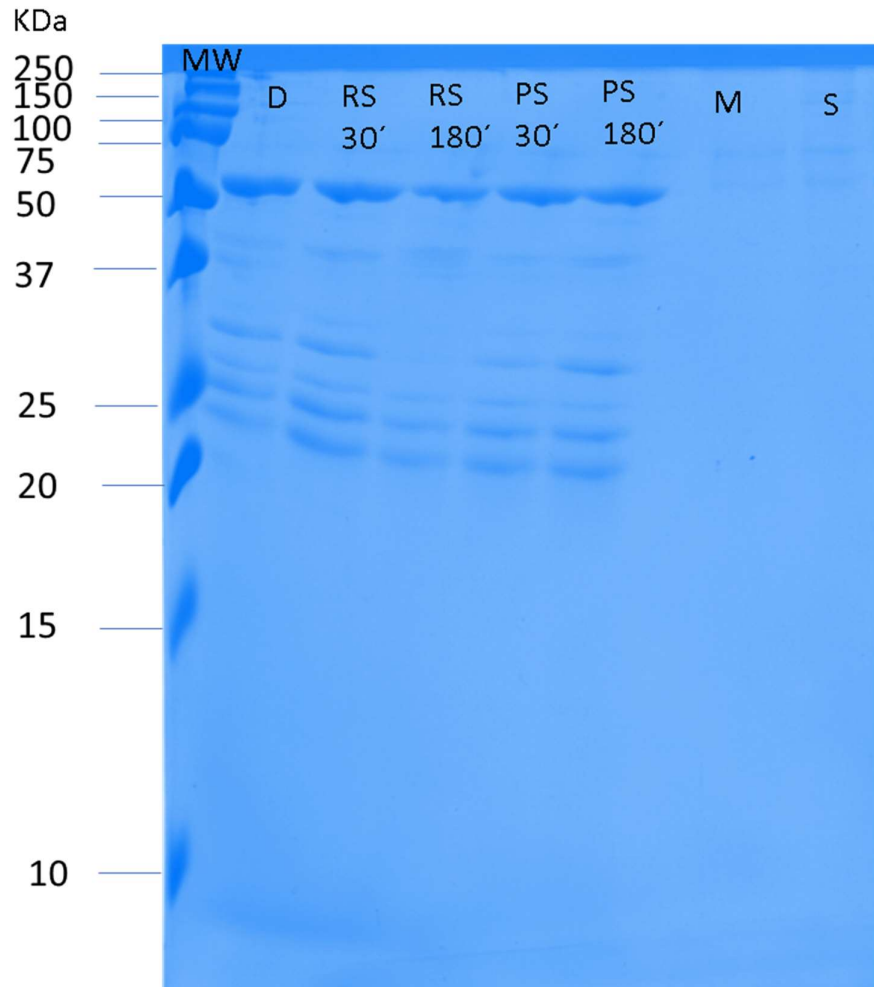


Figure VII.4. Sodium dodecyl sulphate polyacrylamide gel electrophoresis (SDS-PAGE) profile of R-PE encapsulated from different stage *in vitro* simulated digestion (simuGIT). 50 $\mu$ g of protein were loaded into the corresponding lane. MW: Molecular weight marker; D:Duodenn; RS30': Retentate streams at 30min; RS180': Retentate streams at 180min; PS30': Permeate streams at 30 min; PS180': Permeate streams at 180 min; M:mouth; S: stomach.



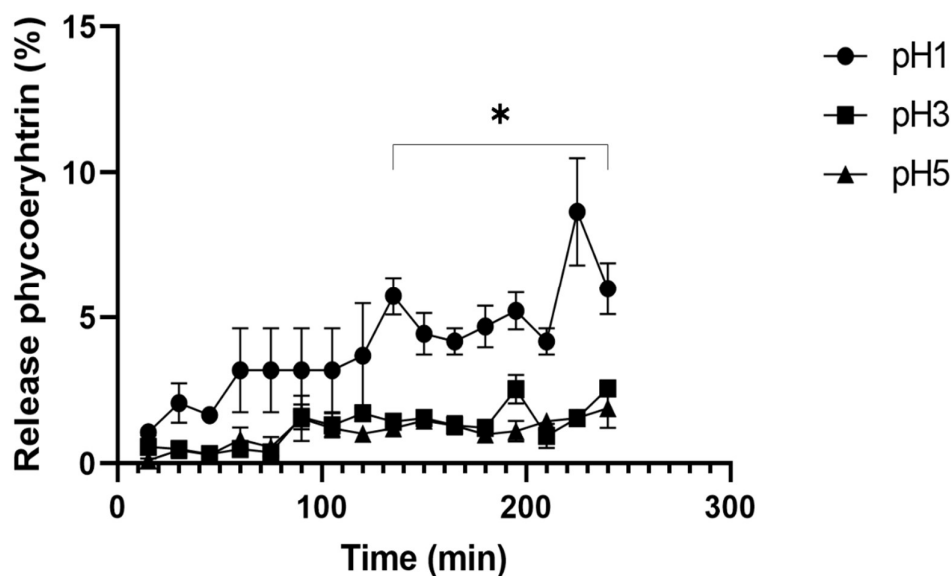


Figure VIII.4. R-PE release from alginate/shellac capsules during 250 min at different pH-values. Points with asterisk indicate significance difference ( $p < 0.05$ ).

The cytotoxicities of encapsulates and non-encapsulates of R-PE (aqueous extract) were determined in the human cancer cells (HCT-116; G-361; U-937) and health cells (1064sk). After the treatment of the cells with increasing concentration of the two samples, cell proliferation was evaluated using MTT assay. As shown in Table II.4 all the samples exhibited relatively inhibition ratios at all concentration levels and demonstrated a dose-dependent inhibition on the growth of cancer cells. It was observed that the lowest  $IC_{50}$  value in G-361 with encapsulates of R-PE was  $4132 \pm 10.86 \mu\text{g mL}^{-1}$ , in U-937  $IC_{50}$  cells was  $1251 \pm 4.83 \mu\text{g mL}^{-1}$ , in HCT-116  $IC_{50}$  cells was  $1076 \pm 8.46 \mu\text{g mL}^{-1}$  (Table II.4). For R-PE aqueous extract (non-encapsulates) the lowest  $IC_{50}$  value in HCT-116 cells  $IC_{50}$  was  $144.5 \pm 3.96 \mu\text{g mL}^{-1}$ , while in U-937  $IC_{50}$  was  $2788 \pm 11.5 \mu\text{g mL}^{-1}$  and in G-361 was  $2702 \pm 12.6 \mu\text{g mL}^{-1}$  (Table II.4). On the other hand, in health's cells line in 1064sK the encapsulates and non-encapsulates was  $3516 \pm 15.3 \mu\text{g mL}^{-1}$  and  $4438 \pm 10.3 \text{mg mL}^{-1}$ , respectively. The highest SI values calculated for encapsulated R-PE also belonged to the three above mentioned cell lines including HCT-116 ( $> 3.27$ ), U-937 ( $> 0.86$ ) and G-361 ( $> 0.26$ ) compared to the other cell

lines (Table II.4). The SI values calculated for R-PE extract for all the cell lines were high, ranging between 30.71 and 1.59, dependent on the cell line, indicating higher effectiveness of R-PE extract on the cancer cell lines compared to R-PE encapsulate. These results suggested show a cytotoxic effect on the cancer and health cells where the R-PE aqueous extract presented relatively high antitumoral activities against HCT-116 cells.

Table II.4. Cytotoxicity index ( $IC_{50}$ ) and selective index (SI) for R-PE encapsulate and non-encapsulate on the different cell lines : 1064 sK (human gingival fibroblasts cell line), HCT-116 (human colon cancer), G-361 (human melanoma), U-937 (human leukemia).

| Samples                          | Health and Antiproliferative active cell lines | Cytotoxicity Index $IC_{50}$ ( $\mu\text{g mL}^{-1}$ ). | Selectivity Index (SI) |
|----------------------------------|--|---|------------------------|
| Encapsulates                     | 1064sK   | $3516 \pm 15.3$   | -                      |
|                                  | HCT-116  | $1076 \pm 8.46$   | 3.27                   |
|                                  | U-937  | $1251 \pm 4.83$   | 0.86                   |
|                                  | G-361  | $4132 \pm 10.86$  | 0.26                   |
| Noun-Encapsulate (R-PE extract). | 1064sK   | $4438 \pm 10.3$   | -                      |
|                                  | HCT-116  | $144.5 \pm 3.96$  | 30.71                  |
|                                  | U-937  | $2702 \pm 12.6$   | 1.59                   |
|                                  | G-361  | $2788 \pm 11.5$   | 1.64                   |

## DISCUSSION

Algae, especially macroalgae, have recently emerged as a vast source of metabolites with unique structures and nutritional and therapeutic activities, and this field is becoming one of the hot challenges in food science and technology (Pimentel et al., 2020). Our work, it's a first

approach in the new generation of potential ingredients based on alginate/shellac as biomaterials for the protection of R-PE to maintain the biological activity and bioavailability under human physiological conditions. To formulate the wall material, alginate/shellac has been validated by other authors with good results in the efficiency of encapsulation for bioactive like riboflavin (Messaud et al., 2016), sunflower oil (Morales et al., 2017) and inclusive in a microorganism (Silva et al., 2016). However, the protection processes for phycobilin pigments have been little explored but have great potential in the food industry according to several studies (Juin et al., 2015; Jacotet-Navarro et al., 2016; Pereira et al., 2020; Dominguez et al., 2020). In this sense, the R-PE was successfully encapsulated by Taguchi optimization, which revealed that the high efficiency is given with design point 1, reaching values close to  $97.5 \pm 0.71\%$  EE (Table I.4). Similar results were obtained by Pan-tai et al., (2018) for Phycocyanin (C-PC), from microalgae *Arthrospira platensis* (Cyanobacteria), under alginate formulation process to beads by ionic gelation reached 98 %EE. It was found that alginate and  $\text{CaCl}_2$  concentration have a significant influence on the EE (%) and bead properties. In the same line, Yan et al., (2014) developed a microencapsulated by an extrusion method using alginate and chitosan as coating materials for the protection of the phycocyanin, from *Arthrospira platensis* (Cyanobacteria), which reached found values around 56% of EE. These values are less than our results, where the differences can be by the combination of the materials and the low concentration of  $\text{CaCl}_2$  (2.5%), in wich the competition between the two polymers to bind calcium ions  $\text{Ca}^{2+}$  affects the final composite gel structure. The observations of Messaoud et al., (2016), found that coating the capsules by  $\text{Ca}^{2+}$  reticulation of shellac led to the formulation of a uniform and smooth layer was closely related to the amount of shellac and  $\text{Ca}^{2+}$ , were recommended concentration of  $\text{CaCl}_2$  2% (W/V). Also, Henning et al., (2012) suggest that concentrations of  $\text{CaCl}_2$  over 2% (W/V) are enough to ensure the formation of cross-linked hydrogel alginate/shellac membranes. However, there found a shrinking

phenomenon of the alginate hydrogels during the coating process. This shrinking might be induced by the depletion of cross-linked calcium ions in the alginate hydrogel as a consequence of chemical reactions between the calcium ions and the shellac. From our observations, we suggest that the range of  $\text{CaCl}_2$  between 5 and 15 % (W/V) depends directly on the interaction with shellac, founded high values of EE (97.5 %) at 5 % (W/V). Further studies are necessary for another aspect that could describe the differences in the thickness of the shellac layers is linked to the total amount of  $\text{H}^+$  ions in the capsules (adjusted by the pH value).

The SEM and fluorescence observation of alginate/shellac beads exhibited a semi-spherical shape thanks to the intrinsic properties (surface tension, density and viscosity of the  $\text{CaCl}_2$  solution before the encapsulation stage (Chan et al., 2009, Morales et al., 2017). According to Chang (2011), beads with SF value lower than 0.05 are considered spherical beads. Therefore, the beads in our study are semi-spherical. The irregular bead shape was observed with high distance (10 cm) and high  $\text{CaCl}_2$ . However, the bead morphology became spherical as the distance of extrusion and  $\text{CaCl}_2$  on the % EE increased. According to Chan et al., (2009), SF was found to be an efficient tool as a sphericity indicator to study the shape of the beads. Additionally, spherical beads as an encapsulation system are more stable than irregular or non-spherical shaped beads as spherical beads have a low surface/volume ratio, producing a lower diffusion of bioactive in the beads. Dried microcapsules presented diameters ranging from 0.8 to 1.20 mm (Table I.4). Despite the large size, these microcapsules may be used in solid foods, in which the texture is not affected by the particle size, such as chocolate and cereal bars (Silva et al., 2016).

The alginate/shellac beads with the highest EE were submitted to *in vitro* dynamic digestion method (SIMUGIT). The percentage of R-PE found in the permeate stream was lower than R-PE encapsulated where we found 6.0% of bioavailability at 180 min of intestinal digestion. The

R-PE bioavailability significantly differed depending on the wall material, after the gastric step the alginate/shellac beads contained  $0.58 \text{ mg g}^{-1}$  of R-PE, which represents a decrease of 89.6% compared with the initial concentration ( $5.58 \text{ mg g}^{-1}$ ). In the same line, in the intestinal stage, the content available and passed through the microfiltration membrane ( $0.05 \text{ }\mu\text{m}$ ) more R-PE was seen to be released, showing a decrease of 94.5 % of R-PE compared to the initial concentration. Thus, the alginate/shellac as wall materials for R-PE have an acceptable mechanism for protection of the pigment allowing it to pass through the mouth, stomach and duodenum barriers and releasing the compound in a controlled intestinal phase. According to Pimmentel et al., (2020), the enriching protein extracts from *Porphyra dioica* (Nori) released at the intestinal level is recommendable because it is in the intestine that the proteins are degraded by enzymes and peptides are absorbed into the bloodstream improving the antioxidant activity. Our DGGE analysis showed that the fraction of the final digest was between 25-50 KDa, where the profile of the extracted protein is consistent with previous results reported by Pimentel et al (2020) and Stack et al., (2017) for red algae. Similar conclusions were reported by Wu et al., (2015), who evaluated the *in vitro* digestion of R-PE found that the final intestinal digestion still contained high antioxidant activity in proteins fraction of  $<3 \text{ kDa}$ . They indicate that digestion-resistant antioxidant peptides of R-PE may be obtained by *in vitro* gastrointestinal proteinase degradation. In the same line, Yabuta et al., (2010) found that the R-PE from *Porphyra* sp extract is readily digested to release the phycoerythrobilin compound during the gastrointestinal digestion process of mammals. Also, they suggested that the various therapeutic activities of phycoerythrin appear to be associated with the phycoerythrobilin compound released during mammalian gastrointestinal digestion. On other hand, Teixé-Roig et al., (2022) reported that in the other phycobiliprotein C-phycoyanin (C-PC) was protected by double emulsions containing pectin and sodium alginate presented high EE and the most suitable to prevent phycocyanin degradation during the

digestion process. This suggested that biological activity can be enhanced and safety after the digestion process. Also, Campos et al., (2020) reported that in the same C-phycoyanin (C-PC) extract can be applied as a stable blue dye in ice creams and highlight the increased antioxidant activity of the C-PC-added products after *in vitro* simulated digestion.

The changes in R-PE encapsulates concentration through digestion have low reports in the literature. This represents the novelty of the research where we considered a positive highlight in new knowledge due to little information. However, is clear that the biological activities of R-PE be maintained after *in vitro* digestion stage demonstrated by Yabuta et al., (2010), Wu et al., (2015), Stack et al., (2017) and Pimentel et al., (2020). In our work, from the R-PE encapsulates release in the final intestinal digestion stage ( $0.31 \text{ mg g}^{-1}$ ) we indicate that is enough for cytotoxic response against on human cancer cells. This allows us to show that the proportion or mixture of the encapsulating wall material is the one indicated.

The  $IC_{50}$  values for HCT-116 ( $1076 \pm 8.46$ ) and U-937 ( $1251 \pm 4.83$ ), as well as the SI values for the R-PE, encapsulated in these cells ( $> 3.27$  for HCT-116 and  $> 0.86$  for U-937) suggest encapsulated as a promising therapeutic candidate, particularly on gastro and blood cancers. Knowing that the greater the SI value is, the more selective it is, and SI values over 10 indicate general toxicity (Quispe et al., 200; Valdes-García et al., 2006), we concluded that compared to R-PE encapsulated, (SI:30.71), R-PE extracts non-encapsulated are better candidates for growth suppression of all the examined cell lines with SI values  $> 10$ . These observations can be attributed that the wall materials (alginate/shellac) could affect the level of growth factors of human cells, especially due to alginate, which has been shown to have catalytic characteristics in human cells (Lee and Mooney, 2012). Future studies in an *in vivo* system are necessary to relate antiproliferative and antioxidant activities as potential nutraceuticals.

## Conclusions

This study provided insights into the process conditions to prepare beads with a high EE of R-PE and the evolution under *in vitro* gastrointestinal digestion microcapsules. The variables process for R-PE encapsulation was obtained using a feeding flow of 20 mL h<sup>-1</sup>, 5 cm of distance and 5 gr L<sup>-1</sup> of CaCl<sub>2</sub>. The encapsulation under optimal conditions showed 97.5% showing a good coincidence with the predictive OTE values (97%). The beads presented a semi-spherical shape and were free of pores with a size of 1.2 mm. The *in vitro* digestion showed that the alginate/shellac beads were 2.5 times higher in bioavailability than non-encapsulated R-PE extract at intestine stage digestion with a concentration of 0.31 mg of R-PE. Finally, the R-PE charged in the encapsulate can be used as a potential delivery system for aqueous extract and give a therapeutic response according to the IC<sub>50</sub> (144 µg mL<sup>-1</sup>) values found for the R-PE for colon cancer. We suggest the encapsulation system of R-PE can be incorporated into a food matrix for nutraceutical applications.

## Acknowledgment.

We want to express our gratitude to Mr. Jaime Zamorano, Director of Development, from the GELYMAR S.A. for collaborate with this research project. We also want to thank to the Photobiology and Biotechnology of Aquatic Organisms research group (FYBOA, RNM-295) and the Institute of Blue Biotechnology and Development (IBYDA), University of Malaga due to the use of laboratory equipment and the financial support by the Project “Blue nutricosmeceutics with cyanobacteria and macroalgae (NAZCA)-Nutricosmeceútica azul con cianobacterias y algas (NAZCA-) PY20-00458 by Junta de Andalucía . P.C.V. thanks to Agency of National Research and Development of Chile ANID (N°21180254), Universidad de La Frontera, Junta de Andalucía and Asociación Iberoamericana de Postgrado (AUIP) for scholarship research.

---

# CHAPTER V:

## **Photobiological effects on biochemical composition in *Porphyridium cruentum* (Rhodophyta) with a biotechnological application.**

This chapter has been published in Journal of Photochemistry and Photobiology.

Castro-Varela, P. A., Celis-Plá, P. S. M., Abdala-Díaz, R., and Figueroa, F. L. (2021). Photobiological Effects on Biochemical Composition in *Porphyridium cruentum* (Rhodophyta) with a Biotechnological Application. *Photochemistry and Photobiology* 97, 1032-1042 doi: 10.1111/php.13426.



---

## **CHAPTER V: Photobiological effects on biochemical composition in *Porphyridium cruentum* (Rhodophyta) with a biotechnological application**

Pablo A. Castro-Varela<sup>1,2</sup>, Paula S.M. Celis-Plá<sup>3,4\*</sup>, Roberto Abdala-Díaz<sup>1</sup>, Félix L. Figueroa<sup>1</sup>

<sup>1</sup>Institute of Blue Biotechnology and Development (IBYDA), Department of Ecology and Geology, Faculty of Sciences, University of Malaga, Málaga, Spain

<sup>2</sup>Doctorate in Engineering Sciences with Specialization in Bioprocesses, Department of Chemical Engineering, University of La Frontera, Temuco, Chile.

<sup>3</sup>Laboratory of Coastal Environmental Research, Center of Advanced Studies, University of Playa Ancha, Traslaviña, Viña del Mar, Chile.

<sup>4</sup>HUB-AMBIENTAL UPLA, Vicerrectoría de Investigación Postgrado e Innovación, University of Playa Ancha, Valparaíso, Chile

**Keywords:** Photobiology, *Porphyridium cruentum*, phycoerythrin, pulse amplitude modulated fluorescence (PAM), microalgae, Omega 3 fatty acids

## ABSTRACT

This study describes the relation of photostimulation capacity and biochemical compounds in the microalgae *Porphyridium cruentum* under saturated irradiance ( $200 \mu\text{mol m}^{-2} \text{s}^{-1}$ ) by white light (WL) and low-pressure sodium vapor (SOX lamps-Control) and supplemented by fluorescent lamps (FL) with different light qualities (blue;  $\lambda_{\text{max}} = 440 \text{ nm}$ , green;  $\lambda_{\text{max}} = 560 \text{ nm}$  and red;  $\lambda_{\text{max}} = 660 \text{ nm}$ ) at low irradiance  $30 \mu\text{mol m}^{-2} \text{s}^{-1}$ . The maximum photosynthetic efficiency ( $F_v/F_m$ ) showed a positive correlation to the light quality by saturating light SOX in mixture with stimulating blue light than the white light (WL) at the harvest day (10 day). The production i.e., maximal electron transport rate ( $\text{ETR}_{\text{max}}$ ) and energy dissipation, i.e., maximal non-photochemical quenching ( $\text{NPQ}_{\text{max}}$ ) had the same pattern throughout the time (3 to 6 days) being the values higher under white light (WL) compared SOX and SOX plus the different light qualities. Total protein levels increased significantly in the presence of SOX light, while phycoerythrin (B-PE) showed significant differences under SOX+ Blue light. Arachidonic acid (ARA) was higher under SOX and SOX plus supplemented different light qualities than that under WL whereas Eicosapentaenoic acid (EPA) was the reverse. The high photomorphogenic potential by SOX light shows promising application for microalgae biotechnology.

## INTRODUCTION

In the last decade, microalgal biotechnology has received great attention as it can potentially reach high biomass yield (Vigani et al., 2015) to extract valuable products and environmental applications (Jerez et al., 2016; Madeira et al., 2017; Peralta et al., 2019). Productivity of microalgae is generally higher than that in higher plants (Madeira et al., 2017) due its higher photosynthetic yield. *In vivo* Chl<sub>a</sub> fluorescence reflects the utilization of light energy, i.e., its distribution between photochemical and non-photochemical processes. Pulse amplitude modulated (PAM) fluorometer has been successfully used on-line to monitor the photosynthetic performance of mass cultures of macro and microalgae and give rapid evidence of stress affecting growth (Jerez et al., 2016; Álvarez-Gómez et al., 2019). The unicellular microalga *Porphyridium cruentum* Nägeli, 1849 (Rhodophyta, Porphyridiales) is a potential source of important biotechnologically compounds with high commercial value. These metabolites include mainly polysaccharides with therapeutic properties (Abdala-Díaz et al., 2010), phycoerythrin (Ibáñez-González et al., 2016; Li et al., 2019a) and polyunsaturated fatty acids (Eicosapentaenoic acid, EPA (C20:5n-3) and Araquidonic acid, ARA (C20:4n-6)) (Cohen, 1990; Sánchez-Saavedra et al., 2018).

Phycoerythrin is the major light-harvesting chromoprotein in red algae and has an interesting market as a natural dye of use in food, pharmaceutical and cosmetics. However, a commercially more interesting application is as a fluorescent agent, to be used in biochemical, molecular and clinical techniques (Ibáñez-González et al., 2016; Li et al., 2019a). On the other hand, EPA has recognized beneficial effects in preventing coronary heart diseases, lowering blood cholesterol and reducing the risk of atherosclerosis (Sirisuk et al., 2018b), while ARA is the biogenic precursor of prostaglandins and leukotrienes, both eicosanoid hormones with important functions in the circulatory and nervous systems (Sato et al., 2017; Tallima and El Ridi, 2018;

Sudhakar et al., 2019; Katiyar and Arora, 2020). In this point, *P. cruentum* has been shown to be a good source of ARA, EPA, pigments as well proteins (Reboloso Fuentes et al., 2000; Safi et al., 2013; Gagnard et al., 2019). This strain is attracted great interest in recent years due to the prospective application for functional food products and/or feed supplements (Vigani et al., 2015; Michalak and Chojnacka, 2018; Sánchez-Saavedra et al., 2018; Gagnard et al., 2019; Sudhakar et al., 2019).

For enhance biomass and metabolites yield, it is necessary to increase photosynthetic efficiency and optimization of light absorption through adjustment of the light harvesting apparatus to achieve optimal balance of photosynthesis/photoprotection, rather than just maximizing light absorption (Larkum, 2003; Jerez et al., 2016; Peralta et al., 2019). The optimization of light represents a critical issue in microalgal biotechnology due to the low photosynthetic quantum efficiency in natural systems (Abu-Ghosh et al., 2016), as well as of the increase ratio surface and volume (Jerez et al., 2016). As excess of light is especially harmful to photosynthetic apparatus, microalgae have evolved different acclimation strategies, to control and process sunlight absorbed at both photosystems (Kianianmomeni and Hallmann, 2014; Rockwell et al., 2014; Wobbe et al., 2016). Improving biomass, for large-scale cultivation, by manipulating incident light could be economically feasible (Wobbe et al., 2016).

Recent work proposes that the LED technology with different colored lights can increase the possibility to provide selected wavebands to plants and algae (Sirisuk et al., 2018a; Hamdani et al., 2019; Landi et al., 2020). Recently, Hamdani et al., (Hamdani et al., 2019) reported how the light quality of LED technology influences the growth and photosynthesis properties of rice, determinate artificial lighting can be used to manipulate the final biomass. In microalgae there are few reports where optimize the monochromatic light by LED technology for the phototropism, photo-morphogenesis, and photosynthesis. However, Ra et al., (Ra et al., 2018)

indicates at photo-morphogenesis level that green LED light induces the total lipids content by over 40 %w/w in three species of *Nannochloropsis salina*, *Isochrysis galbana*, and *Phaeodactylum tricornerutum*. However, further research is needed before drawing a definitive conclusion about the effect of green light on microalgae.

Light plays an essential role in controlling plant physiology and morphology in two ways: 1) as a source of energy; and 2) as an environmental signal acting through photomorphogenic photoreceptors to drive photo-morphogenesis as phytochromes, rhodopsin's or cryptochromes (Chory et al., 1996; Rockwell et al., 2014). Most often, the optimal light wavelength for microalgal biomass accumulation is red light, while lipid and carotenoid accumulation can be increased by using the blue and far-red light wavelengths (Yang and Weathers, 2014). However, in some cases, far-red light wavelengths have been shown to affect microalgal accessory pigments and secondary metabolites used for harvesting of the light in the photosynthesis process (Yang and Weathers, 2014). The PSII in the microalgae, is enhanced by red light wavelengths, while PSI is enhanced by blue and far-red light wavelengths (Baer et al., 2016). In this way, blue and red lights wavelengths and quality light conditions, are the most appropriate for culture in microalgae and should be sufficiently and selectively delivered for photosynthetic activity.

In the culture, the artificial light intensities need to be delivered uniformly over an illuminating surface of vessels to enable a sufficient amount of photosynthetically active radiation (PAR) to reach cells continuously (Ezequiel et al., 2015). For cultivation of the microalgae, three types of artificial light are mainly used 1) fluorescent lamps (FL), 2) the high-intensity discharge (HID), and 3) light-emitting diode (LED), as a principal sources for microalgae cultivation (Blanken et al., 2016). However, this kind of lights (FL, HID and LED) does not emit a complete spectrum of light, it produces light with either an excess of one or

more wavelengths. For example, incandescent light bulbs mostly produce yellow, orange or red light. Standard “cool white” fluorescent bulbs emit mostly yellow-green light (Baer et al., 2016; Wobbe et al., 2016). The sodium lamps low pressure (SOX lamps), emitting mainly at 589 nm, are efficient sources of PAR, that emit relatively low levels of infra-red radiation (IR) and heat (J. C. Sager et al., 1982). Growth rate and photosynthetic activity were optimal under SOX in the red macroalgae (Aguilera et al., 1997, 2000). The microalgae produce an important intracellular metabolite in responses to light stress conditions. Based on the microalgal responses, the specific wavelengths will enhance the productivity of specific intracellular products with artificial light.

In this study, we determinate the growth and photobiological parameters, to know their photo-stimulation capacity at saturated irradiance with supplementation of light qualities (blue, red and green light) at low irradiances (15% of saturated irradiances) and ii) the accumulation of commercially important metabolites. Growth rate, biomass productivity, photosynthetic activity by using *in vivo* chlorophyll *a* fluorescence with pulse amplitude modulated (PAM) fluorometer, antioxidant activity (AA) and the accumulation of commercially important metabolites as soluble proteins (SP), allophycocyanin (A-PC), phycocyanin (R-PC), phycoerythrin (B-PE), total carbohydrates (TC), total lipids (TL), polyunsaturated fatty acids (PUFAs) were determined in the in the red microalgae *Porphyridium cruentum*.

## MATERIALS AND METHODS

### Microalgae strain and culture conditions

The strain *Porphyridium cruentum* Nägeli, 1849 (Rhodophyta, Porphyridiales) was isolated and maintained in the Collection Culture of Marine Microalgae from the Institute of Marine Sciences of Andalucía, Spain (CCMM-ICMA). Primary stock cultures were grown in a 500 mL flask with Vonshak medium (Vonshak et al., 1985) in autoclaved 30 ppt saltwater, at  $20 \pm 1^\circ\text{C}$ , in white light (fluorescent lamps) with a photon flux density (PFD) of  $50 \mu\text{mol photons m}^{-2} \text{s}^{-1}$  and a photoperiod 12:12 (light: dark). In a first stage, the microalgae were acclimated in white light and low-pressure sodium vapor lamps (SOX;  $\lambda_{\text{max}} = 590 \text{ nm}$ ) at different intensities of light; 1) 50, 2) 100, 3) 150, 4) 200 and 5)  $250 \mu\text{mol photons m}^{-2} \text{s}^{-1}$ ) to determine the optimal irradiance of culture on growth and photosynthetic activity in this specific microalga (see supplementary material, Tables S1, S2, Figs. S1 and S2). The acclimation was performed in volume of 250 mL, with an initial cell density of  $500,000 \text{ cells ml}^{-1}$ , with a photoperiod 12:12 (light: dark), at  $20 \pm 1^\circ\text{C}$  of the temperature, with constant aeration for 6 days (See Supporting material, Tables S1, S2, Figs. S1 and S2).

The second stage, for the experimental periods (10 days), the optimal irradiance of  $200 \mu\text{mol m}^{-2} \text{s}^{-1}$  was selected in function of photobiological capacity (i.e.,  $F_v/F_m$ ) and growth (cell density) from the acclimation condition (first stage; 6 days). *P. cruentum* was inoculated in 1-L flask with 650 mL of Vonshak medium. Cultures were initiated with a cell density of  $500,000 \text{ cells ml}^{-1}$  of cell concentration, aerated with filtered air ( $0.22 \mu\text{m}$ ). To evaluate the photomorphogenic potential, four Osram T8/18W fluorescent lamp were used as a white light and one Philips SOX/55W lamps (low pressure sodium vapor) were used as a yellow light and was supplemented by two tubes of General Electric 15W fluorescent lamps (FL) for every one of the qualities of the light: Blue light ( $30 \mu\text{mol m}^{-2} \text{s}^{-1}$ ;  $\lambda_{\text{max}} = 440 \text{ nm}$ ), green light ( $30 \mu\text{mol}$

$\text{m}^{-2} \text{s}^{-1}$ ;  $\lambda_{\text{max}} = 560 \text{ nm}$ ) and red light ( $30 \mu\text{mol m}^{-2} \text{s}^{-1}$ ;  $\lambda_{\text{max}} = 660 \text{ nm}$ ) with a photoperiod 12:12 (light: dark). In all the stages the SOX light was the control condition (See supplementary material; Fig. S3). This selection is necessary to obtain the light color independently than the saturated photosynthesis by the SOX lamp. Three replicates of each condition were established in the acclimatation (first stage) and experimental period (second stage). The irradiance of the lamps was determined by PAR spherical sensor (US-SQS, Walz GmbH, Effeltrich, Germany) connected to the Licor LI-250A radiometer (Licor radiation Sensors Inc., Lincoln, USA).

## **Growth analyses**

### **Cell account**

Growth of each replicate was monitored over a 10-day period by cell counting in a Neubauer chamber every 36 hours (every other day). The maximum growth rate,  $K_{\text{max}}$  (divisions  $\text{day}^{-1}$ ) were determined during the logarithmic growth phase according to Guillard (Guillard, 1973).

### **Dry weight**

The dry weight was determined at the end of the experimental period (10 days), through of the filtering 10-mL aliquots, using Millipore filters of  $0.45 \mu\text{m}$  (dry weight), washing the filtered aliquots with 0.5 M ammonium format ( $\text{NH}_4\text{HCO}_2$ ) and dried at  $80 \text{ }^\circ\text{C}$  until they reached a constant weight.



### ***In vivo* chlorophyll a fluorescence of PSII**

Photosynthetic activity was determined using an equipment pulse amplitude modulated fluorometer Water-PAM (Win-Control v3.25, Walz GmbH, Germany). The photosynthetic activity was measured along the experimental period in each treatment (day-3, day-6, and day-10). *Porphyridium cruentum* was collected in each treatment and then it was placed in the incubation chambers to conduct the Rapid Light Curve (RLC), in samples of 10 mL of the culture, and it was placed in darkness for 15 min to full oxidize to the reaction centres and to determine the basal fluorescence ( $F_o$ ). Afterwards a saturation pulse was applied, reducing the reaction centres, and determining the maximal fluorescence ( $F_m$ ).

Maximal quantum yield of PSII ( $F_v/F_m$ ) was calculated as  $(F_m - F_o)/F_m$  being  $F_v = F_m - F_o$ .  $F_o$  is the basal fluorescence of dark-acclimated after 15 min and  $F_m$  is the maximal fluorescence after a saturation light pulse of  $> 4,000 \mu\text{mol m}^{-2} \text{s}^{-1}$  (39). For RLC conduct, the microalga was incubated for 20 s at increasing irradiances of actinic light (light source: Red LED lamp) emitted by the Water-PAM fluorometer (77, 115, 166, 253, 373, 570, 846 and 1220  $\mu\text{mol photons m}^{-2} \text{s}^{-1}$ ), and thus, to determine the values of intrinsic fluorescence in light ( $F_t$ ) and maximal fluorescence in light ( $F_m'$ ) after the application of the saturation pulse.

Electron Transport Rates (ETR) which represents the electron flux through photosynthetic transport chain, was calculated and expressed per area unit (Schreiber et al., 1995) as follows:

$$\text{ETR} = \Delta F / F_m' \times E \times A \times F_{II} \text{ (}\mu\text{mol electrons m}^{-2}\text{s}^{-1}\text{)} \quad (1)$$

where  $\Delta F/F_{m'}$  is the effective quantum yield ( $\Delta F/F_{m'}$ ) was calculated as  $(F_{m'} - F_t)/F_{m'}$ , being  $\Delta F = F_{m'} - F_t$  (Figueroa et al., 2003).  $E$  is the incident PAR irradiance expressed in  $\mu\text{mol photons m}^{-2} \text{ s}^{-1}$ ,  $F_{II}$  is the fraction of chlorophyll related to PSII (400–700 nm), being 0.15 in red algae (Figueroa et al., 2003).  $A$  is the absorptance (relative units) which is the fraction of light absorbed by the culture and was measured by a method used of thin layer of cell suspension (3 mm) according to (2) as follows:

$$A = 1 - E_p / E_m \quad (2)$$

where  $E_p / E_m$  is the transmittance (T);  $E_p$  is the transmitted irradiance by the microalgal culture and  $E_m$  is the transmitted irradiance by the culture medium, both measured with a cosine-corrected PAR sensor (LI-COR Company, Nebraska, USA).

Maximum Electron Transport Rate ( $ETR_{\text{max}}$ ), these parameters were calculated by fitting RLCs that estimate of maximal photosynthetic capacity (Celis-Plá et al., 2014a), and the photosynthetic efficiency ( $\alpha_{\text{ETR}}$ ). The initial slope of the data of ETR curve vs absorbed irradiance is considered as indicator of the photosynthetic efficiency (Celis-Plá et al., 2014a). These values were obtained from the tangential function (Eilers and Peeters, 1988).

Non-Photochemical Quenching (NPQ) was calculated using values of fluorescence obtained the RLC procedure by using a Water PAM fluorometer according to this equation:

$$\text{NPQ} = (F_m - F_m)/F_{m'} \quad (3)$$

where the maximal fluorescence ( $F_m$ ) after the application of saturation light pulse after the 15 min incubation in darkness and  $F_m'$  is the maximal fluorescence after the application of saturation light pulse after 20-s incubation in each light intensity of the RLC.  $NPQ_{max}$  was calculated by using a tangential model (Eilers and Peeters, 1988).

### **Biochemical analysis**

At the end of exponential phase of the cultivation, the cells were harvested and centrifuges at 1792 g for 10 min at 4 °C. The biomass was lyophilized for 24 h, and then stored at -80 °C until analysis. For each biochemical analysis, an aqueous extract was carried out and used for the analysis of soluble proteins, phycobiliproteins and antioxidant activity. Subsequently, the total carbohydrates, total lipids, and fatty acid profile.

### **Soluble Proteins and Phycobiliproteins analysis**

The determination of the soluble proteins (SP) was performed through the Bradford method (Bradford, 1976). For this analysis, were taken 50 mg of dry weight, and homogenized in 1 ml of phosphate buffer (0.1M, pH 6.5). It was left overnight at 4 °C in darkness for the extraction. The extract was centrifuged (Sartorius 2-16PK, Sigma, Germany) at 1792 g for 10 minutes, then, 10 µL of the supernatant was mixed with 790 µL of phosphate buffer and 200 µL of Bio-Rad (Bio-Rad protein assay, Germany). After 15 min of incubation (room temperature and darkness) the absorbance was measured spectrophotometrically (spectrophotometer UV Mini-1240, Shimadzu, Columbia, USA) at 595 nm. The standard was made with bovine serum albumin.

The concentration of the phycobiliproteins pigments in the phosphate buffer extract processed was determined by spectrophotometry (UV / VIS) at 565 nm, 620 nm and 650 nm using the mathematical relationships (Eq. 4, 5 and 6) proposed by Bennet and Bogorad, (1973). All the data was normalized against 750 nm. The results were expressed by dry weight of biomass.

$$\text{Phycocyanin (R - PC)} = \text{Abs620} - \left[ 0.7 * \left( \frac{\text{Abs650}}{7.38} \right) \right] \quad (4)$$

$$\text{Allophycocyanin (A - PC)} = \text{Abs650} - \left[ 0.19 * \left( \frac{\text{Abs620}}{5.65} \right) \right] \quad (5)$$

$$\text{Phycoerythrin (R - PE)} = \text{Abs565} - [2.8 * \text{R - PC}] - (1.34) * (\text{A - PC}/12.7) \quad (6)$$

### **Antioxidant activity**

The antioxidant activity (AA) was evaluated using the ABTS assay (Re et al., 1999) based on the free radical scavenging. The ABTS<sup>+</sup> was generated by a reaction of 7mM ABTS with 2.45 mM potassium persulfate in phosphate buffer (0.1M; pH: 6.5) and this reaction was stored for 16 h at room temperature before being used. The same extract was used for the proteins assay and phycobiliproteins determination. 940 µL of phosphate buffer was mixed with 10 µL of ABTS solution and 50 µL of the extract. The absorbance was measured, before adding the antioxidant substance and after 8 minutes of reaction, at 727 nm. A standard solution of Trolox was used as reference. The results were expressed as µmol TEAC (Trolox equivalent antioxidant capacity) g<sup>-1</sup> DW.

## **Total carbohydrates**

The quantification of total carbohydrates (TC) according to the phenol-sulfuric acid method was conducted according to Dubois et al., (1956). For this analysis, 5 mg of dry weight were mixed with 5 mL of H<sub>2</sub>SO<sub>4</sub> 1M and incubated during 1 h in a bath at 100 °C. The extraction was conducted at room temperature and it was centrifuged at 1792 g for 10 min. One mL of the supernatant was mixed with 1 mL of phenol 5%, and after 40 min of incubation at room temperature, 5 mL of concentrated H<sub>2</sub>SO<sub>4</sub> was added. Absorbance was measured in a spectrophotometer at 485 nm. Glucose was used as standard.

## **Total lipids and fatty acids analysis**

The content of total lipids (TL) was quantified gravimetrically by a chloroform/methanol (2:1, v/v) extraction Folch et al., (1957), using the extract composed by one hundred mg of freeze-dried biomass in 5 mL of solvent. Afterwards, the non-polar fraction was collected, dried, and weighed to determine the lipid content of the biomass. The content of lipids was expressed in percentage by dry biomass (% DW). Afterwards, the lipid extract was submitted to methylation to elucidate its fatty acid profile.

The lipid extract was subjected to a transesterification in acid medium following the methodology of Christie et al., (1982). The fatty acid methyl esters (FAMES) obtained were diluted in hexane at a concentration of 40 mg mL<sup>-1</sup> and identified by GC-FID using a BPX70 column (SGE Analytical Science, Australia) coupled to a Focus GC (Thermo Scientific, USA) and using helium as carrier. The initial temperature of the column was 140 °C for 10 min, then it was raised to 240 °C at a rate of 2.5 °C min<sup>-1</sup> and maintained at 240 °C for another 10 min. The detection of the FAMES was done through an FID detector and the quantification

according to retention times referenced to a standard pattern of FAMES (Supelco 37 comp. 47885-U). Results are expressed as percentage of identified FAMES (% FAMES).

### **Statistical analysis**

Interactive effects on growth, metabolites and photosynthesis responses among autotrophic treatments was measurements through ANOVA (Underwood, 1996). The fixed factors were time (with two levels) and quality of the light (with five levels). After significant effects, the interaction was evaluated with a posteriori test of Student Newman Keuls (SNK). Homogeneity of variance was tested using the Cochran test and by visual inspection of the residuals (Underwood, 1996). All data conformed to normality and homogeneity of variance. All analyses were performed using SPSS v.21 (IBM, USA). In addition, the Pearson coefficient was calculated to determine the highest correlation between antioxidant activity and extraction of soluble proteins, total carbohydrates, biliproteins, lipids, EPA, ARA,  $F_v/F_m$ ,  $\alpha_{ETR}$ ,  $ETR_{max}$ , and NPQ. Principal Component Analysis (PCA) was performed to detect patterns among parameters based on Euclidean distance using PERMANOVA+ with PRIMER6 package. PCA analyses were conducted to all variables at the end of the experimental period. This procedure corresponding to equivalent ordination to a PC diagram and also calculates the percentage variation explained by each of the axes in the multidimensional scale (PERMANOVA+ for primer: Guide to software and statistical methods | Request PDF).

## RESULTS

### Correlation and Principal component analysis (PCA)

The PCA show a positive correlation of the first axis (65.8% of total variation) with the relation between TL,  $F_v/F_m$ , B-PE, EPA. On the other hand, R-PC, A-PC,  $ETR_{max}$ ,  $\alpha_{ETR}$ , TC, SP ARA and AA were negatively related (Fig. I.5). The light treatments had a high effect upon these factors (Fig. I.5), mostly in terms of B-PE treatments with SOX + B (Fig. I.5). For other side, TL vector its not associate clearly to any variable data. In addition, in the graphic, the combination of the first two axes explained 59.9% of the total variation (Fig. I.5). On the other hand, positive Pearson correlations (Table S5; see supplementary material) ( $p < 0.05$ ) were observed between antioxidant activity and the fatty acid ARA ( $r = 0.538$ ). Also, phycocyanin (R-PC) showed positive correlations with  $ETR_{max}$  and  $\alpha_{ETR}$  results ( $r = 0.645$ ;  $r = 0.597$ , respectively) (see supplementary material Table S5 (see supplementary material)).

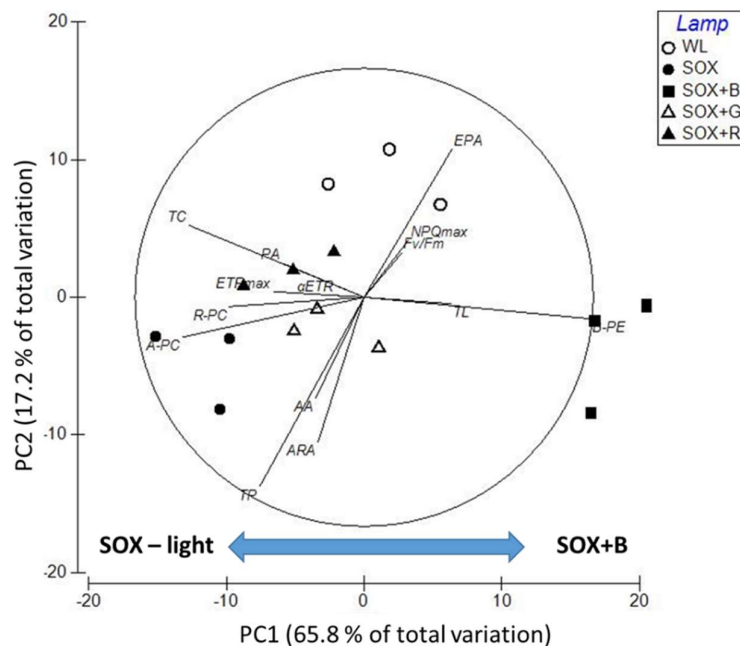


Figure I.5. Principal components diagram in relation to physiological responses in *Porphyridium cruentum* culture at the end of the experimental period respect to the light treatments. WL: White light; SOX(Control): SOX; SOX+B: SOX + Blue; SOX+G: SOX +

Green; SOX+R: SOX +Red. Vectors overlay indicates the relationship between the Principal component ordination (PCO) diagram axes and the physiological and biochemical variables.

### Photosynthetic variables respect to the fluorescence in Chlorophyll *a*

$F_v/F_m$  was significantly affected by the time exposition ( $p < 0.05$ , Fig. II.5).  $F_v/F_m$  increased significantly during the experimental period, showing the highest level at the end of the experimental period (day 10) (Fig.II.5). The  $\alpha_{ETR}$  had a significantly interaction only with the time factor ( $p < 0.05$ , Fig. III.5).  $\alpha_{ETR}$  were similar at 6 and 10 days, only being significantly different in comparison with day 3. No significant differences among the different light qualities were observed.  $ETR_{max}$ , had significant interactions between time exposition and quality of lights ( $p < 0.05$ , Fig. IV.5). At 3 and 6 d culture,  $ETR_{max}$  was higher under WL than that under SOX or SOX + R, G or B light. At 10 d culture,  $ETR_{max}$  decreased compared to 3 and 6 d and no significant differences among the light treatments were observed. Finally, the maximal non-photochemical quenching ( $NPQ_{max}$ ) non presented interactive effects from day 3 at day 10. ( $p > 0.05$ , Fig. V.5). However, white light treatment was significantly highest in comparison to SOX and SOX with supplementation of the day 3 (Fig.V.5and Table S4; see supplementary material).

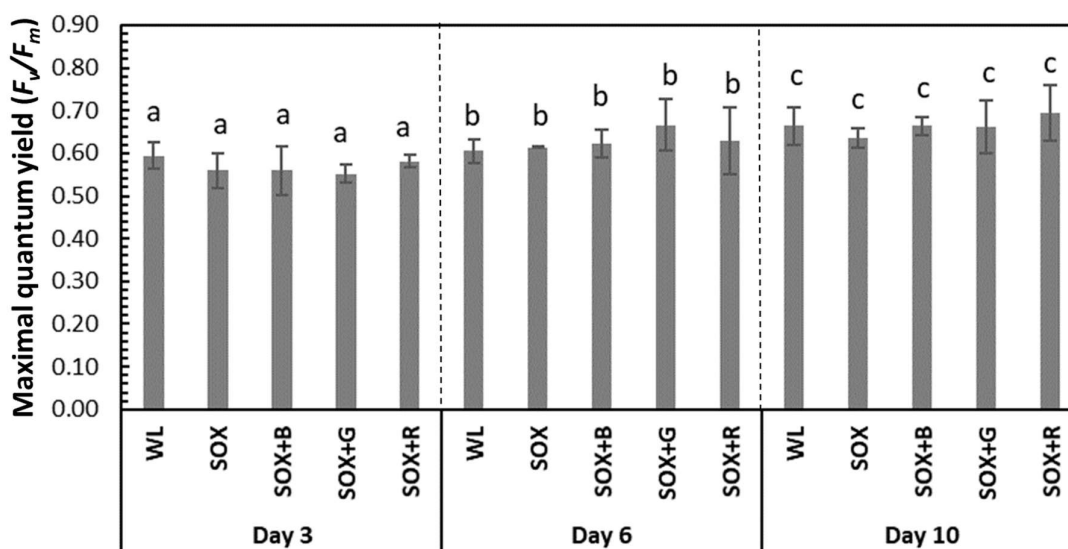


Figure II.5. Maximal quantum yield ( $F_v/F_m$ ) in *Porphyridium cruentum* in function of time and qualities of lights interactions, for the next treatments. WL: White light; SOX(Control): SOX; SOX+B: SOX + Blue; SOX+G: SOX + Green; SOX+R: SOX +Red. Different letters represent



significant differences ( $p < 0.05$ ) according to ANOVA results and the Student Newman Keuls test.

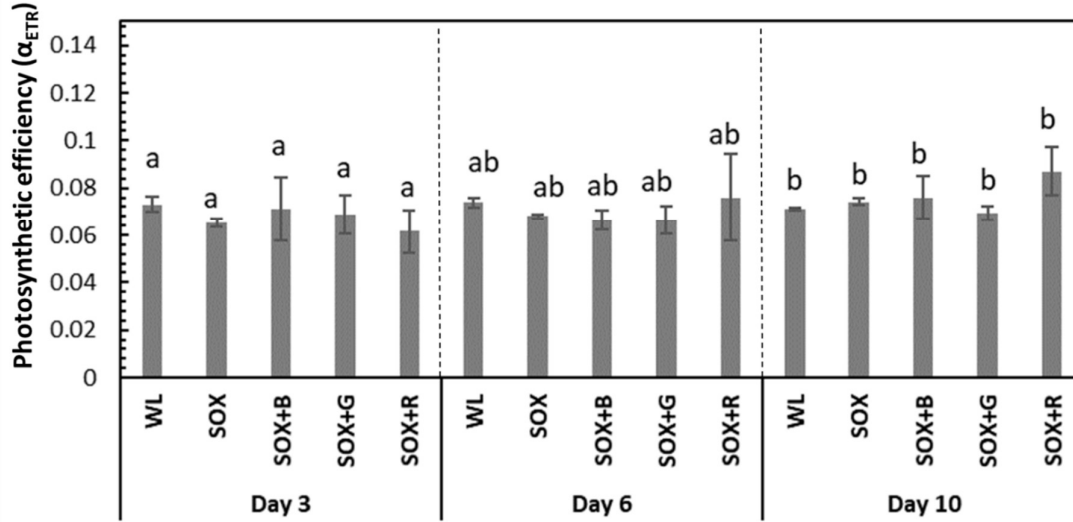


Figure III.5. Photosynthetic efficiency ( $\alpha_{ETR}$ ) in *Porphyridium cruentum* in function of the time and qualities of lights interactions ( $p < 0.05$ ), for the next treatments. WL: White light; SOX(Control): SOX; SOX+B: SOX + Blue; SOX+G: SOX + Green; SOX+R: SOX + Red. Different letters represent significant differences ( $p < 0.05$ ) according to ANOVA results and the Student Newman Keuls test.

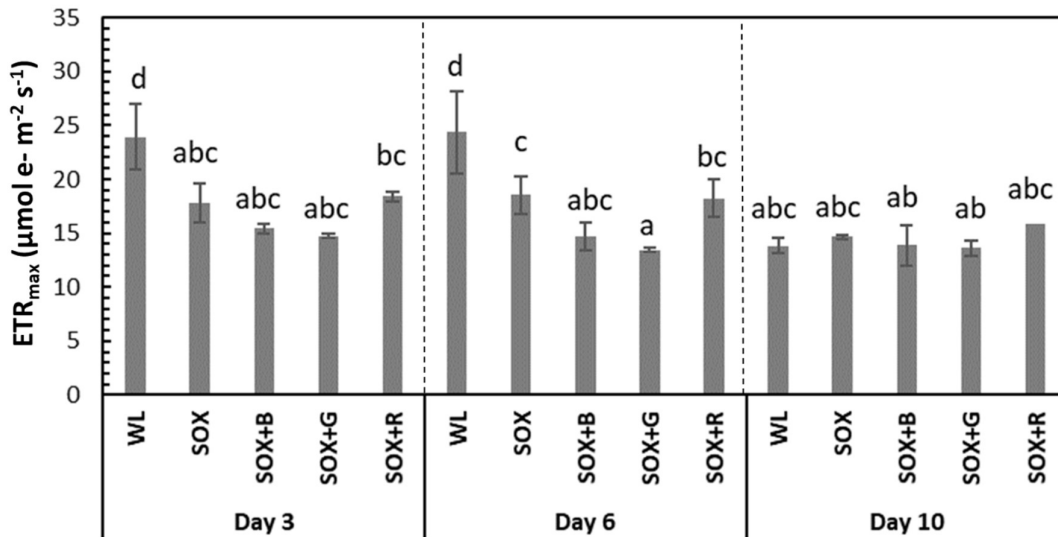


Figure IV.5. Maximal electron transport rate ( $ETR_{max}$ ) or productivity in the culture for *Porphyridium cruentum* culture for the time and qualities of lights interactions. In function of the treatments. WL: White light; SOX(Control): SOX; SOX+B: SOX + Blue; SOX+G: SOX + Green; SOX+R: SOX +Red. Different letters represent significant differences ( $p < 0.05$ ) according to ANOVA results and the Student Newman Keuls test.

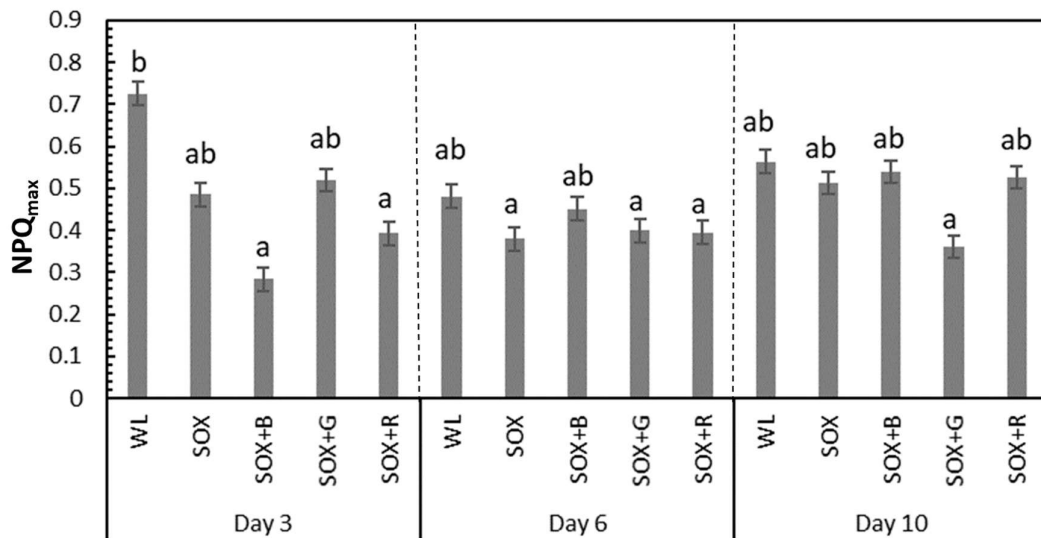


Figure V.5. Maximal non-photochemical quenching ( $NPQ_{max}$ ) or photoprotective indicator in the culture of *P. cruentum*, under time and qualities of lights interactions. In function of the treatments. WL: White light; SOX (Control): SOX; SOX+B: SOX + Blue; SOX+G: SOX + Green; SOX+R: SOX +Red. Different letters represent significant differences ( $p < 0.05$ ) according to ANOVA results and the Student Newman Keuls test.

### Growth rate and biomass productivity

Maximal cell density ( $N_{max}$ ) was higher under WL and SOX than that under SOX plus the different light qualities (Table I.5 and Fig. S2; see supplementary material). However,  $K_{max}$ , DW and biomass productivity did not present significant differences among the different light qualities (Table I.5).

## Effect of quality of light on growth and accumulation of bio-compounds

Phycocerythrin (B-PE) content was significantly affected by SOX+Blue treatments, achieving the highest values of 52.6mg g<sup>-1</sup> DW (Table II.5). At the same time, allophycocyanin (A-PC) content was significantly higher under of SOX light than SOX+Blue treatment while phycocyanin (R-PC) content did not present significant differences (Table II.5). SOX light treatment had significant effect ( $p<0.05$ ) on total protein accumulation and the highest level reported (62.9% DW) than other treatments (Table II.5). Carbohydrates decreased significantly under SOX+B compared to the rest of light treatments (Table II.5). The antioxidant activity (AA) ranges from 14-16  $\mu\text{mol Trolox g}^{-1}$  DW equivalent but not showed significant differences among the light treatments (Table II.5).

Table I.5 Parameters of growth (maximum cell density ( $N_{\text{max}}$ ), maximum growth rate ( $k_{\text{max}}$ ), dry weight (per culture volume) and biomass productivity ( $\text{mg mL}^{-1} \text{ day}^{-1}$ ) obtained in one-liter batch regime under five different combined treatments of light in a harvest day. The average values  $\pm$  standard deviations of 3 replicates per treatment are shown. Different letters indicate

| Treatments | $N_{\text{max}}$<br>( $\times 10^6$ Cell $\text{mL}^{-1}$ ) | $K_{\text{max}}$<br>( $\text{div day}^{-1}$ ) | Dry weight<br>( $\text{mg mL}^{-1}$ ) | Biomass<br>Productivity<br>( $\text{mg mL}^{-1} \text{ day}^{-1}$ ) |
|------------|---|---|---------------------------------------|---|
| WL         | 2.69 $\pm$ 0.4 <sup>c</sup>                                 | 0.28 $\pm$ 0.17 <sup>a</sup>                  | 1.07 $\pm$ 0.38 <sup>a</sup>          | 0.10 $\pm$ 0.03 <sup>a</sup>  |
| SOX        | 2.09 $\pm$ 0.1 <sup>b</sup>                                 | 0.36 $\pm$ 0.10 <sup>a</sup>                  | 0.92 $\pm$ 0.11 <sup>a</sup>          | 0.09 $\pm$ 0.01 <sup>a</sup>  |
| SOX+B      | 1.24 $\pm$ 0.06 <sup>a</sup>                                | 0.13 $\pm$ 0.01 <sup>a</sup>                  | 0.93 $\pm$ 0.09 <sup>a</sup>          | 0.09 $\pm$ 0.009 <sup>a</sup>                                       |
| SOX+G      | 1.59 $\pm$ 0.07 <sup>a</sup>                                | 0.27 $\pm$ 0.01 <sup>a</sup>                  | 1.0 $\pm$ 0.02 <sup>a</sup>           | 0.10 $\pm$ 0.002 <sup>a</sup>                                       |
| SOX+R      | 1.43 $\pm$ 0.06 <sup>a</sup>                                | 0.16 $\pm$ 0.04 <sup>a</sup>                  | 0.91 $\pm$ 0.07 <sup>a</sup>          | 0.09 $\pm$ 0.007 <sup>a</sup>                                       |

significant differences ( $p<0.05$ ) (ANOVA, Student Newman Keuls,  $p<0.05$ ). WL: White light; SOX(Control): SOX; SOX+B: SOX + Blue; SOX+G: SOX + Green; SOX+R: SOX +Red.

Total lipid concentration was not significantly different among the different light treatments (Table III.5). In general, the fatty acid profiles of the strain studied were characterized by high proportions of saturated and monounsaturated fatty acids. Polyunsaturated fatty acids (PUFAs) were preferably accumulated under SOX+Red, SOX+Green and SOX+Blue treatments, with Araquidonic acid (ARA) and eicosapentaenoic acid (EPA) being the most abundant PUFAs detected (Table III.5). The ranged between 20.4 and 23.08% for ARA under SOX conditions evaluated while under white light, ARA content was 16.13% of fatty acids. However, the highest EPA accumulation detected in this study occurred under white light condition (24.41% of total fatty acids) in contrast, under SOX and SOX plus supplemented light qualities the content ranges from (17.41-20.28% of total fatty acids). The saturated fatty acid fractions of Palmitic acid (PA) levels were not significantly different among the treatments (Table III.5).

Table II.5. Biochemical composition (soluble proteins, biliproteins content, total carbohydrates, and antioxidant activity) of the biomass of *Porphyridium cruentum* grown in one-liter batch regime under five different combined treatments of light sources and quality. The average values  $\pm$  standard deviations of 3 replicates per treatment are shown. Different letters indicate significant differences ( $p < 0.05$ ) (ANOVA, Student Newman Keuls,  $p < 0.05$ ). WL: White light; SOX(Control): SOX; SOX+B: SOX + Blue; SOX+G: SOX + Green; SOX+R: SOX +Red.

| Treatment | Soluble proteins by dry biomass (%) | Total carbohydrates by dry biomass (%) | Allophycocyanin by dry biomass (mg g <sup>-1</sup> ) | Phycocyanin by dry biomass (mg g <sup>-1</sup> ) | Phycoerythrin by dry biomass (mg g <sup>-1</sup> ) | Antioxidant activity of aqueous extract TE ( $\mu\text{mol g}^{-1}$ ) |
|-----------|-------------------------------------|--|--|--|--|---|
| WL        | 49.1 $\pm$ 2.7 <sup>a</sup>         | 16.6 $\pm$ 4.7 <sup>b</sup>            | 4.3 $\pm$ 0.4 <sup>ab</sup>                          | 6.1 $\pm$ 0.6 <sup>a</sup>                       | 36 $\pm$ 2.2 <sup>b</sup>                          | 14 $\pm$ 2.0 <sup>a</sup>   |
| SOX       | 62.9 $\pm$ 2.7 <sup>b</sup>         | 17.3 $\pm$ 2.1 <sup>b</sup>            | 5.9 $\pm$ 1.6 <sup>b</sup>                           | 7.4 $\pm$ 2.1 <sup>a</sup>                       | 26.2 $\pm$ 2.3 <sup>a</sup>                        | 15 $\pm$ 0.3 <sup>a</sup>   |
| SOX+B     | 53.8 $\pm$ 4.4 <sup>a</sup>         | 7.4 $\pm$ 0.6 <sup>a</sup>             | 3.1 $\pm$ 0.4 <sup>a</sup>                           | 5.1 $\pm$ 0.1 <sup>a</sup>                       | 52.6 $\pm$ 2.2 <sup>c</sup>                        | 15 $\pm$ 0.5 <sup>a</sup>   |
| SOX+G     | 52.2 $\pm$ 1.3 <sup>a</sup>         | 15.9 $\pm$ 0.4 <sup>b</sup>            | 4.6 $\pm$ 0.4 <sup>ab</sup>                          | 8.0 $\pm$ 3.3 <sup>a</sup>                       | 30.3 $\pm$ 3.8 <sup>ab</sup>                       | 15 $\pm$ 1.2 <sup>a</sup>   |
| SOX+R     | 56.0 $\pm$ 2.5 <sup>a</sup>         | 13.5 $\pm$ 1.0 <sup>ab</sup>           | 4.4 $\pm$ 0.4 <sup>ab</sup>                          | 6.1 $\pm$ 0.7 <sup>a</sup>                       | 33.3 $\pm$ 2.4 <sup>b</sup>                        | 16 $\pm$ 1.6 <sup>a</sup>   |

Table III.5. Total lipids and fatty acids composition of *Porphyridium cruentum* in one-liter batch regime under five treatments of light. Values are expressed as % total lipids and fatty acids by dry biomass. The average values  $\pm$  standard deviations of 3 replicates per treatment are shown. Different letters indicate significant differences ( $p < 0.05$ ) (ANOVA, Student Newman Keuls,  $p < 0.05$ ). WL: White light; SOX(Control): SOX; SOX+B: SOX + Blue; SOX+G: SOX + Green; SOX+R: SOX +Red.

|                             |         | Treatments                    |                               |                               |                               |                               |
|-----------------------------|---------|-------------------------------|-------------------------------|-------------------------------|-------------------------------|-------------------------------|
|                             |         | WL                            | SOX                           | SOX+B                         | SOX+G                         | SOX+R                         |
| Total Lipids                |         | 4.66 $\pm$ 1.07 <sup>a</sup>  | 3.84 $\pm$ 2.85 <sup>a</sup>  | 5.35 $\pm$ 0.94 <sup>a</sup>  | 4.78 $\pm$ 0.29 <sup>a</sup>  | 5.07 $\pm$ 0.86 <sup>a</sup>  |
| Saturated                   |         |                               |                               |                               |                               |                               |
| Palmitic acid (PA)          | C16:0   | 43.68 $\pm$ 0.48 <sup>a</sup> | 43.90 $\pm$ 1.76 <sup>a</sup> | 42.55 $\pm$ 0.64 <sup>a</sup> | 43.48 $\pm$ 2.60 <sup>a</sup> | 44.20 $\pm$ 2.56 <sup>a</sup> |
| Polyunsaturated             |         |                               |                               |                               |                               |                               |
| Arachidonic acid (ARA)      | C20:4n6 | 16.13 $\pm$ 1.4 <sup>a</sup>  | 20.89 $\pm$ 0.72 <sup>b</sup> | 20.47 $\pm$ 1.16 <sup>b</sup> | 23.08 $\pm$ 0.78 <sup>b</sup> | 22.98 $\pm$ 1.0 <sup>b</sup>  |
| Eicosapentaenoic acid (EPA) | C20:5n3 | 24.41 $\pm$ 1.30 <sup>b</sup> | 18.48 $\pm$ 0.89 <sup>a</sup> | 20.28 $\pm$ 1.69 <sup>a</sup> | 17.66 $\pm$ 1.08 <sup>a</sup> | 17.41 $\pm$ 1.63 <sup>a</sup> |

## DISCUSSION

Recent reviews reported that metabolic changes of high-value compounds occur as a response to the light quality (spectrum), and this idea attracted a lot of interest to optimize microalgae cultivation or in the same context, their utilization as bio-crudes or the maximal productivity in the microalgae culture (Ptushenko et al., 2015; Sirisuk et al., 2018a; Jung et al., 2019). Although, these previously cited studies did not consider effects mediated by SOX-light in microalgae (Cohen, 1990; Sánchez-Saavedra et al., 2018; Gaignard et al., 2019; Li et al., 2019a). Previously Aguilera et al., (1997, 2000) describe the positive effects of SOX lamp irradiation on growth and C metabolism in red macroalgae. In this context, the positive effects of SOX light in the massive culture system could increase the accumulation of the metabolites.

Aguilera et al., (1997) demonstrated that the enrichment of the SOX light in red macroalgae *Porphyra leucosticta* produced an increase of growth rate (thallus expansion) and production of photosynthetic pigments compared to fluorescent white light. The similar effect of narrowband SOX light on leaf area was recently shown for Chinese cabbage plants (Ptushenko et al., 2015). However, in our study, the microalgae *P. cruentum* did not present significant differences in DW and biomass production among the different light qualities. In fact, the accumulation of certain compounds as phycoerythrin, allophycocyanin, soluble proteins, carbohydrates, and fatty acids was different in WL compared to SOX or affected by the supplementation of different light qualities.

The photosynthetic responses are affected mainly by time exposure, i.e.,  $F_v/F_m$ , as an indicator of photo-inhibition (Guillard, 1973) increased from 0.58 to 0.66 in presence of the yellow light from day 3 to the end of the experimental period, suggesting low photoinhibition in the culture (Fig. 2, 3). In contrast, Sánchez-Saavedra et al., (2018) report inhibition of photosynthetic activity in *P. cruentum* under the different sources of nitrogen (ammonium and nitrate) and white light levels (50 and 200  $\mu\text{moles m}^{-2} \text{s}^{-1}$ ), i.e., 0.24-0.36. In this case, we suggest the high the physiological plasticity of the *P. cruentum* under different factors. Studies on physiological plasticity of a species allow the prediction of its ecological success (Üveges et al., 2012) and, from an evolutionary perspective, determine its potential for adaptation to future environmental changes (Ellers and Stuefer, 2010; Elisa Schaum and Collins, 2014; Gómez et al., 2016; Haro et al., 2017). The presence of phycobilisomes in the light-harvesting system may lead also to obtain lower values of  $F_v/F_m$  than those obtained in green or brown algae (Figueroa et al., 2013; Schuurmans et al., 2015). However, our  $F_v/F_m$  values were not so low as in comparison with Sanchez-Saavedra et al., (2018). Actually, values from 0.6 to 0.7 are very high considering red algae, indicating an acclimatation to light conditions. For another hand, Villafañe et al., (2005) found that *P. cruentum* is affected by solar ultraviolet radiation

(280–400 nm and 315–400 nm) in the short term (5 days), but can acclimate quickly to high irradiances, adjusting their photosynthesis but not growth rate.

In contrast to the growth rate as DW and biomass productivity, SOX produced different effects than that of WL on photosynthesis. Thus, under SOX alone or with supplementation of B, G, or R light,  $ETR_{max}$  decreased but only at 3 and 6-day culture. In 10 d culture, no significant differences between WL and SOX treatments are present, indicating a stress to light conditions. This stress condition could be associated a short acclimatation or by incremented relation between algal cells per culture media availability. Positive effects of SOX wavelengths on the accumulation of metabolites in *P. cruentum* were founded. Korbee et al., (Korbee et al., 2005a) reported that the growth of the red macroalgae *Porphyra leucosticta* can be enhanced using blue or red lights. Thus, blue light was used as the wavelength for biomass production in the first phase culture. The photosynthetic efficiency in the experimental vessels expressed the efficiency electron transport rate ( $\alpha_{ETR}$ ) increased under SOX supplemented by blue and red light, in both experimental times according to the maximal absorption of B and R light and minimal absorption in G light. The pattern was different on EPA and phycoerythrin content (B-PE) where a positive correlation ( $p < 0.05$ ) and better performance in function of  $F_v/F_m$  under SOX+Blue were found (Fig.1 and 2; Table II.5). Total protein and carbohydrate levels increased in the presence of SOX light, while phycoerythrin (B-PE) present significant differences under SOX light and SOX+B treatment but under only SOX light reached the highest level (Table II.5). In the same direction, allophycocyanin content was significantly higher under SOX light compared to white light and other light treatments. Our findings provide a specific effect of each colored light, which possible to use for the management of these specific compounds.

The strategy condition (SOX light and in mixture with Blue and Red lights) would allow maximizing the photomorphogenic potential of soluble proteins, phycoerythrin, allophycocyanin, and arachidonic acid as specialized additives in the food/feed industry. Similar photomorphogenic potential results were obtained for *Tetraselmis* sp. and *Nannochloropsis* sp. under blue light LEDs (Teo et al., 2014). In contrast, Mattos et al., (Mattos et al., 2015) performed short term oxygen evolution experiments in *Scenedesmus bijuga* and conclude that weakly absorbed colors of light such as green results in higher photosynthetic efficiency for high-density cultures. The green light could stimulate photosynthetic efficiency, however, in our study was not the case. Our work found that a mixture of these light wavelengths (SOX+Green) would not excite the PSII and PSI. Studies in *Evernia prunasstri* (lichen), Segovia et al., (64), suggest the saturation of photosynthesis with SOX light promoted cAMP accumulation and responded to photosynthetic photochemistry most likely through PSII and PSI acting sensors of light quantity.

The mechanisms of the heat of the energy dissipation ( $NPQ_{max}$ ) showed trends to increase in function of the time of the exposition during the experimental period, (from 3 to 10 days). Whereas the  $NPQ_{max}$  was higher under white light conditions, this suggests that was related to photoprotection mechanisms (Celis-Plá et al., 2016). In addition, the phycobiliproteins, such as phycoerythrin (B-PE), increased under the supplementation by blue light. B-PE is the main biliproteins and light-harvesting accessory pigment in *Porphyridium*; moreover, it has been found that the phycobiliproteins such as; allophycocyanin (A-PC), phycocyanin (R-PC), phycoerythrin (B-PE) has the strong antioxidant capacity (Soni et al., 2009). In our study, the PCA analyses show a positive correlation ( $p < 0.05$ ) on the second axis in the relationship between R-PC, A-PC, productivity, photosynthetic efficiency, and antioxidant activity. These results reinforce the possibility of using the phycobiliproteins (aqueous extracts) from *P. cruentum* for nutraceutical or pharmacology applications (Soni et al., 2009; Jung et al., 2016;



Senthilkumar et al., 2018). The A-PC, and B-PE in *P. cruentum* are influenced by yellow and yellow with blue light reached 5.9 and 52.6 mg g<sup>-1</sup> by dry biomass, respectively. The content pigment in algae is highly dependent on the perceived light intensity and quality of light (Lopez-Figueroa et al., 1989; López-Figueroa and Niell, 1990). The photo-regulation of both chlorophyll and biliproteins in red algae is regulated by different B, G, and R light photomorphogenic and non-photosynthetic photoreceptors (López-Figueroa, 1991; Rüdiger and López-Figueroa, 1992). In this way, the next step of this research will include the optimization of SOX and SOX with blue light to get high-efficiency photosynthetic systems of a photobioreactor for indoor production of biliproteins with high-value food products such as A-PC and B-PE.

In the process of photoacclimation, the phycoerythrin content increase under yellow light with wavelength-specific supplementation where the blue light supplementation was the highest, these results suggest that the metabolic change could be associated with the efficient use of the yellow and photomorphogenic effect of blue light, because, the blue light has a special role in metabolism as chlorophyll *a* has a pronounced absorption peak of the light spectrum and has influenced gene expression, activation of the enzyme and metabolic pathway via blue light photoreceptors cryptochromes, aureochromes, and phototropins (Kianianmomeni and Hallmann, 2014; Landi et al., 2020). It could have been expected that pigment content correlates to the biomass specific light absorption rate. If this was in the case our experiments, blue light that promotes the synthesis of ribulose 1,5-biphosphate carboxylase (RuBisCo) and carbonic anhydrase, that are enzyme affecting the carbon dioxide fixation rates and ultimately the accumulation of carbohydrates. Likewise, yellow light with blue supplementation should have resulted in increased carbohydrates content, but our results show the opposite. Probably the saturation of SOX light (equivalent to yellow light) inhibited the carbohydrate metabolism. Besides, the high accumulated amounts of carbohydrates by *P. cruentum* are observed when

there is the presence of external carbon sources, like as mixotrophic and heterotrophic cultures (Fabregas et al., 1999). In fact, in red microalgae the variation of light/dark cycles has been seen to have a significant effect on their accumulation and when there the nitrogen deprivation conditions (Fabregas et al., 1999; Villay et al., 2013; Soanen et al., 2016).

Blue light stimulated N metabolism and C metabolism is decreased whereas and R light stimulated C metabolism (Rüdiger and López-Figueroa, 1992). As the mechanism behind pigment acclimation in response to light quality has not yet unraveled (Jones, 1998; Landi et al., 2020) and the importance of other light acclimation responses has not yet been studied in detail, our observations are difficult to explain. De Mooij et al., (de Mooij et al., 2016) suggests that green microalgae with yellow and blue light treatments reach inactivation of PSII, which reduced the biochemical conversion capacity, however yellow light could still be used at a higher efficiency than, for example, blue light. Therefore, we suggest the high intensity of yellow light must have been the explanation for the good performance. One approach could be possible from the proportion of relative emission spectra where the WL have 45.8% and 31.8% of total percentage of blue and yellow light, respectively (Table S6; see supplementary material). In this sense, the enrichment of this spectra region by SOX+Blue treatment show a clear direction of the nitrogen metabolism to improve culture performance and production of the microalgae *P. cruentum*

Lipid content values, expressed as percentage by dry biomass, obtained in this study ranged from 3.8 to 5.3 % (Table III.5), which were lower values than that reported previously (8 to 19.3%) for *P. cruentum* (Walsby, 1995; Oh et al., 2009; Sánchez-Saavedra et al., 2018; Li et al., 2019c). Light quality did not affect lipid accumulation in *P. cruentum* (Table III.5). These results show that the application of supplemented B, G, and R lights does not negatively affect photosynthesis and subsequently the accumulation of lipids. Considering that the accumulation

of lipids could be a response condition to stress as an energy reservoir produced during photosynthesis under non-optimal conditions. The highest lipid accumulation was observed at the SOX+Blue light quality condition. However, the values were lower, which makes it necessary to investigate in future experiences about the effect of blue light on the accumulation of lipids in this strain. You and Barnett (2004) observed an increase in cell growth when exposing under blue light in *P. cruentum*. They did not determine the lipid content, but growth rates were better than for white light. In contrast, Oh et al., (Oh et al., 2009) demonstrated that with white light, a maximum of 19.3% (w/w) lipid can be obtained by growing *P. cruentum* in batch mode under 18 h/12 h, then 12 h/12 h light/dark periods. In addition, the lipid profile produced by *P. cruentum* is composed of approximately 44% C16 under SOX+Red. This result is comparable with a previous study reporting that the total C16 was 33% in *P. cruentum*, a value lower than that obtained by us, exposed to the high light intensity of white fluorescent lamps (Oh et al., 2009). This study can guide commercial indoor production of *P. cruentum* for high-value food products such as Palmitic acid (C16:0).

When microalgae are cultured for the supply of nutritionally valuable lipid, LC-PUFAs (accumulated mainly as membrane phospholipids) are the principal interest. Although total lipids decreased under SOX lights treatment, the fatty acid profile showed a significant proportion of them corresponded to PUFAs (39.3-40.7 %) (Table III.5) including EPA and ARA, both highly valuable in animal and human nutrition. ARA proportion was higher in SOX+Green (23.08%), while EPA maximum value (24.41%) was achieved when the alga was cultured in white light. The literature, reports have been demonstrated a direct relationship between temperature and lipid quality in different strains of *Porphyridium* (S. Mihova, 1996; Oh et al., 2009). Nevertheless, the temperature is not the sole culture parameter affecting lipid production by red microalgae, as light intensity and quality can also modified as we reported in our study. As shown by Mihova et al., (S. Mihova, 1996), the EPA content of *Porphyridium*

*sordidum* can reach 28% (w/w) of the total fatty acids when it cultivated at low light (150  $\mu\text{moles m}^{-2} \text{s}^{-1}$ ; white light), which is close with our results (24.41% EPA). In another hand, Cohen et al., (Cohen, 1990), with a supplement of nitrogen of potassium > 10 mM, obtained values of 20.7% ARA in *P. cruentum* a value lower than that obtained by us. These differences suggested in relation to the intrinsic differences between strains and differences in the source of nitrogen and light quality employed in the studies. To the authors' knowledge, this is the first time that the lipid profiles in *P. cruentum* were investigated under different wavelengths. The results could help to improve the arachidonic acid, which remains at a desirable level, considering its commercial importance, and potential applications in the functional food sector and/or supplement market.

From a biotechnological point of view, this kind of studies allows the determination of some attributes of commercial interest like culture stability under fluctuating environments or the possibility of handling culture conditions to produce biomass with a different biochemical composition (Gómez et al., 2016; Haro et al., 2017).

## CONCLUSIONS

In this study we reported, in the first time for the experimental period, the feasibility to use SOX light (yellow light) as a photosynthetic light at saturated irradiance of the photosynthesis activity without reducing the concentration of biomass of *P. cruentum*. This study demonstrates that the yellow light with the incidence of blue light as an interesting factor in the culture of red microalgae, to improve high-quality compounds and maintained stable biomass productivity. In spite of we compared just a small number of factors in a very narrow range, the data show that *P. cruentum* has great potential for the production of phycoerythrin pigment for commercial natural colorants or proteins for different markets, such as feed/food. It is proposed the use of SOX light or filters of yellow color with blue light supplementation in the

new generation of the photobioreactor technology to grow species of red algae with the objective to improve the quality of phycoerythrin production.

### **Supplementary Material**

<https://onlinelibrary.wiley.com/action/downloadSupplement?doi=10.1111%2Fphp.13426&file=php13426-sup-0001-TableS1-S7-FigS1-S3.docx>

### **Acknowledgments**

This study was supported by Junta de Andalucía (research group Photobiology and Biotechnology of Aquatic Organisms, RNM-295). The authors thank Julia Vega, member of the Unit of Photobiology of the University of Malaga, for her technical assistance.

---

# CHAPTER VI:

**General discussion, conclusions and future  
perspectives**

## VI.1. General discussion.

Our work contributes to the knowledge for the development of novel extraction techniques with food grade solvents providing high extraction yields on endemic and commercial interest of the red macroalga *Sarcopeltis skottsbergii* from Chile. There is a clear effect using high pressure homogenization (HPH) obtained the most efficient extraction, yielding 5.7 mg R-PE g<sup>-1</sup> DW biomass at the optimal conditions (300 MPa, 2 passes with distilled water), 50-60 % higher than the R-PE yields obtained with ultrasound-assisted extraction (UAE) (Chapter II). The most crucial variable in the extraction process was the pressure level, with the highest concentrations of R-PE using distilled water were obtained. Our results suggest that the release of R-PE can be promoted with distilled water due to accelerated molecule diffusion and solubility of other proteins and the affinity of the carboxylic groups at pH 6.5-7.0. However, heat can also induce the degradation of the extracted bioactive compounds. The high amplitude of UAE (between 75-90% wave amplitude) and HPH (>450MPa) increases the temperature (average of 40°C; data not shown). In this sense, more than 20 min is not recommended for *S. skottsbergii*, assuming that the chloroplast is slightly damaged, explaining the low release of R-PE over this time. From these observations the hypothesis was accepted in relation to the viability and safety (non-aggressive) of the use of high pressure technology until 300 MPa, because of the temperature limitation in the system. Similar results were observed by Pereira et al., (2020), where the pressure at 600 MPa induced an increase in the extracted temperature, promoting pigment denaturation. Simovic et al., (2022) reported that in contrast to high temperature, the high-pressure (HP) treatment showed that a significant concentration at 450 MPa had a less destructive effect on R-PE color intensity from the macroalga *Porphyra purpurea* (Rhodophyta). However, the yields are lower even if a range similar to our range of 100-300 MPa is worked with. This difference may be due to the different species of red algae and geographical latitude because the morphology of the cell wall and accumulation of

metabolites can vary despite R-phycoerythrin being the pigment with the highest proportion in red algae.

The pigments concentration and antioxidant capacity of the water extract from the *S. skottsbergii* show a good correlation (Figure V.II). A great number of authors used the freezing and thawing method for phycobiliproteins extraction (e.g. Phycoerythrin or Phycocyanin) in different species of Red algae and Cyanobacteria (Korbee et al., 2005; Celis-Plá et al., 2014; Astorga-España et al., 2017; Pagels et al., 2019; Niu et al., 2006). However, our observations showed significant antioxidant properties, which were increased with the enhancement of R-PE concentration in water solvent using the UAE and HPH methods. Although our study does not use a chromatographic technique for purification and determines the polyphenols, the concentrated extract of R-PE could be part of a synergy of these compounds in the redox activity attributable to this macroalga.

In Chapter III we evaluated the residue generated from the phycoerythrin aqueous extract using a bio-refinery concept process. The supernatant residue was characterized funded high proportion of polysaccharides (neutral and acid) compounds. From our observations, the high-pressure homogenization offers a process efficiency of depolymerization where we found a high proportion of oligomers. Moreover, it has been seen that the degree of sulfation is much higher in acid than total polysaccharide from aqueous fraction, exhibited significant antioxidant activity in superoxide radical assay (ABTS) and high anti-proliferative effects on G-361, U-937, HCT-116 cancer cells. In the same line, Fenoradosa et al., (2012) reported the performed by high-pressure homogenization on the polysaccharide of the red macroalga *Halymenia durvillei* showed their feasibility and effectiveness and that an advantage of the depolymerization at high pressure was the ease and speed of the preparation. Also, del Río et al., (2021) reported the use of microwave hydrothermal treatment for the multiproduct



valorisation of the invasive macroalgae *Sargassum muticum* allowing a recovery of a liquid phase rich in fucoidan-derived compounds (up to 4.81 gL<sup>-1</sup>), oligomers and phenolics with antioxidant capacity of interest from feed/food sector. In our case, when high pressure homoeogenization was used, clear effect in the depolymerization enhanced of the cytotoxicity index (IC<sub>50</sub>). Ariffin et al., (2005) reported similar results, when effects of carrageenan from the red alga *Eucheuma denticulatum* on cancer human intestine Caco-2 with IC<sub>50</sub>=1000 (µg mL<sup>-1</sup>) was analyzed, while in our assays on HCT-116, the acid polysaccharides from *S. skottsbergii* presented 3.6 times higher cytotoxic. In addition, the incorporation of ultrasound-assisted extraction can enhance the activity as reported Torres et al. (2021) comparing the conventional extraction of carrageenan with ultrasound extraction. The cytotoxic was 3.39 times more effective against the same cancer cell line HT-29 than that reported by Suganya et al (2014). Finally, the biological profile of the products could be influenced by the depolymerization method, since it affects their size and molecular weight. One of the highlights of our work was the low temperatures (40 °C) respect to the traditional extraction method for polysaccharides (>80 °C) reached by the high-pressure processes, finding fractions with interesting biological properties by depolymerization of polysaccharides with low temperature is suggested. Apparently, the fractions rich in glucose and saccharose of carrageenan would be suitable and replicable technology for the generation of compounds for food and biotechnological applications.

Following the diagram process of high extraction yields of R-PE from Chapter II (Figure I.2) and valorization of the residual components from R-PE extraction of Chapter III (Figure I.3), we have grouped in a general scheme which includes Chapter II, III and IV in general discussion (Figure I.6).

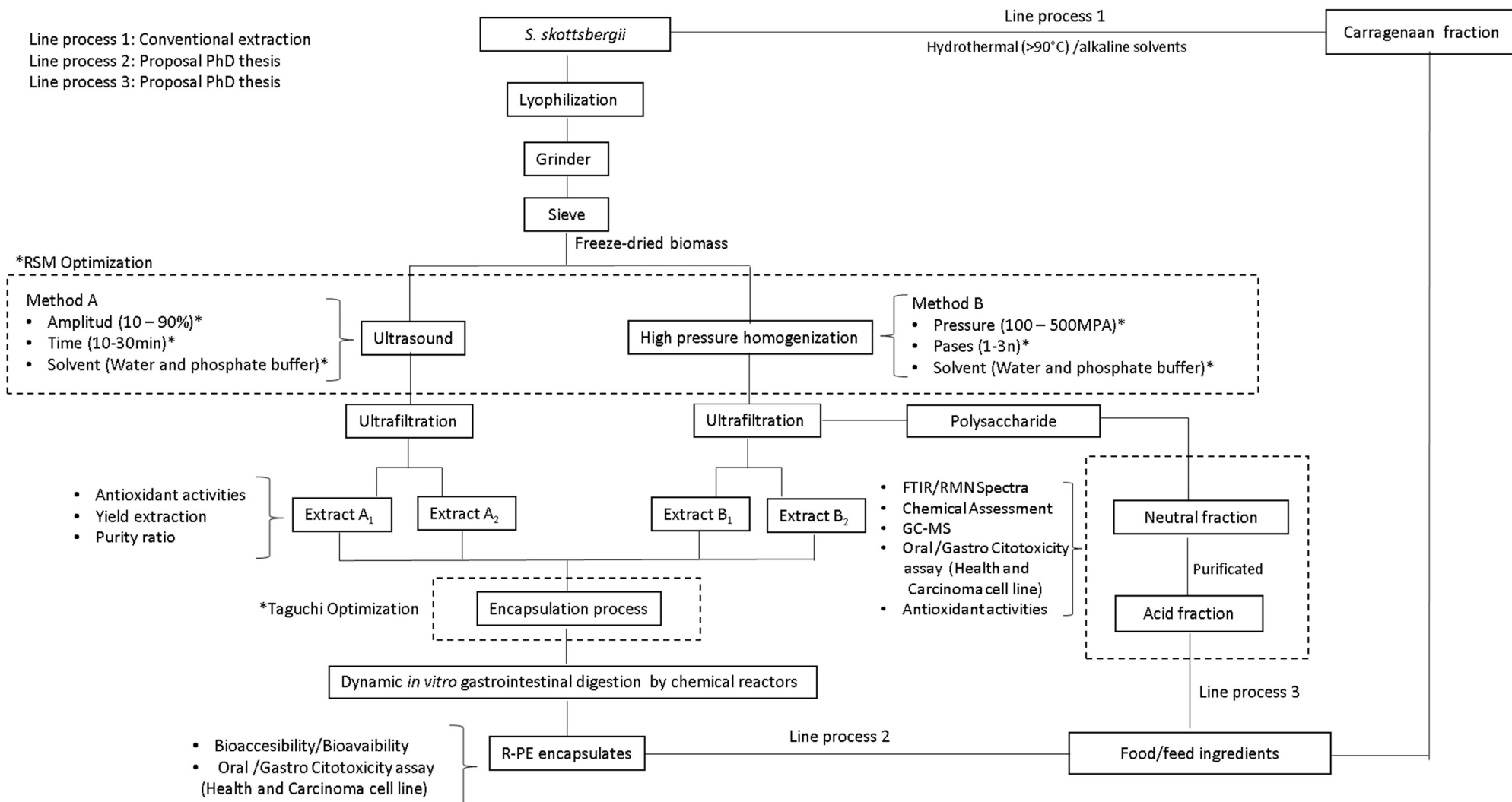


Figure I.6. Schematic of general blue bioprocess from *Sarcopeltis skottsbergii*.

Chapter IV presented how the alginate/shellac mixture as wall material to develop aqueous R-PE can be used as an encapsulation system by external gelation and the effect of encapsulation on the release properties of R-PE during simulated gastrointestinal digestion by dynamic systems (Chemical reactors). The effect of the variables: Feeding flow (90 and 20 mL h<sup>-1</sup>), distance (5 and 10cms) and CaCl<sub>2</sub> (5 and 15 g L<sup>-1</sup>) were optimized by Taguchi method and characterized the bead size, sphericity factor (SF) and total R-PE content of beads. The CaCl<sub>2</sub> concentration and feeding flow were the variables that most affect the R-PE EE reached 97.5±0.5%. The beads obtained were semi-spherical, non-aggregated with a particle size of 1.2mm and SF 0.09. The release of R-PE from alginate/shellac was affected at acid pH 1, showed membrane rupture under acidic conditions; however, the concentration was under the 10% of R-PE total content. To formulate the wall material, alginate/shellac has been validated by other authors with good results in the efficiency of encapsulation for bioactive like riboflavin (Messaud et al., 2016), sunflower oil (Morales et al., 2017) and inclusive in a microorganism (Silva et al., 2016). However, the protection processes for phycobilin pigments have been little explored but have great potential in the food industry according to several studies (Juin et al., 2015; Jacotet-Navarro et al., 2016; Pereira et al., 2020; Domínguez et al., 2020). Similar results were obtained by Pan-tai et al., (2018) for Phycocyanin (C-PC), from microalgae *Arthrospira platensis*, under alginate formulation process to beads by ionic gelation reached 98% EE. It was found that alginate and CaCl<sub>2</sub> concentration have a significant influence on the EE (%) and bead properties. These values are similar with our results, where the differences can be by the combination of the materials and the low concentration of CaCl<sub>2</sub> (2.5%), in which the competition between the two polymers to bind calcium ions Ca<sup>2+</sup> affects the final composite gel structure. The observations of Henning et al., (2012) and Messaoud et al., (2016), found that coating the capsules by Ca<sup>2+</sup> reticulation of shellac led to the formulation of a uniform and the smooth layer closely related to the amount of shellac and Ca<sup>2+</sup>, elucidating

that the cross-linking can be enough at concentration of CaCl<sub>2</sub> 2% (%W/V). Additionally, spherical beads as an encapsulation system are more stable than irregular or non-spherical shaped beads as spherical beads have a low surface/volume ratio, producing a lower diffusion of bioactive in the beads. Dried microcapsules presented diameters ranging from 0.8 to 1.20mm (Table I.4). Despite the large size, these microcapsules may be used in solid foods, in which the texture is not affected by the particle size, such as chocolate and cereal bars (Silva et al., 2016).

From another hand, alginate/shellac as wall materials for R-PE have an acceptable mechanism for protection of the pigment allowing it to pass through the mouth, stomach, duodenum barriers and releasing the compound in a controlled intestinal phase compared with R-PE non-encapsulated, suggesting a protective role. From permeate streams, equivalent to absorption of R-PE encapsulated, the bioavailability was 2.5 times significantly higher than R-PE non-encapsulated. According to Pimentel et al., (2020), the enriching protein extracts from *Porphyra dioica* (Nori) released at the intestinal level is recommendable because it is in the intestine that the proteins are degraded by enzymes and peptides are absorbed into the bloodstream improving the antioxidant activity. Our DGGE analysis showed that the fraction of the final digest was between 25-50 KDa, where the profile of the extracted protein is consistent with previous results reported by Pimentel et al., (2020) and Stack et al., (2017) for red algae. Similar conclusions were reported by Wu et al., (2015), who evaluated the in vitro digestion of R-PE found that the final intestinal digestion still contained high antioxidant activity in proteins fraction of <3 kDa. They indicate that digestion-resistant antioxidant peptides of R-PE may be obtained by in vitro gastrointestinal proteinase degradation.

The changes in R-PE encapsulates concentration through digestion have low reports in the literature. This represents the novelty of the research where we considered a positive highlight

in new knowledge due to little information. However, it is clear that the biological activities of R-PE be maintained after in vitro digestion stage demonstrated by Yabuta et al., (2010), Wu et al., (2015), Stack et al., (2017) and Pimentel et al., (2020). In our work, the percentage of R-PE found in the permeate stream was lower than R-PE encapsulated where we found 6.0% of bioavailability at 180 min of intestinal digestion. The R-PE bioavailability significantly differed depending on the wall material, after the gastric step the alginate/shellac beads contained  $0.31 \text{ mg g}^{-1}$  of R-PE, which represents a decrease of 91.4% compared with the initial concentration ( $5.58 \text{ mg g}^{-1}$ ). However, the R-PE bioavailability is enough for cytotoxic response against on human cancer cells. A high selectivity index ( $> 10$ ) was observed for the R-PE extract on HCT-116 human colon cancer cell line. This allows us to show that the proportion or mixture of the encapsulating wall material is the one indicated and this is possible to use a criterium for future application of the encapsulation in Phycobiliproteins. In this context, in relation of the inventions of process founded (Appendix A4), it was determined that the initial stages of the encapsulating process may be novel and that there is a possible inventive level of the proposal under study, due to the scarce information existing in patents of these stages. However, the final stages of the process may have advantageous characteristics (Point of release at the gastrointestinal level) and possible patenting process.

The cytotoxicity of R-PE was found to be dose dependent, and the effect was observed microscopically all the selected cancer cell lines at their  $\text{IC}_{50}$  values of R-PE were  $144.5 \pm 3.96 \mu\text{g mL}^{-1}$  for HCT-116 (colon carcinoma),  $2702 \pm 12.6 \mu\text{g mL}^{-1}$  for U-937 (leukemia carcinoma) and  $2788 \pm 11.5 \mu\text{g mL}^{-1}$  for G-361 (melanoma carcinoma). From HCT-116 results were in consonance with that HepG2 (liver carcinoma) and A549 (Lung carcinoma) cell line with R-PE obtained from *Portiera hornemannii* (Red algae) (Senthilkumar et al., 2013). Also, R-PE show inhibits growth and induces apoptosis on SKOV-3 cells (Ovarian carcinoma) from *Gracilaria lemaneiformis* (red algae) (Ying et al., 2021). Definitely, the inhibitory effect of

PE on gastro-intestinal cells was a result of interaction with multiple cell lines with potential nutraceutical or pharma applications. Inclusive when the R-PE was encapsulated we observed similar affinity on HCT-116. The  $IC_{50}$  encapsulates was  $1076 \pm 8.46 \mu\text{g mL}^{-1}$  which was low with respect to  $144.5 \pm 3.96 \mu\text{g mL}^{-1}$  from aqueous extract of R-PE. This could be due to the materials used that could be growth cofactors in tumoral cells. The foregoing is difficult to explain since there are no studies to date that include the bioactivity of encapsulated phycobiliproteins.

On the other hand, the same cytotoxic pattern was observed in sulphated polysaccharides, being almost 100 times more cytotoxic than that found with R-PE in *S. skottsbergii*. The lowest  $IC_{50}$  was found in the acid fraction with  $0.642 \pm 1.86 \mu\text{g mL}^{-1}$  for G-361 (melanoma carcinoma) and  $1.2 \pm 5.85 \mu\text{g mL}^{-1}$  for U-937 (leukemia carcinoma). Similar results in acidic fraction polysaccharide were found in *Gracilaria lemaneiformis* (red algae) (Fan et al., 2012). Abdala-Díaz et al., (2019) found high antiproliferative activity in sulfated polysaccharides of *Laminaria ochrikeuca* (brown algae) on human leukemia ( $IC_{50} = 3.72 \text{ mg mL}^{-1}$ ) and malignant melanoma G-361 ( $IC_{50} = 5.42 \text{ mg mL}^{-1}$ ). Also, high potential immunomodulatory was found in *Hypnea spinella* and *Halopithis incurva* (red algae) by strong cytokine IL-6 inducers (Abdala-Díaz et al., 2011). In general, the bioactive properties and their compounds vary from species to species. However, most of the bioactive compounds in seaweeds are typically from the aqueous fraction of the seaweed. Dias et al., (2005) and Ale et al., (2011) have studied these functional materials based on different types of seaweed polysaccharides and the growth inhibitory effects on tumor cells. The results showed that the contents of sulphate groups played a key role in increasing the bioactive properties, acting to promote apoptosis via activation of caspase-3. However, the contents of the sulfate groups depend on the seaweed source and its chemical and structural composition. Additionally, the sulfation pattern (position of sulphate groups in each sugar residue) also affects biological activity.

The incorporation of macroalgae as part of the normal daily diet has been correlated with a lower incidence and decreased risk of mortality for *MetS* diseases such as hyperlipidemia, coronary heart disease, and other cardiovascular diseases based on epidemiological studies of the Japanese diet (Iso, 2011; Nanri et al., 2017; Niu et al., 2015; Yokoyama et al., 2019). A study by Yoshinaga & Mitamura (2019) revealed that just by consuming dried wakame (*Undaria pinnatifida*) (brown algae) with rice can reduce blood glucose and insulin after 30 minutes, indicating that the intake of seaweed could regulate postprandial homeostasis. This is probably due to the known ancestrally traditional practice in the Asia continent whereby seaweeds are boiled, infused with hot water, or prepared as a soup to extract its medicinal properties before being consumed by the patient (Anggadiredja, 2009; Liu et al., 2012).

On the other hand, the generation of R-PE is still a bottleneck for the development of bioprocesses in the food and biotechnology area. Bioprocess reproducibility and scalability are still areas that need to be investigated in order to have a constant supply of the compound of interest. In that sense, the cultivation of macroalgae in Chile has a low development, only one species has managed to be cultivated industrially (*Gracilaria chilensis*), so the rest are obtained from natural banks, risking its extinction and the biological richness of the habitat where it lives. For this reason, an alternative is the development of cultivation technologies that allow satisfying a constant and incremental demand. In a biotechnological perspective, light is a key factor for the production of red algae in photoautotrophic mode, which is the most used type of cultivation due to economic criteria for biomass production on a large scale (Gouveia et al., 2009; Guedes et al., 2014). For this, in Chapter V, yellow light by the application of low pressure sodium vapor lamps (SOX) was used to obtain saturation of photosynthesis in a wavelength band without any known photomorphogenic photoreceptor (Segovia et al., 2003) and without interference with other known non-photosynthetic photoreceptors in the

wavelengths of blue, green, or red light leading to accumulation of compounds through non-photosynthetic pathways (Rüdiger and López-Figueroa 1992; Rockwell et al., 2014).

In photosynthetic organisms, light can be used as a source of environmental information to control metabolic processes such as growth, reproduction, and morphogenesis. In spite of comparing just a small number of factors in a very narrow range, the data show that the red microalga *P. cruentum* has great potential for the production of phycoerythrin pigment (52.6 mg of R-PE g<sup>-1</sup> of biomass) for commercial natural colorants or proteins for different markets, such as feed/food. The production of R-PE was 9.2 times higher productive based on saturating light in microalgae *P. cruentum* than macroalgae *S. skottsbergii*. Obviously, the comparative differences have a limit due to the that they are different species, habitats and extraction methods. However, organisms from the same group, new lines of research are opened for the optimization of the accumulation of R-PE in red macroalgae.

In red macroalgae, there are few reports that optimize the R-PE by LED or Fluorescent Lamps technology. Aguilera et al., (1997, 2000) describe the positive effects of SOX lamp irradiation on growth and C metabolism in red macroalgae. In this context, the positive effects of SOX light in the massive culture system could increase the accumulation of the metabolites. Aguilera et al., (1997) demonstrated that the enrichment of the SOX light in red macroalgae *Porphyra leucosticta* produced an increase of growth rate (thallus expansion) and production of photosynthetic pigments compared to fluorescent white light. Positive effects of SOX wavelengths on the accumulation of metabolites in *P. cruentum* were founded. Korbee et al., (2005) reported that the growth of the red macroalga *Porphyra leucosticta* can be enhanced using blue or red lights. Thus, blue light was used as the wavelength for biomass production in



the first phase culture and in addition B light promote the accumulation of Mycosporine-like amino acids.

It could have been expected that pigment content correlates to the biomass specific light absorption rate. If this was in the case our experiments, blue light that promotes the synthesis of ribulose 1,5-biphosphate carboxylase (RuBisCo) and carbonic anhydrase, that are enzyme affecting the carbon dioxide fixation rates and ultimately the accumulation of carbohydrates. Likewise, yellow light with blue supplementation should have resulted in increased carbohydrates content, but our results show the opposite. The blue light supplementation was the highest, these results suggest that the metabolic change could be associated with the efficient use of the yellow and photomorphogenic effect of blue light, because, the blue light has a special role in metabolism as chlorophyll *a* has a pronounced absorption peak of the light spectrum and has influenced gene expression, activation of the enzyme and metabolic pathway via blue light photoreceptors cryptochromes, aureochromes, and phototropins (Landi et al., 2020).

Finally, the use of SOX light with blue light supplementation is proposed for the new generation of technology in a photobioreactor for the cultivation of red algae species, with the aim of improving the quality of bioprocess production.

## **VI.2. General conclusions/Conclusiones generales**

Given the questions asked and contrasting them with the experimental results of this work, we verify that the hypothesis is accepted at three levels of the objectives:

In the first stage, we development of efficient extraction methods by High-pressure homogenization for R-PE provides an interesting non-aggressive extraction alternative with the biological activity. At the same time, it was possible to recover using a biorefinery concept

from R-PE supernatants, two fractions (neutral and acid) of polysaccharides with the high antiproliferative activity on G-361 (Melanoma cancer cells) and HCT-116 (Colon cancer cells) of interest for the formulation of biotechnological products for the nutraceutical and food industry.

In the second level, the design of membrane architecture mixing alginate and shellac solutions produce an excellent matrix system for the protection of R-PE with 97.5% efficiency of encapsulation. The  $\text{CaCl}_2$  concentration and feeding flow were the variables that most affect the R-PE encapsulation systems. The beads obtained were semi-spherical, non-aggregated with a particle size of 1.2mm.

In the last level, from permeate streams, equivalent to absorption of R-PE encapsulated, the bioavailability was 2.5 times significantly higher than R-PE non-encapsulated. Alginate/shellac as wall materials for R-PE have an acceptable mechanism for protection of the pigment allowing it to pass through the mouth, stomach, duodenum barriers and releasing the compound in a controlled intestinal phase compared with R-PE non-encapsulated, suggesting a protective role. The R-PE bioavailability is enough for cytotoxic response against on human cancer cells. A high selectivity index ( $> 10$ ) was observed for the R-PE extract on HCT-116 human colon cancer cell line.

From an alternative context, the R-PE pigment is possible to produce under the use of SOX light with blue light supplementation is proposed for the new generation of technology in a photobioreactor for the cultivation of red microalgae species, with the aim of improving the quality of biocompounds.

## Conclusiones Generales

Ante las cuestiones planteadas y contrastándolas con los resultados experimentales de este trabajo, comprobamos que la hipótesis se acepta en tres niveles de los objetivos:

En la primera etapa, el desarrollo de métodos eficientes de extracción por homogeneización a alta presión para R-PE proporciona una interesante alternativa de extracción no agresiva con presencia de actividad biológica. Al mismo tiempo, fue posible recuperar utilizando un concepto de biorrefinería a partir de sobrenadantes de R-PE, dos fracciones (neutra y ácida) de polisacáridos con alta actividad antiproliferativa sobre G-361 (células de cáncer de melanoma) y HCT-116 (células de cáncer de colon). Ambas fracciones son de interés para la formulación de productos biotecnológicos para la industria nutracéutica y alimentaria.

En el segundo nivel, el diseño de la arquitectura de membrana mezclando soluciones de alginato y goma laca produce un excelente matrix para la protección de R-PE con una eficiencia de encapsulación del 97,5%. La concentración de  $\text{CaCl}_2$  y el flujo de alimentación fueron las variables que más afectaron los sistemas de encapsulación R-PE. Las perlas obtenidas fueron semiesféricas, no agregadas con un tamaño de partícula de 1,2 mm.

En el último nivel, a partir de corrientes de permeado, equivalente a la absorción de R-PE encapsulado, la biodisponibilidad fue 2,5 veces significativamente mayor que la del R-PE no encapsulado. El alginato/goma laca como materiales de pared para R-PE tienen un mecanismo aceptable para la protección del pigmento que le permite pasar a través de las barreras de la boca, el estómago y el duodeno y liberar el compuesto en una fase intestinal controlada en comparación con el R-PE no encapsulado, lo que sugiere un papel protector. La biodisponibilidad de R-PE es suficiente para la respuesta citotóxica contra las células cancerosas humanas. Se observó un alto índice de selectividad ( $> 10$ ) para el extracto de R-PE en la línea celular de cáncer de colon humano HCT-116.

Desde un contexto alternativo, el pigmento R-PE es posible de producir bajo el uso de luz SOX con luz azul, se propone la suplementación para la nueva generación de tecnología en fotobiorreactores para el cultivo de especies de microalgas rojas, con el objetivo de mejorar la calidad de biocompuestos.

### VI.3. Future perspectives

The development and employment of innovative HPH techniques can have a favorable effect on process efficiency to enhance pigment extraction. This technology involves the use of water as a solvent for extraction allowing an economic alternative to buffering extraction and leading to a reduction in the environmental impact. Another advantage of this methodology is that less heat damage is done to the R-PE molecule, and indirectly the recovery of the polysaccharide with biological activity, as the heat is applied over a shorter period of time. This may be achieved through the development on an industrial scale of the so-called integrated biorefinery systems, and improved processing technology for the production and purification by environment-friendly extraction processes in a fast, cost-effective and non-aggressive way.

On the other hand, we postulate to unwind the bottleneck regarding the availability of the resource, cultivating species of red algae accumulating R-PE in culture systems with photostimulation of yellow light supplemented with blue, as a strategy to maximize production (See Figure II.6).

In the short term, we hope to carry out *in vivo* tests using the zebrafish model for the prospection of polysaccharides as potential food ingredients. As well as the biological activity against viral hemorrhagic septicemia virus (VHSV) on salmonids cell lines (RTG-2), which for now we have an interesting and innovative results which can be use for create a new line of nutraceutical application due to its proven physiological effects for aquaculture industry (See Figure II.6).

Finally, macroalgae are already farmed on a massive scale in Asia, and substantial quantities are also harvested from aquaculture intensity activities. More research has shown the potential for large-scale culture of macroalgae in Pacific waters.

This Ph.D. project its a first approach based to open new research line in relation of downstream process and open the window in others related in effective methodologies to grow, harvest, and bioproduct large quantities of sustainable cultivated macroalgae.

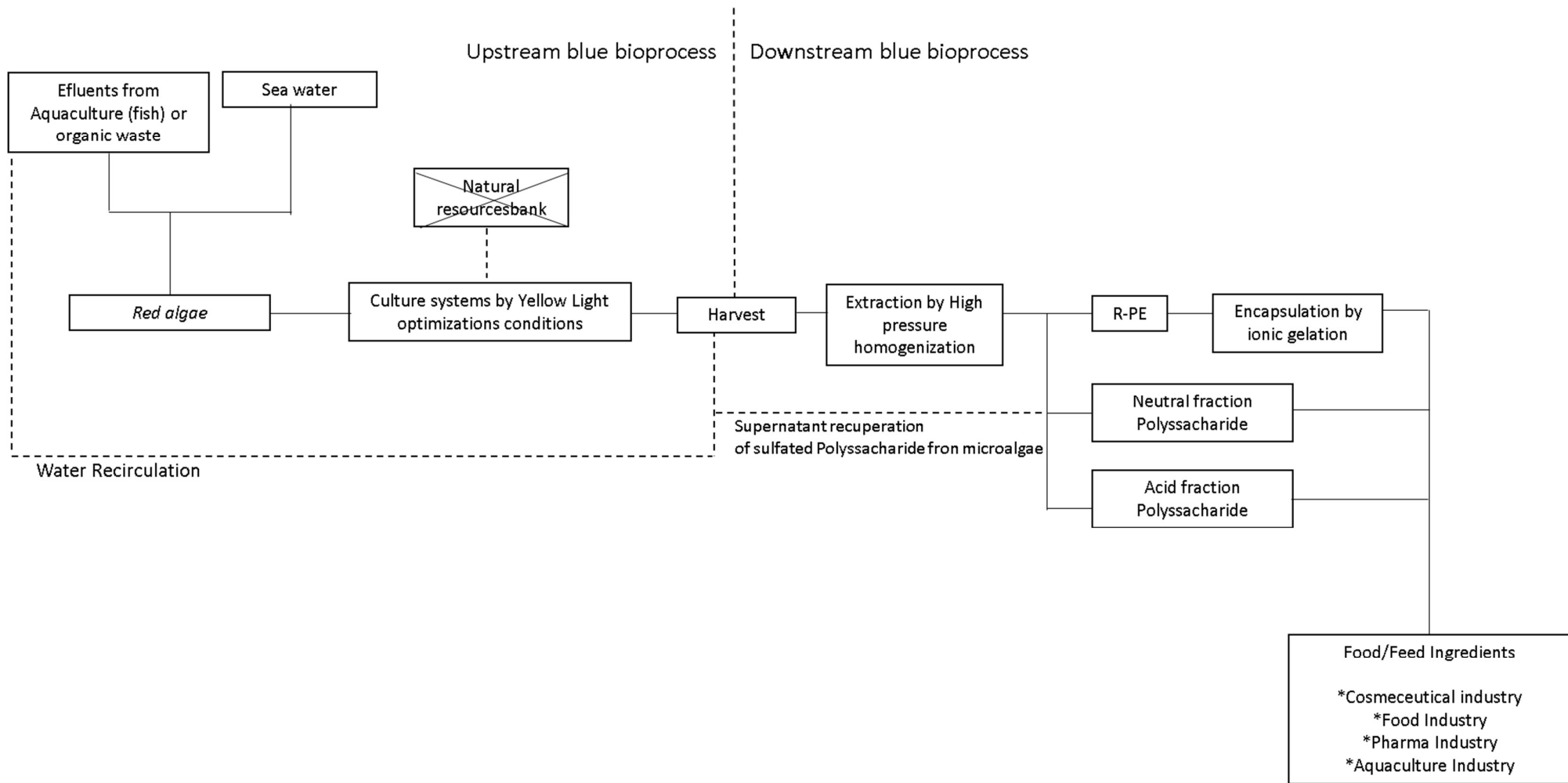


Figure II.6. Schematic of general upstream and downstream blue bioprocess proposal for future applications from red algae (Macro and microalgae).

---

## CHAPTER VII: LIST OF APPENDICES

### Appendix A.

#### A1. List of paper and patents of this thesis

**Castro-Varela P.**, Celis-Pla P.S.M., Figueroa F. and Rubilar M. (2022) Highly Efficient Water-Based Extraction of Biliprotein R-Phycoerythrin From Marine the Red-Macroalga *Sarcopeltis skottsbergii* by Ultrasound and High- Pressure Homogenization Methods. *Frontiers Marine Science*. 9:877177. Doi: 10.3389/fmars.2022.877177

**Castro-Varela P.**, Rubilar M., Rodriguez B., Figueroa L.F., Abdala R. (2022). A sequential recovery extraction and biological activity of water-soluble sulfated polysaccharides from the polar red macroalgae *Sarcopeltis skottsbergii*. (*Submitted to Marine Biotechnology Journal*)

**Castro-Varela, P. A.**, Celis-Plá, P. S. M., Abdala-Díaz, R., and Figueroa, F. L. (2021). Photobiological Effects on Biochemical Composition in *Porphyridium cruentum* (Rhodophyta) with a Biotechnological Application. *Photochemistry and Photobiology*. 97, 1032-1042 Doi: 10.1111/php.13426.

**Castro-Varela Pablo**, Rubilar Mónica, Abdala-Díaz Roberto, Figueroa-López, Félix. *Método para la bioprotección de ficobiliproteínas utilizando un simple y rápido proceso iónico gelificante*. Solicitud de Patente. Dirección de Innovación y Transferencia Tecnológica. Universidad de La Frontera.

#### A2. Other original research papers during PhD studies

**Castro-Varela, P.A.**, Sáez, K and Gómez, P.I. (2021) Effect of urea on growth and biochemical composition of *Porphyridium purpureum* (Rhodophyta) and scaling-up under non-optimal outdoor conditions. *Phycologia*, 10:1-10. <https://doi.org/10.1080/00318884.2021.1953305> .

Gomez PI., Inostroza I., **Castro-Varela P.A.**, Silva J., Clement A., Rojas G., Aguilera Belmonte A. (2021) Comparison of a Chilean strain of the ichthyotoxic phytoflagellate *Heterosigma akashiwo* (Raphidophyceae) with strains from France, Spain and New Zealand. *Phycologia* 61:1, 7-15 <https://doi.org/10.1080/00318884.2021.1991685>



Massocato T, Robles V., Rodrigues B., Castro-Varela P., Pinheiro-Silva L., Oliveira, W., Vega J., Figueroa A., Bonomi-Barufi J., Rorig, L., and Figueroa F.L (2022). Growth, biofiltration and photosynthetic performance of *Ulva* spp. cultivated in fishpond effluents: an outdoor study. *Frontiers Marine Sciences*, 9:981468. [https://doi: 10.3389/fmars.2022.981468](https://doi.org/10.3389/fmars.2022.981468)

Gomez PI., **Castro-Varela P.**, Mayorga J., Flaig D. (2022) Looking beyond *Arthrospira*: comparison of antioxidant and anti-inflammatory properties of ten cyanobacteria strains (*Submitted to Algal Research*).

Massocato, T, Robles, V, Rodrigues, B, **Castro-Varela, P.**, Bonomi-Barufi, Abdala Díaz, R. T. ,J., Rorig, L., Figueroa, F. L. (2022) Characterization, antioxidant and cytotoxicity activity of ulvan polysaccharides from *Ulva pseudorotundata* and *Ulva rigida* and their potential for pharmaceutical and cosmeceutical application. (*Submitted to Marine Biotechnology*).

### **A3. Conference contributions**

**2022.** “A sequential recovery extraction and biological activity of water-soluble sulfated polysaccharides from the polar red macroalgae *Sarcopeltis skottsbergii*”, IV International Congress Seaweed for Health, Universidad de Vigo, modalidad presencial, presentación oral.

**2021.** “Validación Fotobiológica y Antioxidante de extractos concentrados en R-ficoeritrina procesados por Ultrasonido y altapresion de la macroalga *Sarcopeltis skottsbergii*. III Congreso de Jóvenes investigadores del Mar, Universidad de Granada, modalidad presencial, presentación poster.

**2021.** “Highly efficient water-based extraction of biliprotein R-phycoerythrin from marine macroalgae *Sarcopeltis skottsbergii* (Rhodophyta): Optimization of conditions by ultrasound and high-pressure homogenization methods”. International Phycological Applied Algae Congress, University of Tasmania, modalidad Virtual, presentación oral.

**2019.** “Desarrollo de Emulsiones multicapa en polvo como un sistema eficiente de encapsulación de oleoresina de Astaxantina desde la microalga *Haematococcus pluvialis*.”. Congreso Nacional Ciencia y Tecnología de los Alimentos, Universidad de Los Lagos, modalidad presencial.

#### A4. Table of Patents

| Title of the patent   | Country   | Year |
|---|-----------|------|
| “Método para el cultivo de células de algas rojas <i>Acrochaetium moniliforme</i> , método para obtener un extracto de su biomasa y uso de las mismas en cosmética” 1553106 10.04.2015 FR | Francia   | 2016 |
| “Producción de ficoeritrina a partir de alga roja”  | Rusia     | 2014 |
| “Recuperación y purificación de b-ficoeritrina producida por porphyridium cruentum utilizando sistemas de dos fases acuosas y precipitación isoeléctrica”                                 | Mexico    | 2007 |
| “Composiciones de recubrimiento que comprenden un fragmento de una célula biológica o virus, superficies revestidas y métodos para fabricar y utilizar dichas composiciones               | Israel    | 2006 |
| Orange-red dye extracted from red alga - useful as colourant and immunofluorescence label (FR2690452)   | Francia   | 1998 |
| Material colorante derivado de microalgas rojas”  | Australia | 1998 |
| Algal pigment material and its production (JP1999299450)  | Japon.    | 1992 |

---

## REFERENCES

- Abad, P., Arroyo-Manzanares, N., Rivas-Montoya, E. Ochando-Pulido, K.M., Guillamon, E., García-Campaña, A.M. and Martínez-Ferez, A. (2019) Effects of different vehiculization strategies for the allium derivative propyl propane thiosulfonate during dynamic simulation of the pig gastrointestinal tract. *Canadian Journal Animal Science* 99:244–253. <https://doi.org/10.1139/cjas-2018-0063>
- Abdala-Díaz, R. T. A., Chabrilón, M., Cabello-Pasini, A., Gómez-Pinchetti, J. L., and Figueroa, F. L. (2011). Characterization of polysaccharides from *Hypnea spinella* (Gigartinales) and *Halopithys incurva* (Ceramiales) and their effect on RAW 264.7 macrophage activity. *Journal of Applied Phycology* 23, 523–528. doi: 10.1007/S10811-010-9622-7/FIGURES/3.
- Abdala-Díaz, R. T., Casas Arrojo, V., Arrojo Agudo, M. A., Cárdenas, C., Dobretsov, S., and Figueroa, F. L. (2019). Immunomodulatory and Antioxidant Activities of Sulfated Polysaccharides from *Laminaria ochroleuca*, *Porphyra umbilicalis*, and *Gelidium corneum*. *Marine Biotechnology* 21, 577–587. doi: 10.1007/s10126-019-09905-x.
- Abu-Ghosh, S., Fixler, D., Dubinsky, Z., and Iluz, D. (2016). Flashing light in microalgae biotechnology. *Bioresource Technology*. 203, 357–363. doi: 10.1016/j.biortech.2015.12.057.
- Acevedo, F., Hermosilla, J., Sanhueza, C., Mora-Lagos, B., Fuentes, I., Rubilar, M., Concheiroi, A., Alvarez-Lorenzo, C. (2018) Gallic acid loaded PEO-core/zein-shell nanofibers for chemopreventive action on gallbladder cancer cells. *European Journal of Pharmaceutical Sciences* 119: 49-61
- Aguilera, J., Figueroa, F., and Niell, F. X. (1997). Photocontrol of short-term growth in *Porphyra leucosticta* (Rhodophyta). *European Journal of Phycology*. 32, 417–424. doi: 10.1080/09670269710001737359.
- Aguilera, J., Gordillo, F. J. L., Karsten, U., Figueroa, F. L., and Niell, F. X. (2000). Light quality effect on photosynthesis and efficiency of carbon assimilation in the red alga *Porphyra leucosticta*. *Journal of Plant Physiology* 157, 86–92. doi: 10.1016/S0176-1617(00)80140-6.
- Álvarez-Gómez, F., Korbee, N., Casas-Arrojo, V., Abdala-Díaz, R. T., and Figueroa, F. L. (2019). UV photoprotection, cytotoxicity and immunology capacity of red algae extracts. *Molecules* 24, 1–16. doi: 10.3390/molecules24020341.
- Álvarez-Viñas, M., Flórez-Fernández, N., Torres, M. D., and Domínguez, H. (2019). Successful Approaches for a Red Seaweed Biorefinery. *Marine Drugs* 2019, Vol. 17, Page 620 17, 620. doi: 10.3390/MD17110620.
- Alexandre, E. M. C., Araújo, P., Duarte, M. F., de Freitas, V., Pintado, M., and Saraiva, J. A. (2017). Experimental Design, Modeling, and Optimization of High-Pressure-Assisted Extraction of Bioactive Compounds from Pomegranate Peel. *Food and Bioprocess Technology* 10, 886–900. doi: 10.1007/s11947-017-1867-6.

- Angell, A. R., Mata, L., de Nys, R., and Paul, N. A. (2016). The protein content of seaweeds: a universal nitrogen-to-protein conversion factor of five. *Journal of Applied Phycology* 28, 511–524. doi: 10.1007/S10811-015-0650-1/FIGURES/5.
- Anderson, M.J., Gorley, R.N. and Clarke, K.R. (2008) PERMANOVA + for PRIMER: Guide to Software and Statistical Methods. PRIMER-E, Plymouth.
- Ardiles, P., Cerezal-Mezquita, P., Salinas-Fuentes, F., Órdenes, D., Renato, G., and Ruiz-Domínguez, M. C. (2020). Biochemical Composition and Phycoerythrin Extraction from Red Microalgae: A Comparative Study Using Green Extraction Technologies. *Processes* 8, 1628. doi: 10.3390/PR8121628.
- ASAE S319.3 Method of Determining and Expressing Fineness of Feed Materials by Sieving Available at: <https://dokumen.tips/documents/asae-s3193-method-of-determining-and-expressing-fineness-of-feed-materials-by-sieving.html> [Accessed January 25, 2022].
- Astorga-España, M. S., Mansilla, A., Ojeda, J., Marambio, J., Rosenfeld, S., Mendez, F., Rodrigues J.P. and Ocaranza P. (2017). Nutritional properties of dishes prepared with sub-Antarctic macroalgae—an opportunity for healthy eating. *Journal of Applied Phycology* 29, 2399–2406. doi: 10.1007/s10811-017-1131-5.
- Araiza-Calahorra, A., and Sarkar, A. (2019). Pickering emulsion stabilized by protein nanogel particles for delivery of curcumin: Effects of pH and ionic strength on curcumin retention. *Food Structure*. 21, 100113. doi: 10.1016/J.FOOSTR.2019.100113.
- Assunção, J., Pagels, F., Tavares, T., Malcata, F. X., & Guedes, A. C. (2022). Light Modulation for Bioactive Pigment Production in *Synechocystis salina*. *Bioengineering* 2022, Vol. 9, Page 331, 9(7), 331. <https://doi.org/10.3390/BIOENGINEERING9070331>
- Barba, F. J., Grimi, N., and Vorobiev, E. (2015). New Approaches for the Use of Non-conventional Cell Disruption Technologies to Extract Potential Food Additives and Nutraceuticals from Microalgae. *Food Engineering Reviews* 7(1), 45–62. doi: 10.1007/s12393-014-9095-6.
- Baer, S., Heining, M., Schwerna, P., Buchholz, R., and Hübner, H. (2016). Optimization of spectral light quality for growth and product formation in different microalgae using a continuous photobioreactor. *Algal Research* 14, 109–115. doi: 10.1016/j.algal.2016.01.011.
- Bagchi, D. (2006) Nutraceuticals and functional foods regulations in the United States and around the world. *Toxicology* 221:1–3.
- Bradford, M. M. (1976). A rapid and sensitive method for the quantitation of microgram quantities of protein utilizing the principle of protein-dye binding. *Analytical Biochemistry* 72, 248–254. doi: 10.1016/0003-2697(76)90527-3.
- Bennett, A., and Bogobad, L. (1973). Complementary chromatic adaptation in a filamentous blue-green alga. *Journal of Cell Biology* 58, 419–435. doi: 10.1083/jcb.58.2.419.
- Benavides, J., and Rito-Palomares, M. (2006). Simplified two-stage method to B-phycoerythrin recovery from *Porphyridium cruentum*. *J Chromatogr B Analyt Technol Biomed Life Sci* 844, 39–44. doi: 10.1016/J.JCHROMB.2006.06.029.

- Belay, A. (2002) The potential application of *Spirulina (Arthrospira)* as a nutritional and therapeutic supplement in health management. *Journal of the American Nutraceutical Association*. 5, 27–48.
- Ben Messaoud, G., Sanchez-Gonzalez, L., Jacquot, A., Probst, L., Jeandel-Elmira, C., Desobry, S. (2016) Physico-chemical properties of alginate/shellac aqueous core capsules: Influence of membrane architecture on riboflavin release. *Carbohydrate Polymers*. 144, 428-437.
- Bischoff-Bäsmann, B., and Wiencke, C. (1996). Temperature requirements for growth and survival of Antarctic Rhodophyta. *Journal of Phycology* 32, 525-535. doi: 10.1111/j.0022-3646.1996.00525.x.
- Boehlke, C., Zierau, O., Hannig, C. (2015) Salivary amylase—the enzyme of unspecialized euryphagous animals. *Archives of Oral Biology*. 60,1162–1176.
- Buschmann, A., Hernández, M., Aranda, C., Chopin, T., Neori, A., Halling, C., Troell, M. (2008) Mariculture waste management. In Jorgensen S, Fath B (eds) *Ecological Engineering*. vol. 3 of Encyclopedia of Ecology, Oxford: Elsevier, p. 2211-2217.
- Burgain, J., Gaiani, C., Linder, M., and Scher, J. (2011). Encapsulation of probiotic living cells: From laboratory scale to industrial applications. *Journal of Food Engineering*. 104, 467–483. doi: 10.1016/J.JFOODENG.2010.12.031.
- Bhat, B., and Madyastha, K. (2000) C-phycoerythrin: A potent peroxyl radical scavenger in vivo and in vitro. *Biochemical and Biophysical Research Communications*. 275(1), 20–25.
- Blanken, W., Postma, P. R., de Winter, L., Wijffels, R. H., and Janssen, M. (2016). Predicting microalgae growth. *Algal Research* 14, 28–38. doi: 10.1016/j.algal.2015.12.020.
- Blois, M. S. (1958). Antioxidant Determinations by the Use of a Stable Free Radical. *Nature* 1958 181:4617 181, 1199–1200. doi: 10.1038/1811199a0.
- Bradford, M. M. (1976). A rapid and sensitive method for the quantitation of microgram quantities of protein utilizing the principle of protein-dye binding. *Analytical Biochemistry* 72, 248–254. doi: 10.1016/0003-2697(76)90527-3.
- Brodkorb, A., Egger, L., Alming, M., Alvito, P., Assunção, R., Ballance, S., et al., (2019). INFOGEST static in vitro simulation of gastrointestinal food digestion. *Nature Protocols* 14, 991–1014. doi: 10.1038/s41596-018-0119-1.
- Castro-Varela, P. A., Celis-Plá, P. S. M., Abdala-Díaz, R., and Figueroa, F. L. (2021). Photobiological Effects on Biochemical Composition in *Porphyridium cruentum* (Rhodophyta) with a Biotechnological Application. *Photochemistry and Photobiology* 97, 1032-1042 doi: 10.1111/php.13426.
- Castro-Varela, P., Celis-Pla, P. S. M., Figueroa, F. L., and Rubilar, M. (2022). Highly Efficient Water-Based Extraction of Biliprotein R-Phycocyanin From Marine the Red-Macroalga *Sarcopeltis skottsbergii* by Ultrasound and High-Pressure Homogenization Methods. *Frontiers Marine Sciences*. 0, 988. doi: 10.3389/FMARS.2022.877177.

- Campos A., M., Cavalcante Braga, A. R., Sala, L., and Juliano Kalil, S. (2020). Colour stability and antioxidant activity of C-phycoerythrin-added ice creams after in vitro digestion. *Food Research International*. 137, 109602. doi: 10.1016/J.FOODRES.2020.109602
- Carbonell-Capella, JM., Buniowska, M., Barba, FJ., Esteve, MJ., Frigola, A. (2014) Analytical methods for determining bioavailability and bioaccessibility of bioactive compounds from fruits and vegetables: a review. *Comprehensive Reviews in Food Science and Food Safety*.13:155–171.
- Celis-Plá, P. S. M., Korbee, N., Gómez-Garreta, A., and Figueroa, F. L. (2014). Seasonal photoacclimation patterns in the intertidal macroalga *Cystoseira tamariscifolia* (Ochrophyta). *Scientia Marina*. 78(3), 377-88. doi: 10.3989/scimar.04053.05a.
- Celis-Plá, P. S. M., Bouzon, Z. L., Hall-Spencer, J. M., Schmidt, E. C., Korbee, N., and Figueroa, F. L. (2016). Seasonal biochemical and photophysiological responses in the intertidal macroalga *Cystoseira tamariscifolia* (Ochrophyta). *Marine Environmental Research*. 115, 89–97. doi: 10.1016/j.marenvres.2015.11.014.
- Celis-Plá, P. S. M., Korbee, N., Gómez-Garreta, A., and Figueroa, F. L. (2014). Patrones estacionales de fotoaclimatación en el alga intermareal, *Cystoseira tamariscifolia* (Ochrophyta). *Scientia Marina* 78, 377–388. doi: 10.3989/scimar.04053.05A.
- Ciko, A. M., Jokić, S., Šubarić, D., and Jerković, I. (2018). Overview on the application of modern methods for the extraction of bioactive compounds from marine macroalgae. *Marine Drugs* 16(10), 348. doi: 10.3390/md16100348.
- Cofrades, S., Serdaroglu, M., Jimenez-Colmenero, F. (2013). Functional ingredients from algae for foods and nutraceuticals. In: Dominguez H(ed) Functional ingredients from algae for foods and nutraceuticals. *Woodhead Publishing Series in Food Science, Technology and Nutrition*. N°19: 609- 633
- Cohen, Z. (1990). The production potential of eicosapentaenoic and arachidonic acids by the red alga *Porphyridium cruentum*. *Journal of American Oil Chemistry Society*. 67, 916–920. doi: 10.1007/BF02541847.
- Cotas, J., Leandro, A., Pacheco, D., Gonçalves, A. M. M., and Pereira, L. (2020a). A Comprehensive Review of the Nutraceutical and Therapeutic Applications of Red Seaweeds (Rhodophyta). *Life* 10. doi: 10.3390/LIFE10030019.
- Cotas, J., Marques, V., Afonso, M. B., Rodrigues, C. M. P., and Pereira, L. (2020b). Antitumour Potential of *Gigartina pistillata* Carrageenans against Colorectal Cancer Stem Cell-Enriched Tumourspheres. *Marine Drugs*. 2020, Vol. 18, Page 50 18, 50. doi: 10.3390/MD18010050.
- Chan, E. (2011) Preparation of Ca-alginate beads containing high oil content: Influence of process variables on encapsulation efficiency and bead properties. *Carbohydrate Polymers*, 84(4), 1267-1275.
- Chan, E. S., Lee, B. B., Ravindra, P., and Poncelet, D. (2009). Prediction models for shape and size of ca-alginate macrobeads produced through extrusion–dripping method. *Journal of Colloid and Interface Sciences*. 338, 63–72. doi: 10.1016/J.JCIS.2009.05.027.

- Chemat, F., Rombaut, N., Sicaire, A. G., Meullemiestre, A., Fabiano-Tixier, A. S., and Abert-Vian, M. (2017). Ultrasound assisted extraction of food and natural products. Mechanisms, techniques, combinations, protocols and applications. A review. *Ultrasonics Sonochemistry* 34, 540-560. doi: 10.1016/j.ultsonch.2016.06.035.
- Chevalier, P., Consentino, GP., De la Noue, J., Rakhit, S. (1987) Comparative study on the diffusion of an IgG from various hydrogel beads. *Biotechnology Techniques*. 1 : 201–206.
- Chew, S. C., and Nyam, K. L. (2016). Microencapsulation of kenaf seed oil by co-extrusion technology. *Journal of Food Engineering* 175, 43–50. doi: 10.1016/J.JFOODENG.2015.12.002.
- Christie, W. W. (1982) A simple procedure for rapid transmethylation of glycerolipids and cholesteryl esters. *Journal of Lipid Research*. 23(7), 1072–1075.
- Choi, D., Park, C., Kim, I., Chun, H., Park, K., Han, D. (2010) Fabrication of core-shell microcapsules using PLGA and alginate for dual growth factor delivery system. *Journal of Controlled Release*, 147, 193–201
- Chory, J., Chatterjee, M., Cook, R. K., Elich, T., Fankhauser, C., Li, J., et al., (1996). From seed germination to flowering, light controls plant development via the pigment phytochrome. *Proceedings of the National Academy of Sciences*. 93, 12066–12071. doi: 10.1073/pnas.93.22.12066.
- Dammeyer, T., Frankenberg-Dinkel, N. (2006) Insights into phycoerythrobilin biosynthesis point toward metabolic channeling. *Journal of Biological Chemistry*, 281(37), 27081–27089.
- Denis, C., Massé, A., Fleurence, J., and Jaouen, P. (2009). Concentration and pre-purification with ultrafiltration of a R-phycoerythrin solution extracted from macro-algae *Grateloupia turuturu*: Process definition and up-scaling. *Separation and Purification Technology* 69, 37–42. doi: 10.1016/j.seppur.2009.06.017.
- Devi, N., Sarmah, M., Khatun, B., and Maji, T. K. (2017). Encapsulation of active ingredients in polysaccharide–protein complex coacervates. *Advances in Colloid and Interface Science* 239, 136–145. doi: 10.1016/J.CIS.2016.05.009.
- Del Río, P. G., Gullón, B., Pérez-Pérez, A., Romani, A., and Garrote, G. (2021). Microwave hydrothermal processing of the invasive macroalgae *Sargassum muticum* within a green biorefinery scheme. *Bioresource Technology* 340, 125733. doi: 10.1016/J.BIORTECH.2021.125733.
- De Felice, S. L. (1992). The nutraceutical initiative: a recommendation for U. S. economic and regulatory reforms. *Genet. Eng. News*. 12, 13–15.
- De Mooij, T., de Vries, G., Latsos, C., Wijffels, R. H., and Janssen, M. (2016). Impact of light color on photobioreactor productivity. *Algal Research*. 15, 32–42. doi: 10.1016/j.algal.2016.01.015.
- Dominguez, H. (2013) Algae as a source of biologically active ingredients for the formulation of functional foods and nutraceuticals”. In: Dominguez H(ed) Functional ingredients from algae for foods and nutraceuticals. *Woodhead Publishing Series in Food Science, Technology and Nutrition*. No.256: 1-19.

- Doyon, M. And Labrecque, J. (2008). Functional foods: A conceptual definition.. *British Food Journal.*, 110 , 1133–1149
- Dubois, M., Gilles, K. A., Hamilton, J. K., Rebers, P. A., and Smith, F. Colorimetric Method for Determination of Sugars and Related Substances. *Analytical Chemistry.* 1956, 28, 350–356.
- Dupont, D., Alric, M., Blanquet-Diot, S., Bornhorst, G., Cueva, C., Deglaire, A., Denis, S., Ferrua, M., Havenaar, R., Lelieveld, J., Mackie, A., Marzorati, M., Menard, O., Minekus, M., Miralles, B., Recio, I., Van den Abbeele, P. (2018) Can dynamic in vitro digestion systems mimic the physiological reality?. *Critical Review Food Science Nutrition.* 1-17.
- Eilers, P. H. C., and Peeters, J. C. H. (1988). A model for the relationship between light intensity and the rate of photosynthesis in phytoplankton. *Ecological Modelling* 42, 199–215. doi: 10.1016/0304-3800(88)90057-9.
- Elisa Schaum, C., and Collins, S. (2014). Plasticity predicts evolution in a marine alga. *Proceedings of the Royal Society B: Biological Sciences* 281. doi: 10.1098/rspb.2014.1486.
- Ellers, J., and Stuefer, J. F. (2010). Frontiers in phenotypic plasticity research: New questions about mechanisms, induced responses and ecological impacts. *Evolutionary Ecology.* 24, 523–526. doi: 10.1007/s10682-010-9375-4.
- Esmaeili, C., Heng, L. Y., Chiang, C. P., Rashid, Z. A., Safitri, E., and Malon Marugan, R. S. P. (2017). A DNA biosensor based on kappa-carrageenan-polypyrrole-gold nanoparticles composite for gender determination of Arowana fish (*Scleropages formosus*). *Sensors and Actuators B: Chemical* 242, 616–624. doi: 10.1016/J.SNB.2016.11.061.
- Ezequiel, J., Laviale, M., Frankenbach, S., Cartaxana, P., and SerÔdio, J. (2015). Photoacclimation state determines the photobehaviour of motile microalgae: The case of a benthic diatom. *Journal of Experimental Marine Biology and Ecology.* 468, 11–20. doi: 10.1016/j.jembe.2015.03.004.
- Fabregas, J., Garcia, D., Morales, E., Lamela, T., And Otero, A. (1999). Mixotrophic production of phycoerythrin and exopolysaccharide by the microalga. *Cryptogamie Algologie.* 20, 89–94. doi: 10.1016/s0181-1568(99)80009-9.
- Fenoradosoa, T. A., Laroche, C., Delattre, C., Dulong, V., Cerf, D. le, Picton, L., et al., (2012). Rheological Behavior and Non-enzymatic Degradation of a Sulfated Galactan from *Halymenia durvillei* (Halymeniales, Rhodophyta). *Applied Biochemistry and Biotechnology.* 2012 167:5 167, 1303–1313. doi: 10.1007/S12010-012-9605-Z.
- Ferruzzi, M and Blakeslee, J. (2007) Digestion, absorption, and cancer preventative activity of dietary chlorophyll derivatives, *Nutrition Research.* 27(1)1-12. <https://doi.org/10.1016/j.nutres.2006.12.003>.
- Figuroa, F. L., Conde-Álvarez, R., and Gómez, I. (2003). Relations between electron transport rates determined by pulse amplitude modulated chlorophyll fluorescence and oxygen evolution in macroalgae under different light conditions. *Photosynthesis Research* 75, 259–275. doi: 10.1023/A:1023936313544.
- Figuroa, F. L., Jerez, C. G., and Korbee, N. (2013). Chlorophyll fluorescence and biomass productivity in microalgae Use of in vivo chlorophyll fluorescence to estimate photosynthetic



activity and biomass productivity in microalgae grown in different culture systems. *Latin American Journal Of Aquatic Research*. 41(5), 801-819. <https://dx.doi.org/103856/vol41-issue5-fulltext-1>

- Figuerola, F. (1991) Red, blue and green photoreceptors controlling chlorophyll, biliprotein and total protein synthesis in the red alga *Chondrus crispus*. *British Phycological Journal*. 26: 383 – 392.
- Figuerola, F. L., Aguilera, J. And Niell, F. X. (1995) Red and blue light regulation of growth and photosynthetic metabolism in *Porphyra umbilicalis* (L.) Kützing (Bangiales , Rhodophyta). *European Journal of Phycology*. 30: 11 – 18.
- Folch, J., Lees, M., And Sloane Stanley, G. H. (1957). A simple method for the isolation and purification of total lipides from animal tissues. *Journal of Biochemical Chemistry*. 226, 497–509. doi: 10.3989/scimar.2005.69n187.
- Fukumoto, L. R., and Mazza, G. (2000). Assessing antioxidant and prooxidant activities of phenolic compounds. *Journal of Agricultural and Food Chemistry* 48(8), 3597–3604. doi: 10.1021/jf000220w.
- Galland-Irmouli, A. V., Pons, L., Luçon, M., Villaume, C., Mrabet, N. T., Guéant, J. L. and Fleurence J. (2000). One-step purification of R-phycoerythrin from the red macroalga *Palmaria palmata* using preparative polyacrylamide gel electrophoresis. *Journal of Chromatography B: Biomedical Sciences and Applications* 739(1),117-123 doi: 10.1016/S0378-4347(99)00433-8.
- Gaignard, C., Gargouch, N., Dubessay, P., Delattre, C., Pierre, G., Laroche, C., et al., (2019). New horizons in culture and valorization of red microalgae. *Biotechnology Advances* 37, 193–222. doi: 10.1016/j.biotechadv.2018.11.014.
- Gajaria, T. K., Suthar, P., Baghel, R. S., Balar, N. B., Sharnagat, P., Mantri, VA. (2017) Integration of protein extraction with a stream of byproducts from marine macroalgae: A model forms the basis for marine bioeconomy. *Bioresource Technology*. 243, 867–873.
- Ge, X., Wan, Z., Song, N., Fan, A., and Wu, R. (2009). Efficient methods for the extraction and microencapsulation of red pigments from a hybrid rose. *Journal of Food Engineering* 94, 122–128. doi: 10.1016/J.JFOODENG.2009.02.021.
- Gereniu, C. R. N., Saravana, P. S., and Chun, B. S. (2018). Recovery of carrageenan from Solomon Islands red seaweed using ionic liquid-assisted subcritical water extraction. *Separation and Purification Technology* 196, 309–317. doi: 10.1016/J.SEPPUR.2017.06.055.
- González, E., Gómez-Caravaca, A.M., Giménez, B. Cebrian, R., Maqueda, M., Martinez-Ferez, A., Segura-Carretero, A. and Robert, P. (2019) Evolution of the phenolic compounds profile of olive leaf extract encapsulated by spray-drying during in vitro gastrointestinal digestion. *Food Chemistry* 279:40–48. <https://doi.org/10.1016/j.foodchem.2018.11.127>
- Gómez-Ordóñez, E., Jiménez-Escrig, A., and Rupérez, P. (2010). Dietary fibre and physicochemical properties of several edible seaweeds from the northwestern Spanish coast. *Food Research International* 43(9), 2289-2294. doi: 10.1016/j.foodres.2010.08.005.

- Gómez, P. I., Haro, P., Lagos, P., Palacios, Y., Torres, J., Sáez, K., et al., (2016). Intraspecific variability among Chilean strains of the astaxanthin-producing microalga *Haematococcus pluvialis* (Chlorophyta): An opportunity for its genetic improvement by simple selection. *Journal of Applied Phycology* 28, 2115–2122. doi: 10.1007/s10811-015-0777-0.
- Gómez-Ordóñez, E., Jiménez-Escrig, A., and Rupérez, P. (2014). Bioactivity of sulfated polysaccharides from the edible red seaweed *Mastocarpus stellatus*. *Bioactive Carbohydrates and Dietary Fibre*. 3, 29–40. doi: 10.1016/J.BCDF.2014.01.002.
- Gómez-Pinchetti, J.L., Suárez Álvarez, S., Güenaga Unzetabarrenechea, Figueroa, F.L., Garía Reina, G. (2011). Posibilidades para el desarrollo de sistemas integrados con macroalgas en las islas canarias y su entrono. Editado por Cetmar (centro tecnológico del mar) Vigo, España isbn: 978-84-615-4974-0. pp. 74-93
- Goula, A. M., Ververi, M., Adamopoulou, A., & Kaderides, K. (2017). Green ultrasound-assisted extraction of carotenoids from pomegranate wastes using vegetable oils. *Ultrasonics Sonochemistry*, 34, 821–830. <https://doi.org/10.1016/J.ULTSONCH.2016.07.022>
- González-Ballesteros, N., and Rodríguez-Argüelles, M. C. (2020). Seaweeds: A promising bionanofactory for ecofriendly synthesis of gold and silver nanoparticles. *Sustainable Seaweed Technologies*, 507–541. doi: 10.1016/B978-0-12-817943-7.00018-4.
- Gombotz, R. and Wee F (2012) Protein release from alginate matrices. *Advanced Drug Delivery Reviews* .64:194–205
- Guan, J., Li, L., and Mao, S. (2017). Applications of Carrageenan in Advanced Drug Delivery. *Seaweed Polysaccharides: Isolation, Biological and Biomedical Applications*, 283–303. doi: 10.1016/B978-0-12-809816-5.00015-3.
- Guillard, R. R. L. (1973). Division rates. 289–311.
- Guldhe, A., Singh, B., Rawat, I., Ramluckan, K., Bux, F., 2014. Efficacy of drying and cell disruption techniques on lipid recovery from microalgae for biodiesel production. *Fuel* 128, 46–52.
- Ghosh, T., and Mishra, S. (2020). Studies on Extraction and Stability of C-Phycocerythrin From a Marine Cyanobacterium. *Frontiers in Sustainable Food Systems*. 4, 102. doi: 10.3389/FSUFS.2020.00102/BIBTEX.
- Glazer, A.N., Apell, G.S., Hixson, C.S., Bryant, D.A., Rimon, S. and Brown, D.M. (1976). Biliproteins of cyanobacteria and Rhodophyta: Homologous family of photosynthetic accessory pigments. *Proceedings of the National Academy of Sciences of the United States of America* 73(2), 428–431. <https://doi.org/10.1073/pnas.73.2.428>.
- Gropper, SS. and Smith, JL. (2013) Advanced human nutrition and metabolism, 6th edn. Wadsworth, Belmont.
- Hafting, JT., Critchley AT, Cornish ML, Hubley SA, Archibald AF. (2012) On-land cultivation of functional seaweed products for human usage. *Journal of Applied Phycology*. 24:385–392.
- Hagemann, M., (2011) Molecular biology of cyanobacterial salt acclimation, *FEMS Microbiology Reviews*. Volume 35(1), 87–123, <https://doi.org/10.1111/j.1574-6976.2010.00234.x>

- Hasan R. and Chakrabarti, R. (2009). Use of algae and aquatic macrophytes as feed in small-scale aquaculture: a review. *FAO Fisheries and Aquaculture Technical* 531, Rome, FAO. 123p.
- Hamdani, S., Khan, N., Perveen, S., Qu, M., Jiang, J., Govindjee, et al., (2019). Changes in the photosynthesis properties and photoprotection capacity in rice (*Oryza sativa*) grown under red, blue, or white light. *Photosynthesis Research*. 139, 107–121. doi: 10.1007/s11120-018-0589-6.
- Haro, P., Sáez, K., and Gómez, P. I. (2017). Physiological plasticity of a Chilean strain of the diatom *Phaeodactylum tricornutum*: the effect of culture conditions on the quantity and quality of lipid production. *Journal of Applied Phycology* 29, 2771–2782. doi: 10.1007/s10811-017-1212-5.
- Hardouin, K., Bedoux, G., Burlot, A. S., Nyvall-Collén, P., and Bourgoignon, N. (2014). Enzymatic recovery of metabolites from seaweeds: Potential applications. *Advances in Botanical Research*. 71, 279-320. doi: 10.1016/B978-0-12-408062-1.00010-X.
- Häder, D. P., and Figueroa, F. L. (1997). Photoecophysiology of Marine Macroalgae. *Photochemistry and Photobiology*, 66(1), 1–14. <https://doi.org/10.1111/J.1751-1097.1997.TB03132.X>
- Heffernan, N., Smyth, T. J., FitzGerald, R. J., Vila-Soler, A., Mendiola, J., Ibáñez, E., et al., (2016). Comparison of extraction methods for selected carotenoids from macroalgae and the assessment of their seasonal/spatial variation. *Innovative Food Science & Emerging Technologies* 37, 221–228. doi: 10.1016/J.IFSET.2016.06.004.
- Henning, S., Leick, S., Kott, M., Rehage H. and Suter D. (2012). Sealing liquid-filled pectinate capsules with a shellac coating, *Journal of Microencapsulation*, 29:2, 147-155, DOI: 10.3109/02652048.2011.635220.
- Holdt, S.L., Kraan, S., 2011. Bioactive compounds in seaweed: functional food applications and legislation. *Journal of Applied Phycology*. 23, 543–597.
- Holst, B., Williamson, G. (2008) Nutrients and phytochemicals: from bioavailability to bioefficacy beyond antioxidants. *Current Opinion Biotechnology*. 19:73–82
- Hosokawa, M., Kudo, M., Maeda, H., Kohno, H., Tanaka, T., Miyashita, K (2004) Fucoxanthin induces apoptosis and enhances the antiproliferative effect of the PAR  $\gamma$ -ligand, troglitazone on colon cancer cells. *Biochimica et Biophysica Acta (BBA): General Subjects*. 1675: 113-119.
- Huang, Y.-Z., Jin, Z., Wang, Z.-M., Qi, L.-B., Song, S., Zhu, B.-W. and Dong, X-P. (2021). Marine Bioactive Compounds as Nutraceutical and Functional Food Ingredients for Potential Oral Health. *Frontiers in Nutrition* 8, 1011. doi: 10.3389/FNUT.2021.686663/BIBTEX.
- Ishikawa, C., Takufu, S., Kadokaru, T., Sawada, S., Tomita, M., Okudaira, T., et al., (2008) Antiadult T cell leukemia effects of brown algae fucoxanthin and its deacetylated product, fucoxanthinol. *International Journal of cancer*. 123, 2702-2712.
- Ibáñez-González, M. J., Mazzuca-Sobczuk, T., Redondo-Miranda, R. M., Molina-Grima, E., and Cooney, C. L. (2016). A novel vortex flow reactor for the purification of B-phycoerythrin from *Porphyridium cruentum*. *Chemical Engineering Research and Design*. 111, 24–33. doi: 10.1016/j.cherd.2016.03.032.

- Jacotet-Navarro, M., Rombaut, N., Deslis, S., Fabiano-Tixier, A. S., Pierre, F. X., Bily, A., et al., (2016). Towards a “dry” bio-refinery without solvents or added water using microwaves and ultrasound for total valorization of fruit and vegetable by-products. *Green Chemistry*. 18. doi: 10.1039/c5gc02542g.
- Jerez, C. G., Malapascua, J. R., Sergejevová, M., Masojídek, J., and Figueroa, F. L. (2016). *Chlorella fusca* (Chlorophyta) grown in thin-layer cascades: Estimation of biomass productivity by in-vivo chlorophyll a fluorescence monitoring. *Algal Research*. 17, 21–30. doi: 10.1016/j.algal.2016.04.010.
- Jiménez-Escrig, A., Gómez-Ordóñez, E., and Rupérez, P. (2011). Brown and red seaweeds as potential sources of antioxidant nutraceuticals. *Journal of Applied Phycology*. 2011 24:5 24, 1123–1132. doi: 10.1007/S10811-011-9742-8.
- Jones, R. I. (1998). P.G. Falkowski and J.A. Raven. Aquatic photosynthesis. Blackwell Science, 1997. Pp. 375. Price 39.50 (p/b). ISBN 0 86542 387 3. *Journal of Experimental Botany* 49, 621–621. doi: 10.1093/jxb/49.320.621.
- Joye, I. J., and McClements, D. J. (2014). Biopolymer-based nanoparticles and microparticles: Fabrication, characterization, and application. *Current Opinion in Colloid & Interface Science*. 19, 417–427. doi: 10.1016/J.COCIS.2014.07.002.
- Jung, J. H., Sirisuk, P., Ra, C. H., Kim, J. M., Jeong, G. T., and Kim, S. K. (2019). Effects of green LED light and three stresses on biomass and lipid accumulation with two-phase culture of microalgae. *Process Biochemistry*. 77, 93–99. doi: 10.1016/j.procbio.2018.11.014.
- Jung, S. M., Park, J. S., Shim, H. J., Kwon, Y. S., Kim, H. G., and Shin, H. S. (2016). Antioxidative effect of phycoerythrin derived from *Grateloupia filicina* on rat primary astrocytes. *Biotechnology and Bioprocess Engineering* 21, 676–682. doi: 10.1007/s12257-016-0369-0.
- Juin, C., Chérouvrier, J. R., Thiéry, V., Gagez, A. L., Bérard, J. B., Joguet, N., et al., (2015). Microwave-assisted extraction of phycobiliproteins from *Porphyridium purpureum*. *Applied Biochemistry and Biotechnology* 175. doi: 10.1007/s12010-014-1250-2.
- Jubeau, S., Marchal, L., Pruvost, J., Jaouen, P., Legrand, J., and Fleurence, J. (2013). High pressure disruption: A two-step treatment for selective extraction of intracellular components from the microalga *Porphyridium cruentum*. *Journal of Applied Phycology* 25, 983–989. doi: 10.1007/s10811-012-9910-5.
- Kazir, M., Abuhassira, Y., Robin, A., Nahor, O., Luo, J., Israel, A., Golberg, A., Livney YD. (2019) Extraction of proteins from two marine macroalgae, *Ulva* sp. and *Gracilaria* sp., for food application, and evaluating digestibility, amino acid composition and antioxidant properties of the protein concentrates. *Food Hydrocolloids* .87:194-203.
- Katiyar, R., and Arora, A. (2020). Health promoting functional lipids from microalgae pool: A review. doi: 10.1016/j.algal.2020.101800.
- Kannaujiya, V. K., Sundaram, S., and Sinha, R. P. (2017). Advances in production technology. In: Kannaujiya VK, Sundaram, Sinha RP (eds) Phycobiliproteins: recent developments and future applications. *Springer*, 83–97. doi: 10.1007/978-981-10-6460-9.

- Kang, J. Y., Chun, B. S., Lee, M. C., Choi, J. S., Choi, I. S., and Hong, Y. K. (2016). Anti-inflammatory Activity and Chemical Composition of Essential Oil Extracted with Supercritical CO<sub>2</sub> from the Brown Seaweed *Undaria pinnatifida*. <http://dx.doi.org/10.1080/0972060X.2014.989181> 19, 46–51. doi: 10.1080/0972060X.2014.989181.
- Kawsar, S., Yuki, F., Matsumoto, R., Yasumitsu, H., and Yasuhiro, O. (2011). Protein R-phycoerythrin from marine red alga *Amphiroa anceps*: extraction, purification and characterization. *Phytologia Balcanica*. 17(3), 347-354.
- Kianianmomeni, A., and Hallmann, A. (2014). Algal photoreceptors: In vivo functions and potential applications. *Planta* 239, 1–26. doi: 10.1007/s00425-013-1962-5.
- Kong, F. and Singh, R. P. (2010) A human gastric simulator (HGS) to study food digestion in human stomach. *Journal of Food Science*. 75, E627–E635
- Korbee, N., Huovinen, P., Figueroa, F. L., Aguilera, J., and Karsten, U. (2005). Availability of ammonium influences photosynthesis and the accumulation of mycosporine-like amino acids in two *Porphyra* species (Bangiales, Rhodophyta). *Marine Biology* 146, 645–654. doi: 10.1007/s00227-004-1484-6.
- Kotake Nara, E., Kushiro, M., Zhang, H., Sugawara, T., Miyashita, K., & Nagao, A (2001) Carotenoids affect proliferation of human prostate cancer cells. *Journal of nutrition*. 131, 3303.
- Kumar, P.; Sharma, N.; Ranjan, R.; Kumar, S.; Bhat, Z.; Jeong, D (2013) Perspective of membrane technology in dairy industry: A review. *Asian-Australasian Journal of Animal Science*. 2013, 26, 1347.
- Khanra, S., Mondal, M., Halder, G., Tiwari, O. N., Gayen, K., and Bhowmick, T. K. (2018). Downstream processing of microalgae for pigments, protein and carbohydrate in industrial application: A review. *Food and Bioproducts Processing*. 110, 60–84. doi: 10.1016/j.fbp.2018.02.002.
- Klimas, M., Brethour, C. And Bucknell, D. (2008). International market trends analysis for the functional foods and natural health products industry in the United States, Australia, the United Kingdom and Japan. Market Research Report . pp.142.
- Lamparter,, T. (2004). Evolution of cyanobacterial and plant phytochromes, *FEBS Letters*, 573, doi: 10.1016/j.febslet.2004.07.050.
- Larkum, A. W. D. (2003). “Light-Harvesting Systems in Algae,” in (Springer, Dordrecht), 277–304. doi: 10.1007/978-94-007-1038-2\_13.
- Lange, L., Bak, U. G., Hansen, S. C. B., Gregersen, O., Harmsen, P., Karlsson, E. N., Meyer, A., Mikkelsen, M. D., van den Broek, L., and Hreggviðsson, G. Ó. (2020). Opportunities for seaweed biorefinery. *Sustainable Seaweed Technologies*. 3–31. <https://doi.org/10.1016/B978-0-12-817943-7.00001-9>.
- Landi, M., Zivcak, M., Sytar, O., Brestic, M., and Allakhverdiev, S. I. (2020). Plasticity of photosynthetic processes and the accumulation of secondary metabolites in plants in response to monochromatic light environments: A review. *Biochimica et Biophysica Acta – Bioenergetics*. 1861, 148131. doi: 10.1016/j.bbabi.2019.148131.

- Lee, K. Y., and Mooney, D. J. (2012). Alginate: properties and biomedical applications. *Prog Polym Sci* 37, 106. doi: 10.1016/J.PROGPOLYMSCI.2011.06.003.
- Le Guillard, C., Dumay, J., Donnay-Moreno, C., Bruzac, S., Ragon, J. Y., Fleurence, J., and Bergé, J.P. (2015). Ultrasound-assisted extraction of R-phycoerythrin from *Grateloupia turuturu* with and without enzyme addition. *Algal Research*. 12, 522-528. doi: 10.1016/j.algal.2015.11.002.
- Lewinska, D., Bukowski, J., Ko\_zuchowski, M., Kinasiewicz, A. and Werynski, A. (2008) Electrostatic microencapsulation of living cells. *Biocybernetics and Biomedical Engineering* 28:69–84.
- Li, L., Ni, R., Shao, Y., and Mao, S. (2014). Carrageenan and its applications in drug delivery. *Carbohydrate Polymers*. 103, 1–11. doi: 10.1016/J.CARBPOL.2013.12.008.
- Li, S., Ji, L., Shi, Q., Wu, H., and Fan, J. (2019a). Advances in the production of bioactive substances from marine unicellular microalgae *Porphyridium* spp. *Bioresource Technology*. 292, 122048. doi: 10.1016/j.biortech.2019.122048.
- Li, X., Li, W., Zhai, J., Wei, H., and Wang, Q. (2019b). Effect of ammonium nitrogen on microalgal growth, biochemical composition and photosynthetic performance in mixotrophic cultivation. *Bioresource Technology*. 273, 368–376. doi: 10.1016/j.biortech.2018.11.042.
- Li, W., Su, H.-N., Pu, Y., Chen, J., Liu, L.-N., Liu, Q. and Qin S. (2019c). Phycobiliproteins: Molecular structure, production, applications, and prospects. *Biotechnology Advances* 37, 340–353. doi: <https://doi.org/10.1016/j.biotechadv.2019.01.008>.
- Liu, X., Luo, G., Wang, L., and Yuan, W. (2019). Food and Bioproducts Processing Optimization of antioxidant extraction from edible brown algae *Ascophyllum nodosum* using response surface methodology. *Food and Bioproducts Processing*. 114, 205–215. doi: 10.1016/j.fbp.2019.01.003.
- Liu, L., Heinrich, M., Myers, S., and Dworjanyn, S. A. (2012). Towards a better understanding of medicinal uses of the brown seaweed *Sargassum* in Traditional Chinese Medicine: a phytochemical and pharmacological review. *Journal of Ethnopharmacol.* 142, 591–619. doi: 10.1016/J.JEP.2012.05.046.
- Limmatvapirat, S., Panchapornpon, D., Limmatvapirat, C., Nunthanid, J., Luangtana-Anan, M., and Puttipipatkachorn, S. (2008). Formation of shellac succinate having improved enteric film properties through dry media reaction. *European journal of pharmaceuticals and biopharmaceutics : official journal of Arbeitsgemeinschaft fur Pharmazeutische Verfahrenstechnik e.* 70, 335–344. doi: 10.1016/J.EJPB.2008.03.002.
- Lourenço, S. O., Barbarino, E., De-Paula, J. C., Pereira, L.O.D.S., and Lanfer Marquez, U. M. (2002). Amino acid composition, protein content and calculation of nitrogen-to-protein conversion factors for 19 tropical seaweeds. *Phycological Research*. 50, 233-241. doi: 10.1046/j.1440-1835.2002.00278.x.
- López-Figueroa, F. (1991). Red, green and blue light photoreceptors controlling chlorophyll a, biliprotein and total protein synthesis in the red alga *Chondrus crispus*. *British Phycological Journal*. 26, 383–393. doi: 10.1080/00071619100650351.

- López-Figueroa, F., and Niell, F. X. (1990). Effects of light quality on chlorophyll and biliprotein accumulation in seaweeds. *Marine Biology* 104, 321–327. doi: 10.1007/BF01313274.
- López-Figueroa, F., Perez, R., and Niell, F. X. (1989). Effects of red and far-red light pulses on the chlorophyll and biliprotein accumulation in the red alga *Corallina elongata*. *Journal of Photochemistry and Photobiology, B: Biology* 4, 185–193. doi: 10.1016/1011-1344(89)80004-1.
- Luo, A. X., He, X. J., Zhou, S. D., Fan, Y. J., Luo, A. S., and Chun, Z. (2010). Purification, composition analysis and antioxidant activity of the polysaccharides from *Dendrobium nobile*. *Carbohydrate Polymers* 79, 1014–1019. doi: 10.1016/J.CARBPOL.2009.10.033.
- Lupo, B., Maestro, A., Gutierrez, J. M., and Gonzalez, C. (2015) Characterization of alginate beads with encapsulated cocoa extract to prepare functional food: Comparison of two gelation mechanisms. *Food Hydrocolloids*. 49: 25-34
- Madeira, M. S., Cardoso, C., Lopes, P. A., Coelho, D., Afonso, C., Bandarra, N. M., et al., (2017). Microalgae as feed ingredients for livestock production and meat quality: A review. *Livestock Science* 205, 111–121. doi: 10.1016/j.livsci.2017.09.020.
- Madene, A., Jacquot, M., Scher, J., and Desobry, S. (2006). Flavour encapsulation and controlled release – a review. *International Journal of Food Science & Technology* 41, 1–21. doi: 10.1111/J.1365-2621.2005.00980.X.
- Manilal, A., Sujith, S., Kiran, G. S., Selvin, J., Shakir, C., Gandhimathi, R., Panikkar, MVN. (2009) Biopotentials of seaweeds collected from southwest coast of India. *Journal of Marine Science and Technology*. 17(1), 67–73.
- Mancini, M., Moresi, M., and Rancini, R. (1999). Uniaxial compression and stress relaxation tests on alginate gels. *Journal of Texture Studies* 30, 639–657. doi: 10.1111/J.1745-4603.1999.TB00235.X.
- Manivannan, K., Thirumaran, G., Devi, G. K., Anantharaman, P., and Balasubramanian, T. (2009). Proximate composition of different group of seaweeds from Vedhai Coastal Waters (Gulf of Mannar): Southeast coast of India. *Middle-East Journal of Scientific Research*.. pp.92.
- Mamatha, B. S., Namitha, K. K., Senthil, A., Smitha, J., and Ravishankar, G. A. (2007). Studies on use of Enteromorpha in snack food. *Food Chemistry* 101(4), 1707-1713. doi: 10.1016/j.foodchem.2006.04.032.
- Martinsen, A., Skjak-Braek, G., Smidsrod, O., Zanetti, F., Paoletti, S. (1991) Comparison of different methods for determination of molecular weight and molecular weight distribution of alginates. *Carbohydrate Polymers*. 15: 171–193.
- Martone, P. T., Estevez, J. M., Lu, F., Ruel, K., Denny, M. W., Somerville, C., et al., (2009). Discovery of Lignin in Seaweed Reveals Convergent Evolution of Cell-Wall Architecture. *Current Biology* 19, 169–175. doi: 10.1016/J.CUB.2008.12.031.
- Mateos-Aparicio, I., Martera, G., Goñi, I., Villanueva-Suárez, M. J., and Redondo-Cuenca, A. (2018). Chemical structure and molecular weight influence the in vitro fermentability of polysaccharide extracts from the edible seaweeds *Himathalia elongata* and *Gigartina pistillata*. *Food Hydrocolloids* 83, 348–354. doi: 10.1016/J.FOODHYD.2018.05.016.

- Mattos, E. R., Singh, M., Cabrera, M. L., and Das, K. C. (2015). Enhancement of biomass production in *Scenedesmus bijuga* high-density culture using weakly absorbed green light. *Biomass and Bioenergy* 81, 473–478. doi: 10.1016/j.biombioe.2015.07.029.
- Michalak, I., and Chojnacka, K. (2014). Algal extracts: Technology and advances. *Engineering in Life Sciences* 14, 581–591. doi: 10.1002/elsc.201400139.
- Michalak, I., and Chojnacka, K. (2018). *Introduction: Toward Algae-Based Products*. doi: 10.1007/978-3-319-74703-3\_1.
- Mittal, R., Sharma, R., and Raghavarao, K. S. M. S. (2019). Aqueous two-phase extraction of R-Phycoerythrin from marine macro-algae, *Gelidium pusillum*. *Bioresource Technology* 280, 277–286. doi: 10.1016/j.biortech.2019.02.044.
- Mittal, R., Tavanandi, H. A., Mantri, V. A., and Raghavarao, K. S. M. S. (2017). Ultrasound assisted methods for enhanced extraction of phycobiliproteins from marine macro-algae, *Gelidium pusillum* (Rhodophyta). *Ultrasonics Sonochemistry* 38, 92–103. doi: 10.1016/j.ultsonch.2017.02.030.
- Minekus, M., Alminger, M., Alvito, P., Ballance, S., Bohn, T., Bourlieu, C., et al., (2014). A standardised static in vitro digestion method suitable for food – an international consensus. *Food & Function* 5, 1113–1124. doi: 10.1039/C3FO60702J.
- Moreira, A. S., González-Torres, L., Olivero-David, R., Bastida, S., Benedi, J., and Sánchez-Muniz, F. J. (2010). Wakame and Nori in Restructured Meats Included in Cholesterol-enriched Diets Affect the Antioxidant Enzyme Gene Expressions and Activities in Wistar Rats. *Plant Foods for Human Nutrition* 65(3), 290–8. doi: 10.1007/s11130-010-0179-z.
- Morales, E., Rubilar, M., Burgos-Díaz, C., Acevedo, F., Penning, M., and Shene, C. (2017). Alginate/Shellac beads developed by external gelation as a highly efficient model system for oil encapsulation with intestinal delivery. *Food Hydrocolloids* 70, 321–328. doi: 10.1016/j.foodhyd.2017.04.012.
- Mouritsen, O. G., Rhatigan, P., and Pérez-Lloréns, J. L. (2018). World cuisine of seaweeds: Science meets gastronomy. *International Journal of Gastronomy and Food Science* 14, 55–65. doi: 10.1016/J.IJGFS.2018.09.002.
- Munier, M., Jubeau, S., Wijaya, A., Morañais, M., Dumay, J., Marchal, L., Jaouen, P. and Fleurence, J. (2014). Physicochemical factors affecting the stability of two pigments: R-phycoerythrin of *Grateloupia turuturu* and B-phycoerythrin of *Porphyridium cruentum*. *Food chemistry*. 150:400–407. <https://doi.org/10.1016/j.foodchem.2013.10.113>
- Mollet, J. C., Rahaoui, A., and Lemoine, Y. (1998). Yield, chemical composition and gel strength of agarocolloids of *Gracilaria gracilis*, *Gracilariopsis longissima* and the newly reported *Gracilaria cf. vermiculophylla* from Roscoff (Brittany, France). *Journal of Applied Phycology* 1998 10:1 10, 59–66. doi: 10.1023/A:1008051528443.
- Niu, J. F., Wang, G. C., and Tseng, C. K. (2006). Method for large-scale isolation and purification of R-phycoerythrin from red alga *Polysiphonia urceolata* Grev. *Protein Expression and Purification*. 49(1), 23–31. doi: 10.1016/j.pep.2006.02.001.



- Ngo, D.H., Wijesekara, I., Vo, T.S., Van Ta, Q., Kim, S.K. (2011) Marine food-derived functional ingredients as potential antioxidants in the food industry: an overview. *Food Research International*. 44, 523-529.
- Oh, S. H., Han, J. G., Kim, Y., Ha, J. H., Kim, S. S., Jeong, M. H., Jeong H.S., Kim, N.Y., Cho, J.S., Yoon, W.B., Lee, S.Y., Kang, D.H. and Lee, H.Y. (2009). Lipid production in *Porphyridium cruentum* grown under different culture conditions. *Journal of Bioscience and Bioengineering* .108, 429–434. doi: 10.1016/j.jbiosc.2009.05.020.
- Okai, Y., Hiqashi Okai, K., Yano, Y., and Otani, S (1996) Identification of antimutagenic substances in an extract of edible red alga, *Porphyra tenera* (Asadusa-nori). *Cancer Letters*, 100, 235-240.
- Ooi, L., Heng, L. Y., and Mori, I. C. (2015). A high-throughput oxidative stress biosensor based on *Escherichia coli* roGFP2 cells immobilized in a k-carrageenan matrix. *Sensors (Basel)* 15, 2354–2368. doi: 10.3390/S150202354.
- Pagels, F., Guedes, A. C., Amaro, H. M., Kijjoa, A., and Vasconcelos, V. (2019). Phycobiliproteins from cyanobacteria: Chemistry and biotechnological applications. *Biotechnology Advances* 37, 422–443. doi: 10.1016/J.BIOTECHADV.2019.02.010.
- Pagels, F., Bonomi-Barufi, J., Vega, J., Abdala-Díaz, R., Vasconcelos, V., Guedes, A. C., and Figueroa, F. L. (2020). Light quality triggers biochemical modulation of *Cyanobium* sp. photobiology as tool for biotechnological optimization. *Journal of Applied Phycology*, 32(5), 2851–2861. <https://doi.org/10.1007/S10811-020-02179-0/FIGURES/6>
- Palthur, M. P., Palthur, S. S. And Chitta, S. K. (2010a). Nutraceuticals: A conceptual definition. *International Journal of Pharmacy and Pharmaceuticals Sciences*. 2 ,19–27.
- Parsons, T.T. and Strickland, J.D.H. (1963) Discussion of Spectrophotometric Determination of Marine-Plant Pigments, with Revised Equations for Ascertaining Chlorophylls and Carotenoids. *Journal of Marine Research* 21, 155-163.
- Parages, M. L., Rico, R. M., Abdala-Díaz, R. T., Chabrilón, M., Sotiroudis, T. G., and Jiménez, C. (2012). Acidic polysaccharides of *Arthrospira* (Spirulina) *platensis* induce the synthesis of TNF- $\alpha$  in RAW macrophages. *Journal of Applied Phycology*. 2012 24:6 24, 1537–1546. doi: 10.1007/S10811-012-9814-4.
- Pan-utai, W., and Iamtham, S. (2019). Physical extraction and extrusion entrapment of C-phycoyanin from *Arthrospira platensis*. *Journal of King Saud University - Science* 31, 1535–1542. doi: 10.1016/J.JKSUS.2018.05.026.
- Patel, A. R., Schatteman, D., de Vos, W. H., and Dewettinck, K. (2013). Shellac as a natural material to structure a liquid oil-based thermo reversible soft matter system. *RSC Advances* 3, 5324–5327. doi: 10.1039/C3RA40934A.
- Pawar, S. N., and Edgar, K. J. (2012). Alginate derivatization: a review of chemistry, properties and applications. *Biomaterials*. 33, 3279–3305. doi: 10.1016/J.BIOMATERIALS.2012.01.007.
- Petrusevski, B.; Bolier, G.; Van Breemen, A.; Alaerts, G. (1995) Tangential flow filtration: A method to concentrate freshwater algae. *Water Res.* 29, 1419–1424.

- Pereira, L., Amado, A. M., Critchley, A. T., van de Velde, F., and Ribeiro-Claro, P. J. A. (2009). Identification of selected seaweed polysaccharides (phycocolloids) by vibrational spectroscopy (FTIR-ATR and FT-Raman). *Food Hydrocolloids*. 23, 1903–1909. doi: 10.1016/J.FOODHYD.2008.11.014.
- Pereira, T., Barroso, S., Mendes, S., Amaral, R. A., Dias, J. R., Baptista, T., et al., (2020). Optimization of phycobiliprotein pigments extraction from red algae *Gracilaria gracilis* for substitution of synthetic food colorants. *Food Chemistry* 321, 126688. doi: 10.1016/j.foodchem.2020.126688.
- Peralta, E., Jerez, C. G., and Figueroa, F. L. (2019). Centrate grown *Chlorella fusca* (Chlorophyta): Potential for biomass production and centrate bioremediation. *Algal Research* 39, 101458. doi: 10.1016/j.algal.2019.101458.
- Pérez Lloréns, JL, Hernández Carrero, I, Vergara Oñate, JJ, Brun Murillo, FG , Lón, A. (2016). Las algas se comen: un periplo por la biología, historia, las curiosidades y la gastronomía . Servicio de Publicaciones UCA , ISBN:978-84-9828-567-3
- PERMANOVA+ for primer: Guide to software and statistical methods | Request PDF Available at: [https://www.researchgate.net/publication/285237419\\_PERMANOVA\\_for\\_primer\\_Guide\\_to\\_software\\_and\\_statistical\\_methods](https://www.researchgate.net/publication/285237419_PERMANOVA_for_primer_Guide_to_software_and_statistical_methods) [Accessed September 8, 2020].
- Piornos, J.A., Burgos-Díaz, C., Morales, E., Rubilar, M., and Acevedo, F. (2017). “Highly efficient encapsulation of linseed oil into alginate/lupin protein beads: Optimization of the emulsion formulation”. *Food Hydrocolloid*, 63, 139-148.
- Pimentel, F. B., Cermeño, M., Kleekayai, T., Harnedy, P. A., FitzGerald, R. J., Alves, R. C., Oliveira M.B. (2020). Effect of in vitro simulated gastrointestinal digestion on the antioxidant activity of the red seaweed *Porphyra dioica*. *Food Research International* 136, 109309. doi: 10.1016/J.FOODRES.2020.109309.
- Ponthier, E., Domínguez, H., and Torres, M. D. (2020). The microwave assisted extraction sway on the features of antioxidant compounds and gelling biopolymers from *Mastocarpus stellatus*. *Algal Research* 51, 102081. doi: 10.1016/J.ALGAL.2020.102081.
- Popa, E. G., Reis, R. L., and Gomes, M. E. (2015). Seaweed polysaccharide-based hydrogels used for the regeneration of articular cartilage. *Critical Review Biotechnology*. 35, 410–424. doi: 10.3109/07388551.2014.889079.
- Phawaphuthanon, N., Behnam, S., Koo, S. Y., Pan, C. H., Chung, D. (2014). Characterization of core-shell calcium-alginate macrocapsules fabricated by electro-coextrusion. *International Journal of Biological Macromolecules*. 65(267-274). <https://doi.org/10.1016/j.ijbiomac.2014.01.031>.
- Ptushenko, V. V., Avercheva, O. V., Bassarskaya, E. M., Berkovich, Y. A., Erokhin, A. N., Smolyanina, S. O., et al., (2015). Possible reasons of a decline in growth of Chinese cabbage under a combined narrowband red and blue light in comparison with illumination by high-pressure sodium lamp. *Scientia Horticulturae* 194, 267–277. doi: 10.1016/j.scienta.2015.08.021.
- Ra, C. H., Sirisuk, P., Jung, J. H., Jeong, G. T., and Kim, S. K. (2018). Effects of light-emitting diode (LED) with a mixture of wavelengths on the growth and lipid content of microalgae. *Bioprocess and Biosystems Engineering* .41, 457–465. doi: 10.1007/s00449-017-1880-1.

- Rafiquzzaman, S. M., Rahman, M. A., and Kong, I. S. (2017). Ultrasonic-Assisted Extraction of Carrageenan. *Seaweed Polysaccharides: Isolation, Biological and Biomedical Applications*, 75–81. doi: 10.1016/B978-0-12-809816-5.00005-0.
- Ramírez, M.E. y B. Santelices 1991. Catálogo de las algas marinas bentónicas de la Costa del Pacífico Temperado de Sudamérica. Monografías Biológicas 5. Pontificia Universidad Católica de Chile. Santiago, Chile. 433pp.
- Re, R., Pellegrini, N., Proteggente, A., Pannala, A., Yang, M., and Rice-Evans, C. (1999). Antioxidant activity applying an improved ABTS radical cation decolorization assay. *Free Radical Biology and Medicine*. 26, 1231–1237. doi: 10.1016/S0891-5849(98)00315-3.
- Reboloso Fuentes, M. M., Ación Fernández, G. G., Sánchez Pérez, J. A., and Guil Guerrero, J. L. (2000). Biomass nutrient profiles of the microalga *Porphyridium cruentum*. *Food Chemistry* 70, 345–353. doi: 10.1016/S0308-8146(00)00101-1.
- Ritchie, R. J. (2008). Universal chlorophyll equations for estimating chlorophylls a, b, c, and d and total chlorophylls in natural assemblages of photosynthetic organisms using acetone, methanol, or ethanol solvents. *Photosynthetica* .46,115–126. doi: 10.1007/s11099-008-0019-7.
- Rocha De Souza, M. C., Marques, C. T., Guerra Dore, C. M., Ferreira Da Silva, F. R., Oliveira Rocha, H. A., and Leite, E. L. (2006). Antioxidant activities of sulfated polysaccharides from brown and red seaweeds. *Journal of Applied Phycology*.19:2 19, 153–160. doi: 10.1007/S10811-006-9121-Z.
- Rockwell, N. C., Duanmu, D., Martin, S. S., Bachy, C., Price, D. C., Bhattacharya, D., et al., (2014). Eukaryotic algal phytochromes span the visible spectrum. *Proc Natl Acad Sci USA* 111, 3871–3876. doi: 10.1073/pnas.1401871111.
- Rodrigues, R.D.P., de Castro, F. C., Santiago-Aguiar, R. S. de, and Rocha, M. V. P. (2018). Ultrasound-assisted extraction of phycobiliproteins from *Spirulina* (Arthrospira) *platensis* using protic ionic liquids as solvent. *Algal Research* 31, 454-462. doi: 10.1016/j.algal.2018.02.021.
- Roleda, M. Y., Dethleff, D., and Wiencke, C. (2008). Transient sediment load on blades of Arctic *Saccharina latissima* can mitigate UV radiation effect on photosynthesis. *Polar Biology* 31, 765–769. doi: 10.1007/s00300-008-0434-z.
- Rostamabadi, H., Assadpour, E., Tabarestani, H. S., Falsafi, S. R., and Jafari, S. M. (2020). Electrospinning approach for nanoencapsulation of bioactive compounds; recent advances and innovations. *Trends in Food Science & Technology* 100, 190–209. doi: 10.1016/J.TIFS.2020.04.012.
- Román, R. B., Álvarez-Pez, J. M., Fernández, F. G. A., and Grima, E. M. (2002). Recovery of pure b-phycoerythrin from the microalga *Porphyridium cruentum*. *Journal of Biotechnology* 93(1),73-85. doi: 10.1016/S0168-1656(01)00385-6.
- Roy, D., and Pabbi, S. (2022). A simple improved protocol for purification of C-phycoerythrin from overproducing cyanobacteria and its characterization. *Journal of Applied Phycology* 34, 799–810. doi: 10.1007/S10811-021-02649-Z/TABLES/5.

- Rüdiger, W., and López-Figueroa, F. (1992). Photoreceptors in algae. *Photochemistry and Photobiology* 55, 949–954. doi: 10.1111/j.1751-1097.1992.tb08542.x.
- Safi, C., Charton, M., Pignolet, O., Pontalier, P. Y., and Vaca-Garcia, C. (2013). Evaluation of the protein quality of *Porphyridium cruentum*. *Journal of Applied Phycology* 25, 497–501. doi: 10.1007/s10811-012-9883-4.
- Sánchez-Saavedra, M. del P., Castro-Ochoa, F. Y., Nava-Ruiz, V. M., Ruiz-Güereca, D. A., Villagómez-Aranda, A. L., Siqueiros-Vargas, F., et al., (2018). Effects of nitrogen source and irradiance on *Porphyridium cruentum*. *Journal of Applied Phycology* 30, 783–792. doi: 10.1007/s10811-017-1284-2.
- Sato, N., Moriyama, T., Mori, N., and Toyoshima, M. (2017). Lipid metabolism and potentials of biofuel and high added-value oil production in red algae. *World Journal of Microbiology and Biotechnology* 33. doi: 10.1007/s11274-017-2236-3.
- Sanjeewa, K. K. A., and Jeon, Y.-J. (2018). Edible brown seaweeds: a review. *Journal of Food Bioactives*. 2, 37–50–37–50. doi: 10.31665/JFB.2018.2139.
- Sager, J.C., Edwards, J.L., and Klein W.H. (1982). Light Energy Utilization Efficiency for Photosynthesis. *Transactions of the ASAE* 25, 1737–1746. doi: 10.13031/2013.33799.
- Sekar, S., and Chandramohan, M. (2008). Phycobiliproteins as a commodity: Trends in applied research, patents and commercialization. *Journal of Applied Phycology*. 20, 113–136. doi: 10.1007/s10811-007-9188-1.
- Senthilkumar, N., Suresh, V., and Thangam, R. (2013). International Journal of Biological Macromolecules Isolation and characterization of macromolecular protein R-Phycoerythrin from *Portieria hornemannii*. *International Journal of Biological Macromolecules* 55, 150–160. doi: 10.1016/j.ijbiomac.2012.12.039.
- Senthilkumar, N., Thangam, R., Murugan, P., Suresh, V., Kurinjimalar, C., Kavitha, G., Sivasubramanian S. and Rengasamy R. (2018). Hepato-protective effects of R-phycoerythrin-rich protein extract of *Portieria hornemannii* (Lyngbye) Silva against DEN-induced hepatocellular carcinoma. *Journal of Food Biochemistry*. 42, 1–11. doi: 10.1111/jfbc.12695.
- Silva, M. P., Tulini, F. L., Ribas, M. M., Penning, M., Fávoro-Trindade, C. S., and Poncelet, D. (2016). Microcapsules loaded with the probiotic *Lactobacillus paracasei* BGP-1 produced by co-extrusion technology using alginate/shellac as wall material: Characterization and evaluation of drying processes. *Food Research International*. 89, 582–590. doi: 10.1016/J.FOODRES.2016.09.008.
- Simovic, A., Combet, S., Cirkovic Velickovic, T., Nikolic, M., and Minic, S. (2022). Probing the stability of the food colourant R-phycoerythrin from dried Nori flakes. *Food Chemistry*. 374, 131780. doi: 10.1016/J.FOODCHEM.2021.131780.
- Sirisuk, P., Ra, C. H., Jeong, G. T., and Kim, S. K. (2018a). Effects of wavelength mixing ratio and photoperiod on microalgal biomass and lipid production in a two-phase culture system using LED illumination. *Bioresource Technology*. 253, 175–181. doi: 10.1016/j.biortech.2018.01.020.

- Sirisuk, P., Sunwoo, I. Y., Kim, S. H., Awah, C. C., Hun Ra, C., Kim, J. M., et al., (2018b). Enhancement of biomass, lipids, and polyunsaturated fatty acid (PUFA) production in *Nannochloropsis oceanica* with a combination of single wavelength light emitting diodes (LEDs) and low temperature in a three-phase culture system. *Bioresource Technology* 270, 504–511. doi: 10.1016/j.biortech.2018.09.025.
- Soanen, N., Da Silva, E., Gardarin, C., Michaud, P., and Laroche, C. (2016). Improvement of exopolysaccharide production by *Porphyridium marinum*. *Bioresource Technology* 213, 231–238. doi: 10.1016/j.biortech.2016.02.075.
- Souza, B. W. S., Cerqueira, M. A., Bourbon, A. I., Pinheiro, A. C., Martins, J. T., Teixeira, J. A., et al., (2012). Chemical characterization and antioxidant activity of sulfated polysaccharide from the red seaweed *Gracilaria birdiae*. *Food Hydrocolloids* 27, 287–292. doi: 10.1016/J.FOODHYD.2011.10.005.
- Soni, B., Visavadiya, N. P., and Madamwar, D. (2009). Attenuation of diabetic complications by C-phycoerythrin in rats: Antioxidant activity of C-phycoerythrin including copper-induced lipoprotein and serum oxidation. *British Journal of Nutrition* 102, 102–109. doi: 10.1017/S0007114508162973.
- Sotomayor-Gerding, D., Oomah, D., Acevedo, F., Morales, E., Bustamante, M., Shene, C., Rubilar, M. (2016) High carotenoid bioaccessibility through linseed oil nanoemulsions with enhanced physical and oxidative stability. *Food Chemistry*. 199, 463–470.
- Soni, B., Kalavadia, B., Trivedi, U., and Madamwar, D. (2006). Extraction, purification and characterization of phycocyanin from *Oscillatoria quadripunctulata*-Isolated from the rocky shores of Bet-Dwarka, Gujarat, India. *Process Biochemistry*. 41, 2017–2023. doi: 10.1016/j.procbio.2006.04.018.
- Sudhakar, M. P., Jagatheesan, A., Perumal, K., and Arunkumar, K. (2015). Methods of phycobiliprotein extraction from *Gracilaria crassa* and its applications in food colourants. *Algal Research*. 8, 115-120doi: 10.1016/j.algal.2015.01.011.
- Sudhakar, M. P., Kumar, B. R., Mathimani, T., and Arunkumar, K. (2019). A review on bioenergy and bioactive compounds from microalgae and macroalgae-sustainable energy perspective. *Journal of Cleaner Production*. 228, 1320–1333. doi: 10.1016/j.jclepro.2019.04.287.
- Sun, L., Wang, S., Gong, X., Zhao, M., Fu, X., and Wang, L. (2009). Isolation, purification and characteristics of R-phycoerythrin from a marine macroalga *Heterosiphonia japonica*. *Protein Expression and Purification*. 64, 146–154. doi: 10.1016/j.pep.2008.09.013.
- Sun, Y., Wang, H., Guo, G., Pu, Y., and Yan, B. (2014). The isolation and antioxidant activity of polysaccharides from the marine microalgae *Isochrysis galbana*. *Carbohydrate Polymers* 113, 22–31. doi: 10.1016/J.CARBPOL.2014.06.058.
- Sun, Y., Yang, B., Wu, Y., Liu, Y., Gu, X., Zhang, H., et al., (2015). Structural characterization and antioxidant activities of  $\kappa$ -carrageenan oligosaccharides degraded by different methods. *Food Chemistry*. 178, 311–318. doi: 10.1016/J.FOODCHEM.2015.01.105.
- Suganya, A. M., Sanjivkumar, M., Chandran, M. N., Palavesam, A., and Immanuel, G. (2016). Pharmacological importance of sulphated polysaccharide carrageenan from red seaweed

*Kappaphycus alvarezii* in comparison with commercial carrageenan. *Biomedicine and Pharmacotherapy* 84, 1300–1312. doi: 10.1016/J.BIOPHA.2016.10.067.

- Schreiber, U., Bilger, W., and Neubauer, C. (1995). Chlorophyll Fluorescence as a Noninvasive Indicator for Rapid Assessment of In Vivo Photosynthesis in Ecophysiology of Photosynthesis. *Springer Berlin Heidelberg*. 49–70. doi: 10.1007/978-3-642-79354-7\_3.
- Schuurmans, R. M., van Alphen, P., Schuurmans, J. M., Matthijs, H. C. P., and Hellingwerf, K. J. (2015). Comparison of the Photosynthetic Yield of Cyanobacteria and Green Algae: Different Methods Give Different Answers. *Plos one* 10, e0139061. doi: 10.1371/journal.pone.0139061.
- Schell, D., and Beermann, C. (2014). Fluidized bed microencapsulation of *Lactobacillus reuteri* with sweet whey and shellac for improved acid resistance and in-vitro gastro-intestinal survival. *Food Research International*. 62, 308–314. doi: 10.1016/J.FOODRES.2014.03.016.
- Shao, P., Chen, X., and Sun, P. (2013). In vitro antioxidant and antitumor activities of different sulfated polysaccharides isolated from three algae. *International Journal of Biological Macromolecules*. 62, 155–161. doi: 10.1016/J.IJBIOMAC.2013.08.023.
- Sheng, J., Yu, F., Xin, Z., Zhao, L., Zhu, X., and Hu, Q. (2007). Preparation, identification and their antitumor activities in vitro of polysaccharides from *Chlorella pyrenoidosa*. *Food Chemistry* 105, 533–539. doi: 10.1016/J.FOODCHEM.2007.04.018.
- Sharma, R., Bhunia, B., Mondal, A., Kanti Bandyopadhyay, T., Devi, I., Oinam, G., Prasanna, R., Abraham, G. and Tiwari, O.N. (2020). Statistical optimization of process parameters for improvement of phycobiliproteins (PBPs) yield using ultrasound-assisted extraction and its kinetic study. *Ultrason Sonochem* 60,1350-4177. doi: 10.1016/J.ULTSONCH.2019.104762.
- Suh S.S., Hwang, J., Park, M., Seo, H.H., Kim, H.S, Lee, J.H., Moh, S.H., Lee, T.K.(2014). Anti-inflammation activities of mycosporine-like amino acids (MAAs) in response to UV radiation suggest potential anti-skin aging activity. *Marine Drugs*. 14;12(10):5174-87. doi: 10.3390/md12105174. PMID: 25317535; PMCID: PMC4210892.
- Stack, J., Tobin, P. R., Gietl, A., Harnedy, P. A., Stengel, D. B., and FitzGerald, R. J. (2017). Seasonal variation in nitrogenous components and bioactivity of protein hydrolysates from *Porphyra dioica*. *Journal of Applied Phycology* 2017 29:5 29, 2439–2450. doi: 10.1007/S10811-017-1063-0.
- Stummer, S., Salar-Behzadi, S., Unger, F. M., Oelzant, S., Penning, M., and Viernstein, H. (2010). Application of shellac for the development of probiotic formulations. *Food Research International* 43, 1312–1320. doi: 10.1016/J.FOODRES.2010.03.017.
- Smith, J. P., Daifas, D. P., El-Khoury, W., Koukoutsis, J., and El-Khoury, A. (2004). Shelf life and safety concerns of bakery products—A review. *Critical Reviews in Food Science and Nutrition*. 44(1), 19–55.
- Tabarsa, M., You, S., Dabaghian, E.H., Surayot, U. (2018) Water-soluble polysaccharides from *Ulva intestinalis*: Molecular properties, structural elucidation and immunomodulatory activities. *Journal of Food Drug Analytical*. 26, 599–608.

- Tan, H. T., Khong, N. M. H., Khaw, Y. S., Ahmad, S. A., and Yusoff, F. M. (2020). Optimization of the Freezing-Thawing Method for Extracting Phycobiliproteins from *Arthrospira* sp. *Molecules* 25, 3894. doi: 10.3390/MOLECULES25173894.
- Tan, L. H., Chan, L. W., Heng, P. W. S. (2009) Alginate/starch composites as wall material to achieve microencapsulation with high oil loading.. *Journal of Microencapsulation*. 26(3), 263-271.
- Tallima, H., and El Ridi, R. (2018). Arachidonic acid: Physiological roles and potential health benefits – A review. *Journal of Advanced Research* 11, 33–41. doi: 10.1016/j.jare.2017.11.004.
- Tecson, M. G., Abad, L. v., Ebajo, V. D., and Camacho, D. H. (2021). Ultrasound-assisted depolymerization of kappa-carrageenan and characterization of degradation product. *Ultrasonics Sonochemistry* 73, 105540. doi: 10.1016/J.ULTSONCH.2021.105540.
- Teixé-Roig, J., Oms-Oliu, G., Ballesté-Muñoz, S., Odriozola-Serrano, I., and Martín-Belloso, O. (2022). Encapsulation and controlled release of phycocyanin during the in vitro digestion using polysaccharide-added double emulsions (W1/O/W2). *Food Structure* 31, 100249. doi: 10.1016/J.FOOSTR.2021.100249.
- Teo, C. L., Atta, M., Bukhari, A., Taisir, M., Yusuf, A. M., and Idris, A. (2014). Enhancing growth and lipid production of marine microalgae for biodiesel production via the use of different LED wavelengths. *Bioresource Technology* 162, 38–44. doi: 10.1016/j.biortech.2014.03.113.
- Torres, M. D., Flórez-Fernández, N., and Domínguez, H. (2019). Integral Utilization of Red Seaweed for Bioactive Production. *Mar Drugs* 17. doi: 10.3390/MD17060314.
- Torres, M. D., Flórez-Fernández, N., and Dominguez, H. (2021). Ultrasound-Assisted Water Extraction of *Mastocarpus stellatus* Carrageenan with Adequate Mechanical and Antiproliferative Properties. *Marine Drugs* 2021, Vol. 19, Page 280 19, 280. doi: 10.3390/MD19050280.
- Thangam, R., Sundarraj, S., Vivek, R., Suresh, V., Sivasubramanian, S., Paulpandi, M., et al., (2015). Theranostic potentials of multifunctional chitosan-silver-phycoerythrin nanocomposites against triple negative breast cancer cells. *RSC Advances* 5. doi: 10.1039/c4ra14043e.
- Thangam, R., Suresh, V., Asenath Princy, W., Rajkumar, M., Senthilkumar, N., Gunasekaran, P., Kannan, S. (2013) C-Phycocyanin from *Oscillatoria tenuis* exhibited an antioxidant and in vitro antiproliferative activity through induction of apoptosis and G0/G1 cell cycle arrest". *Food Chemistry*, 140, 262–272.
- Thoisen, C., Hansen, B. W., and Nielsen, S. L. (2017). A simple and fast method for extraction and quantification of cryptophyte phycoerythrin. *MethodsX* 4, 209–213. doi: 10.1016/j.mex.2017.06.002.
- Tjahjana, J., Pengkajian, A. B., Teknologi, P., and Mh, J. (2009). Ethnobotany study of seaweed diversity and its utilization in warambadi, panguhalodo areas of east sumba district. *Jurnal Teknologi Lingkungan* 10, 297–310. doi: 10.29122/JTL.V10I3.1476.

- Ulagesan, S.; Nam, T.-J.; Choi, Y.-H. Extraction and Purification of R-Phycoerythrin Alpha Subunit from the Marine Red Algae *Pyropia Yezoensis* and Its Biological Activities. *Molecules* 2021, 26, 6479. <https://doi.org/10.3390/molecules2621647>
- Underwood, A. J. (1996). *Experiments in Ecology*. Cambridge University Press doi: 10.1017/cbo9780511806407.
- Üveges, V., Tapolczai, K., Krienitz, L., and Padisák, J. (2012). Photosynthetic characteristics and physiological plasticity of an *Aphanizomenon flos-aquae* (Cyanobacteria, Nostocaceae) winter bloom in a deep oligo-mesotrophic lake (Lake Stechlin, Germany). *Hydrobiologia* 698, 263–272. doi: 10.1007/s10750-012-1103-3.
- Vadiraja, B. B., Gaikwad, N. W., and Madyastha, K. (1998) Hepatoprotective effect of C-Phycocyanin: Protection for carbon tetrachloride and R- (+)-pulegone-mediated hepatotoxicity in rats. *Biochemical and Biophysical Research Communications*, 249(2), 428–431.
- Vijayabaskar, P., and Vaseela, N. (2012). In vitro antioxidant properties of sulfated polysaccharide from brown marine algae *Sargassum tenerrimum*. *Asian Pacific Journal of Tropical Disease* 2, S890–S896. doi: 10.1016/S2222-1808(12)60287-4.
- Vigani, M., Parisi, C., Rodríguez-Cerezo, E., Barbosa, M. J., Sijtsma, L., Ploeg, M., et al., (2015). Food and feed products from micro-algae: Market opportunities and challenges for the EU. *Trends in Food Science and Technology* 42, 81–92. doi: 10.1016/j.tifs.2014.12.004.
- Villafañe, V. E., Gao, K., and Helbling, E. W. (2005). Short- and long-term effects of solar ultraviolet radiation on the red algae *Porphyridium cruentum*(S. F. Gray) Nägeli. *Photochemical and Photobiological Sciences* 4, 376–382. doi: 10.1039/b418938h.
- Villay, A., Laroche, C., Roriz, D., El Alaoui, H., Delbac, F., and Michaud, P. (2013). Optimisation of culture parameters for exopolysaccharides production by the microalga *Rhodella violacea*. *Bioresource Technology* 146, 732–735. doi: 10.1016/j.biortech.2013.07.030.
- Vonshak, A., Cohen, Z., and Richmond, A. (1985). The feasibility of mass cultivation of *Porphyridium*. *Biomass* 8, 13–25. doi: 10.1016/0144-4565(85)90032-0.
- Xu, S. Y., Huang, X., and Cheong, K. L. (2017). Recent Advances in Marine Algae Polysaccharides: Isolation, Structure, and Activities. *Marine Drugs*. 15, Page 388 15, 388. doi: 10.3390/MD15120388.
- Walsby, A. E. (1995). *Microalgae: Biotechnology and Microbiology*. By E. W. Becker. Cambridge: Cambridge University Press (1994), pp. 230. *Experimental Agriculture* 31, 112–112. doi: 10.1017/S0014479700025126.
- Walter, A., de Carvalho, J. C., Soccol, V. T., de Faria, A. B. B., Ghiggi, V., and Soccol, C. R. (2011). Study of phycocyanin production from *Spirulina platensis* under different light spectra. *Brazilian Archives of Biology and Technology*. 54(4), 675–682. <https://doi.org/10.1590/S1516-89132011000400005>
- Wani, S. M., Jan, N., Wani, T. A., Ahmad, M., Masoodi, F. A., and Gani, A. (2017). Full length article. *Journal of the Saudi Society of Agricultural Sciences* 2, 119–126. doi: 10.1016/J.JSSAS.2015.03.006.



- Westermeyer, R. and Ramírez, C. (1978). Algas marinas de Niebla y Mehuín (Valdivia-Chile). *Medio Ambiente* 3: 44-49.
- Wijffels, R., Kruse, O. & Hellingwerf, O. (2013) Potential of industrial biotechnology with cyanobacteria and eukaryotic microalgae. *Current Opinion in Biotechnology*. 24(3): 405–413.
- Wobbe, L., Bassi, R., and Kruse, O. (2016). Multi-Level Light Capture Control in Plants and Green Algae. *Trends in Plant Science* 21, 55–68. doi: 10.1016/j.tplants.2015.10.004.
- Wu, Q., Fu, X. P., Sun, L. C., Zhang, Q., Liu, G. M., Cao, M. J., et al., (2015). Effects of physicochemical factors and in vitro gastrointestinal digestion on antioxidant activity of R-phycoerythrin from red algae *Bangia fusco-purpurea*. *International Journal of Food Science and Technology* 50, 1445–1451. doi: 10.1111/IJFS.12775.
- Yabuta, Y., Fujimura, H., Kwak, C. S., Enomoto, T., and Watanabe, F. (2010). Antioxidant Activity of the Phycoerythrobilin Compound Formed from a Dried Korean Purple Laver (*Porphyra* sp.) during in Vitro Digestion. *Food Science and Technology Research* 16, 347–352. doi: 10.3136/FSTR.16.347.
- Yaich, H., Garna, H., Besbes, S., Paquot, M., Blecker, C., and Attia, H. (2011). Chemical composition and functional properties of *Ulva lactuca* seaweed collected in Tunisia. *Food Chemistry* 128(4), 895-901. doi: 10.1016/j.foodchem.2011.03.114.
- Yan, M. de, Lin, H. Y., and Hwang, P. A. (2019). The anti-tumor activity of brown seaweed oligo-fucoidan via lncRNA expression modulation in HepG2 cells. *Cytotechnology* 71, 363–374. doi: 10.1007/S10616-019-00293-7.
- Yan, M., Liu, B., Jiao, X., and Qin, S. (2014). Preparation of phycocyanin microcapsules and its properties. *Food and Bioprocess Processing* .92, 89–97. doi: 10.1016/J.FBP.2013.07.008.
- Yang, Y., and Weathers, P. (2014). Red light and carbon dioxide differentially affect growth, lipid production, and quality in the microalga *Ettlia oleoabundans*. *Applied Microbiology and Biotechnology* 99, 489–499. doi: 10.1007/s00253-014-6137-1.
- Yang, Y.C. and Wei, M.C. (2015) Kinetic and characterization studies for three bioactive compounds extracted from *Rabdosia rubescens* using ultrasound, *Food and Bioprocess Processing*. 94:101-113. <https://doi.org/10.1016/j.fbp.2015.02.001>.
- Ye, H., Zhou, C., Sun, Y. Zgǎhang, X., Hu, Q. and Zeng, X. (2009) Antioxidant activities in vitro of ethanol extract from brown seaweed *Sargassum pallidum* .*European Food Research Technology* . 230, 101. <https://doi.org/10.1007/s00217-009-1147-4>.
- Ye, H.; Wang, K.; Zhou, C.; Liu, J.; Zeng, X. (2008) Purification, antitumor and antioxidant activities in vitro of polysaccharides from the brown seaweed *Sargassum pallidum*. *Food Chem.* 111, 428-432.
- Yi, M., Fang, X., Wen, L., Guang, F., & Zhang, Y. (2019). The Heterogeneous Effects of Different Environmental Policy Instruments on Green Technology Innovation. *International Journal of Environmental Research and Public Health*. 16(23), 4660. <https://doi.org/10.3390/IJERPH16234660>

- Youssouf, L., Lallemand, L., Giraud, P., Soulé, F., Bhaw-Luximon, A., Meilhac, O., et al., (2017). Ultrasound-assisted extraction and structural characterization by NMR of alginates and carrageenans from seaweeds. *Carbohydrate Polymers* 166, 55–63. doi: 10.1016/J.CARBPOL.2017.01.041.
- You, T., and Barnett, S. M. (2004). Effect of light quality on production of extracellular polysaccharides and growth rate of *Porphyridium cruentum*. *Biochemical Engineering Journal* 19, 251–258. doi: 10.1016/j.bej.2004.02.004.
- Yuan, H., Zhang, W., Li, X., Lü, X., Li, N., Gao, X., et al., (2005). Preparation and in vitro antioxidant activity of kappa-carrageenan oligosaccharides and their oversulfated, acetylated, and phosphorylated derivatives. *Carbohydr Res* 340, 685–692. doi: 10.1016/J.CARRES.2004.12.026.
- Zainal Ariffin, S. H., Yeen, W. W., Zainol Abidin, I. Z., Megat Abdul Wahab, R., Zainal Ariffin, Z., and Senafi, S. (2014). Cytotoxicity effect of degraded and undegraded kappa and iota carrageenan in human intestine and liver cell lines. *BMC Complementary and Alternative Medicine* 14, 1–16. doi: 10.1186/1472-6882-14-508/FIGURES/8.
- Zhang, H., Jiang, F., Zhang, J., Wang, W., Li, L., and Yan, J. (2022). Modulatory effects of polysaccharides from plants, marine algae and edible mushrooms on gut microbiota and related health benefits: A review. *International Journal of Biology Macromolecules*. 204, 169–192. doi: 10.1016/J.IJBIOMAC.2022.01.166.
- Zhou, J., Hu, N., Wu, Y. L., Pan, Y. J., and Sun, C. R. (2008). Preliminary studies on the chemical characterization and antioxidant properties of acidic polysaccharides from *Sargassum fusiforme*. *Journal of Zhejiang University Science B*. 9:9 9, 721–727. doi: 10.1631/JZUS.B0820025.